Vol. 57 • No. 11

November 2014

Microwave Journal .com

MVP
Keysight Signal Analyzer

horizon house®
Founded in 1958

MCL B 744
ADP-2-10
MCL B 744
ADP-2-10
MCL B 744
ADP-2-10
MCL
GBA-12
071838

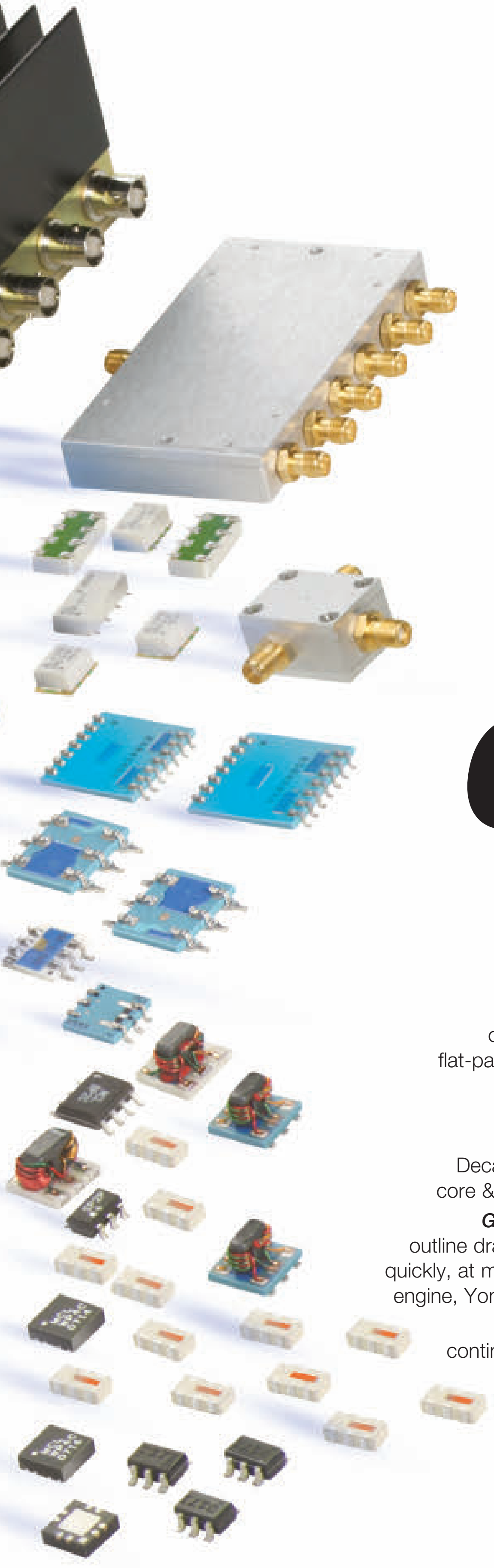

POWER SPLITTERS/ COMBINERS

NOW! from **2 kHz to 18 GHz** as low as **79¢**

The Industry's Largest Selection includes THOUSANDS of models, from 2 kHz to 18 GHz, at up to 300 watts power, in coaxial, flat-pack, surface-mount and rack-mount housings for 50 and 75 Ω systems.

From 2-way through 48-way designs, with 0°, 90°, or 180° phase configurations, Mini-Circuits power splitters/combiners offer outstanding performance for insertion loss, isolation, and VSWR. Decades of experience with multiple technologies make it all possible, from core & wire, microstrip, and stripline, to semiconductors and LTCC ceramics.

Get easy-to-find, detailed data and performance curves, S-parameters, outline drawings, PCB layouts, and everything else you need to make a decision quickly, at minicircuits.com. Just enter your requirements, and our patented search engine, Yoni2, searches *actual test data* to find the models that meet your needs.

All Mini-Circuits catalog models are in stock, continuously replenished, and backed by our 1-year guarantee. We even list *current stock quantities and real-time availability*, as well as pricing, to help our customers plan ahead and make quick decisions. So why wait? Take a look at minicircuits.com today!

RoHS Compliant
Product availability is listed on our website.

Mini-Circuits®

www.minicircuits.com P.O. Box 350166, Brooklyn, NY 11235-0003 (718) 934-4500 sales@minicircuits.com

448 rev N

Technology On the Move™

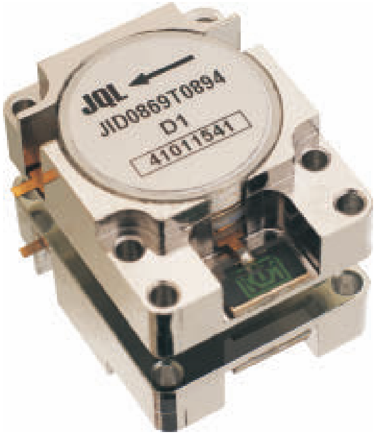

Drop-in Isolators

Cavity Filters

Surface Mount Circulators

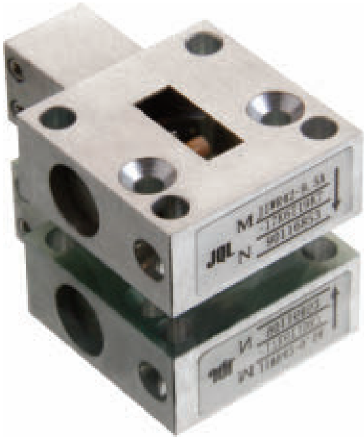

Waveguide Isolators

Power Combiners

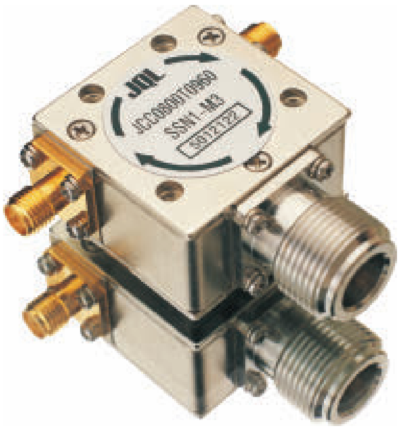

Coaxial Circulators

JQL

Tel:1(888)236-9828(US&Canada)
1(630)930-9917(Worldwide)
www.jqlelectronics.com   sales@jqlelectronics.com


Relax
We've got you covered
Your supplier of high performance, precise equipment for AWGN
NOISEWAVE
The new wave in NOISE
Ph. (973) 386-1119 • Fax (973) 386-1131 • info@noisewave.com • www.noisewave.com

Microwave Journal

CONTENTS

November 2014
Vol. 57 • No. 11
Passive & Control Components
mwjournal.com

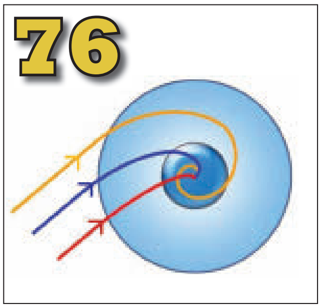

AUGMENTED REALITY: HOW IT WORKS

STEP 1
Download the free Layar app from the iTunes (iOS) or Google Play (Android) store.

STEP 2
Launch the app to view enhanced content on any page with the layar logo.

STEP 3
Frame the entire page in the screen and tap to experience enhancements (tap screen again for full screen view).

Refer to page 152 for this month's participants

AR pages may expire after 60 days.

57 YEARS OF PUBLISHING EXCELLENCE

NATIONAL INSTRUMENTS

AWR A National Instruments Company™

Try NI AWR Design Environment Today!

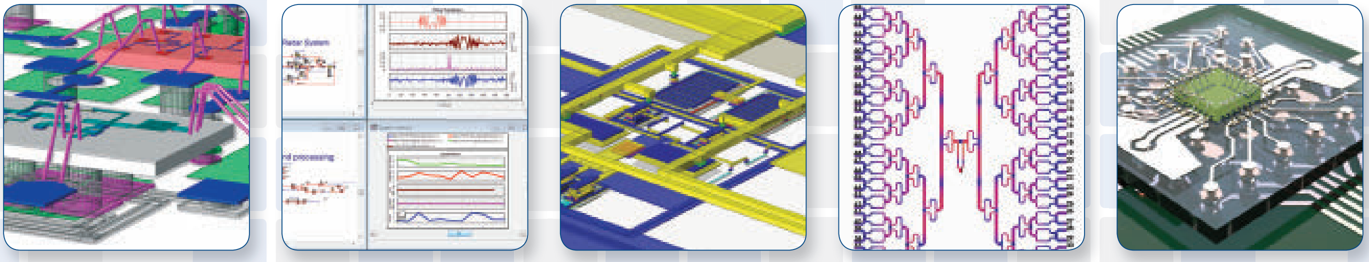

Microwave Office | Visual System Simulator | Analog Office | AXIEM | Analyst

Try NI AWR Design Environment

today and see for yourself how easy and effective it is to streamline your design process, improve end product performance, and accelerate time to market for MMICs, RFICs, RF PCBs, microwave modules, 3D/planar passive interconnects, antennas, communication systems, and more.

>> Learn more at ni.com/awr

NI AWR Design Environment consists of a comprehensive software product portfolio that offers a variety of high-frequency design tools that embrace system simulation, circuit simulation, and electromagnetic analysis.

- Microwave Office for MMIC, module, and RF PCB design
- Visual System Simulator for RF/comms. systems design
- Analog Office for analog and RFIC design
- AXIEM for 3D planar electromagnetic analysis
- Analyst for 3D FEM EM simulation and analysis

Visit **awrcorp.com/whatsnew** for a complete list of features found in the current version of NI AWR Design Environment.

Microwave Journal

CONTENTS

mwjournal.com

Product Features

Tech Briefs

Departments

Microwave Journal (USPS 396-250) (ISSN 0192-6225) is published monthly by Horizon House Publications Inc., 685 Canton St., Norwood, MA 02062. Periodicals postage paid at Norwood, MA 02062 and additional mailing offices.

POSTMASTER: Send address corrections to *Microwave Journal*, PO Box 3256, Northbrook, IL 60065-3256 or e-mail mwj@omeda.com. Subscription information: (847) 291-5216. This journal is issued without charge upon written request to qualified persons working in the RF & microwave industry. Other subscriptions are: domestic, $120.00 per year, two-year subscriptions, $185.00; foreign, $200.00 per year, two-year subscriptions, $370.00; back issues (if available) and single copies, $10.00 domestic and $20.00 foreign. Claims for missing issues must be filed within 90 days of date of issue for complimentary replacement.

STAFF

Publisher: Carl Sheffres
Editor: Patrick Hindle
Technical Editor: Gary Lerude
Managing Editor: Jennifer DiMarco
Associate Technical Editor: Cliff Drubin
Multimedia Staff Editors:
Barbara Walsh and Leslie Nikou
Consulting Editor: Harlan Howe, Jr.
Consulting Editor: Frank Bashore
Consulting Editor: David Vye
Consulting Editor: Raymond Pengelly
Web Editor: Chris Stanfa
Client Services Manager:
Kristen Anderson
Audience Development Manager:
Carol Spach
Traffic Manager: Edward Kiessling
Director of Production & Distribution:
Robert Bass
Art Director: Janice Levenson
Graphic Designer: Sachiko Stiglitz

EUROPE

International Editor: Richard Mumford
Office Manager: Nina Plesu

CORPORATE STAFF

CEO: William M. Bazzy
President: Ivar Bazzy
Vice President: Jared Bazzy

Executive Editorial Office
685 Canton Street, Norwood, MA 02062
Tel: (781) 769-9750
FAX: (781) 769-5037
e-mail: mwj@mwjournal.com

European Editorial Office
16 Sussex Street, London SW1V 4RW, England
Tel: Editorial: +44 207 596 8730 Sales: +44 207 596 8740
FAX: +44 207 596 8749

Subscription Services
Send subscription inquiries and address changes to:
Tel: (847) 291-5216
e-mail: mwj@omeda.com

BPA WORLDWIDE

www.mwjournal.com

Printed in the USA

Microwave Journal Online

Scan page using layar app

Visit us @ mwjournal.com

eLEARNING free webinars

EMC Simulation in Modern Electronics
Presented by: CST 11/6

MMIC Design Overview
Sponsored by: National Instruments (formerly AWR) 11/6

Passive Components: Dividers, Couplers, Combiners
Sponsored by: Mini-Circuits 11/12

Efficient Simulation of Optical Devices
Presented by: CST 11/13

Essential Thermal Mechanical Concepts Needed in Today's Microwave Circuit Designs
Sponsored by: Rogers Corp. 11/13

Modeling a DDR4 Memory Channel
Presented by: CST 11/20

Modeling Material Properties
Presented by: CST 11/25

Web Survey

What filter technology will win the most duplexer sockets in small cell base stations?

Look for our multiple choice survey online at mwjournal.com

September Survey
What city do you like the most for EuMW?

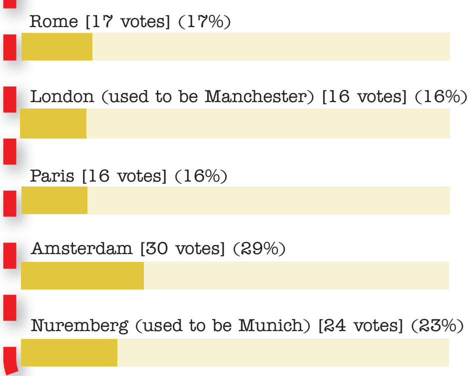

Marc E. Smith, president and CEO of **XMA**, discusses the company's heritage from Omni Spectra, expansion into other product areas and future plans.

Executive Interview

WHITE PAPERS

molex — A Simple Approach to Signal Via Stubs for Coaxial PCB Connector Launches

RichardsonRFPD (An Arrow Company) / Arrow RF & Power — Integrated GaN Amplifiers: an Optimized Solution for Mid-Level Broadband RF Power

COM

DECEMBER 2014

SUNDAY	MONDAY	TUESDAY	WEDNESDAY	THURSDAY	FRIDAY	SATURDAY
30	1 ◄ **Precise Time and Time Interval Systems and Applications**, Boston, Mass. (Dec. 1–4)	2 ◄ **ARFTG 84th Microwave Measurement Conference**, Boulder, Colo. (Dec. 2–5)	3	4 **Webinar: Antennas for Automotive Applications** Sponsored by CST; **Webinar: RF System Design, Prototype & Production with X-Parameters in One Pass** Sponsored by KEYSIGHT TECHNOLOGIES	5	6
7	8	9	10	11 **Webinar: Simulation-Enabled 5G Antenna Design** Sponsored by CST; **Webinar: Non Destructive Testing of Composite Materials** Sponsored by KEYSIGHT TECHNOLOGIES	12	13
14	15 ◄ **IMaRC**, Bangalor, India (Dec. 15–17)	16	17	18	19	20
21	22	23	24	25	26	27
28	29	30	31	1	2	3

Visit mwjournal.com/events

Coming**Events**

CALL FOR PAPERS

EDI CON 2015
November 30, 2014

IMS 2015
December 8, 2014

WAMICON 2015
January 5, 2015

mwjournal.com

NOVEMBER

electronica 2014
November 11–14, 2014 • München, Germany
www.electronica.de

CommuniCast Myanmar 2014
November 18–20, 2014 • Yangon, Myanmar
www.communicastmyanmar.com

DECEMBER

Precise Time and Time Interval Systems and Applications
December 1–4, 2014 • Boston, Mass.
www.ion.org/ptti

ARFTG 84th Microwave Measurement Conference
December 2–5, 2014 • Boulder, Colo.
www.arftg.org

IMaRC 2014
IEEE MTT-S International Microwave and RF Conference
December 15–17, 2014 • Bangalor, India
www.imarc-ieee.org

JANUARY 2015

RWW 2015
Radio and Wireless Week
January 25–28, 2015 • San Diego, Calif.
www.radiowirelessweek.org

DesignCon
January 27–30, 2015 • Santa Clara, Calif.
www.designcon.com

MARCH

Mobile World Congress
March 2–5, 2015 • Barcelona, Spain
www.mobileworldcongress.com

CS International Conference 2015
March 11–12, 2015 • Frankfurt, Germany
www.cs-international.net

IEEE EMC & SI 2015
March 15–21, 2015 • Santa Clara, Calif.
www.emc2015usa.emcss.org

Satellite 2015
March 16–19, 2015 • Washington, DC
www.satshow.com

APRIL

Microwave & RF 2015
April 1–2, 2015 • Paris, France
www.microwave-rf.com

WAMICON 2015
IEEE Wireless and Microwave Technology Conference
April 13–15, 2015 • Cocoa Beach, Fla.
www.wamicon.org

EDI CON 2015
Electronic Design Innovation Conference
April 14–16, 2015 • Beijing, China
www.ediconchina.com

MAY

AUVSI's Unmanned Systems 2015
May 4–7, 2015 • Atlanta, Ga.
www.auvsi.org

RFIC 2015
IEEE Radio Frequency Circuits Symposium
May 17–19, 2015 • Phoenix, Ariz.
www.rfic-ieee.org

IMS 2015
IEEE MTT-S International Microwave Symposium
May 17–22, 2015 • Phoenix, Ariz.
www.ims2015.org

Space Tech Expo 2015
May 19–21, 2015 • Long Beach, Calif.
www.spacetechexpo.com

85th ARFTG Microwave Measurement Symposium
May 22, 2015 • Phoenix, Ariz.
www.arftg.org

EW Europe 2015
May 26–28, 2015 • Stockholm, Sweden
www.eweurope.com

Honored to Join You

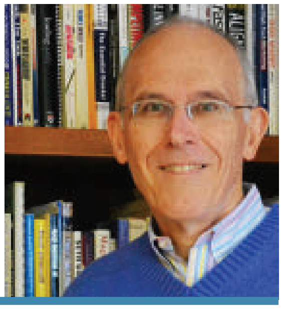

Gary Lerude
Microwave Journal *Technical Editor*

As the new technical editor of *Microwave Journal*, I welcome you to our November issue. What a privilege it is for me to be here and contribute to such a quality and long-lasting publication.

Life is neither predictable nor linear, often bringing unexpected turns that forever change us. Such is my story. Long, long ago, as a senior in high school, I faced the difficult choice of which career to pursue: engineering or journalism / mass communication. Both were of keen interest, fostered by my part-time job at a radio station. I chose electrical engineering.

By the time I was a senior in college, I had decided to apply my EE degree to audio engineering, designing loudspeakers or power amplifiers. However, the economy was in a recession and although I had quite a few interviews, no real job offers followed. I did land an engineering position, ironically working at the other end of the frequency spectrum.

That job experience and another degree led me to Texas Instruments (TI), where I was introduced to microstrip, an early version of COMPACT, and GaAs. TI gave me the opportunity to be a "midwife" at the birth of the GaAs MMIC industry. When Raytheon acquired TI's defense business in 1997, I left to join MACOM, where I played several marketing, product management and business development roles, serving both commercial and defense markets.

Cobham's acquisition of MACOM six years ago prompted me to join TriQuint, where I was reunited with many former TI colleagues. TriQuint had purchased TI's MMIC segment after the U.S. Department of Justice forced Raytheon to divest it, as a condition of purchasing TI's defense business. At TriQuint, I held product and strategic marketing and business development roles focused on the infrastructure markets: base station, point-to-point radio, VSAT, optical networking and CATV.

David Vye's departure from *Microwave Journal* last summer created an opening for a technical editor. When Pat Hindle, who took on David's role, posted the opening on LinkedIn, I was surprised at how much it resonated with me. After all these years, I saw the chance to pursue my long-standing interest in journalism and media, while using my industry experience and technical background.

And so, somewhat unexpectedly, I find myself writing this column, honored to join the talented and dedicated team that publishes the most prestigious of the RF and microwave media, a publication that has informed me throughout my career. I see my role as helping to make you more effective, productive and informed in your respective roles, while maintaining our high standards for the quality of content.

Ours is a small industry. I look forward to renewing acquaintance with those of you I have met over the years and meeting many of you I do not yet know. I want to hear and help tell the stories of the work you are doing and the impact you are having on society. But enough about me.

Our November issue includes two interesting articles on the challenges facing today's filter designers. With data consumption growing exponentially, every bit of frequency spectrum is in demand, and filters allow the myriad services, commercial and military, to coexist without interfering with each other.

Last year's article on Möbius strips, used as printed resonators for oscillators, was one of the most popular *Microwave Journal* has published. As a follow up, Ulrich Rohde and Ajay Poddar are back with the first of a three-part series that provides a broader treatment of the topic.

Two technical articles address aspects of power amplifier design: second harmonic tuning of a broadband GaN PA to maximize efficiency, and PCB thermal management, which is critical to ensure reliability. Rounding out the issue is an article on a low phase noise oscillator.

Our November supplement focuses on mobile communications and infrastructure. You have probably noticed that industry interest in 5G is accelerating, including R&D investigating the feasibility of using the millimeter wave spectrum. Addressing a major question, NYU WIRELESS has contributed an encouraging article reporting on propagation at 28 and 73 GHz.

For circuits and systems, we have technical features on a Q-Band transceiver and an 8 × 8 MIMO subsystem for 802.11ac Wi-Fi. Sky Light Research provides a market perspective on the long-haul, point-to-point radio market.

As interesting and complex as the communications technology and products are, we often take for granted the test systems needed to design and manufacture them. Two articles provide insight into this: Keysight Technologies writes about the role of the test system in optimizing the design of envelope tracking (ET) power amplifiers, and National Instruments contributes a tutorial on six key measurements necessary to characterize LTE receivers.

This range of topics reminds me once again that we live in an amazing age. We should be proud to be part of an industry that provides the RF and microwave technologies that help make it so. ■

Redefining RF and Microwave Instrumentation

with open software and modular hardware

Scan page
using layar app

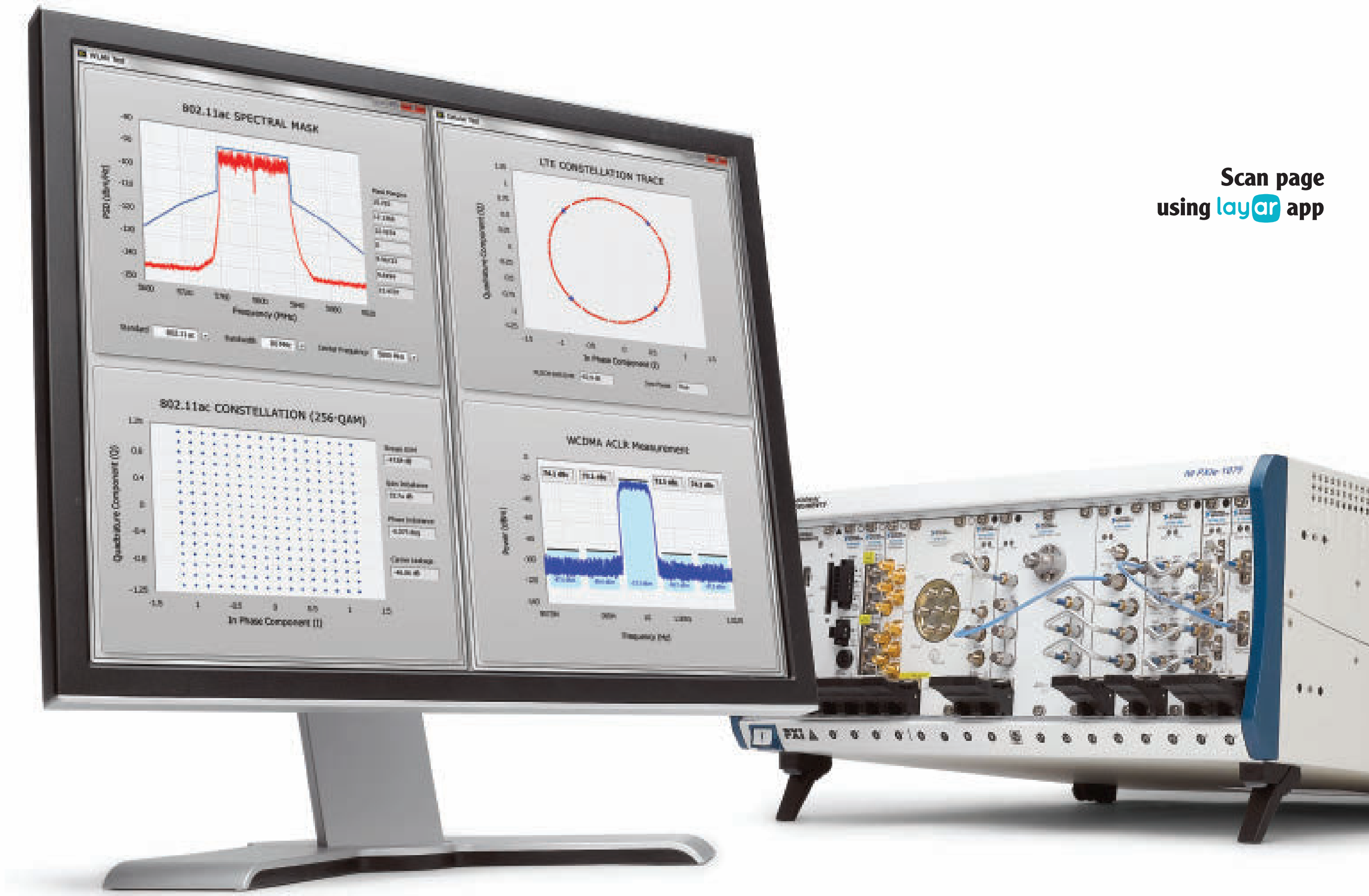

Achieve speed, accuracy, and flexibility in your RF and microwave test applications by combining National Instruments open software and modular hardware. Unlike rigid traditional instruments that quickly become obsolete by advancing technology, the system design software of NI LabVIEW coupled with NI PXI hardware puts the latest advances in PC buses, processors, and FPGAs at your fingertips.

WIRELESS TECHNOLOGIES

National Instruments supports a broad range of wireless standards including:

LTE	GSM/EDGE
802.11a/b/g/n/ac	CDMA2000/EV-DO
WCDMA/HSPA/HSPA+	Bluetooth

>> Learn more at ni.com/redefine

800 813 5078

NATIONAL INSTRUMENTS™

Keysight W1715EP SystemVue MIMO channel builder

Keysight N9040B UXA signal analyzer
with 89600 VSA software

Keysight MIMO PXI test solution
with N7624/25B Signal Studio software for LTE-Advanced/LTE FDD/TDD and 89600 VSA software

Keysight E7515A UXM wireless test set
with E7530A/E7630A LTE-Advanced/LTE test/lab application software

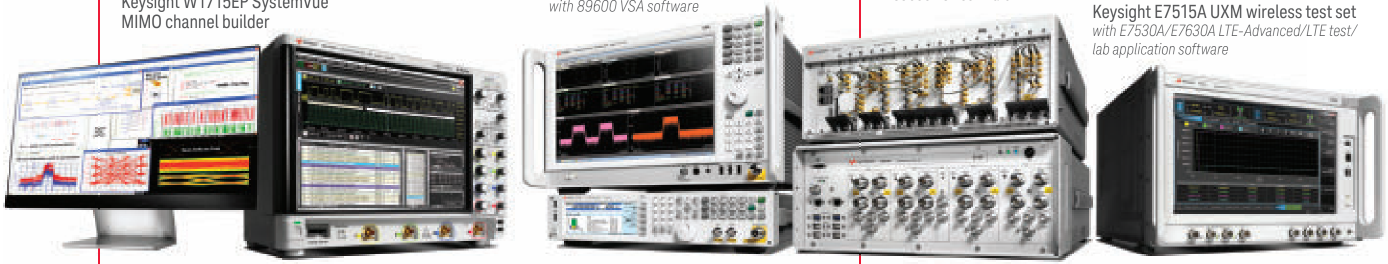

Keysight Infiniium S-Series high-definition oscilloscope
with N8807A MIPI DigRF v4 (M-PHY) protocol decode software

Keysight N5182B MXG X-Series RF vector signal generator
with N7624/25B Signal Studio software for LTE-Advanced/LTE FDD/TDD

Keysight E6640B EXM wireless test set
with V9080/82B LTE FDD/TDD measurement applications and N7624/25B Signal Studio software for LTE-Advanced/LTE FDD/TDD

HARDWARE + SOFTWARE

The more complex your LTE-A design, the more you need help from test and measurement experts. Keysight is the only company that offers benchtop, modular and software solutions for every step of the LTE-A design process. From R&D to manufacturing, we can give you the expertise, instruments and applications you need to succeed.

- *Complete LTE-Advanced design and test lifecycle*
- *Identical software algorithms across platforms*
- *300+ software applications for the entire wireless lifecycle*

PEOPLE

We know what it takes for your designs to meet LTE-A standards. After all, Keysight engineers have played major roles in LTE-A and other wireless standards bodies, including 3GPP. Our engineers even co-authored the first book about LTE-A design and test. We also have hundreds of applications engineers. You'll find them all over the world, and their expertise is yours for the asking.

- *Representation on every key wireless standards organization globally*
- *Hundreds of applications engineers in 100 countries around the world*
- *Thousands of patents issued in Keysight's history*

KEYSIGHT TECHNOLOGIES

Unlocking Measurement Insights

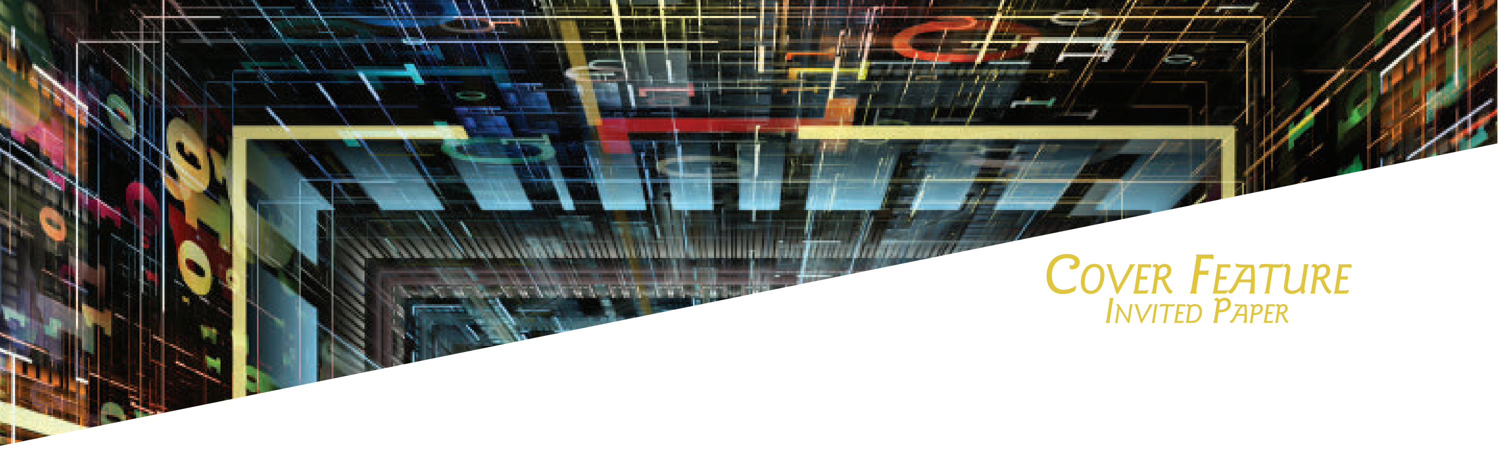

Recent Market Driven Filter Advances

David Howett, Michael P. Busse
Microwave Products Group, Salisbury, Maryland
David Rawlinson
BSC, York, United Kingdom
Jeff Burkett, Tim Dolan, Rafi Hershtig
K&L Microwave, Salisbury, Maryland
Douglas King
Pole/Zero Corp., West Chester, Ohio

Recent marketplace realities have included looming budget cuts, competition with low-cost competitors and regular large program contract delays, all highlighting the increasing importance of versatile, configurable, reusable RF modules and hardware. Size, weight and power (SWaP) innovation and wider bandwidth, multimode, smaller platforms are the mantra.

RECENT FILTER INNOVATIONS AND MARKET DRIVERS

The history of advances in the development of RF and microwave filters is well documented, and broad innovation goals have remained essentially the same over decades. Better performance, smaller size, lower cost and greater power-handling are some of the general "wants" engineers are always working to achieve. However, certain observations about recent industry trends can be made. For instance, filter innovation in the last 10 years has been spurred by material advances and ever-increasing electromagnetic simulation speeds and capabilities. Accordingly, lumped component products are supporting higher power-handling, cavity filters are shrinking in size/volume (by a factor of two or more) with little loss of Q, tunable filters are achieving higher power-handling at smaller sizes and low passive intermodulation (low PIM) products are being cost-effectively manufactured in higher volume.

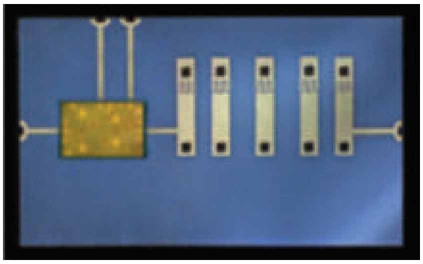

▲ *Fig. 1 Thin film/GaN integration.*

The industry has observed the following trends:

1. Ceramic material advances, particularly specialized material consistency, have facilitated higher yields on ceramic resonator filters and on higher-performance ceramic substrate printed filters. Additionally, advanced ceramic materials have made dielectrically-loaded waveguide super high Q filters possible. Single-, dual- and triple-mode "puck" filters provide better performance at a smaller size.
2. Newly developed materials or substrates that enable practical thin film filter implementation are equally at home supporting GaAs and GaN bare-die integration, allowing further size reduction in multifunction module construction. As an example, ***Figure 1*** shows a BSC product with GaN integration on thin film.
3. In addition to virtual prototyping of various innovative mechanical realizations, 3D modeling and printing and other computing advances have allowed more complex

phase, delay, and matching criteria in specifications, as well as in real-time testing and verification.

4. System computing technology has expanded possibilities for filtering cancellation techniques, driving some agile filter technology. Various methodologies have been tried, with mixed results. Standard techniques and components like varactor diodes cannot handle the system power requirements. Millions of dollars have been invested in novel agile materials that remain unproven. High power pin diodes have filled some voids, but much work remains. MEMS technology has not yet effectively aided band tuning/agility.
5. High-frequency MMICs shrink cost and size of various filter assemblies, for example, up/down-converters, making them increasingly filter-dependent in terms of size and cost, adding to pressure for filter design innovation in commercial and military arenas.
6. Commercial and military system frequency spectrum overcrowding has vastly increased demand for notch filters, simultaneously escalating demand for size and performance improvements in band-reject realizations.
7. Even with spectrum interferers addressed, the push for greater speeds, more data and more connected users has created the need for low PIM systems and low PIM test equipment. PIM is directly related to noise, noise to bandwidth and bandwidth to supportable speed.
8. Cavity-like performance and Q are being sought in surface mount formats.
9. Amplifier semiconductor materials have lowered noise figures, allowing higher filter insertion loss to be traded for smaller filter size while maintaining overall system cascaded noise.

Against the backdrop of these broad trends, innovation in filter design and the usage of specialized filter products continues. Military and commercial telecommunications, along with certain medical industry technologies, prompt advances in materials, packaging, design and arrangement of filters to meet key market challenges. This article focuses on five current innovative approaches to address present and future market needs.

THIN FILM APPROACH TO MINIATURIZED RF INTEGRATION

Traditional thin film microwave hybrid circuit designs have declined in many applications, displaced over the years by the evolution of MMICs and the development of low-cost packaging. These advances enabled active microwave design to be realized on soft-board materials at frequencies above 60 GHz. More recently, the advent of special ceramic materials has facilitated the realization of high-performance miniature filtering using thin film, enabling the integration of such filtering into multifunctional subsystems.

While many thin film circuits have featured a degree of filtering as an adjunct, until the development of modern substrates, thin film was not widely regarded as a suitable technology for high-performance miniaturized filters. Alumina substrates could not be readily exploited for filtering applications due to low filter Q, relatively poor thermal properties and an ε_r yielding impractical size and relatively poor selectivity.

On the application side, SWaP reduction remains critical, particularly in the UAV and space environments. Modern information gathering and distribution systems are tending toward greater dependence on small airborne platforms in military and civilian contexts. A plethora of fixed and rotary-wing vehicles are affordably available in a wide variety of shapes and sizes, creating opportunities for military and commercial enterprises alike.

With greater dependence on RF systems for control, navigation and telemetry, the proportion of payload size and weight allocated to RF modules is significant, especially when factoring in the usual complement of EW and ECM equipment found onboard military UAVs. Smaller, lighter and more efficient onboard systems extend the

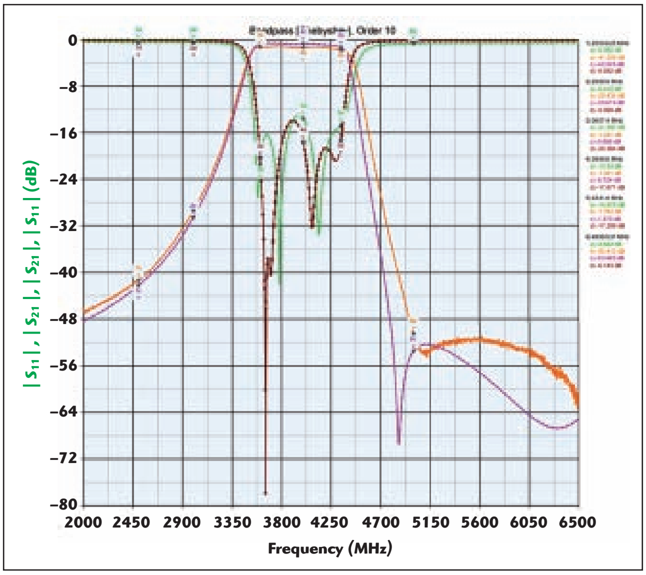

▲ *Fig. 2 Measured 4 GHz bandpass response (orange/green) against simulation (purple/red).*

mission time and capabilities of the craft. SWaP considerations are fundamentally important in the realm of spacecraft systems, and with the widespread use of RF technology in space, cost-per-kilogram to achieve orbit and the small form factor of modern satellites dictate that "smaller and lighter" is always better.

Analysis of the size and weight composition of RF systems shows that two key aspects contribute significantly: discrete RF filters and the inherently modular construction of subsystems. Clearly, shrinking filter size and integrating further would offer discernible advantages. The challenge is that filter size is limited by the laws of physics. Common dielectrics, such as air or PTFE, produce relatively large resonators and cavity volume, while integration of self-contained machined housings, often from different manufacturers, can be far from seamless or space-efficient.

Comparing volumes, a typical 8-section lumped element filter at 2 GHz might be 2.0" × 0.6" × 0.4" in size, and an equivalent air cavity combline would be even larger at 5.9" × 1.8" × 0.9". A thin film approach drastically reduces size to about 0.4" × 0.4" × 0.14" (including cover). This reduction in size is facilitated by the high dielectric constant of the ceramic substrate base, typically featuring an ε_r of more than 25. The unloaded Q of interdigital and combline structures realized in thin film is in the range 250 to 400. By comparison, conventional lumped element and capacitively-coupled ceramic coaxial resonator devices have Q values of 50 to 300 and 300 to 600, respectively. In many cases, thin film offers comparable selectivity.

The design process starts by forming a transmission line model, developing the filter order and preliminary physical layout required. This simplistic model uses a homogenous distribution of the substrate's dielectric properties and simple conductor parameters to speed initial development. The next step is to import the result from the transmission line model into a Finite Element Analysis (FEA) package. At this stage, the virtual prototype can be modelled in detail, including auxiliary parameters such as conductor surface roughness and parasitic effects. The simulation takes into account the inherent coupling between non-adjacent resonators that forms a transmission zero on the high side of the filter passband in interdigital and combline designs, as shown in ***Figure 2***. Edge vias are then matched into both the filter and the interfacing transmission lines.

After the FEA process, the optimized filter geometry is assembled onto photolithographic masks and developed onto laser-drilled, gold-sputtered substrates. Surface conductor thickness of typically 5 µm maintains an adequate multiple of skin depths to achieve optimum conductivity. Depending on the application, thin film devices can be interfaced by soldering or bonding, mounted by reflow or conductive epoxy, enclosed in self-contained shielding or channelized. In mass production contexts, thin film devices are ideally suited to pick-and-

5.0 NOW AVAILABLE
comsol.com/release/5.0

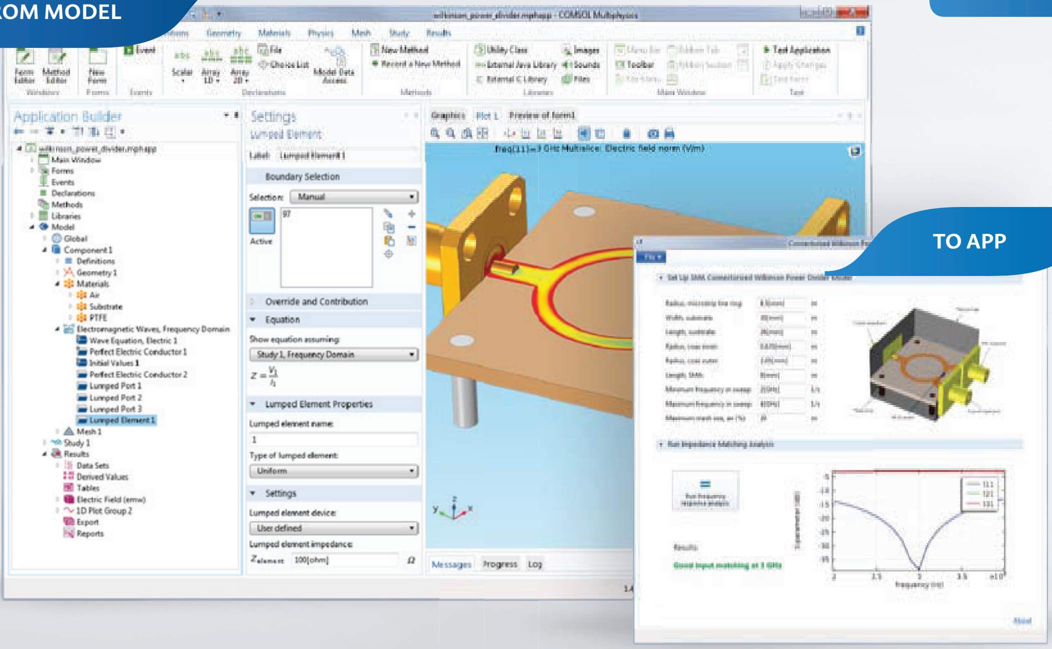

Verify and Optimize your Designs with COMSOL Multiphysics®

NOW FEATURING THE APPLICATION BUILDER

The Application Builder provides you with tools to easily design a custom interface for your multiphysics models. Use COMSOL Server to distribute your apps to colleagues and customers worldwide.

Visit comsol.com/release/5.0

PRODUCT SUITE

COMSOL Multiphysics
COMSOL Server

ELECTRICAL
AC/DC Module
RF Module
Wave Optics Module
Ray Optics Module
MEMS Module
Plasma Module
Semiconductor Module

MECHANICAL
Heat Transfer Module
Structural Mechanics Module
Nonlinear Structural Materials Module
Geomechanics Module
Fatigue Module
Multibody Dynamics Module
Acoustics Module

FLUID
CFD Module
Mixer Module
Microfluidics Module
Subsurface Flow Module
Pipe Flow Module
Molecular Flow Module

CHEMICAL
Chemical Reaction Engineering Module
Batteries & Fuel Cells Module
Electrodeposition Module
Corrosion Module
Electrochemistry Module

MULTIPURPOSE
Optimization Module
Material Library
Particle Tracing Module

INTERFACING
LiveLink™ *for* MATLAB®
LiveLink™ *for* Excel®
CAD Import Module
Design Module
ECAD Import Module
LiveLink™ *for* SOLIDWORKS®
LiveLink™ *for* Inventor®
LiveLink™ *for* AutoCAD®
LiveLink™ *for* Revit®
LiveLink™ *for* PTC® Creo® Parametric™
LiveLink™ *for* PTC® Pro/ENGINEER®
LiveLink™ *for* Solid Edge®
File Import *for* CATIA® V5

COMSOL

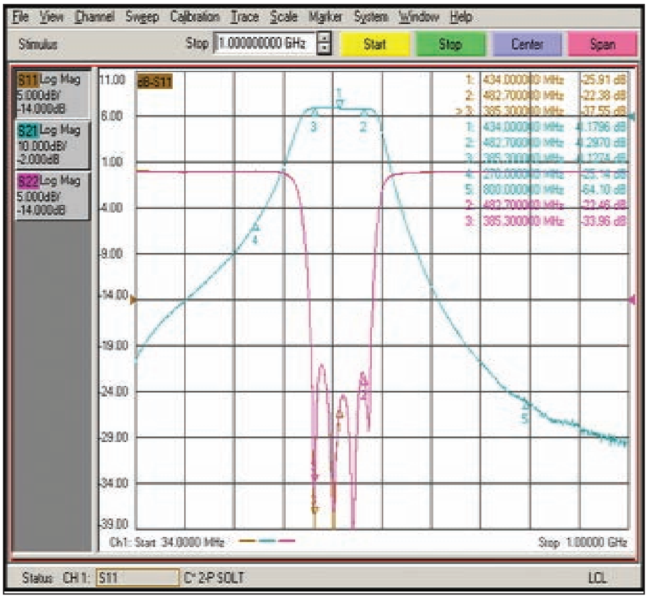

▲ *Fig. 3 90 MHz bandwidth filter data.*

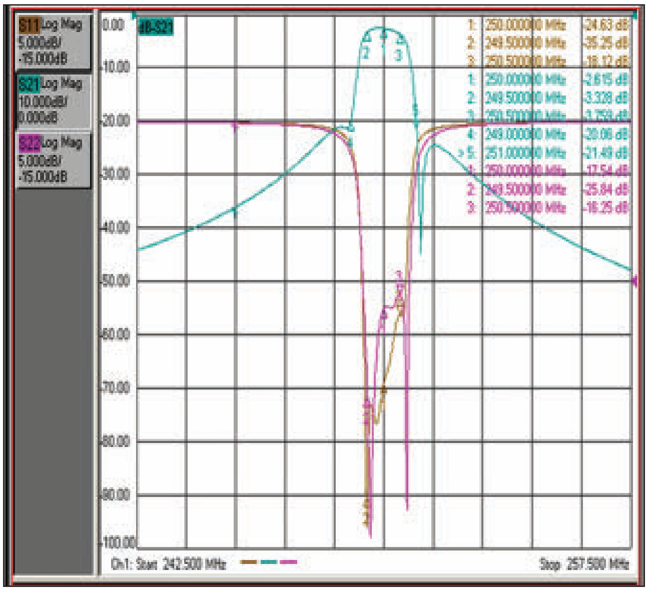

▲ *Fig. 4 1 MHz bandwidth filter data.*

place assembly processes.

Such flexibility and miniaturization allows conventionally large filter-based modules – for example, switched filter banks or pre-selectors, in which filtering accounts for most of the volume and mass – to be drastically reduced in size. The ability to realize filter structures on the same conductor plane as other components in the RF chain obviates the need for discrete filter packaging, connectors or glass-to-metal seals and eliminates associated discontinuities.

Newly developed substrates enabling practical thin film filter implementation are equally suitable for GaAs and GaN bare-die integration, allowing further size reduction in multifunction module construction. Given the advantages, it seems likely that integration of active components and passive filtering will become more commonplace in future module design (see Figure 1).

NEW TEM STRUCTURE FOR SIZE REDUCTION

Transverse Electromagnetic (TEM) mode structures in the form of resonators have been a staple in RF and microwave filter design for decades. Recent innovations represent a significant improvement for certain applications. The primary innovation consists of a revised layout for TEM structure resonators that exploits total cavity volume to lower frequencies with only minimal Q degradation. With this new approach, overall filter volume is significantly decreased. Newly devised coupling methods achieve wider percentage bandwidths, along with elliptical responses in the real and imaginary domains.

Figures 3 and ***4*** show measured results for filters with 90 and 1 MHz bandwidths. The first has nine sections, and the second has four. Corresponding filter dimensions are 5.0" × 5.0" × 2.5" and 3.2" × 3.2" × 2.2", respectively.

Has Amplifier Performance or Delivery Stalled Your Program?

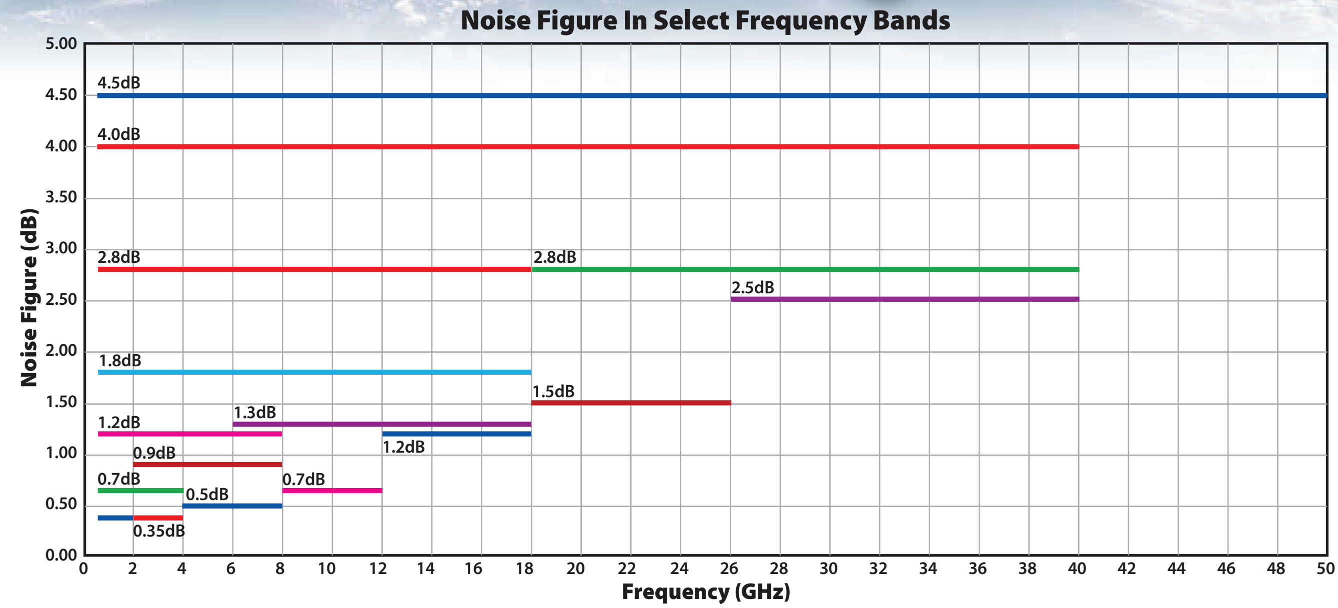

B&Z TECHNOLOGIES
Innovating to Excel

www.bnztech.com

Lowering the frequency of operation without drastic degradation of unloaded Q is particularly advantageous in the VHF to UHF frequency range. With bandwidth limitations almost removed, relative bandwidths ranging from 0.5 to 40 percent have been realized. In addition to smaller bandpass filters, cavity size reduction enables compact band-reject filters with small footprints and high performance. The TEM structure supports high power applications typically associated with the UHF to VHF frequency range. In essence, the classic TEM resonator structure has been rethought by eliminating the portions contributing only weakly to supporting electric or magnetic fields. The new structure is lighter and produces greater electrical length. Using this approach, a full 90 percent of band-reject filter volume arises from the volume of the resonator cavities, compared to a much lower percentage in the classic case.

THIN FILM LUMPED COMPONENT FILTERS

An innovative and versatile thin film lumped element approach supports highpass, lowpass, bandpass and notch designs using the same basic structure, simply by removing or reconfiguring specific components. The resulting filters exhibit broad spurious-free stopbands, small physical size, excellent amplitude and phase match and high reliability due to the thin film construction.

Thin film microstrip filters are important components in modern hybrid integrated subassemblies. For filters in such applications, subsystem designers often use edge-coupled, commensurate line, hairpin and other well-known distributed topologies. Distributed topologies, however, have certain limitations. Constructing broadband distributed filters in conventional microstrip is challenging due to the large impedance ratios required, and realizing elliptic responses exhibiting finite transmission zeros in distributed networks is difficult. At lower microwave frequencies, the physical size of distributed filters is relatively large. Finally, distributed filters by their nature present challenges for realization of broad stopbands free of spurious responses.

Lumped element microwave filters address many of these limitations, but present difficulties of their own when used in thin film assemblies. Lumped component filters are usually constructed using parallel plate chip capacitors and air-wound inductors soldered into a small housing. Skilled manual labor is required to build and tune such filters. While the volume occupied is small compared to distributed counterparts, it is often difficult to integrate lumped component filters into an otherwise all thin film assembly.

At microwave frequencies, a hybrid lumped/distributed structure is an excellent solution enjoying the best of both worlds. Typical construction consists of an alumina carrier, single layer caps and printed inductors. Possible end launches include coplanar with edge wraps, coplanar with filled vias and microstrip.

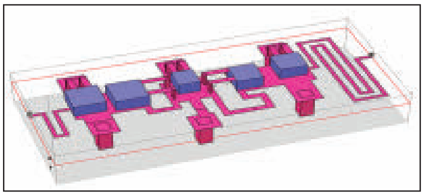

Fig. 5 CAD representation of thin film lumped component filter.

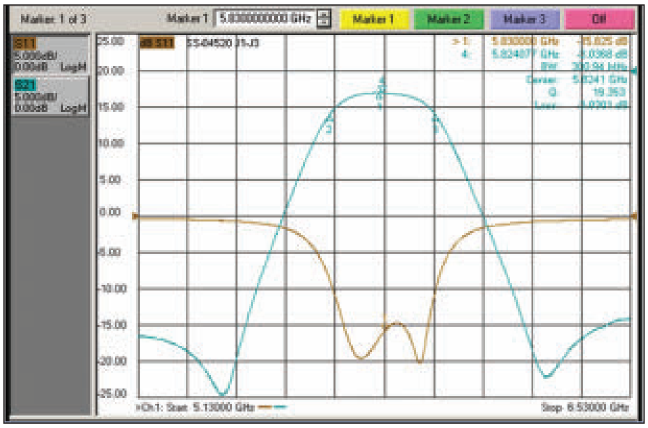

Fig. 6 Measured response of hybrid thin film lumped component filter.

▲ *Fig. 7 Microminiature 5.83 GHz C-Band filter.*

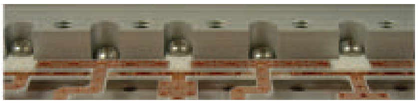

▲ *Fig. 8 K&L's patented low PIM high power series capacitor.*

A hybrid C-Band filter was designed and manufactured to demonstrate the feasibility, size and performance advantages of this approach. ***Figure 5*** shows the CAD representation of the 5.83 GHz filter producing the measured response shown in ***Figure 6***. ***Figure 7*** shows the relative physical size of the 5.83 GHz filter, which is approximately 0.26" × 0.13" × 0.1".

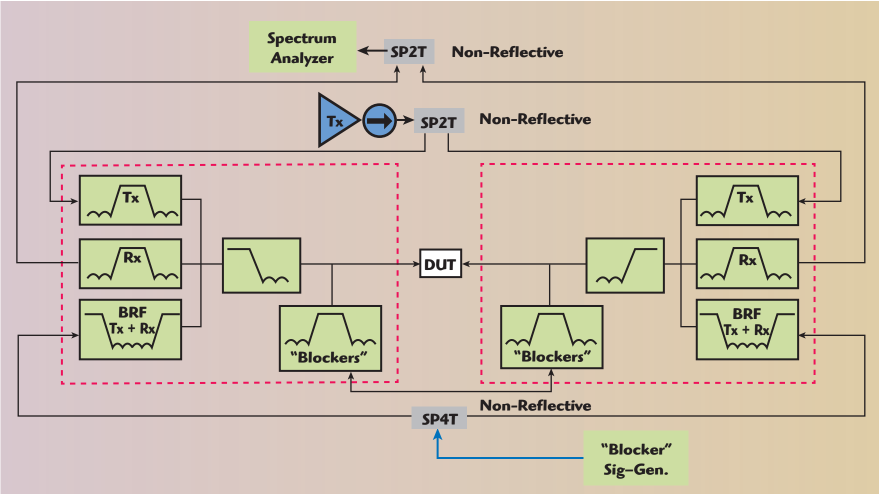

▲ *Fig. 9 4G/LTE test setup.*

EXPANDING 4G/LTE FILTERING SOLUTIONS

The ongoing 4G/LTE rollout's emphasis on increased data transmission and resolution of co-location issues for signal types ranging from earlier generation cellular to GPS have made the testing of supporting components ever more critical and challenging. Commercial telecommunication applications mandate full testing and understanding of the performance of virtually every component in a device or system.

Special filtering solutions simplify testing and can, in some cases, make seemingly impossible tests relatively easy. In response to customer needs, various test scenarios have been developed utilizing custom filters that increase dynamic range. These test setups employ filter building blocks and technologies, such as a patented low PIM capacitor and complex multiplexers and tunable filters with adjustable bandwidths.

Conceivably, individualized "brute force" PIM distortion testing in the LTE frequency bands could require large numbers of individual fixed frequency filters due to the number of LTE frequency and bandwidth combinations. Two recently-developed adjustable bandwidth tunable filters capable of tuning both bandwidth and center frequency could replace as many as 105 fixed frequency filters.

SPECIALIZED FILTERS AND TEST CONFIGURATIONS

The highpass/lowpass duplexer is a basic filtering element in many test setup schemes. While the lowpass filter can be made of one piece for low PIM purposes, the highpass construction poses a great challenge. Multiple solder joints and dissimilar metals can be intermodulation sources, directly impacting the dynamic range of the sys-

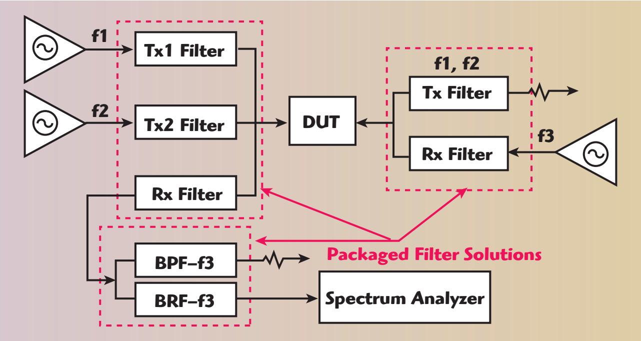

▲ *Fig. 10 Triple beat test configuration.*

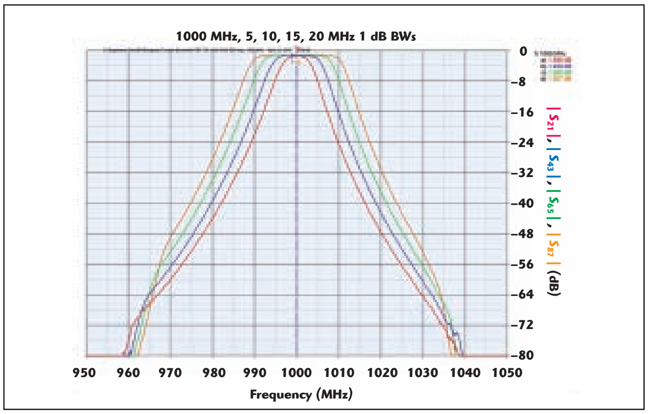

▲ *Fig. 11 Tunable bandwidth capability of adjustable bandwidth filter.*

tem. In June 2014, K&L Microwave was awarded US Patent 8742869 B2 for the low PIM high power series capacitor shown in ***Figure 8***. This paved the way for various broadband low PIM and wideband structures.

Ultimately, testing of components for use in 4G/LTE systems requires input of the planned transmit (Tx) frequency simultaneously with "blocker" signals applied in virtually any input/output combination. ***Figure 9*** shows a test configuration that allows the engineer to input the appropriate Tx signal along with any blockers required. The setup permits Tx and blockers to be swapped from input to output ports of the device under test (DUT), and supports forward and reverse measurement of DUT performance without moving any connections or cable locations.

One of the most difficult tests required in today's environment is the "triple beat" test. Three frequencies are simultaneously injected into the DUT. Two are typical uplink, or Tx, frequencies that could be experienced by the device in normal operation. For this particular test, these two signals are spaced just 1 MHz apart, so that they occur in a single channel. The third signal is a blocker from the receive (Rx) band, simulating interfering signals that may be encountered in actual operation.

Traditionally, this test is set up using isolators to protect the amplifiers, hybrid quadratures to combine the signals, filtering to clean up injected signals and attenuators to protect the spectrum analyzer's input. Isolators potentially create additional spurious frequencies that are not part of the test, while the hybrid quadratures require amplifiers to provide 3.5 dB of additional power. Further, the attenuators directly reduce the dynamic range of the spectrum analyzer. Taken together, these factors significantly reduce the test setup's effectiveness.

Figure 10 shows a test configuration that eliminates most of the issues associated with the typical triple beat test setup. A "standard" Tx/Rx diplexer is used at the output to terminate the injected Tx signals and as an injection port for the blocker in the center of the Rx channel. The Rx channel of the input triplexer then feeds the test signal to a bandpass/bandstop diplexer on the path to the spectrum analyzer. This diplexer has both the bandpass and bandstop filters tuned to the blocker frequency. The bandstop portion of the diplexer passes the test signal to the spectrum analyzer while removing the injected blocker signal. The blocker signal is properly terminated at the output of the bandpass port. This configuration provides clean signal paths with little to no spurious interferers created by the test setup.

In addition to proper termination of injected signals, this configuration offers another advantage related to the return loss of the filters and reduc-

tion of reflected signals. With 20 dB return loss at each of the filter ports, reflections back into the test environment are minimized. In other setups, reflections from test components create uncharacterized spurious signals that introduce uncertainty. Further, proper termination of all injected signals improves the dynamic range of the overall system. Now Tx signals, terminated through diplexers or triplexers, have no opportunity to reflect into the system and mix with others, creating potential problems. Injected blocker signals terminated before the spectrum analyzer minimize any mixing that might take place inside the analyzer. This configuration provides a clean and reliable setup.

TUNABLE DEVICES WITH ADJUSTABLE BANDWIDTHS

While the testing of many components is best accomplished with multiplexers, some device specifications require a single filter to provide a clean signal to the test system. In such cases, vast numbers of individual filters can be required because of the number of LTE frequency and bandwidth combinations. An "adjustable bandwidth tunable filter" can be an effective alternative to minimize the number of fixed frequency filters for reduced space, greater utility and lower cost. ***Figure 11*** shows plots for a filtering solution that tunes both its bandwidth and center frequency. Two of these filters will cover any bandwidth from 5 to 20 MHz and any center frequency from 700 to 2700 MHz. The figure shows the variable bandwidth capability at 1000 MHz. Two digitally-controlled filter assemblies of this kind could replace as many as 105 fixed frequency filters, simplifying testing and reducing cost.

MITIGATING SELF-GENERATED INTERFERENCE

Self-generated communications interference is a problem faced by many RF and microwave communications customers. Recent tunable filter advances are mitigating past problems and enhancing future systems. Examples of recently introduced solutions are:

- Microwave digital high-speed (< 100 ns) voltage-tuned agile filters extending into S-Band (with coverage through X-Band planned) in miniature, reflowable SMT packages.
- Highly integrated filter products with significant SWaP reduction compared to legacy filters that maintain 5 W in-band power over the entire military tactical radio tuning range in single- and dual-channel configurations.
- Mini SMT bandpass filter options from 30 MHz to 3 GHz.
- Narrowband and wideband interference cancellers, some of which do not require an interferer reference, thereby enabling cancellation of off-platform interferers.
- Deep notch filters to create communications channels in wideband, high power signals.
- Miniature, lightweight (0.5 lb) filter and power amplifier cascades for co-site interference issues inherent in UAV retransmission applications.

MILITARY RADIO CO-SITE INTERFERENCE MITIGATION

Military radios often operate in close proximity to additional radios, giving rise to co-site interference. Mili-

tary radios must be able to operate in severe co-site interference environments. ***Figure 12*** shows a typical spectrum of a transmitted signal evaluated at the co-site receiver input location over the receive bandwidth under two conditions of co-site transmit-to-receive antenna isolation, 30 and 40 dB. The receiver sensitivity superimposed on the chart represents the minimum signal required for acceptable demodulation in the receiver. Antenna isolation of 30 dB yields a broadband noise level that exceeds the sensitivity level of the receiver over the entire band. Hence, weak or distant signals within the receiver's inherent capability would be "lost" in the noise created by the co-site transmitter.

Greater isolation can effectively be achieved through the use of selective filtering at the transmitter to minimize broadband noise. Selective filtering is applied following the primary noise sources in the transmit signal chain, having the overall effect of lowering the broadband noise without necessitating an increase in antenna isolation.

As an example, a 2 percent instantaneous 3 dB bandwidth Maxi-Pole® filter with the tuning range of 90 to 200 MHz would have an insertion loss of approximately 5 dB (4.8 dB actual). This selectivity characteristic is shown in ***Figure 13***. For greater selectivity, multiple filters can be placed in cascade with low noise amplifiers (LNA) for inter-filter isolation and filter loss recovery, followed by a power amplifier designed for efficient operation and low noise output. ***Figure 14*** shows three filters in a cascade with LNAs and a power amplifier for enhanced broadband noise performance. The noise performance of this arrangement, referred to as Integrated Cosite Equipment (ICE) at Pole/Zero, is 20 to 40 dB superior to the transmitter for measurements taken more than 4 MHz from the transmit carrier.

Figure 14 shows a technique to mitigate co-site interference, decrease transmitter spurious output and increase output power available from the transmitter. ***Figure 15*** shows the additional selectivity achieved.

Multiple transmitters coupled to antennas in close proximity create a condition called reverse intermodulation, characterized by the coupling of energy from one transmitter into

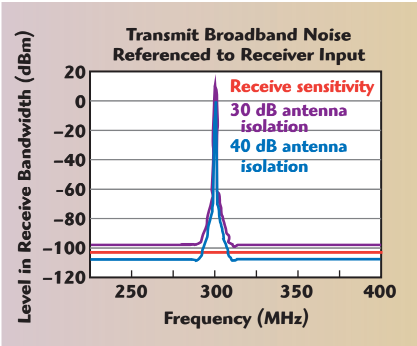

▲ *Fig. 12 Typical spectrum of a transmitted signal.*

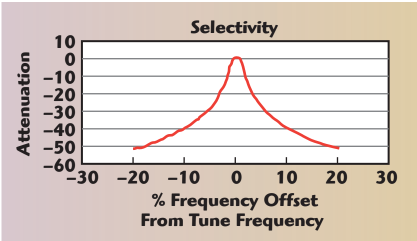

▲ *Fig. 13 Basic Maxi-Pole® filter selectivity.*

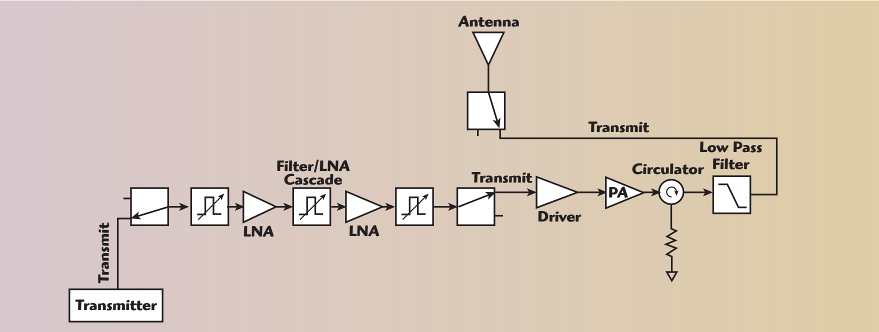

Fig. 14 Transmit filtering block diagram.

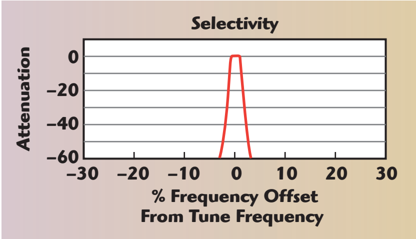

Fig. 15 Selectivity characteristic of a transmit filter/LNA cascade.

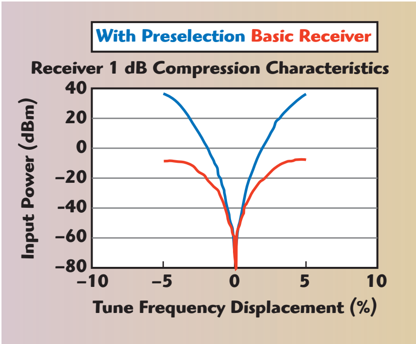

Fig. 16 Receiver 1 dB compression characteristics.

the antenna of another, creating a simultaneous flow of reverse and forward energy. Coupled energy mixes in the nonlinearities in the output network of the transmitter to create an infinite number of intermodulation products. The products are then re-propagated to the collocated receivers, creating products of sufficient level to preclude reception at those frequencies. Thus, a co-site transmitter's output carrier signal can significantly degrade the performance of the receiver.

The 1 dB compression point of an amplifier is the actual output power where the small signal gain extrapolation exceeds the actual gain by 1 dB. For co-site communications analysis, this concept is modified to accommodate the variation in this parameter due to the presence of selectivity in the system and the effect of multiple inputs to the receiver. The compression characteristics of a receiver are evaluated prior to detection with a desired signal 1 dB above sensitivity level. An interfering signal at various displacements from tune frequency is increased in amplitude until the desired signal degrades to the sensitivity level. This level is designated as the 1 dB desensitization point and is representative of the debilitating effect the interferer has on the desired signal. The red curve in ***Figure 16*** represents this characteristic for a typical receiver.

Microwave components from

Your time-trusted source

Mil Spec Compliant RF/Microwave Control Components since 1960

I-Q Vector Modulators

- 500 MHz to 40 GHz
- Broadband 2 to 18 GHz model
- Simultaneous Phase & Amplitude Control
- High Modulation Rate – >50 MHZ
- High Resolution & Accuracy
- Guaranteed Monotonic

Phase Shifters/ Frequency Translators

- 500 MHz to 40 GHz
- Full 360 Degree Phase Control
- Translation Rates – Up to 500 kHz
- Digital & Analog Control
- Guaranteed Monotonic

Attenuators

- 200 MHz to 40 GHz
- Up to 80 dB Attenuation
- Digital and Analog Control
- Guaranteed Monotonic

To learn more or get our new full line catalog please contact us.

Switches

- 200 MHz to 40 GHz
- SPST to SP16T
- Non-Reflective & Reflective
- High Speed – Rise/Fall <10 nanoseconds
- Phase & Amplitude Matched models
- Low Cost Hermetic models

KRATOS | GENERAL MICROWAVE

ELECTRONIC PRODUCTS DIVISION

227A Michael Drive, Syosset New York 11791
Tel: 516 - 802 - 0900, Fax: 516 - 802 - 0897
E-mail: kratosgeneralmicrowave@kratosdefense.com
www.kratosepd.com

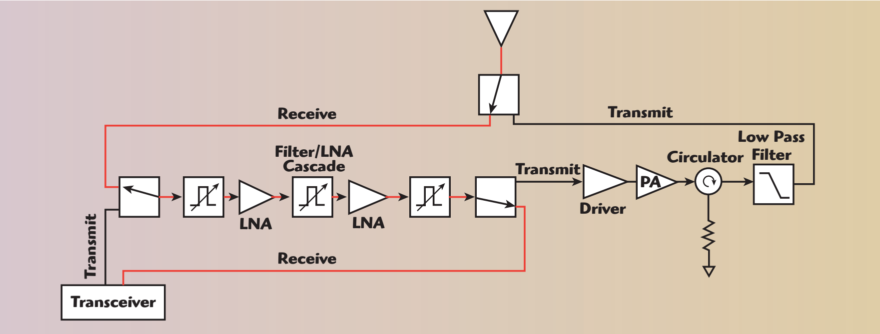

▲ *Fig. 17 Half duplex Tx/Rx integrated co-site equipment.*

While a 1 dB drop in system gain is seemingly subtle, empirical evidence suggests that as the interferer increases above the 1 dB desensitization point, it is not uncommon for the desired signal level to drop as much as 4 dB for every increase of 1 dB in interferer.

The use of a receive filter or filter/LNA cascade similar to that used in the transmit chain can create "preselection" of the energy from the receive antenna and reduce the relative level of the co-site interferer to the desired signal. ***Figure 17*** shows the same filter/LNA cascade from Figure 14 configured for receive operation. The net effect of this level of preselection is shown graphically by the blue curve in Figure 16. Under this condition, the debilitating effect of co-site interference is mitigated by the selectivity of the preselector.

As in the transmit environment, nonlinear effects in the receive chain can be the source of additional co-site interference. The preselection filter serves to minimize the level of the interfering signals prior to the receive nonlinearity, thereby minimizing any resulting products created within the receiver.

CONCLUSION

The Microwave Products Group (MPG) has established an Engineering Innovation Council comprised of senior design professionals from all four business units. Some of the new technologies and inventions in this article are direct results of that collaboration. Anticipating future requirements after an extensive review of the current state of technology in the RF and microwave community, the MPG R&D and engineering teams are actively applying their collective expertise to developing tomorrow's products. MPG welcomes opportunities to leverage an evolving technology roadmap to meet customers' immediate and emerging communication and signal control needs.

Certain aspects of the innovations presented in this article represent the intellectual property of MPG's parent Dover Corp. and are protected by patents, pending patents and information filings on these proprietary rights. ■

ACKNOWLEDGMENT

The authors thank Kevin W. Asplen for his help preparing this article.

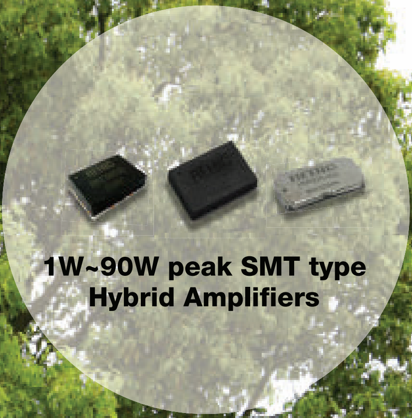
1W~90W peak SMT type
Hybrid Amplifiers


10W~1kW(peak)
GaN Pallet & Module

Most Valuable **Product**

Leading-Edge Signal Analyzer

Keysight Technologies
formerly Agilent Technologies electronic measurement business
Santa Rosa, Calif.

For decades, spectrum analyzers have been used in the development and characterization of radar and electronic-warfare (EW) systems. However, traditional swept measurements are rapidly becoming insufficient for today's agile and adaptive systems. That is driving the need for a solution that delivers significant speed, flexibility and performance, and also has the headroom to handle next-generation needs. That is why Keysight Technologies created the new UXA signal analyzer. As the new flagship of the X-Series signal analyzers, the UXA leverages proprietary technologies to achieve new benchmarks in performance.

ADDRESSING LEADING-EDGE REQUIREMENTS

The UXA enables analysis of today's wideband systems by providing 510 MHz of instantaneous bandwidth and extending up to 900 MHz bandwidth using the IF output. The instrument provides industry-leading performance in three key areas: phase noise, wideband spurious-free dynamic range (SFDR) and wideband flatness.

For those who need even more performance, optional real-time spectrum analysis (RTSA) covers the full analysis bandwidth and provides 100 percent probability of intercept (POI) for signals with durations as short as 3.837 μs (at 510 MHz bandwidth). The optional external atomic frequency reference provides exceptional long-term stability.

To enhance usability, the UXA provides a streamlined, touch-driven interface through a 14.1" display. The multi-touch display simplifies measurement set up through the familiar X-Series menu structure. By providing wider, deeper views of elusive and wideband signals — known and unknown — the UXA enables users to see more and take their designs farther.

ACHIEVING EXCEPTIONAL PURITY AND CLARITY

Progress in RF and microwave technologies is a complementary, back-and-forth process: new technologies lead to better tools, these lead to enhanced technologies, and the cycle continues. This type of interplay has driven the development of the UXA. Several of its exceptional performance figures are the result of a new analog-to-digital converter (ADC) and a new digital-to-analog converter (DAC). Both are proprietary, Keysight-designed devices, op-

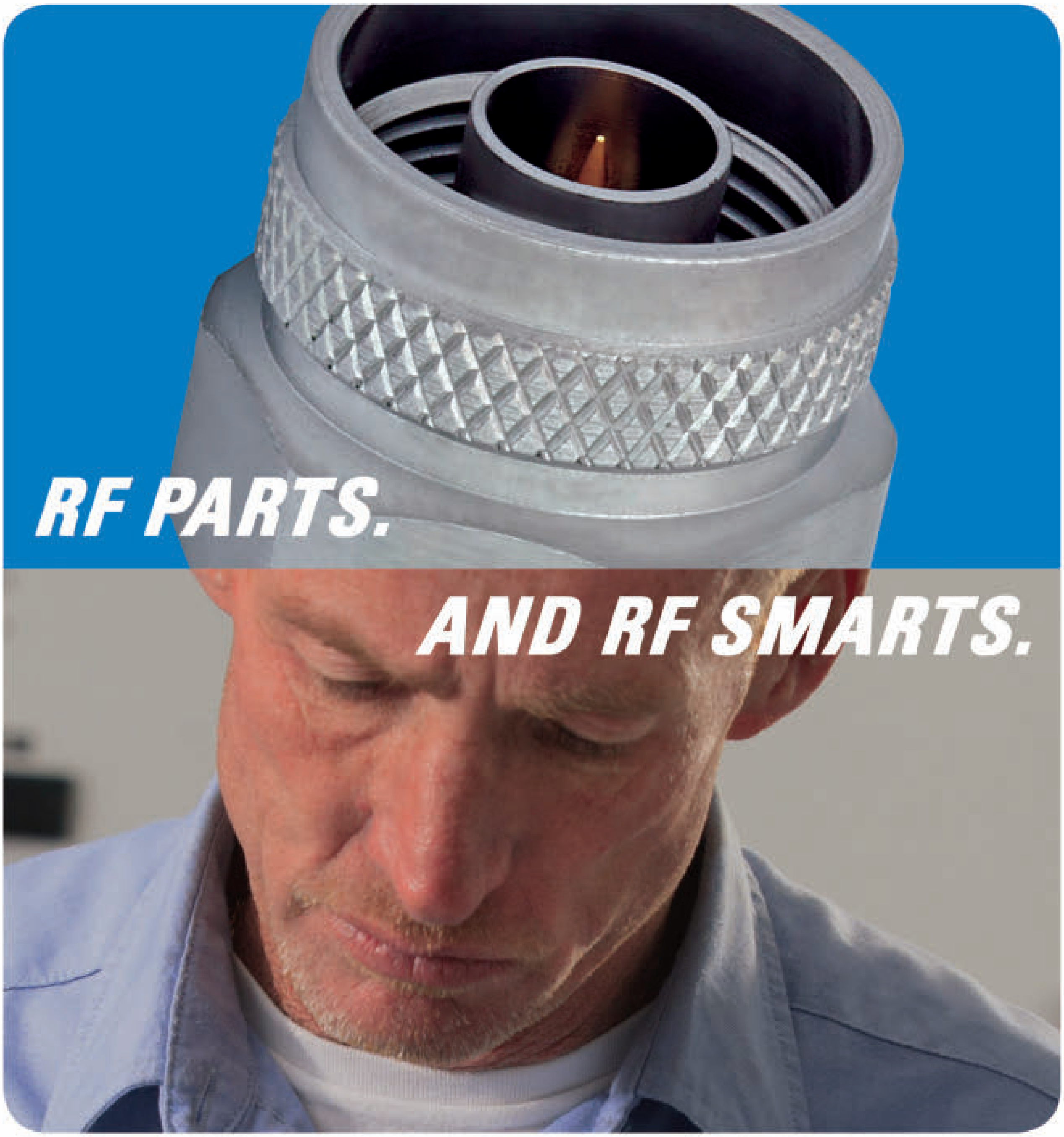
RF PARTS.
AND RF SMARTS.

timized for RF and microwave applications such as radar, EW and wireless communications.

The metrology-grade ADC provides a combination of bandwidth and low distortion that is ideal for optimizing today's ultra-wideband systems. Using this technology, the UXA can maintain very high SFDR over its maximum instantaneous bandwidth, as shown in ***Figure 1***. In this measurement, the largest spurious product is more than 88 dB below the level of the main signal.

This is useful for design tasks such as evaluating the sensitivity of wideband EW equipment and tuning the operation of digital predistortion compensation in the latest multi-band or wideband wireless systems.

The ADC does not operate in isolation. To maximize converter performance, the UXA employs a wideband RF front end assembly with flatness of less than ±0.7 dB over the full IF bandwidth.

While the ADC is clearly important to analyzer performance, the value of a wideband DAC is less obvious. Here, the Keysight-proprietary DAC is essential to fundamental performance improvements, providing an outstanding combination of phase noise and low spurious distortion.

The DAC is the central component of a direct digital synthesizer (DDS), which complements the traditional PLL-based local oscillator (LO) found in spectrum and signal analyzers. Because the LO is used in all frequency-conversion operations, its purity and frequency stability are reflected in the signal analyzer's spurious and phase noise performance figures.

The phase noise benefits of the DDS-based LO are impressive, especially at low and moderate carrier offsets, as shown in ***Figure 2***. One remarkable consequence of the DDS-based architecture is the absence of a pedestal in the analyzer's phase noise curve when the DDS is used by itself, without a PLL. The shape and corner frequency of the pedestal are governed by the PLL's loop-filter characteristics, which are sometimes user-adjustable as a way to optimize phase noise performance in specific offset regions.

In the UXA, the absence of a pedestal means that improved performance is available over a wide range of offsets up to about 1 MHz. For very wide offsets, a PLL is used along with the DDS to get a lower phase noise floor from the YIG-tuned oscillator. When needed, the PLL also provides loop filtering and avoidance of DDS spurs.

As with the ADC, the DAC does not operate in isolation. For example, the close-in phase noise performance of the UXA is the result of a new frequency-reference assembly. The design of the reference was optimized to take advantage of the DDS characteristics and improve phase noise performance, especially for offsets narrower than 100 Hz.

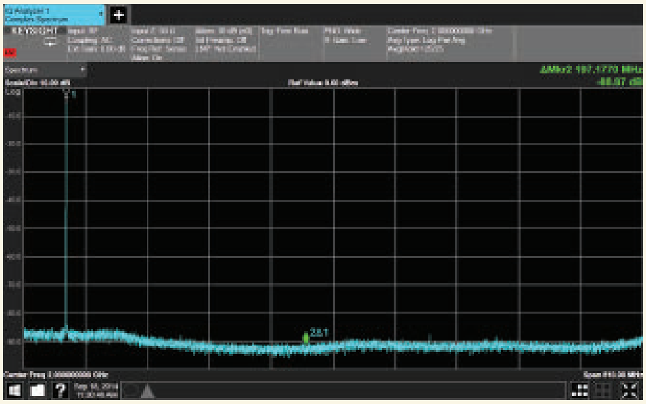

▲ *Fig. 1 The Keysight proprietary ADC maintains high dynamic range over the UXA's full 510 MHz bandwidth.*

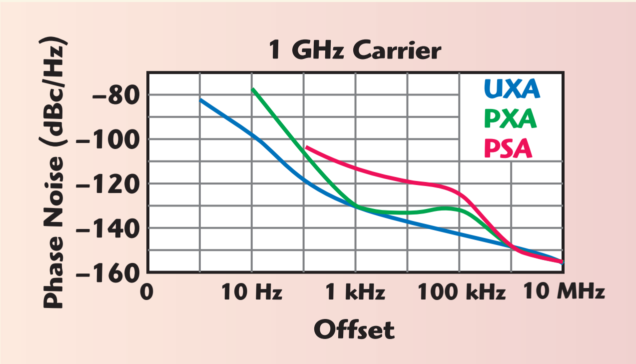

▲ *Fig. 2 Compared with its high-performance predecessors — the Keysight PXA and PSA — the UXA offers improved phase noise, especially at close-in and medium offsets.*

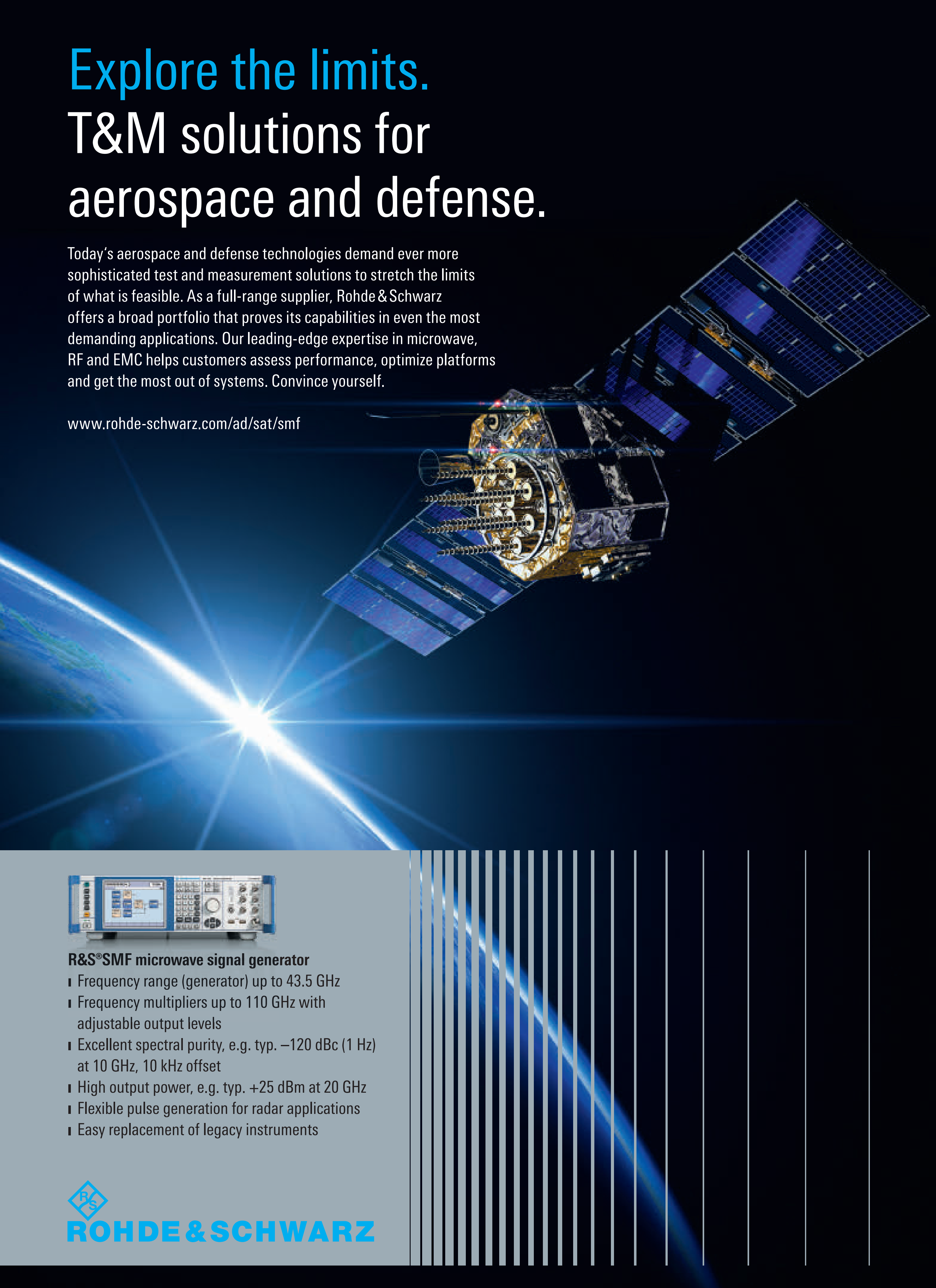
Explore the limits.
T&M solutions for aerospace and defense.
Today's aerospace and defense technologies demand ever more sophisticated test and measurement solutions to stretch the limits of what is feasible. As a full-range supplier, Rohde & Schwarz offers a broad portfolio that proves its capabilities in even the most demanding applications. Our leading-edge expertise in microwave, RF and EMC helps customers assess performance, optimize platforms and get the most out of systems. Convince yourself.
www.rohde-schwarz.com/ad/sat/smf
R&S®SMF microwave signal generator
Frequency range (generator) up to 43.5 GHz
Frequency multipliers up to 110 GHz with adjustable output levels
Excellent spectral purity, e.g. typ. –120 dBc (1 Hz) at 10 GHz, 10 kHz offset
High output power, e.g. typ. +25 dBm at 20 GHz
Flexible pulse generation for radar applications
Easy replacement of legacy instruments
ROHDE & SCHWARZ

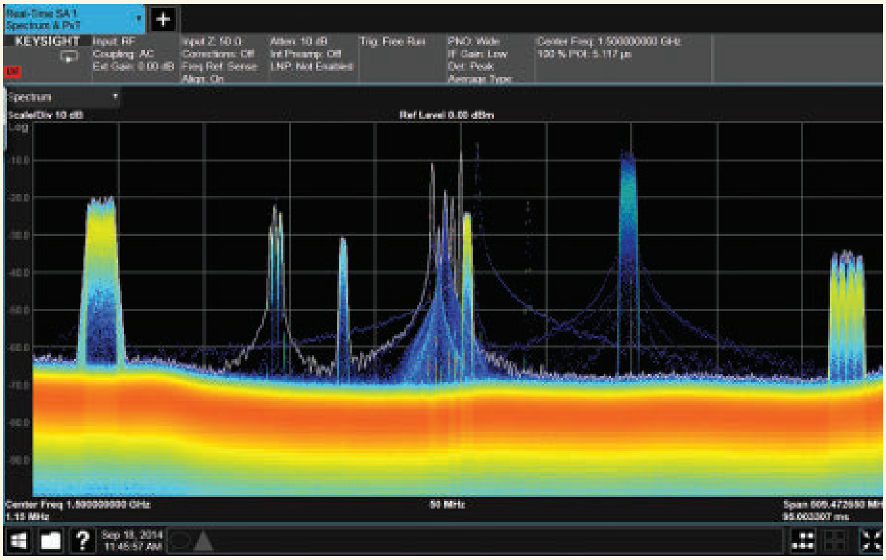

Fig. 3 The UXA sets new benchmarks for real-time bandwidth. The spectral density display is a powerful way to reveal fleeting or otherwise elusive signals and signal behaviors.

EXTENDING REAL-TIME PERFORMANCE

The 510 MHz instantaneous bandwidth is coupled to ultra-fast digital signal processing (DSP) to more than triple the widest real-time bandwidth currently available in a general-purpose signal analyzer. With the RTSA capability, the UXA provides 100 percent POI — with full amplitude accuracy — for signals with durations as short as 3.517 μs and it can detect elusive signals as short as 3.33 ns (see ***Figure 3***).

Real-time analysis is also used to implement frequency-mask and time-qualified triggers. As a result, the UXA can distinguish between spectrally similar signals based on their time characteristics, and it can trigger on pulses shorter or longer than others. As an example, this capability could be used to find transient interferers in the middle of a dense wireless signal environment or to identify specific emitters in spectra from a battlefield.

SEEING THROUGH COMPLEX SIGNALS

The full instantaneous bandwidth of the UXA is also available for use with Keysight's 89600 VSA software, either inside the analyzer or through a networked PC. Frequency-mask, time-qualified and other real-time triggers can be configured to initiate individual measurements and gap-free signal captures for post-processing.

Since signals are captured in complete vector form, post-processing can include changes to center frequency and span with no need to capture new data. This technique can capture several signals at once, potentially including multiple frequency channels or bands. Individual signals can then be extracted from the capture for any type of analysis, including demodulation and time alignment or detection of cause and effect.

The wide acquisition bandwidth of the UXA expands the VSA's multi-measurement capability. For example, simultaneous demodulation measurements can be made from a single acquisition, covering different modulation types and bandwidths. Analysis can include modulated signals, interferers and other signal types, all at the same time.

CONTINUING THE CYCLE

The UXA X-Series signal analyzer is the latest iteration in the complementary, back-and-forth cycle of improvement that encompasses new technologies, new tools and new developments. Built on Keysight-proprietary technologies, the UXA delivers unsurpassed purity and clarity in signal analysis. The excellent IF section enables a deeper understanding of what is happening inside a system and ultimately helps designers determine if a particular project is meeting or exceeding its performance goals.

VENDORVIEW

Keysight Technologies Inc.
Santa Rosa, Calif.
www.keysight.com

RF Amplifiers and Sub-Assemblies for Every Application

Delivery from Stock to 2 Weeks ARO from the catalog or built to your specifications!

- Competitive Pricing & Fast Delivery
- Military Reliability & Qualification
- Various Options: Temperature Compensation, Input Limiter Protection, Detectors/TTL & More
- Unconditionally Stable (100% tested)

ISO 9001:2000 and AS9100B CERTIFIED

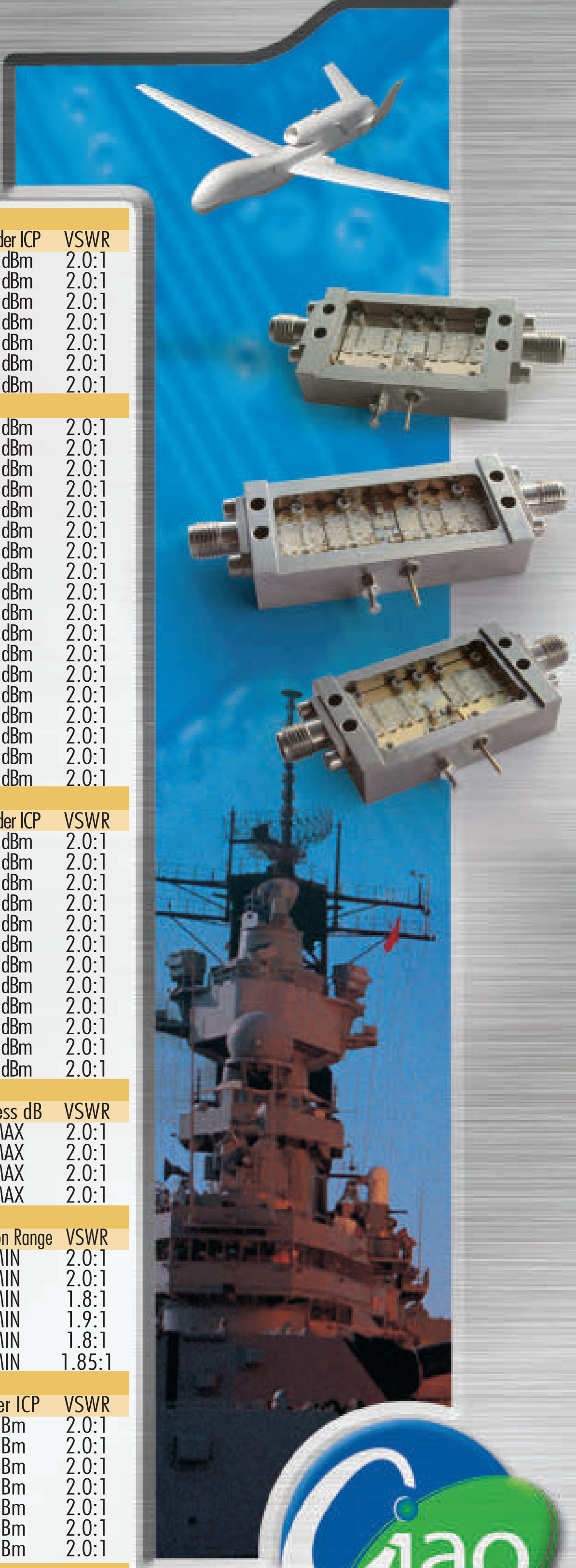

OCTAVE BAND LOW NOISE AMPLIFIERS

Model No.	Freq (GHz)	Gain (dB) MIN	Noise Figure (dB)	Power-out @ P1-dB	3rd Order ICP	VSWR
CA01-2110	0.5-1.0	28	1.0 MAX, 0.7 TYP	+10 MIN	+20 dBm	2.0:1
CA12-2110	1.0-2.0	30	1.0 MAX, 0.7 TYP	+10 MIN	+20 dBm	2.0:1
CA24-2111	2.0-4.0	29	1.1 MAX, 0.95 TYP	+10 MIN	+20 dBm	2.0:1
CA48-2111	4.0-8.0	29	1.3 MAX, 1.0 TYP	+10 MIN	+20 dBm	2.0:1
CA812-3111	8.0-12.0	27	1.6 MAX, 1.4 TYP	+10 MIN	+20 dBm	2.0:1
CA1218-4111	12.0-18.0	25	1.9 MAX, 1.7 TYP	+10 MIN	+20 dBm	2.0:1
CA1826-2110	18.0-26.5	32	3.0 MAX, 2.5 TYP	+10 MIN	+20 dBm	2.0:1

NARROW BAND LOW NOISE AND MEDIUM POWER AMPLIFIERS

Model No.	Freq (GHz)	Gain (dB) MIN	Noise Figure (dB)	Power-out @ P1-dB	3rd Order ICP	VSWR
CA01-2111	0.4 - 0.5	28	0.6 MAX, 0.4 TYP	+10 MIN	+20 dBm	2.0:1
CA01-2113	0.8 - 1.0	28	0.6 MAX, 0.4 TYP	+10 MIN	+20 dBm	2.0:1
CA12-3117	1.2 - 1.6	25	0.6 MAX, 0.4 TYP	+10 MIN	+20 dBm	2.0:1
CA23-3111	2.2 - 2.4	30	0.6 MAX, 0.45 TYP	+10 MIN	+20 dBm	2.0:1
CA23-3116	2.7 - 2.9	29	0.7 MAX, 0.5 TYP	+10 MIN	+20 dBm	2.0:1
CA34-2110	3.7 - 4.2	28	1.0 MAX, 0.5 TYP	+10 MIN	+20 dBm	2.0:1
CA56-3110	5.4 - 5.9	40	1.0 MAX, 0.5 TYP	+10 MIN	+20 dBm	2.0:1
CA78-4110	7.25 - 7.75	32	1.2 MAX, 1.0 TYP	+10 MIN	+20 dBm	2.0:1
CA910-3110	9.0 - 10.6	25	1.4 MAX, 1.2 TYP	+10 MIN	+20 dBm	2.0:1
CA1315-3110	13.75 - 15.4	25	1.6 MAX, 1.4 TYP	+10 MIN	+20 dBm	2.0:1
CA12-3114	1.35 - 1.85	30	4.0 MAX, 3.0 TYP	+33 MIN	+41 dBm	2.0:1
CA34-6116	3.1 - 3.5	40	4.5 MAX, 3.5 TYP	+35 MIN	+43 dBm	2.0:1
CA56-5114	5.9 - 6.4	30	5.0 MAX, 4.0 TYP	+30 MIN	+40 dBm	2.0:1
CA812-6115	8.0 - 12.0	30	4.5 MAX, 3.5 TYP	+30 MIN	+40 dBm	2.0:1
CA812-6116	8.0 - 12.0	30	5.0 MAX, 4.0 TYP	+33 MIN	+41 dBm	2.0:1
CA1213-7110	12.2 - 13.25	28	6.0 MAX, 5.5 TYP	+33 MIN	+42 dBm	2.0:1
CA1415-7110	14.0 - 15.0	30	5.0 MAX, 4.0 TYP	+30 MIN	+40 dBm	2.0:1
CA1722-4110	17.0 - 22.0	25	3.5 MAX, 2.8 TYP	+21 MIN	+31 dBm	2.0:1

ULTRA-BROADBAND & MULTI-OCTAVE BAND AMPLIFIERS

Model No.	Freq (GHz)	Gain (dB) MIN	Noise Figure (dB)	Power-out @ P1-dB	3rd Order ICP	VSWR
CA0102-3111	0.1-2.0	28	1.6 Max, 1.2 TYP	+10 MIN	+20 dBm	2.0:1
CA0106-3111	0.1-6.0	28	1.9 Max, 1.5 TYP	+10 MIN	+20 dBm	2.0:1
CA0108-3110	0.1-8.0	26	2.2 Max, 1.8 TYP	+10 MIN	+20 dBm	2.0:1
CA0108-4112	0.1-8.0	32	3.0 MAX, 1.8 TYP	+22 MIN	+32 dBm	2.0:1
CA02-3112	0.5-2.0	36	4.5 MAX, 2.5 TYP	+30 MIN	+40 dBm	2.0:1
CA26-3110	2.0-6.0	26	2.0 MAX, 1.5 TYP	+10 MIN	+20 dBm	2.0:1
CA26-4114	2.0-6.0	22	5.0 MAX, 3.5 TYP	+30 MIN	+40 dBm	2.0:1
CA618-4112	6.0-18.0	25	5.0 MAX, 3.5 TYP	+23 MIN	+33 dBm	2.0:1
CA618-6114	6.0-18.0	35	5.0 MAX, 3.5 TYP	+30 MIN	+40 dBm	2.0:1
CA218-4116	2.0-18.0	30	3.5 MAX, 2.8 TYP	+10 MIN	+20 dBm	2.0:1
CA218-4110	2.0-18.0	30	5.0 MAX, 3.5 TYP	+20 MIN	+30 dBm	2.0:1
CA218-4112	2.0-18.0	29	5.0 MAX, 3.5 TYP	+24 MIN	+34 dBm	2.0:1

LIMITING AMPLIFIERS

Model No.	Freq (GHz)	Input Dynamic Range	Output Power Range Psat	Power Flatness dB	VSWR
CLA24-4001	2.0 - 4.0	-28 to +10 dBm	+7 to +11 dBm	+/- 1.5 MAX	2.0:1
CLA26-8001	2.0 - 6.0	-50 to +20 dBm	+14 to +18 dBm	+/- 1.5 MAX	2.0:1
CLA712-5001	7.0 - 12.4	-21 to +10 dBm	+14 to +19 dBm	+/- 1.5 MAX	2.0:1
CLA618-1201	6.0 - 18.0	-50 to +20 dBm	+14 to +19 dBm	+/- 1.5 MAX	2.0:1

AMPLIFIERS WITH INTEGRATED GAIN ATTENUATION

Model No.	Freq (GHz)	Gain (dB) MIN	Noise Figure (dB)	Power-out @ P1-dB	Gain Attenuation Range	VSWR
CA001-2511A	0.025-0.150	21	5.0 MAX, 3.5 TYP	+12 MIN	30 dB MIN	2.0:1
CA05-3110A	0.5-5.5	23	2.5 MAX, 1.5 TYP	+18 MIN	20 dB MIN	2.0:1
CA56-3110A	5.85-6.425	28	2.5 MAX, 1.5 TYP	+16 MIN	22 dB MIN	1.8:1
CA612-4110A	6.0-12.0	24	2.5 MAX, 1.5 TYP	+12 MIN	15 dB MIN	1.9:1
CA1315-4110A	13.75-15.4	25	2.2 MAX, 1.6 TYP	+16 MIN	20 dB MIN	1.8:1
CA1518-4110A	15.0-18.0	30	3.0 MAX, 2.0 TYP	+18 MIN	20 dB MIN	1.85:1

LOW FREQUENCY AMPLIFIERS

Model No.	Freq (GHz)	Gain (dB) MIN	Noise Figure dB	Power-out @ P1-dB	3rd Order ICP	VSWR
CA001-2110	0.01-0.10	18	4.0 MAX, 2.2 TYP	+10 MIN	+20 dBm	2.0:1
CA001-2211	0.04-0.15	24	3.5 MAX, 2.2 TYP	+13 MIN	+23 dBm	2.0:1
CA001-2215	0.04-0.15	23	4.0 MAX, 2.2 TYP	+23 MIN	+33 dBm	2.0:1
CA001-3113	0.01-1.0	28	4.0 MAX, 2.8 TYP	+17 MIN	+27 dBm	2.0:1
CA002-3114	0.01-2.0	27	4.0 MAX, 2.8 TYP	+20 MIN	+30 dBm	2.0:1
CA003-3116	0.01-3.0	18	4.0 MAX, 2.8 TYP	+25 MIN	+35 dBm	2.0:1
CA004-3112	0.01-4.0	32	4.0 MAX, 2.8 TYP	+15 MIN	+25 dBm	2.0:1

CIAO Wireless can easily modify any of its standard models to meet your "exact" requirements at the Catalog Pricing.

Visit our web site at **www.ciaowireless.com** for our complete product offering.

Ciao wireless

Ciao Wireless, Inc. 4000 Via Pescador, Camarillo, CA 93012

Tel (805) 389-3224 Fax (805) 389-3629 sales@ciaowireless.com

Electronic Warfare Systems Market $10.2 B in 2014

VIEW VIDEO

The global electronic warfare (EW) systems market is expected to reach $10.2 billion by the end of 2014 and is estimated to increase to $13.2 billion by 2024, representing a CAGR of 2.68 percent. The global market is expected to achieve a cumulative value of $125.7 billion during the forecast period. Demand for EW systems is anticipated to be driven by rapid technological advancements in the domain and the growing need for intelligence, surveillance and reconnaissance (ISR) capabilities globally.

The EW systems market is expected to be dominated by North America, followed by Asia-Pacific and Europe. Modern warfare places a greater emphasis on information superiority and situational awareness, and this is expected to be a major factor driving spending in this sector. This theory is further supported by increasing investments by most major militaries across the world, which focus on acquiring electronic warfare systems for airborne, ground based and naval platforms.

> Demand for EW systems is anticipated to be driven by rapid technological advancements in the domain and the growing need for intelligence, surveillance and reconnaissance (ISR) capabilities globally.

The U.S. is the highest spender in the global EW systems market, with a large number of programs being pursued in all three segments. The Asia-Pacific region is the second largest spender, with most major militaries in the region formulating large scale procurement programs for the purchase of airborne, naval, and ground based platforms, which widely incorporate the use of EW systems. The next major market is Europe, with a major portion of the spending attributable to Russia, the UK and France. In the Middle East, all major defense spending nations have increased focus on protecting their oil and gas infrastructure, as they are involved in territorial disputes.

Raytheon Awarded Contract to Build New USAF Radar

The U.S. Air Force awarded Raytheon Co. a $19.5 million contract for engineering and manufacturing development of a new expeditionary radar that will detect, identify and track drones, missiles and aircraft. The total contract, including all options, is estimated at $71.8 million and includes the procurement of an additional three radar systems, for a total of six radar systems and product support. The radar, called the Three Dimensional Expeditionary Long Range Radar, or 3DELRR, is one of the first programs under the DoD's Better Buying Power initiative to be designed for exportability, enabling U.S. forces, allies and security partners to benefit from the system.

"By choosing Raytheon's 3DELRR solution, the Air Force is purchasing an affordable, exportable radar," said David Gulla, vice president, Global Integrated Sensors at Raytheon Integrated Defense Systems. "Raytheon's 3DELRR design is interoperable with coalition systems and capable of meeting the requirements of many international customers."

Raytheon's 3DELRR system is a gallium nitride (GaN)-based radar that operates in C-Band. By using GaN, Raytheon was able to affordably increase the radar's range, sensitivity and search capabilities. C-Band also offers the military increased flexibility because that portion of the spectrum is relatively uncongested.

> "Raytheon's 3DELRR design is interoperable with coalition systems and capable of meeting the requirements of many international customers."

"As the U.S. and other countries look to replace aging battlefield radars with low-cost yet cutting edge and highly capable systems, Raytheon's 3DELRR can meet that growing demand," said Andrew Hajek, Raytheon's 3DELRR program director.

3DELRR will replace radars, such as the Vietnam-era AN/TPS-75, which are no longer able to keep pace with current and emerging threats.

Harris Receives $88 M from a Nation in the Middle East for a Wideband Tactical Communications System

Harris Corp. has received an $88 million order to provide a country in the Middle East with Falcon III ® wideband tactical radios and accessories as part of an overall modernization effort.

The system leverages the latest software-defined radios from the Harris Falcon III ® RF-7800 family. This includes the RF-7800H, the first wideband HF tactical radio, delivering expanded data capabilities for long range, beyond-line-of-sight environments; the RF-7850M, for wideband mobile ad-hoc networking; and the RF-7800S, a lightweight soldier personal radio for full-duplex voice and data communications over two kilometers. The order also includes vehicular and base station systems, accessories, spares and training services.

"Harris' strong presence in the region, combined with our continued investment in a leading-edge Falcon portfolio of tactical communications products and systems, enables us to transition our customers from legacy,

For More Information
Visit mwjournal.com for more defense news

voice-dominated communications to modern networked wideband system solutions," said Brendan O'Connell, president, international business, Harris RF Communications. "These advanced communications systems will support the customer's current and future operational requirements for simultaneous secure voice and high-bandwidth data across a wide range of missions."

Elbit Begins Testing the WideBridge Solution for Mission Critical Secure Broadband Services with the DHS

The U.S. Department of Homeland Security (DHS) Science & Technology Directorate awarded Elbit Systems of America LLC, a contract to deliver a technology demonstration of mission critical secure broadband services for first responders and public safety users.

This demonstration will include the WideBridge™, an innovative solution that integrates mission critical capabilities with FIPS certified BlackBerry® BES10 secure workspace and Etherstack's P.25 networks interoperability proven capabilities. The solution was developed at Elbit Systems Land and C4I division with the objective of delivering the most advanced interoperable broadband communication services using FirstNet and commercial LTE networks suitable for federal, state and local public safety agencies nationwide.

WideBridge enables any-to-any secure, interoperable, multimedia services with seamless connectivity between various commercial broadband cellular networks, FirstNet LTE Band 14 and the existing P.25 Land Mobile Radio (LMR) infrastructure.

Mission critical services supported by WideBridge include Push-to-Talk (PTT), Push-to-View (PTV), voice and video conferencing, video streaming from agents and video sensors in the network, map activated multimedia services, situational awareness information dissemination (command and control), P.25 interoperability and a revolutionary off-network "Direct Mode" broadband connectivity using self-forming ad-hoc mesh networks for local mission teams.

DHS intends to use this solution for testing the new concept of accessing secure multimedia services for public safety users through LTE broadband networks. As of September 2014, WideBridge system tests have begun at the Public Safety Communications Research Lab in Boulder, Colo. After successful demonstration, these tests will be followed by field testing of the system in early 2015.


Scan page
using layar app
Reactel, Incorporated
Reacting First to All Your Filter Needs.
When Being the First to React
Makes all the Difference in the World
• RF & Microwave Filters
• Diplexers & Multiplexers
• Multifunction Assemblies
• Ceramic Filters
REACTEL, INC.
Reactel, Incorporated is your source for RF & Microwave Filters, Multiplexers
and Multifunction Assemblies covering DC - 50 GHz.
Trust in Reactel's highly skilled engineers and technicians to quickly
develop and produce the most reliable products for your filter requirements.
- Submitting a request for immediate attention will never be easier.
- Full featured App contains expanded RFQ capability,
catalog, data sheets and more.
- Available for iPad, iPod and Android devices via the
App Store and Google Play.
Available on the App Store
Google play
8031 Cessna Avenue • Gaithersburg, Maryland 20879 • Phone: (301) 519-3660
For general inquiries, please email reactel@reactel.com • http://twitter.com/reacteljim
Go online to www.reactel.com to download your Reactel catalog today.
RoHS Compliant
@reacteljim

GSA Report Confirms Smartphones Driving LTE Growth

The latest update to the "Status of the LTE Ecosystem" report published by the Global mobile Suppliers Association (GSA) confirms that 183 manufacturers have announced 2,218 LTE-enabled user devices, including operator and frequency variants. 978 new products were announced during the past year, representing 79 percent annual growth. The number of manufacturers increased by 52.5 percent in the same period.

Smartphones are the main user device category and the main growth driver. 1,045 smartphone products have been launched, translating to an improved share of 47 percent of all LTE device types. This compares with 455 smartphones and 36 percent share a year ago. 98 percent of LTE smartphones are multimode, capable of operating on at least one 3G technology in addition to LTE.

1800 MHz (3GPP Band 3) continues to be the most prominent band for LTE network deployments globally and also has the largest device ecosystem with 944 user devices. Over 42 percent of all LTE devices can operate in this spectrum.

This report covers LTE Frequency Division Duplexing (FDD) and Time Division Duplexing (TDD) devices. The majority of terminals operate in the FDD mode. The TDD mode also has a fast maturing ecosystem with 644 devices announced. The ecosystems for TDD Bands 38 (2.6 GHz) and 40 (2.3 GHz) dominate and are virtually identical, each supported by more than 420 user terminals. Band 41 (2.6 GHz) is well represented with 261 products, followed by Band 39 (250 products). Another rise in the number of devices supporting Bands 42 and 43 (3.5 GHz) is noted.

Alan Hadden, president of GSA, said, "Operators worldwide are investing strongly in improving the customer experience, efficiencies and growth. 25 percent of LTE devices support Category 4 (150 Mbps peak downlink speed). 16 devices support Category 6 (300 Mbps)."

APT700 FDD spectrum (Band 28) is highly attractive for operators in most regions for LTE deployments. Recent service launches in the Asia-Pacific region are driving the growing choice of compatible user terminals. There are now 55 Band 28 user devices, with over 80 percent being smartphones.

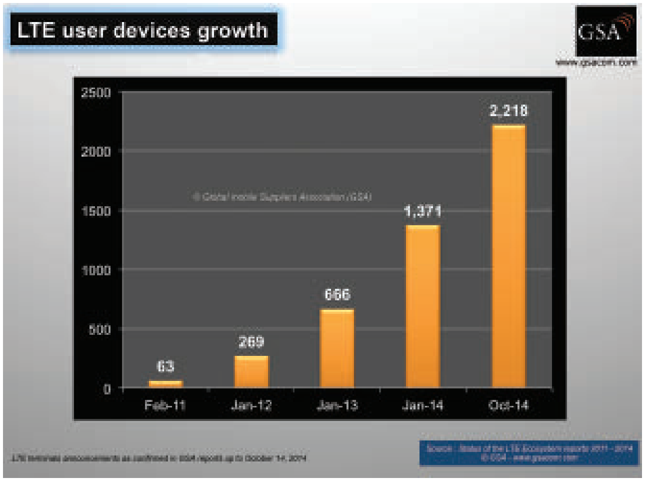

Thales & Bharat Electronics Form Joint Venture in India

Navratna Defence Public Sector Undertaking Bharat Electronics Ltd. (BEL) and Thales announced that the Ministry of Corporate Affairs, Government of India, has approved the incorporation of their joint venture company, BEL-THALES Systems Ltd. This joint venture company will primarily focus on the design, development, marketing, supply and support of civilian and select defense radars for India and the global markets.

BEL holds a 74 percent stake while Thales holds 26 percent of the equity in the joint venture company. The initial product portfolio of BEL-THALES Systems Ltd. will be comprised of innovative solutions for air surveillance, including air traffic management and select ground-based military radars. The ultimate objective of the joint venture is to expand its scope in fields other than radars within the defense electronics domain.

> "...meeting the needs of both Indian and export customers ..."

BEL-THALES Systems will seek to work closely with Government laboratories and the Indian industry and will consequently become a decisive contributor for innovation in various fields of defense electronics.

Expressing his confidence in this joint venture, S. K. Sharma, chairman and managing director of BEL, said, "We have always valued our partnership with Thales. We are confident that our joint venture company will benefit from the significant technology transfers and support from Thales, and from the extensive industrial and design skills of BEL."

Eric Lenseigne, managing director of Thales in India, said, "The incorporation of this joint venture company marks an important milestone in our 60-year-old association with BEL, and takes it to the next level. We will constantly support BEL-Thales Systems to become a centre of excellence, offering solutions specifically aimed at meeting the needs of both Indian and export customers – in line with the government's 'Make in India' approach."

DOCOMO Trials NFV Using Multi-Vendors' Virtualization Systems

NTT DOCOMO, INC. has completed proof-of-concept (PoC) trials that have verified the feasibility of network functions virtualization (NFV) using the software and equipment of six world-leading information and communication technology (ICT) vendors – Alcatel-Lucent, Cisco,

For More Information — **Visit mwjournal.com for more international news**

Ericsson, Huawei, NEC and Nokia Networks.

The PoC trials will help leverage technologies for next-generation virtualized mobile networks. Using the virtualized Evolved Packet Core (EPC), the core network of LTE systems, the trials successfully verified the interoperability of each vendor's EPC software with a different vendor's equipment, such as scalable data processing capability for congested data traffic and immediate network recovery in the event of hardware failure.

The verified technologies will enable communication software designed originally for dedicated hardware to run on multipurpose hardware. In the future, such technologies will allow mobile operators to combine network hardware and software components of any vendor for deployment of network systems.

"Thanks to collaborative efforts in the mobile network industry, NFV is soundly moving toward practical realization, rather than just ending up as a pie-in-the-sky dream," said Seizo Onoe, executive vice president and chief technology officer at NTT DOCOMO. "I am delighted that we have confirmed the feasibility of NFV through multi-vendor initiatives with many of the top ICT players."

Network virtualization is expected to offer key advantages, such as operational sustainability with improved connectivity for dense data traffic and during natural disasters, as well as in the event of hardware failure. It will also accelerate delivery of new services and drive more efficient infrastructure investment.

Europe and Canada Collaborate on ICT and Telecom R&D Projects

The EUREKA ICT cluster Celtic-Plus and the Quebec-based, industry-university consortium Prompt have agreed to sign a memorandum of understanding to strengthen their collaboration in ICT and telecommunication-related R&D projects. Celtic-Plus is an industry-driven European research initiative to define, perform and finance through public and private funding, common research projects in the area of telecommunications, new media, future Internet, and applications and services focusing on a new Smart Connected World paradigm.

Both organizations are key players in stimulating collaborative privately-publicly funded ICT projects in Europe and Canada. Celtic-Plus and Prompt are already performing thematically connected work in similar domains; closer collaboration will be beneficial for the global ICT research communities and for ICT and telecommunication markets.

Jacques Magen, Celtic-Plus group chairman said, "I am very much looking forward to collaborating with Prompt. This will provide both the Celtic-Plus and Prompt research and innovation communities the opportunity to perform additional collaborative research in new common projects." Charles Despins, Prompt president and CEO concurred, "Prompt's community, members and staff are highly pleased to see the emergence of this collaboration with Celtic-Plus and the compelling opportunities it will provide."

Global Driverless Vehicle Shipments to Reach 14 Million by 2030

VIEW VIDEO

Global driverless vehicle shipments will increase from 1.1 million in 2024 to more than 42 million in 2035, with an installed driverless vehicle base reaching 176 million according to ABI Research.

"While autonomous driving under the control of a human standby driver is quickly gaining acceptance, robotic vehicles mostly remain out of bounds, especially for car manufacturers, despite Google's recent announcement to start prototype testing. However, only driverless vehicles will bring the full range of automation benefits including car sharing; driverless taxis and delivery vans; social mobility for kids, elderly and impaired; and overall economic growth through cheaper and smoother transportation critical in an increasing number of smart mega cities. Many barriers remain but the path towards robotic vehicles is now firmly established with high rewards for those first-to-market," says VP and practice director Dominique Bonte.

Though there is progress on the technological side — both on sensor hardware and Artificial Intelligence — user acceptance, security, liability issues and regulation remain huge bottlenecks. Single-mode driverless vehicles face the biggest hurdles towards adoption as Google has already experienced, forced by the California Department of Motor Vehicles to test its prototypes with a steering wheel and brake and acceleration pedals firmly in place.

> "...Many barriers remain but the path towards robotic vehicles is now firmly established with high rewards for those first-to-market."

While the evolutionary character of autonomous driving, gradually appearing in small incremental steps is often highlighted, removing the driver out of the equation represents a disruptive transition. However, this paradigm shift offers the opportunity to address mounting safety concerns about manual-autonomous handover management in co-pilot vehicles, rendering sophisticated HMI and driver monitoring systems superfluous. Removing the ambiguity about who is in charge — the vehicle or the driver — is acknowledged by Google as a critical step forward.

LTE Reinvigorates the Broadband Wireless Access Marketplace

LTE has turbocharged the mobile Internet experience for users, which is reflected in rapid adoption of LTE-capable smartphones along with other mobile devices. It has also reinvigorated the broadband wireless marketplace. According to ABI Research, 1.26 billion households do not have DSL, cable or fiber-optic broadband. Fixed and mobile telcos are looking to LTE to make the connection. "By the end of 2014, ABI Research anticipates there will be 14.5 million residential and commercial premises with fixed LTE broadband access. By 2019, that figure should grow to 123 million," commented Jake Saunders, VP and 4G practice director at ABI Research.

Chipset and CPE vendors are stepping up efforts to prime the market by manufacturing lower cost devices for both the consumer and enterprise segments. Chinese vendors like Huawei and ZTE along with American brands such as NETGEAR and Novatel Wireless have partnerships with North American carriers like Verizon Wireless, Sprint and AT&T to provide exclusive LTE routers that utilize the carrier's individual 4G networks.

4G Fixed Wireless Modems
World Market Forecast: 2014 to 2019

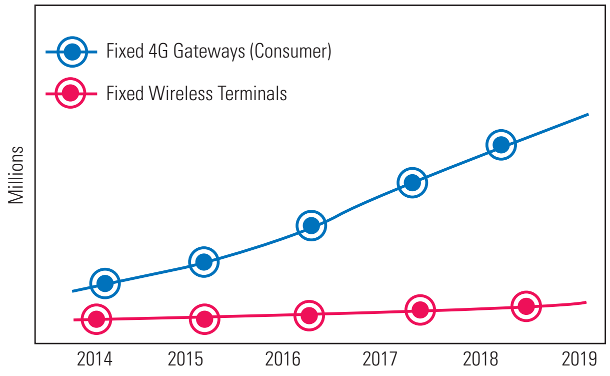

Source: ABI Research

Proliferation of Wireless Technologies Stokes Demand for RF Test Equipment

Telecom operators' increased adoption of wireless technology for mission-critical applications has revved up the global market for general purpose (GP) test equipment. As the link between cloud networks and devices (mobile phones, tablets, notebooks) results in more complex devices under test (DUT), the need for radio frequency test equipment will only intensify.

New analysis from Frost & Sullivan, Global Outlook for Electronic Test Equipment, finds that the market earned revenues of $3.45 billion in 2013 and estimates this to reach $4.64 billion in 2018. The study covers the product segments of oscilloscopes, signal generators, spectrum/signal analyzers, network analyzers, power meters, logic analyzers, electronic counters and multimeters.

"Faster connectivity through the deployment of 5G will also escalate the demand for higher frequency bands," said Frost & Sullivan measurement & instrumentation analyst, Prathima Bommakanti. "This, in turn, will drive the demand for GP test equipment in the microwave range."

For More Information Visit mwjournal.com for more commercial market news

In product categories such as multimeters, which have demonstrated minimal technological progress, purchases are based upon price and availability rather than functions/features. This affects the overall growth of the market.

The best way forward in a competitive market is to offer a balance between price and performance. Modular GP test equipment will be particularly effective in this scenario as it reduces the cost of test by increasing throughput and scalability, while simultaneously lowering power consumption and space requirements.

Pulsed RF Power Semiconductor Device Markets to Exceed $300M by 2019

Markets for pulsed RF power devices up to 18 GHz are expected to show continued growth over the next five years despite the current economic turmoil and cuts in defense spending. While association with consumer spending fuels the volatility of many global electronics markets, pulsed RF power devices are supported by quite different priorities.

"Many RF power semiconductor manufacturers are on a quest to find markets unrelated to mobile wireless infrastructure," notes ABI Research director Lance Wilson. "Device prices in wireless infrastructure are falling, and the total available market is flattening out."

Some markets that use pulsed RF power devices, such as transportation safety and military, are experiencing solid growth even in the midst of today's economic downturn. These devices are used in radars for military, weather and marine applications, and in the current worldwide upgrade of the air traffic control system. There is also a market segment devoted to the avionics transponder and air navigation market, which is also lifted by the overall air traffic control upgrade.

Intrinsically less "optional" than many consumer markets, these segments are therefore less sensitive to economic upheavals than consumer-driven markets, although they are not totally immune to the macro economy.

Understanding this, many semiconductor manufacturers are attempting to enter this space; however, some factors may complicate their efforts. Pulsed RF power device markets are becoming very competitive technologically: gallium nitride and silicon carbide devices are vying for market share along with the more established silicon and gallium arsenide based technologies. The market may not be able to support all the new entrants.

Among the leaders for high-power RF pulsed semiconductor devices are: MACOM, TriQuint, Microsemi, NXP Semiconductors, Cree, Sumitomo Electric Device Innovations and Integra Technologies.

Around the **Circuit**

Barbara Walsh, Multimedia Staff Editor

MERGERS & ACQUISITIONS

Cobham plc announced that its acquisition of **Aeroflex Holding Corp.**, previously announced on May 20, 2014, has been successfully completed following the receipt of regulatory and shareholder approvals. The transaction has an enterprise value of approximately $1.46B. Approximately 70 percent of Aeroflex's revenue is focused on commercial markets with exposure to wireless, space, microelectronics, industrial, energy and other sectors. This will increase the proportion of Cobham's commercial revenue from 35 to nearly 42 percent of the total, on a pro forma basis, and build upon Cobham's focus on connectivity capabilities, customers and characteristics.

RF Micro Devices Inc. and **TriQuint Semiconductor Inc.** revealed that the holding company under which the companies will combine in a merger of equals will be named **Qorvo™ Inc.** The companies also unveiled the new Qorvo logo and stock trading symbol, which they will begin using immediately upon closing of the merger. The name Qorvo (pronounced kor-vo) conveys the combined company's ability to deliver the core technologies and innovation that will enable customers to launch their next-generation designs even faster.

Microsemi Corp., a provider of semiconductor solutions differentiated by power, security, reliability and performance, announced CNT Acquisition Corp., a wholly-owned subsidiary of Microsemi, successfully completed the acquisition of **Centellax**. The terms of the transaction were not disclosed. Centellax makes high-speed analog and wireless semiconductor products for optical networking and ethernet devices. The acquisition will expand Microsemi's line of products and provide access to technology that will benefit customers.

Averna, a developer of test solutions and services for communications and electronics device-makers worldwide, announced that it has acquired U.S.-based **Cal-Bay Systems**, a privately owned provider of test systems, test and measurement solutions, automated testing and vibration monitoring tools. This move strengthens Averna's presence in the medical-device, vibration monitoring and consumer electronics markets, as well as provides the company with strategic positioning on the West Coast. Averna has acquired 100 percent of shares of Cal-Bay Systems for an undisclosed amount and will take on management of its U.S. and European offices.

Anite announced the acquisition of **Xceed Technologies Inc.**, to meet the growing market requirements for data analysis and post-processing, and to further expand its network testing product portfolio. Xceed Technologies Inc. will be integrated into Anite's Network Testing business unit. The acquisition of Xceed is in line with Anite's strategy to reinforce its position as a global leader in wireless test solutions. Anite's established global market and technology leadership in network testing, combined with Xceed's recognized expertise in data analytics, post-processing and reporting solutions, will enable Anite's Network Testing business to transform its position in the data mining and post-analysis market.

COLLABORATIONS

Rohde & Schwarz announced it has entered into a Manufacturing Test License (MTL) agreement with **Broadcom Corp**. Through the MTL agreement, Rohde & Schwarz can provide certified verification test solutions to Broadcom WLAN and Bluetooth® customers. The Broadcom Manufacturing Test License agreement is a license and validation program that gives test equipment vendors access to Broadcom WLAN and Bluetooth® software tools and Broadcom technical support resources. The program is designed to provide Broadcom OEM customers with validated test systems that reduce time-to-market and improve manufacturing efficiency and product quality.

AVX Corp., a manufacturer of passive components and interconnect solutions, has expanded its partnership with **Modelithics**, an RF/microwave simulation model provider, with the addition of 45 new Modelithics® substrate scalable equivalent circuit models. Designed to speed up design decisions and circuit level optimizations when used in combination with the industry's leading electronic design automation tools, including Keysight Advanced Design System (ADS), Keysight Genesys and NI AWR Microwave Office, highly accurate, substrate scalable models are now available for AVX thin film couplers, multilayer organic (MLO™) diplexers and a variety of RF/microwave capacitors and inductors.

Mouser Electronics Inc., announced that it has signed a global distribution agreement with **Broadcom Corp**. As Broadcom's first eCommerce distributor, Mouser Electronics will offer same-day shipping on a variety of Broadcom mass market products, including the industry-leading Wireless Internet Connectivity for Embedded Devices (WICED™) platform. Broadcom's WICED Wi-Fi and WICED Smart development platforms provide original equipment manufacturers (OEM) with a complete, simplified implementation of wireless connectivity, resulting in faster time-to-market for a broad range of Internet of Things (IoT) innovations.

Isola Group S.a.r.l., announced a major qualification win in partnership with **KSG Leiterplatten GmbH** and **InnoSenT GmbH**. The joint conversion project among the three companies successfully tailored the dielectric properties of Isola's high-performance I-Tera® MT laminate material to match the properties of an incumbent product. Isola's dielectric substrates will now be used on existing volume products produced by InnoSenT, and the printed circuit boards will be manufactured by KSG. The conversion to Isola's materials provides InnoSenT with higher performance material without modifying the metallization of the PCB.

For More Information For up-to-date news briefs, visit mwjournal.com

Around the **Circuit**

Tazca Connects partners with **Haleakala R&D** to test plasma smart antennas on commercial 4G LTE. Next generation antenna extends 4G LTE ranges for wireless internet service providers, providing cost-effective, higher speed broadband for underserved communities in rural areas. Tazca Connects high speed Internet service is powered by an innovative LTE software platform from Lemko Corp., bringing cost-effective 4G LTE connectivity to residents and businesses in rural areas.

Lockheed Martin Aeronautics, **Aarhus University** faculty of science and technology and **Terma** have partnered on an F-35 master internships program taking place at Lockheed Martin Aeronautics' facility in Fort Worth. The F-35 Master Internships give students from Aarhus University the opportunity to learn, explore and acquire valuable and different skills than those taught at the university during five months of full work in the aerospace industry. The idea comes from The Netherlands, where Delft University of Technology, Fokker Technologies and Lockheed Martin Aeronautics have been successfully running the F-35 internships since 2004.

NEW STARTS

Presto Engineering Inc. announced that is has tripled the capacity of its San Jose, Calif.-based engineering hub, and has added new RF device testing equipment to its Caen, France-based hub. Presto's Caen hub will support all aspects of RF as well as analog and mixed signal devices. The Caen hub is the only back-end service house in Europe with 12-inch wafer probe capabilities coupled with the most advanced RF automated test equipment (ATE). Presto's San Jose hub will focus on high-frequency RF testing at millimeter wavelengths.

Navratna Defence Public Sector Undertaking Bharat Electronics Ltd. (BEL) and **Thales** announced that the Ministry of Corporate Affairs, Government of India, has approved the incorporation of their joint venture company, **BEL-THALES Systems Ltd.** This joint venture company will primarily focus on the design, development, marketing, supply and support of civilian and select defense radars for India and the global markets.

Murata announced the launch of their new global website, at www.murata.com. Using the recently released new corporate visual identity, the site has a fresh, modern and tablet-friendly design. Aimed to increase customer satisfaction, ease navigation and access to relevant technical application content, the site now incorporates the complete line-up of Murata products and more application related content.

ACHIEVEMENTS

The **Rockwell Collins** ARC-210 radio recently became the first airborne radio to operate over the U.S. government's newest satellite constellation – the Mobile User Objective System (MUOS). The MUOS system is based on cellular phone technology and represents a paradigm shift for Department of Defense communications. The U.S. Air Force Research Laboratory (AFRL) conducted two weeks of MUOS ground and airborne testing. During the first week of testing, the ARC-210 was deployed in a ground environment for system operational tests that included conducting Over the Air Provisioning of the radios and passing IP data.

API Technologies Corp., a provider of high performance RF/microwave, power and security solutions for high-reliability applications, announced that it has been awarded a new patent for antenna technology for GPS and asset tracking applications. U.S. Patent Number 8810474, titled "Antenna with High K Backing Material," features an API-designed topology to boost antenna performance. API's unique design reduces weight and delivers consistent performance even when surrounded by a metallic structure, such as the body of a UAV/UAS or missile casing. Given its low-profile, surface mount design, the antenna is easily disguisable and well-suited for covert applications.

Pasternack Enterprises Inc. has been awarded the 4-Star Supplier Excellence Award by Raytheon's Integrated Defense Systems (IDS) business. This is the second consecutive year that Pasternack has been honored with a Supplier Excellence Award from Raytheon IDS. Pasternack was one of 87 companies recognized by Raytheon's Integrated Defense Systems business for 4-Star honors.

Cree Inc., a leader in GaN RF devices, has earned the U.S. Department of Defense (DoD) manufacturing readiness level eight (MRL 8) designation. Awarded for its production of GaN MMICs, this designation verifies Cree's ability to provide assured, affordable and commercially viable production capabilities and capacities for items essential to national defense. The designation was granted upon Cree's successful completion of the DoD's Defense Production Act (DPA) Title III Gallium Nitride on Silicon Carbide Production Capacity Program.

Frost & Sullivan recognized **RADX Technologies** with the 2014 Global Frost & Sullivan Award for New Product Innovation. RADX entered the test and measurement market with the introduction of the LibertyGT commercial off-the-shelf (COTS) Software Defined Synthetic Instrument (SDSI) product line that synthesizes a wide range of instruments while enabling concurrent operation for high throughput to address key end-user demands. This product features an innovative touchscreen design that has been optimized for reconfigurability, technology insertion and user programmability.

CONTRACTS

Harris Corp. has received an $88 million order to provide a country in the Middle East with Falcon III ® wideband tactical radios and accessories as part of an overall modernization effort. The system leverages the latest software-defined radios from the Harris Falcon III ® RF-7800 family. This includes the RF-7800H, the first wideband HF tactical radio, delivering expanded data capabilities for long-range, beyond-line-of-sight environments; the RF-7850M, for wideband mobile ad-hoc networking; and the RF-7800S, a lightweight soldier personal radio for full-duplex voice and data communications over two kilometers.

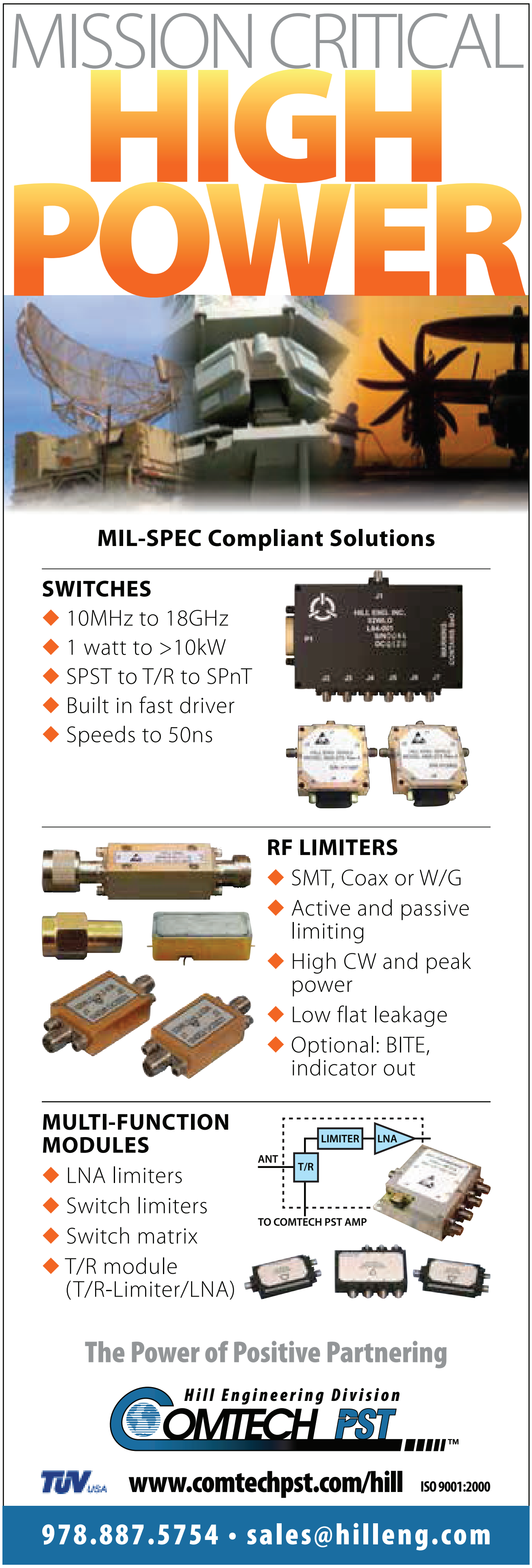

Around the **Circuit**

ViaSat Inc. has been awarded $54 million from the **Space and Naval Warfare Systems Command (SPAWAR)** for co-development and qualification of Tactical Targeting Network Technology (TTNT) capabilities for the Multifunctional Information Distribution System Joint Tactical Radio System (MIDS JTRS). The MIDS JTRS joint development by ViaSat and Data Link Solutions is part of the U.S. government program to provide a migration path from the MIDS-LVT terminal to a certified, reprogrammable, software-defined radio architecture for tactical data links.

Mercury Systems announced it received a $27 million purchase order relating to a sensor processing application. The order was booked in the company's first fiscal quarter 2015 and is expected to be shipped by its first fiscal quarter 2016. The order follows a $39 million order received in the company's fourth fiscal quarter 2014, also from a leading defense prime contractor, for radar subsystems for a missile defense application. That order is expected to be shipped over the next several quarters.

Exelis has been awarded a follow-on contract from **Lockheed Martin** to manufacture composite missile bodies and structures for Lots 11 and 12 of the Joint Air-to-Surface Standoff Missile (JASSM®). The value of the award is approximately $20 million. Exelis will manufacture complex composite structures for more than 400 baseline and extended-range versions of the JASSM. Exelis will fabricate the high-quality, affordable structures using automated composite braiding and resin-transfer mold technologies.

Teledyne Technologies Inc. announced that its **Teledyne Webb Research** business unit has been awarded a five year Indefinite Delivery Indefinite Quantity (IDIQ) contract for the procurement of Autonomous Profiling Explorer (APEX) profiling floats by the **U.S. Naval Oceanographic Office (NAVOCEANO)** with a contract value of $9.9 million, including options. The APEX is a marine system used for persistent measurements of water column properties. Commonly measured parameters include temperature and salinity at different depths in the ocean, feed numerical climate and weather prediction models

PEOPLE

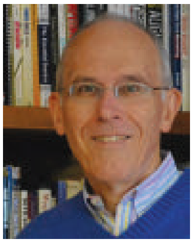

▲ *Gary Lerude*

Gary Lerude joined *Microwave Journal*'s staff, serving as technical editor. He was previously at TriQuint Semiconductor, where he held business development, strategic marketing, and product marketing management roles for TriQuint's GaAs and GaN infrastructure products. Lerude had similar responsibilities at MACOM, where he covered both commercial and defense markets. Prior to MACOM, he was with Texas Instruments, where he describes his role as "midwife" to the birth of TI's GaAs MMIC technology and merchant business. He holds a BSEE, MS in Systems Engineering and Engineers Degree in EE.

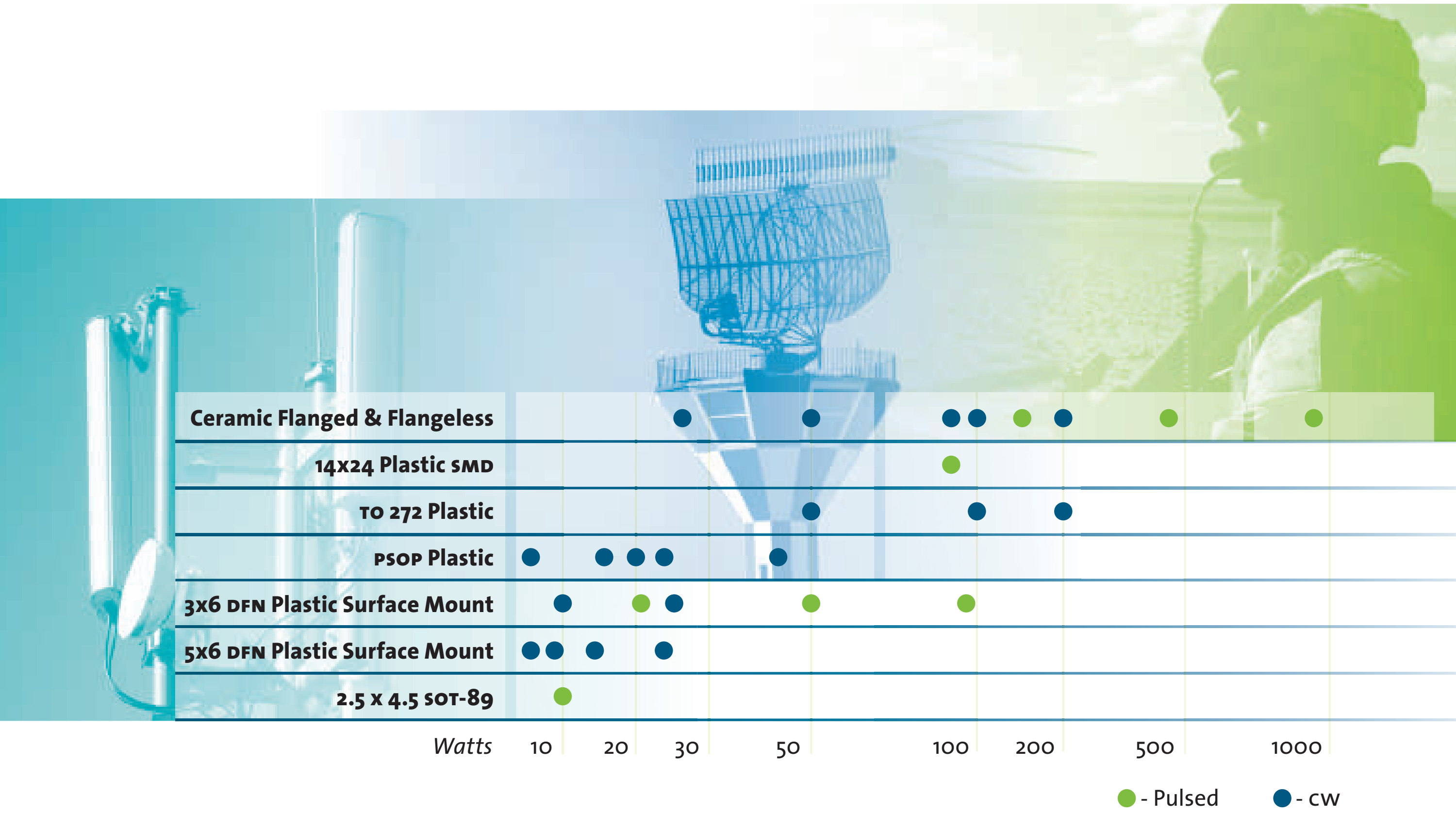

Shattering the Barriers to Mainstream GaN Adoption

MACOM revolutionizes RF applications by securing the supply of the industry's only proven, performance-driven GaN portfolio

MACOM GaN transistors improve upon the high-power handling and voltage operation of LDMOS with the high-frequency performance of GaAs. Improved bandwidth, efficiency and power density give your applications greater power in a variety of packages.

Leveraging deep experience in RF, MACOM engineers are expanding our power transistor family to fuel the future of military and commercial radar as well as other commercial applications. These rugged devices deliver greater flexibility and multi-function capability in your radar communications.

Our growing pulsed power GaN portfolio includes 5W-90W Pk transistors in DFN and SOT-89 plastic packaging, up to 1000W ceramic packages and L-, S-band fully matched modules. Our new CW GaN portfolio includes ceramic package transistors up to 200W, DFN packages from 5W to 25W and TO-272 plastic packages from 50W to 200W.

Only MACOM shatters the final barriers to mainstream GaN adoption by offering dual sourcing for surety of supply.

MACOM™
Partners from RF to Light

Get Samples & Learn How MACOM is Shattering the Barriers to Mainstream GaN Adoption at www.macom.com/gan

Around the **Circuit**

▲ *Mike Clark*

Crane Aerospace & Electronics, a segment of Crane Co., has announced the appointment of **Mike Clark** to senior director of Microwave Solutions of the Electronics Group. In this role, Clark will report directly to Bob Tavares, president of Crane Electronics Group. Clark will be responsible for operations of all Electronics Group Microwave Solutions locations, including Beverly, Mass., Chandler, Ariz., and West Caldwell, N.J. He will be located in Chandler, Ariz.

▲ *Alexander Chenakin*

Anritsu Co. announced the appointment of **Dr. Alexander Chenakin** as a director of R&D for the Anritsu Microwave Measurement Division (MMD). A renowned expert in the test and measurement industry who holds multiple patents and has earned numerous awards, Chenakin will oversee the Anritsu R&D team responsible for developing the company's next-generation synthesized source product line. Dr. Chenakin is well recognized in the field of frequency synthesis and is referred to as the inventor of QuickSyn® technology. In 2009, he received the ARMMS RF & Microwave Society's best contribution award for his work on fast-switching frequency synthesizers.

▲ *Martin Spooner*

Intelliconnect (Europe) Ltd. has appointed **Martin Spooner** to the new position of engineering director. His responsibilities will include development of new connector products, cable assembly capabilities and the development of Intelliconnect's manufacturing capabilities in the UK and Europe. In addition, Spooner will be taking the lead in the company's mission to achieve SC21, a change program designed to accelerate the competitiveness of the aerospace and defense industry.

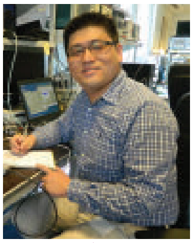

▲ *William Tse*

Nujira Ltd. has appointed **William Tse** as field application engineer manager (FAE) in China. He will focus on supporting customers in China and Taiwan, an increasingly important market for envelope tracking driven by the growth of LTE networks, including FDD and TDD variants in the region. Tse will also be helping to build upon Nujira's existing relationships with chipset, PA and test equipment partners across the region and participate in industry events and seminars.

REP APPOINTMENTS

Copper Mountain Technologies announced the appointment of several new Tier 1 Manufacturers Representatives. **Testech Inc.** is headquartered in Richardson, Texas, with

NARDA

Celebrating **60 Years!**

60TH ANNIVERSARY narda an L3 company

SERVICE • SUPPORT • SELECTION

Narda started in 1954 as a small group of engineers on Long Island offering new and innovative technology to a growing RF and microwave industry. Sixty years later, Narda has become the global standard for quality and durability by continually producing the industry's most reliable RF and microwave components. ***We thank you for sixty years of loyalty to Narda Microwave, and look forward to serving you in the years to come.***

narda

an L3 company

www.nardamicrowave.com • 631.231.1700

Six decades of technological innovation

Around the **Circuit**

offices in Fort Worth, Austin, Houston and Edmund, Okla. **ProTEQ Solutions** is headquartered in Nashua, N.H., with multiple offices supporting the entire New England territory. **Aztec Enterprises** is headquartered in Denver, Colo., with offices in Phoenix, Ariz. and Salt Lake City, Utah. Testech, ProTEQ and Aztec all have considerable experience in the RF/microwave and test and measurement industries.

DITF (Diablo Industries Thin Film), an ISO9001:2008 certified, ITAR registered premier manufacturer of thin film interconnects and related solutions, welcomed **APC-Novacom** as their new representative to the UK and Ireland. APC-Novacom was established in 1991 serving the defense, communication, medical and instrumentation companies of the UK and Ireland.

Intercept Technology Inc. announced expanded representation in Canada with a new reseller, **Kaltron Associates Ltd.** With offices in Toronto, Ottawa, Montreal and Vancouver, Kaltron has been providing software and hardware solutions to companies across Canada since 1996. Kaltron's expansion into selling Intercept's EDA software solutions presents a natural progression for the Kaltron sales team, complemented by a robust customer following.

MtronPTI, a leader in precision frequency control and custom RF solutions for defense, aerospace, telecommunications and industrial markets announced frequency expansion to 80 GHz, millimeter waves for filters and diplexers. The additional products are the result of a business partnership with **Microwavefilters & TVC S.r.l.** (MW&TVC) in Milan who will now represent MtronPTI exclusively in the Italian market.

IN MEMORIAM

Robert T. Fallon passed away on October 14, 2014 at the age of 77. Fallon attended Northeastern University, graduating in 1960 with a degree in chemical engineering. He worked as an RF/microwave semiconductor engineer throughout his career at Raytheon, Sylvania, Microwave Associates (now MACOM) and Massachusetts Bay Technologies (MBT). In 1963, he co-founded and was president of Parametric Industries (PI), Winchester, Mass. and in 1986 co-founded Micrometrics, Londonderry, N.H. Fallon received recognition of achievement from NASA in 1969 for his contributions to the Apollo 11 space program. His passion was in semiconductors and he was often referred to as Dr. Diode in the industry because of his wealth of knowledge in the field, whether it a design, manufacturing or application inquiry. Fallon is survived by his former wife Maryanne, four children and eight grandchildren.

CUSTOM RACK MOUNT TEST SOLUTIONS

Built Your Way and Delivered within 2 Weeks!

Signal Routing & Attenuation Control for Production Test, R&D and More!

Mini-Circuits' new ZTM-Series RF test matrices dramatically accelerate custom solutions for a wide range of applications in test environments. Choose from our lineup of extra-long-life SP4T, SPDT and transfer switches, and programmable attenuators with attenuation ranges of 0 to 30, 60, or 90 dB. We'll build and ship a solution tailored to your exact requirements *within just 2 weeks!*

It's that simple! Give us a call and talk to our engineers about how Mini-Circuits' ZTM-Series custom rack mount test solutions can improve efficiency, increase throughput, and save cost in your business!

Features

- *Rugged 19" Rack Mountable Chassis*
- *Customizable Front Panel Layout*
- *Light Weight*
- *USB and Ethernet Control*
- *User-friendly GUI and DLLs Included*
- *Qualified to 100 Million Switch Cycles*
- *Affordable Cost*
- *Delivery within 2 Weeks!*

Choose from hundreds of possible configurations!

SPDT Switches
DC – 18 GHz

SP4T Switches
DC – 18 GHz

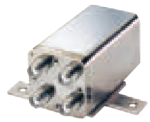

Transfer Switches
DC – 18 GHz

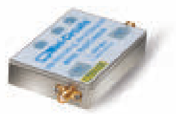

0 – 30, 60, or 90 dB
Programmable Attenuators
1 MHz – 6 GHz

Mini-Circuits®

www.minicircuits.com P.O. Box 350166, Brooklyn, NY 11235-0003 (718) 934-4500 sales@minicircuits.com

Editor's Note: One of our most popular articles last year was our November cover story "Printed Resonators: Möbius Strip Theory and Applications." Therefore the authors decided to present a new three part series covering the theory, applications and future possibilities of Möbius metamaterials and Möbius strip resonators. This is part one of the series that will run in consecutive months starting in November.

Möbius Strips and Metamaterial Symmetry: Theory and Applications

Ulrich L. Rohde
Brandenburgische Technische Universitat, Cottbus, Germany
Ajay K. Poddar
Synergy Microwave, Paterson, N.J.

The inherent disposition of scientists and philosophers is to envision, to explore and to speculate about new things in this vast cosmos. The vastness of cosmos makes us believe that we live in higher dimensions, or Möbius-shaped universes, where one can traverse the entire path without crossing the boundary or edge, if any, with no ending.

For scientists, the Möbius surface is a topological exploration that exhibits unusual mechanical, acoustic and electronic properties to the limit that it violates the Hückel rules.[1] ***Figure 1*** shows the typical Möbius structure and defines the spatial relationships of shape that span dimensions in such a way that its metrical properties are barely changed (i.e., the properties of an object are unchanged when stretched or distorted). Some nanostructures have identical elastic properties.

A necessary and sufficient condition for a Möbius surface to develop is that its Gaussian curvature must vanish everywhere. In a curve with non-vanishing curvature, there exists a unique flat ruled surface (rectifying developable) on which this curve is a geodesic (see ***Figure 1a***) described by Starostin and Heijden[2],

$$\vec{x}(s,t)=\vec{r}(s)+t\left[\vec{b}(s)+\eta(s)\vec{t}(s)\right] \quad (1)$$

$$\tau(s)=\eta(s)k(s),$$
$$s=[0,L],\ t=[-w,w] \quad (2)$$

where $\vec{r}$ is a parameterization of a strip with center line r, length L and width 2w; and where $\vec{t}$ is the unit tangent vector, $\vec{b}$ the unit binormal, k the curvature and τ the torsion of the centerline. The parameterized lines s = const. are the generators, which make an angle β = arc [Tan(1/η)] with the positive tangent direction.

As illustrated in ***Figure 1a***, one can move along the length of a Möbius strip and return to its starting point having traversed the entire length of the strip without ever crossing an edge. In ***Figure 1b***, find the path that the four flies take if they all travel the same route without meeting, and without retracing their path until they reach their original position. Keep track of which side of the path you are on.[3] Knots using a miniature Möbius strip made from silica (see ***Figure 1c***) are used for next generation liquid crystal (liquid crystal used in the flat panel displays on computers, TVs and smartphones all make use of its light-modulating properties).[4]

The unique properties of a Möbius strip results from the fact that its shape minimizes the deformation energy, which is entirely due to

Master Your Power
Source Module with
Electronic Attenuation
90.000 000 000 000 GHz
10.00 dBm
S12MS-AG-EA2
60 to 90 GHz
Millimeter Wave Source Module
THROUGH ELECTRONIC CONTROL:
POWER FLATNESS AND POWER LEVELING ARE ONLY A CLICK AWAY
Innovation in Millimeter Wave Solutions
www.omlinc.com
(408) 779-2698
OML

bending, described by

$$V = \frac{1}{2} D \int_0^L \int_{-w}^{w} k_1^2(s,t)\,dt\,ds \qquad (3)$$

where $D = 2h^3E/[3(1-\nu^2)]$, where 2h is the thickness of the strip, and E and ν are the Young's modulus and Poisson's ratio of the material.

A Möbius transformation f(z) is a fractional linear transformation to complex numbers:

$$f(z) = \frac{az+b}{cz+d}; \quad (a,b,c,d, \in \mathbb{C} \text{ and } ad - bc \neq 0) \qquad (4)$$

$$\text{where } z \in \mathbb{C} \rightarrow z = r[\cos(\theta) + i\sin(\theta)]$$

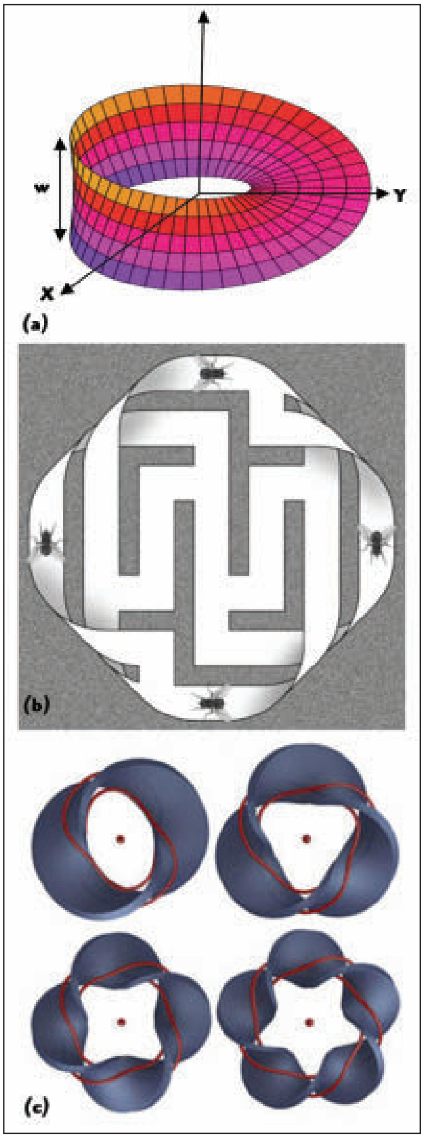

Fig. 1 *Möbius strip (a) Möbius fly maze (courtesy of David Phillips)*[3] *(b) Möbius strip made from silica (c).*[4]

From equation 4, the basic properties of Möbius transformations f(z) are described below: f(z) can be expressed as a composition of affine transformations (scaling: $z \rightarrow tz$, translation: $z \rightarrow z + p$, rotation: $z \rightarrow e^{i\theta}z$, complex conjugation: $z \rightarrow \bar{z}$, inversion: $z \rightarrow \frac{1}{z}$), where $t, p \in \mathbb{C}i$, f(z) maps $\mathbb{C}$ one-to-one onto itself, and is continuous; f(z) maps circles and lines to circles and lines; f(z) is conformal.

Equation 4, a powerful transformation, develops the Möbius surface as a topological structure that thus far has been limited to mathematical imagination. It can now be realized using metamolecules of different designs, enabling linear time algorithms for selecting optimal transformation, mapping, mesh generation, image processing, cryptography and other branches of engineering useful in the physical world and day to day life.

THEORY & APPLICATIONS

Möbius Strips - Building

Figure 2 depicts an award winning building based on principles of the Möbius strip.[5] The wall becomes the roof, the roof becomes the floor, and seamlessly, the floor becomes the roof again. The outer envelope of the structure surpasses architectural design principles in its relationship between wall and ceiling. This structure can offer stability against earthquakes and other seismic and acoustic vibrations as well as provide uniform heating and cooling inside the building.

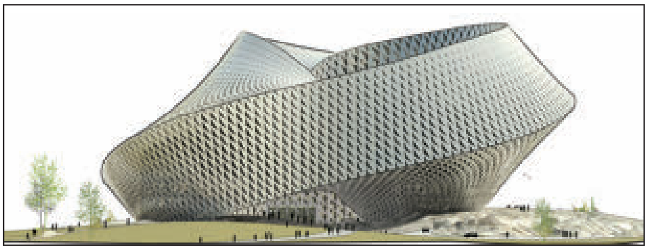

Fig. 2 *Proposed Möbius style National Library building in Kazakhstan.*[5]

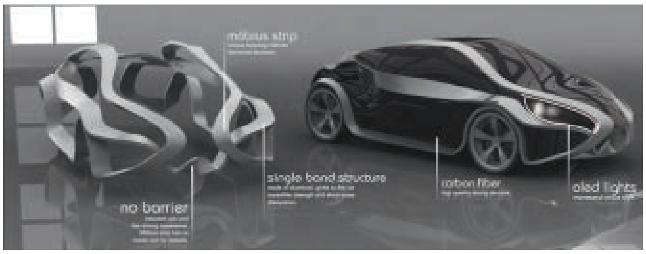

Fig. 3 *Proposed Möbius car.*[6]

Möbius Strips - Automobile

Figure 3 depicts a Möbius car designed by Tommaso Gecchelin.[6] The continuously bent symmetry translates into a superb aerodynamic automotive design. This features a body that uses the concept of the Möbius strip to unify the interior and exterior in a unique and uncanny way, proving outstanding stability against collision as well as high fuel efficiency.

Möbius Strips - Belts, Recording Tape

If conveyor belts were made in the shape of Möbius strips they would wear evenly because they are flipped during each rotation, while ordinary belts wear on only one side. Similarly, recording tapes in the shape of Möbius strips may be used in devices for uninterrupted recording, potentially doubling recording and playing times.

Möbius Strips - Black Holes

A black hole is a region with a massive gravitational field that absorbs everything within its vicinity. This is due to its massive gravitational potential, influencing motion of matter propagating in a curved space-time to form a circle.[7] This is similar to electromagnetic-wave propagation in a curved space or in an inhomogeneous Möbius metamaterial medium. Hence, one could use electromagnetic waves and Möbius metamaterial to mimic celestial mechanics by comparing the refractive index to the metric of gravity.[8] A recently published result demonstrates the electromagnetic black hole by using metamaterials at microwave frequencies. It shows the phenomena of an electromagnetic wave bending and trapping spirally into the artificially created electromagnetic black hole.[9] Cheng et al., reported a model of black hole (see ***Figure 4***) composed of a gradient-index metamaterial shell and a lossy dielectric core that can absorb electromagnetic waves coming from all directions

efficiently with an absorption rate of 99 percent.[10] The absorption rate can be increased to 100 percent by incorporating a higher dimension Möbius metamaterial gradient index shell. This could yield wide applications in the thermal emitting, energy harvesting and high-Q factor evanescent mode resonators.

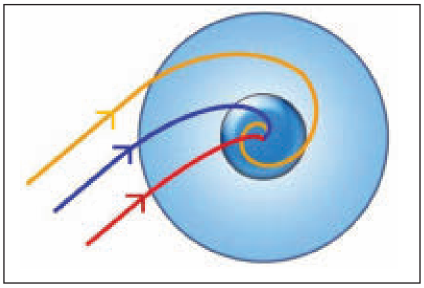

▲ *Fig. 4 Black hole model composed of a gradient-index metamaterial shell and a lossy dielectric core.*[10]

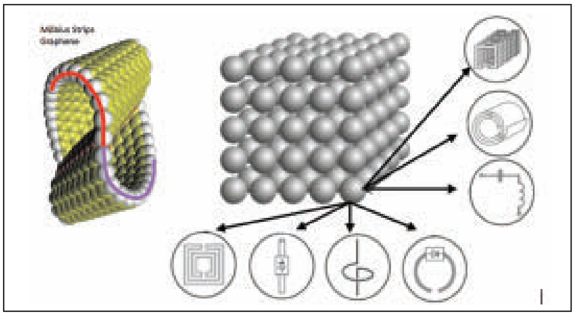

▲ *Fig. 5 A typical structure of the Möbius strips formed by Graphene.*[11]

Möbius Strips - Graphene

Graphene has received much attention for its remarkable structural and superior electronic properties. A single layer of graphite exhibits mechanical properties like planar paper or plastic with a large bulk modulus along its plane and is easily bent or curved.[11] These unique characteristics enable graphene to wrap into carbon nanotubes without deformation, making it a promising material for building Möbius metamaterial strips employed in microwave and optical components for modern communication systems. ***Figure 5*** shows Möbius strips formed into graphene nanoribbons that behave as topological insulators possessing topology-induced thermal and magnetic properties.[11]

Wang investigated the stability and total magnetic moment (TMM) of Möbius strips with fixed length and different widths.[11] Möbius strips formed by Graphene nano-ribbons were found to be extraordinarily stable. These unique magnetic properties enable Möbius strip graphene-based building blocks in spintronic devices.

Möbius Strips - Passive Electrical Components

Resistors, inductors and capacitors are basic electrical components used for building electronic circuitry. In an ideal circuit, resistors would contribute only resistance, capacitors only capacitance, and inductors only inductance. This is not the case at high frequencies, however, due to unwanted electromagnetic coupling and associated parasitics.

Resistor: A resistor is an electrical component designed to reduce current flow and lower voltage in an electronic circuit. Its function as a resistor, however, is affected by parasitic reactance due to the current

passing through it. A magnetic field formed on the inside and outside creates self-inductance L in series with resistance R. In addition, capacitance between turns of wire as well as between various metal objects, is equivalently represented as parasitic capacitance C.

The L and C of a resistor cause a phase shift Ø and time constant τ at frequency ω between the current and the voltage, described by

$$\text{Ø}_{Resistor} = \omega\tau = \frac{\omega L}{R}\left(1-\omega^2 LC\right) - \omega RC \quad (5)$$

$$\text{Ø}_{Resistor} \rightarrow 0\left(\text{for } \frac{L}{R} = RC, \omega^2 LC \ll 1\right) \quad (6)$$

From equation 6, L/R=RC and $\omega^2 LC << 1$, the a phase shift Ø and time constant τ will tend to zero. For this reason, despite the self-inductance and parasitic capacitance associated with the resistor, a reasonably acceptable time constant can be realized at radio frequencies.

At microwave and millimeter wave frequencies, however, it is not possible to achieve $\omega^2 LC << 1$; therefore, a simple resistor acts like a complex impedance. The solution to this problem is the Möbius strip resistor.[12] ***Figure 6*** shows the typical Möbius strip resistor where the inner and outer layers are connected to a terminal.

The conductive layer is a single continuous length of material having regions that are spaced from one another in the direction normal to the surface of the Möbius resistor, part of a common continuous length of conductive material affixed to the surface of a dielectric layer. The continuity of the respective dielectric and conductive layers is only in the circumferential direction running the length of the Möbius resistor, and not in the direction transverse to its length. Direct current applied at the terminal, which is between two points on the conductive surface of the Möbius resistor, will flow substantially in the circumferential direction and not in the transverse direction due to the interruption of continuity between regions of the conductive surface in the normal direction by the layer of dielectric material.

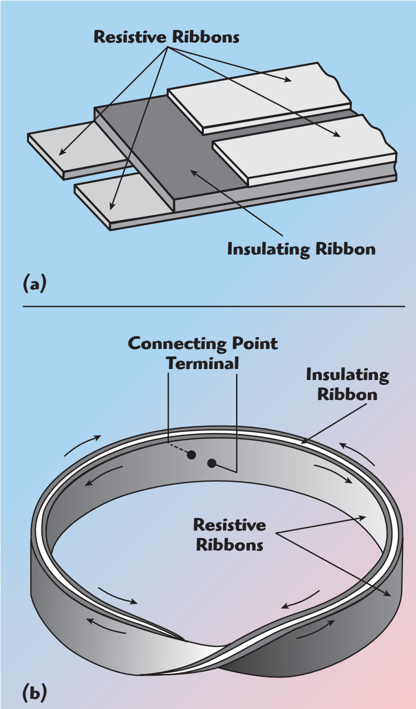

▲ *Fig. 6 Möbius strips resistor (a) and current flow direction (b).*[12]

Enabling LTE Advances with Premium Filters

Solving complex LTE interference challenges is a key design consideration for next-gen smartphones, as the information provided below makes clear. With every model you create, you need to develop multiple platforms tailored for different regions, and then factor in global roaming, too. As band counts rise and higher filter performance is required, TriQuint is leveraging its advanced filter technologies, such as NoDrift™ and LowDrift™ BAW and SAW, to help you tackle the industry's toughest interference problems.

Key Frequency Bands

Band	Mobile Phone Tx Band (MHz)	Mobile Phone Rx Band (MHz)	Duplexer / Filter Mode	LTE Bandwidths	Recommended Filter / Duplexer Technology	Region(s) of Usage
1	1920 - 1980	2110 - 2170	FDD	5, 10, 15, 20	SAW	Asia, EMEA, Japan
2	1850 - 1910	1930 - 1990	FDD	1.4, 3, 5, 10, 15, 20	LowDrift BAW	LatAm, N. Amer.
3	1710 - 1785	1805 - 1880	FDD	1.4, 3, 5, 10, 15, 20	LowDrift BAW	Asia, EMEA
4	1710 - 1755	2110 - 2155	FDD	1.4, 3, 5, 10, 15, 20	SAW	LatAm, N. Amer.
5	824 - 849	869 - 894	FDD	1.4, 3, 5, 10	SAW	LatAm, N. Amer.
7	2500 - 2570	2620 - 2690	FDD	5, 10, 15, 20	LowDrift BAW	Asia, EMEA
8	880 - 915	925 - 960	FDD	1.4, 3, 5, 10	SAW / LowDrift SAW	EMEA, LatAm
12	699 - 716	729 - 746	FDD	1.4, 3, 5, 10	SAW	N. Amer.
13	777 - 787	746 - 756	FDD	5, 10	NoDrift SAW	N. Amer.
17	704 - 716	734 - 746	FDD	5, 10	SAW	N. Amer.
20	832 - 862	791 - 821	FDD	5, 10, 15, 20	SAW / LowDrift SAW	EMEA
23	2000 - 2020	2180 - 2200	FDD	1.4, 3, 5, 10, 15, 20	LowDrift BAW	N. Amer.
25	1850 - 1915	1930 - 1995	FDD	1.4, 3, 5, 10, 15, 20	LowDrift BAW	N. Amer.
26	814 - 849	859 - 894	FDD	1.4, 3, 5, 10, 15	LowDrift SAW	Japan, N. Amer.
27	807 - 824	852 - 869	FDD	1.4, 3, 5, 10	SAW	LatAm
28	703 - 748	758 - 803	FDD	3, 5, 10, 15, 20	SAW	Asia, LatAm
29	N/A - N/A	717 - 728	FDD	3, 5, 10	SAW	N. Amer.
30	2305 - 2315	2350 - 2360	FDD	5, 10	NoDrift BAW	N. Amer.
32	N/A - N/A	1452 - 1496	FDD	5, 10, 15, 20	SAW	Japan, EMEA
34	2010 - 2025	2010 - 2025	TDD	5, 10, 15	SAW	China
38	2570 - 2620	2570 - 2620	TDD	5, 10, 15, 20	SAW	Asia, EMEA
39	1880 - 1920	1880 - 1920	TDD	5, 10, 15, 20	SAW	China
40	2300 - 2400	2300 - 2400	TDD	5, 10, 15, 20	LowDrift BAW	China, India
41	2496 - 2690	2496 - 2690	TDD	5, 10, 15, 20	LowDrift BAW	China, N. Amer.
42	3400 - 3600	3400 - 3600	TDD	5, 10, 15, 20	LowDrift BAW	Japan, EMEA
43	3600 - 3800	3600 - 3800	TDD	5, 10, 15, 20	LowDrift BAW	EMEA

Leveraging Advanced Filter Technology for Regional Demands

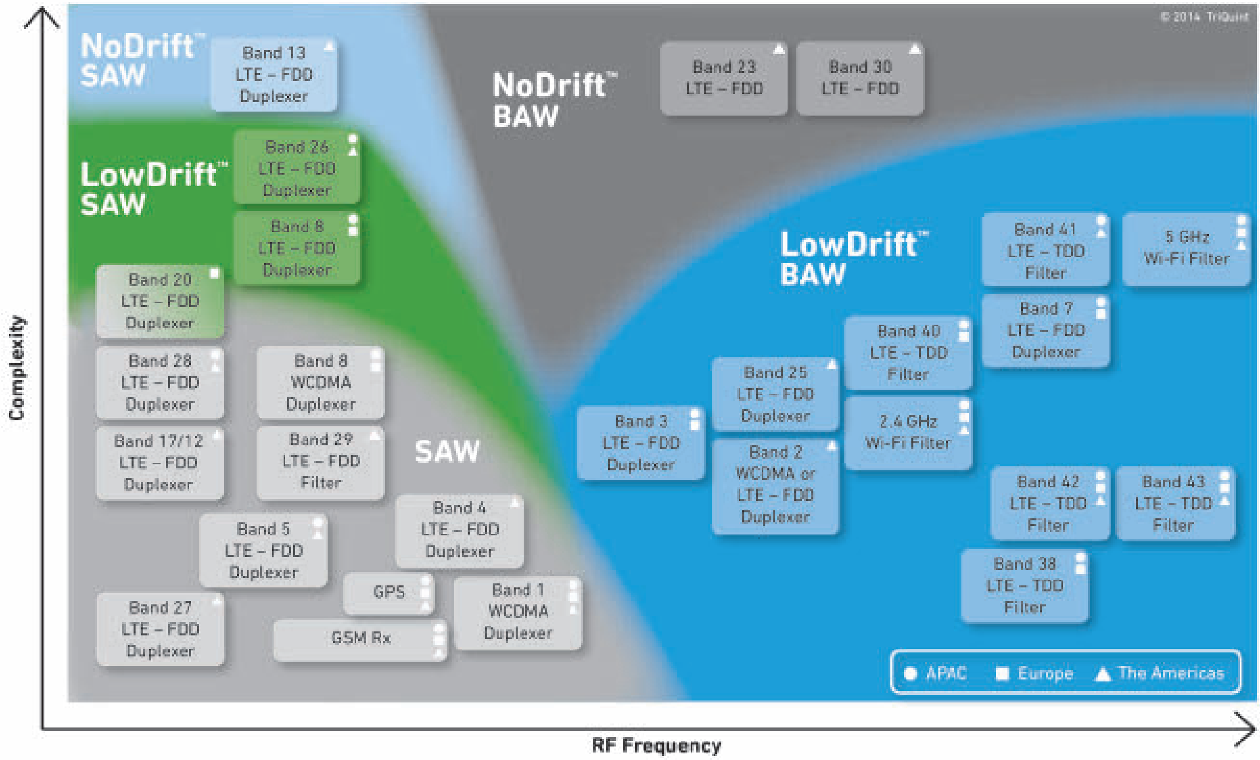

Solving the Toughest RF Challenges

As LTE rolls out, the spectrum crunch is forcing new frequency bands to be squeezed next to existing ones, often with minimal band guards. You can count on TriQuint's specialty filters to meet the most stringent performance requirements for global and regional applications, including vexing LTE / Wi-Fi coexistence issues and those especially demanding specifications that require ultra-stable filtering performance over temperature variations. Whether you're designing smartphones or the network infrastructure that connects them, TriQuint simplifies RF design and boosts performance by integrating our premium filters with other components like broadband amplifiers into tiny space-saving modules with more functionality.

Crowded Spectrum Drives Filter Complexity / Performance

Spectrum Example for Asia / EMEA

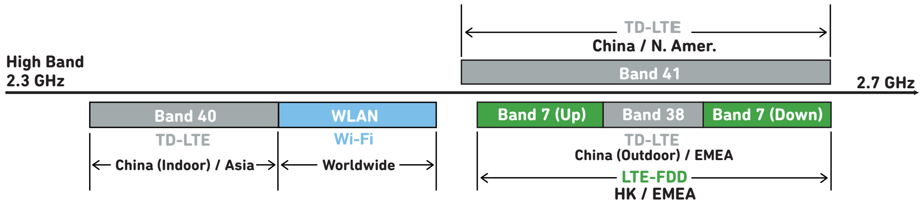

Spectrum Example for North America

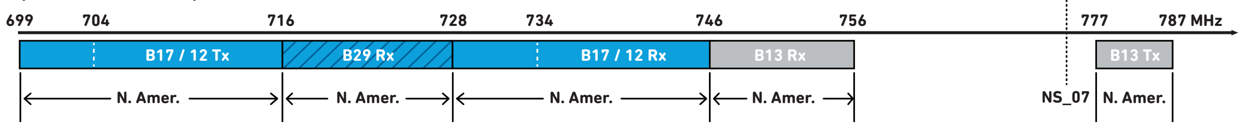

TriQuint Advanced Filtering Solutions

Bands	Part #	Description	Filter Technology	Size (mm)	Features
Band 38 and 40	885043	LTE B38 / 40 Tx Filter	LowDrift BAW	1.7x1.3x0.5	2-in-1 Filter for Full Band 40 Coverage with Low Loss
Band 7	TQM976027	LTE SE / SE Duplexer	LowDrift BAW	2.0x1.6x0.9	Excellent Insertion Loss
Band 41	TQQ0041	LTE B41 Rx Filter	LowDrift BAW	2.0x2.0x0.8	Low IL and High Wi-Fi Attenuation
Band 13	TQQ1013	LTE SE / SE Duplexer	NoDrift SAW	2.5x2.0x0.9	Solution for Public Safety NS_07 Requirements
Band 25 (BC14)	TQM963014	LTE SE / SE Duplexer	LowDrift BAW	2.6x2.1x0.9	Excellent Triple Beat Performance
Band 2 (PCS) (BC1)	TQM966002	PCS SE / SE Duplexer	LowDrift BAW	2.5x2.0x0.9	Excellent Triple Beat Performance
Band 25	TQM966025	LTE Diversity Receive Filter	LowDrift BAW	2.5x2.0x0.8	2.6dB Insertion Loss and 40dB Tx Attenuation
Band 25 / 26	TQQ2526	LTE Duplexer Bank – BAW / TC-SAW	LowDrift BAW & LowDrift SAW	2.8x4.7x1.0	Diplexed Duplexer for B25 / 26 Applications
Band 38	885026	LTE B38 Tx / Rx Filter	LowDrift BAW	1.4x1.2x0.5	Tx or Rx B38 Filter
Band 40	885049	LTE B40 Tx / Rx Filter	LowDrift BAW	1.4x1.2x0.5	Tx or Rx B40 Filter
WLAN	885033	LTE / Wi-Fi Coexist Filter	LowDrift BAW	1.4x1.2x0.5	WLAN BPF Filter B38 / 40 Reject
WLAN	885032	LTE / Wi-Fi Coexist Filter	LowDrift BAW	1.4x1.2x0.5	WLAN BPF Filter B7 / 41 Reject
BC0 / B13	857031	BC0 Notch Filter for Applications SVLTE	LowDrift SAW	2.5x2.0x0.6	Low Loss, High Attenuation and High Linearity
BC0 / B13	857061	B13 Notch Filter for SVLTE Applications	LowDrift SAW	2.5x2.0x0.6	Low Loss, High Attenuation and High Linearity
Band 13	856879	LTE SE / BAL Duplexer	LowDrift BAW	2.5x2.0x0.6	1.5dB (Tx) / 1.6dB (Rx) Insertion Loss
WLAN	885062	LTE / Wi-Fi Coexist Filter	LowDrift BAW	1.4x1.2x0.5	+28dBm MCS7, Hi Rej B38 / B40, Hermetic MSL0, Temp -40 to 95°C
WLAN	885071	LTE / Wi-Fi Coexist Filter	LowDrift BAW	1.4x1.2x0.5	+29dBm MCS7, Hi Rej B7 / B41, Hermetic MSL0, Temp -40 to 95°C
WLAN	885070	LTE Coexist / Wi-Fi Bandedge Filter	LowDrift BAW	1.7x1.3x0.5	+30dBm MCS7, Bandedge Rej 2390 & 2483.5MHz, Hermetic MSL0, Temp -40 to 95°C
SDARS	885014	2332.5 MHz BAW Filter	NoDrift BAW	1.7x1.3x0.5	Enables Coexistence of SDARS with WCS Radios

Application of an alternating voltage at the connecting point terminal induces a field in the dielectric opposing the flow of a resultant alternating current whereby the Möbius resistor exhibits a capacitive type reactance at frequencies other than those corresponding to a wavelength equal to the length of the Möbius strip or an integral multiple of its length. As a result, the Möbius resistor has the property of passing attenuated components of an applied signal having a wavelength that is not equal to the length of the Möbius strip or an integral multiple of its length.[13]

Consider that the strip is made of good electrical conducting material so that charges and currents flowing on the strip will end up on the boundary. From Ampere's law, total flux $\O_B$ through the Möbius strip is given by the line integral of the current I around the boundary ∂M. Starting at any given point on the boundary and evaluating the integral as one moves along the edge for one complete cycle of the Möbius strip M yields:

$$\oint_{\delta M} I.dl = \oint_{\delta M} \delta\O = \O_B = 0 \quad (7)$$

From equation 7, the total flux for the Möbius strip is zero. Using this equation, Davis[12] designed and patented the Möbius resistor, where current passing through resistor's input terminal splits into two equal pulses traveling in opposing directions due to the fact that the impedances of the two paths to the output terminal are equal. As shown in Figure 6, when the two pulses have each traveled halfway along the surface of the resistor reaching the twist (180°), they will be of equal and opposite phase, and thus will cancel. This implies net potentials tend to zero when they reach the output terminal. To achieve this result, it is necessary for the two terminals to be directly opposite, or else the pulses will not be 180° out of phase and thus will not completely cancel (implying the presence of residual magnetism). Due to the cancellation of electromagnetic fields, the Möbius resistor can be non-reactive and will maintain its properties even when folded or deformed. The characteristics of a Möbius resistor do not change with its length or form. It can be wound around a cylindrical core or a thin card, and it can even be formed into a ball, allowing it to wrap around and minimize the space it occupies.[3]

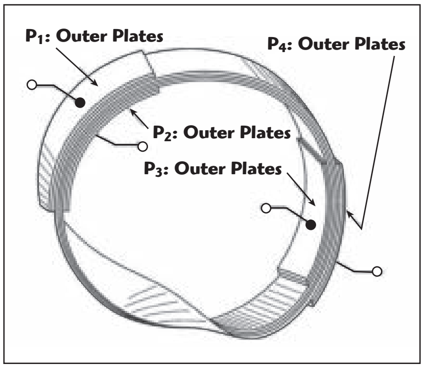

▲ *Fig. 7 Möbius strips capacitor.*[13]

Capacitor: The Möbius resistor has zero-residual self-inductance; however, an intrinsic negligible capacitive effect exists that can have significant utility if used for intended purposes. By modifying the material composition of the Möbius resistor from being primarily resistive to being primarily conductive, the capacitive side effect is enhanced. It is this capacitive effect of the Möbius resistor that is used by Brown[13] for designing the Möbius capacitor. This structure is constructed by layering the continuous conductive surface of the typical Möbius resistor with a second dielectric material, then layering this dielectric with two separate conductive surfaces of a size compatible with the Möbius resistor. The layout of Möbius capacitor is such that the conductive surfaces are diametrically opposite to each other; while simultaneously, the normal of each conductive surface is parallel to the normal of the surface of the Möbius resistor at all points along the surface. ***Figure 7*** shows a typical Möbius capacitor where the outer plates (P_1, P_2, P_3 and P_4) are connected via outside ribbon conductors.[12]

If a sinusoidal voltage $v_1(t)$ is applied at P1 then the voltage at P_2 is described by

$$v_2(t) = V_m \text{Sin}\,\omega\left(t + \frac{l}{u}\right), \omega = 2\pi f \quad (8)$$

where $v_1(t) = V_m\text{Sin}\,\omega t$, V_m is the maximum amplitude, l is the length of the Möbius-resistor (if loop opened, circumference of loop equals to length of loop), u is the propagation speed between P_1 and P_2, f is the frequency, and $t = (\frac{l}{u})$ is the wave propagation time between two opposite points P_1 and P_2 on the conductive surface (separated circumferentially by a distance equal to the length l of the Möbius strip).

From equation 8, the potential difference δv across points P_1 and P_2 at any time t is:

$$dv = v_1(t) - v_2(t) =$$

$$V_m\text{Sin}\,\omega t - V_m\text{Sin}\,\omega\left(t + \frac{l}{u}\right) \quad (9)$$

The current i(t) between two normally opposite points P_1 and P_2 on the conductive surface of the Möbius strip as shown in Figure 6 given by the derivative of equation 8 with respect to time t:

$$i(t) = C\left(\frac{dv}{dt}\right) = \omega CV_m \quad (10)$$

$$\left[\text{Cos}\,\omega t - \text{Cos}\,\omega\left(t + \frac{l}{u}\right)\right] = \omega CV_m$$

$$\left[\text{Cos}\,\omega t - \text{Cos}\,\omega t \times \text{Cos}\frac{\omega l}{u} + \text{Sin}\,\omega t \times \text{Sin}\frac{\omega l}{u}\right]$$

$$i(t) = \omega CV_m \quad (11)$$

$$\left[\text{Cos}\,\omega t\left(1 - \text{Cos}\frac{\omega l}{u}\right) - \text{Sin}\,\omega t \times \text{Sin}\frac{\omega l}{u}\right]$$

From equation 11, if l = λ (length of Möbius strip is equal to the wavelength of field propagation) then the frequency of the wave reduces to $f = \frac{u}{l}$, and the resulting current i(t) between two normally opposite points P_1 and P_2 on the conductive surface of the Möbius strip becomes zero:

$$i(t)_{l=\lambda\rightarrow\left(f=\frac{u}{l}\right)} = \omega CV_m \quad (12)$$

$$[\text{Cos}\,\omega t(1 - \text{Cos}\,2\pi) -$$

$$\text{Sin}\,\omega t \times \text{Sin}\,2\pi] = 0$$

From equation 12, when the wavelengths are equal to the length of the loop or are integer multiples, the Möbius strip in parallel with a circuit across P_1 and P_2 will allow a resonant frequency and its harmonics to pass through the circuit unattenuated but will attenuate other frequencies.

Resonator: The concept of the Möbius strip resonator is based on the fact that a signal coupled to a strip will not encounter any obstruction when travelling around the loop, the loop will behave like an infinite transmission line, enabling a high quality factor (Q) resonator tank. This characteristic enables many radio and microwave applications, such as a compact resonator with the resonant frequency which is

half the size of identically constructed linear coils, a Tesla coil for global transmission of electricity without wires and high temperature superconductors.

Jeffrey Pond reported a Möbius strip filter (see ***Figure 8***),[14,15] in which the Möbius twist provides additional phase shift to facilitate a resonant condition and frequency selectivity in a compact size. The "twist" is implemented using two via connections through the substrate.

Möbius Strips – Metamaterial Symmetry

Symmetry is defined as a system feature or property, conserved when the system undergoes an alteration. In general, spatial symmetries are easily observed but others, such as optical symmetries in metamaterials, are concealed. Recent publications describe electromagnetic Möbius symmetries introduced into metamaterial (metamolecular), made from metals and dielectrics.[16-17] The electromagnetic symmetry discovered in metamaterials is equivalent to the structural symmetry of a Möbius strip, with the number of twists controlled by the sign change of the electromagnetic coupling between the meta-atoms. The negative index artificial material (metamaterial) with different coupling signs exhibit resonant frequencies that depend only on the number of turns

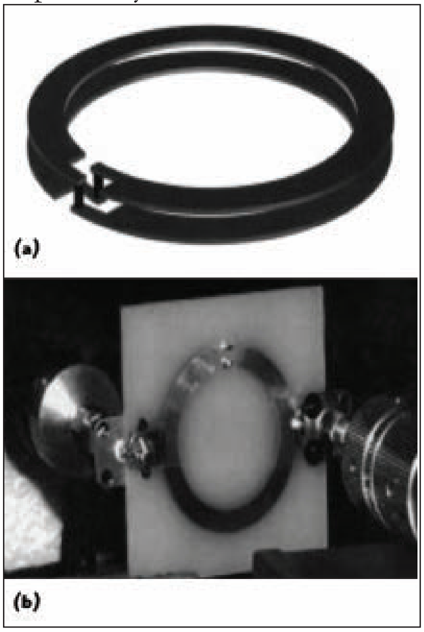

Fig. 8 Möbius strips filter (Möbius "twist" implemented with two vertical interconnects). Planar implementation (a) and photograph of a Möbius BPF realized on a Teflon substrate (b).[15]

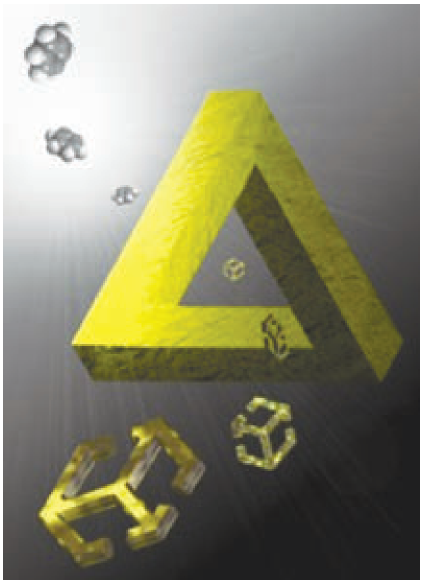

Fig. 9 Möbius symmetry in metamolecular trimmers made from metals and dielectrics (courtesy of National Science Foundation).[17]

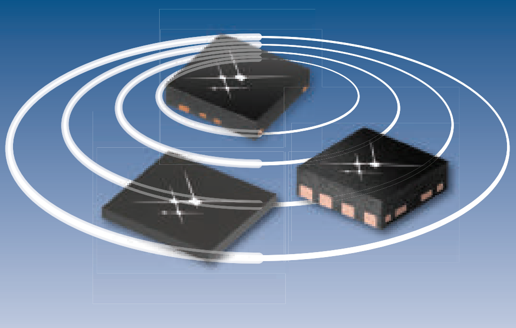

SKYWORKS®

Broadband RF and Analog Solutions

Automotive

SKYA21001 Broadband SPDT RF Switch

- Ideal for infotainment, telematics, and remote keyless entry applications
- AEC-Q100 qualification in process
- Low insertion loss 0.3 dB @ 900 MHz

Aerospace and Defense

SKY16602-632LF Low Threshold Level Limiter Module

- Ideal for WLAN, VSAT, S-band radar, military communication transceivers, jammers, and GPS applications
- Broadband 0.20 to 4.0 GHz
- Low threshold level of 0.5 dB @ 2.5 GHz

Connected Home

SKY66109-11 2.4 ZigBee® / Smart Energy Front-end Module

- Ideal for connected home, security, smart energy, and smart thermostat applications
- 20–23 dBm RF power @ 2.4–2.5 GHz
- 2 dB NF with 11.5 dB gain in Rx mode

Media

SKY85806 802.11ac Dual-band Front-end Module

- Ideal for wireless high fidelity, set-top box, USB dongle, and personal computer applications
- Highly integrated 2.4 GHz PA, 5 GHz PA, 2.4 GHz LNA, 5.8 GHz LAN, transmitter filter, diplexers, and T/R switches
- Power accuracy improvement with integrated logarithmic power detector

Wearables

SKY66110 and SKY66111 Bluetooth® Low Energy (BLE) Front-end Modules

- Super-efficient BLE FEMs provide increased battery life
- 25–30% more efficient when used with chipset
- Reduces overall system current consumption

USA: 781-376-3000 • Asia: 886-2-2735 0399 • Europe: 33 (0)1 43548540 • Email: sales@skyworksinc.com

www.skyworksinc.com • NASDAQ: SWKS •

but not the locations of the "twists," thus confirming its Möbius symmetry topological nature.

Figure 9 illustrates the hyperspace Möbius mechanism that transforms ordinary benzene molecules into metamolecules with Möbius symmetry (the topological phenomenon that yields a half-twisted strip with two surfaces but only one side).[16] Figure 9 shows a three-body system like a trimmer with metallic resonant meta-atoms configured as coupled split-ring resonators, symbolized as metamolecules exhibiting topological Möbius-cyclic-symmetry (C3-symmetry) through three rotations of 120°. Möbius twists result from a change in the signs of the electromagnetic coupling constants between the constituent meta-atoms.[17]

CONCLUSION

Since its discovery, the Möbius strip has captured the imaginations of mathematicians and engineers everywhere, and it continues to fascinate modern generations with its non-orientability and one-sidedness. The unique features of Möbius strips promise new inventions, recurring in an endless loop; one might say that the future resides on the surface of Möbius strips. ■

Note: This article will be continued with Part II (Möbius Metamaterial Resonator) and Part III (Möbius Metamaterial Oscillators) in the December 2014 and January 2015 issues, respectively.[18]

References

1. Hückel, *Grundzüge der Theorie ungesättiger und aromatischer Verbindungen*, Verlag Chem, Berlin, 1938, pp. 77-85.
2. E.L. Starostin and G.H.M. van der Heijden, "The Shape of a Möbius Strip," *Nature Materials*, Vol. 6, July 2007, pp. 563-567.
3. C.A. Pickover, *The Möbius Strip: Dr. August Möbius's Marvelous Band in Mathematics, Games, Literature, Art, Technology, and Cosmology*, Thunder's Mouth Press, New York, N.Y., 2006.
4. "Möbius Strip Ties Liquid Crystal in Knots," *R&D Magazine*, August 20, 2013, www.rdmag.com/news/2013/08/m%C3%B6bius-strip-ties-liquid-crystal-knots, accessed September 2014.
5. D. Basulto, "National Library in Astana, Kazakhstan / BIG," *ArchDaily*, August 25, 2009, www.archdaily.com/33238/national-library-in-astana-kazakhstan-big/, accessed September 2014.
6. T. Gecchelin, "Möbius Concept Car Design," *Automotive Design, Engineering, Industrial Design*, 2010, http://tommasogecchelin.prosite.com/208236/812241/gallery/Möbius-concept-car-design, accessed September 2014.
7. A.J. Kox, M.J. Klein and R. Schulmann Kox, *The Collected Papers of Albert Einstein*, Vol. 6, Princeton University Press, 1997.
8. D.A. Genov, S. Zhang and X. Zhang, "Mimicking Celestial Mechanics in Metamaterials," *Nature Physics*, Vol. 5, July 2009, pp. 687-692.
9. E.E. Narimanov and A.V. Kildishev, "Optical Black Hole: Broadband Omni-Directional Light Absorber," *Applied Physics Letters*, Vol. 95, July 2009.
10. Q. Cheng, T.J. Cui, W.X. Jiang and B.G. Cai, "An Electromagnetic Black Hole Made of Metamaterials, *Cornell University Library*, April 30, 2010, http://arxiv.org/abs/0910.2159, accessed September 2014.
11. X. Wang, X.H. Zheng, M. Ni, L. Zou and Z. Zeng,"Theoretical Investigation of Mobous Strips Formed From Graphene," *Applied Physics Letters*, Vol. 97, No. 12, September 2010, pp. 123103 - 123103-3.
12. R.L. Davis, "Non-Inductive Electrical Resistor," *US Patent 3267406A*, August 16, 1966.
13. T.J. Brown, "Möbius Capacitor," *US Patent 4599586*, July 8, 1986.
14. J.M. Pond, "Möbius Resonator and Filter," *US Patent 6445264*, September 3, 2002.
15. J.M. Pond, "Möbius Dual Mode Resonators and Bandpass Filters," *IEEE Transactions on Microwave Theory and Techniques*, Vol. 48, No. 12, December 2000, pp. 2465-2471.
16. C.W. Chang, M. Liu, S. Nam, S. Zhang, Y. Liu, G. Bartal and X. Zhang," Optical Möbius Symmetry in Metamaterials," *Physical Review Letters*, Vol. 105, December 2010, pp. 235501-1-235501-4.
17. Lynn Yarris, "Strange New Twist: Berkeley Researchers Discover Möbius Symmetry in Metamaterials," *Berkeley Lab*, 20 December 2010, http://newscenter.lbl.gov/2010/12/20/Möbius-symmetry-in-metamaterials/#sthash.Ezqlm5Pr.dpuf, accessed September 2014.
18. A.K. Poddar, "Slow-Wave Resonator Based Tunable Multi-Band Multi-Mode Injection-Locked Oscillators," Research Report, RF and Microwave Techniques Brandenburg University of Technology Cottbus-Senftenberg 2014," https://www-docs.tu-cottbus.de/mikrowellentechnik/public/poddar_report_long_ebook.pdf.

Temperature-Compensated Filter Technologies Solve Crowded Spectrum Challenges

Phil Warder, David Schnaufer
TriQuint Semiconductor
Note: TriQuint and RFMD have announced plans to merge under the name of Qorvo.

The extraordinary growth in mobile wireless data is generating a continuous need for new spectrum bands in which operators can deploy LTE services to accommodate the traffic. As a result, global spectrum has become increasingly crowded, with a highly fragmented and complex array of spectrum licenses spread across multiple operators

Manufacturers are now creating smartphones that support many bands, as they seek to minimize the number of different handset models and enable global roaming. Some of these LTE bands are very close to bands used for other wireless applications such as Wi-Fi and satellite radio. Due to these trends, devices must include a growing number of high-performance filters to prevent interference between these closely spaced frequency bands.

As frequency bands squeeze closer together, filter temperature drift has emerged as a significant challenge. Traditional filter technologies, in which the frequency response shifts as the temperature changes, are often not able to meet the challenging requirements in mobile devices that must operate over a wide temperature range. Solving these challenges requires new filter processes with a much more stable response to temperature variation.

Another challenge facing device designers is limited space, as they seek to pack more filters into each device. This applies not just to smartphones but also to the growing range of other mobile and fixed wireless devices including automotive electronics and small-cell base stations. New packaging technologies play an important role in reducing filter size, making it easier to fit more of them into each device. These packaging technologies are particularly valuable for components such as LTE diversity filters in which compact size is the primary consideration.

Filtering requirements will become even more stringent in the future as more new bands are defined and operators deploy faster LTE Advanced networks to support escalating demand for video and other bandwidth-intensive applications. The data rate increases provided by LTE Advanced will depend in part on Carrier Aggregation (CA), an LTE Advanced feature that enables operators to combine fragments of spectrum to create wider channels. CA will need high-performance filters to meet the requirements for low insertion loss and isolation of each component carrier.

Also on the horizon are new 3.5 GHz bands that will open up wide expanses of a previously unexploited spectrum, and the proposed use of LTE Advanced in an unlicensed 5 GHz spectrum (LTE-U). These developments will be important in enabling operators to support more users via network densification.

THE NEED FOR TEMPERATURE-COMPENSATED FILTERS

The key filter performance parameters are low loss of the desired signals in the passband and sufficient attenuation of undesired interference in the stopband. These parameters must be met over environmental and production variations. Historically, designers have built allowances for each of these sources of variation into the system. However, the design challenges have increased as bands have be-


38GHz
60GHz
24GHz
79GHz

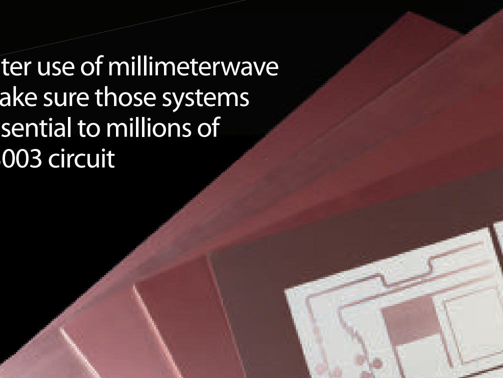

▲ *Fig. 1 Band 13 and public safety coexistence challenge.*

come more closely spaced.

In some cases, the transition between the passband and stopband is as small as 2 MHz. In such cases, it is almost impossible to meet the requirements using traditional filter technologies. This is because the variation in response, which is dominated by temperature drift, can exceed the width of the transition band. The result is unacceptable interference, high insertion loss, or both.

The solution is to design filters using a process that greatly reduces temperature drift. TriQuint has developed such fabrication processes for both of the primary filter technologies: surface acoustic wave (SAW) filters, which are most effective for lower frequencies up to about 1.9 GHz; and bulk acoustic wave (BAW) filters, which are typically used for higher frequencies above 1.5 GHz. As shown in ***Table 1***, these new processes produce filters with dramatically reduced temperature sensitivity. For example, the standard SAW process produces filters with temperature variation of -35 to -45 ppm/°C. In comparison, temperature variation for NoDrift™ SAW filters is almost eliminated, at 0 ± 2 ppm/°C. For LowDrift™ BAW filters, temperature drift is -17 to -22 ppm/°C; with NoDrift™ BAW, this is reduced to 0 ± 2 ppm/°C.

These new SAW and BAW filters are effective within the same frequency ranges as standard SAW and BAW. The reduced sensitivity to temperature change makes these processes a good choice for challenging specifications including several new 3G and 4G duplexers and filters.

TABLE 1

COMPARING STANDARD AND TEMPERATURE-COMPENSATED SAW AND BAW FILTERS

SAW Processes	
Process	***Temperature Drift***
Standard SAW	-35 to -45 ppm/°C
LowDrift™ SAW	-22 ppm/°C
NoDrift™ SAW	0 ± 2 ppm/°C
BAW Processes	
Process	***Temperature Drift***
Standard FBAR	-22 to -31 ppm/°C
LowDrift™ BAW	-17 ppm/°C
NoDrift™ BAW	0 ± 2 ppm/°C

BAND 13

A specific example where temperature-compensated filters are needed is Band 13. The challenge, shown in ***Figure 1***, is that the Band 13 uplink at 777 to 787 MHz is very close to narrowband public safety communications in the 769 to 775 MHz region. This problem was anticipated by 3GPP, the organization responsible for LTE standards. To avoid interference problems, 3GPP defined a network signaling case (NS_07) whereby the network signals mobile devices when there is a narrowband public safety system in the area. In response to this signal, mobile devices must reduce emissions in the 769 to 775 MHz range by 22 dB.

In initial Band 13 deployments, the only feasible way to achieve this emissions improvement was to reduce the output power of the mobile device. The required power reduction is a function of the number and location of the reference blocks in the uplink transmission; worst-case reductions are significant, ranging as high as 12 dB.

Because a power reduction of this size significantly impacts system performance, the operators using Band 13 have long wanted a solution capable of addressing the interference issue without the reductions in output power. To meet the specification, filtering solutions need to provide 22 dB of attenuation at 775 MHz while still passing 777 MHz, the lower edge of Band 13. Complicating the problem is the need to provide this attenuation over a wide temperature range, typically from -20° to + 85°C.

Table 2 compares the drift of standard, the new SAW filters over this temperature range. Given that the space between the passband and the stopband is only 2 MHz, it is clear that only these SAW filters, the most temperature-stable of the filter processes, can meet the requirements. ***Figure 2***

Vector Signals at the touch of a button

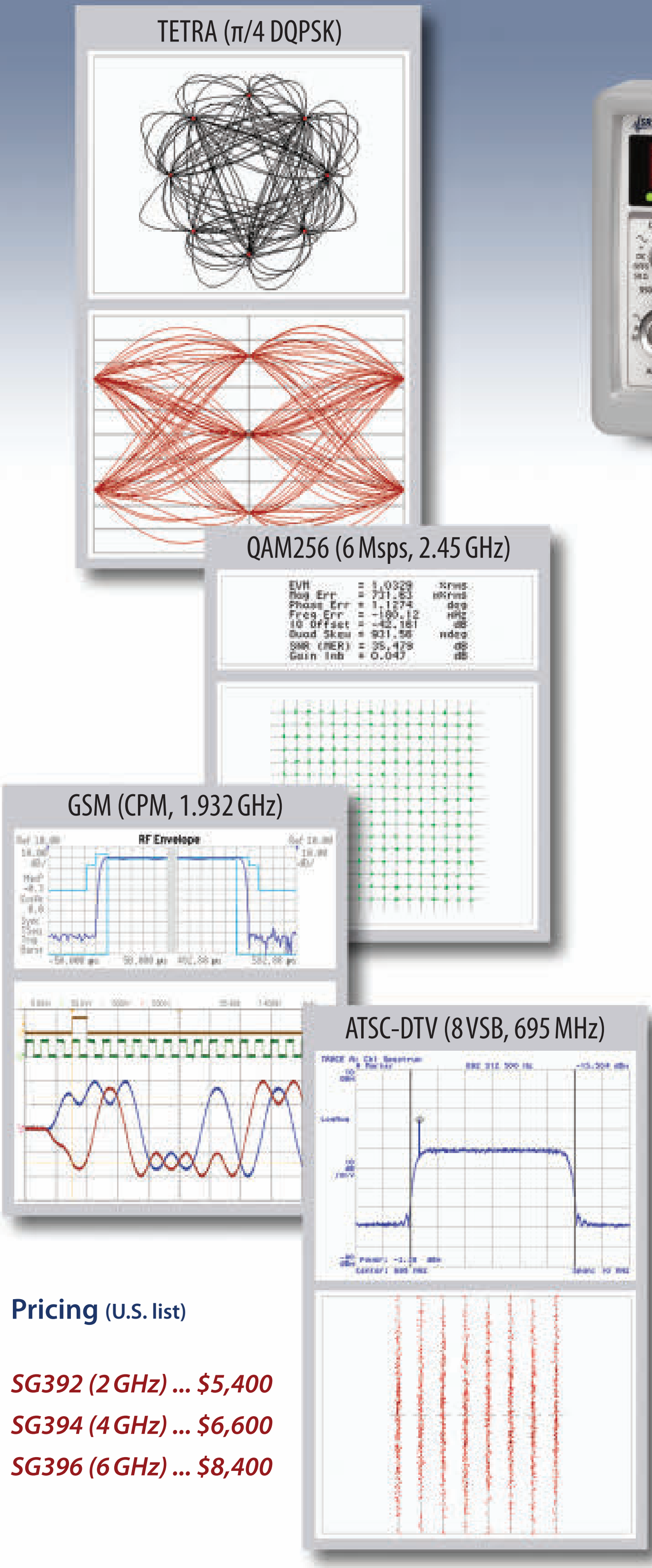

- 2 GHz, 4 GHz & 6 GHz models
- Dual baseband arb generators
- Vector & analog modulation
- I/Q modulation inputs (300 MHz RF BW)
- ASK, FSK, MSK, PSK, QAM, VSB & custom I/Q
- Presets for GSM, EDGE, W-CDMA, APCO-25, DECT, NADC, PDC, ATSC-DTV & TETRA
- GPIB, RS-232 & Ethernet interfaces

The SG390 Series ***Vector Signal Generators*** — taking communications testing to a new level.

The SG390 series has outstanding features and performance: complete vector and analog modulation, dual baseband arb generators, I/Q inputs with 300 MHz RF bandwidth, low phase noise, and an OCXO timebase are all included.

We've also made communications testing quick and easy — everything is available from the front panel of your instrument. Pulse shaping filters, TDMA gating signals, additive white noise, and event markers are all there. Use the built-in pattern or PRBS generators to create data, or upload your own symbol data. Map your symbols to any constellation and transmit at rates up to 6 Msps — it's that simple.

Pricing (U.S. list)

SG392 (2 GHz) ... $5,400

SG394 (4 GHz) ... $6,600

SG396 (6 GHz) ... $8,400

SRS Stanford Research Systems
Tel: (408)744-9040 • www.thinkSRS.com

TABLE 2
COMPARING TEMPERATURE DRIFT OF STANDARD AND TEMPERATURE-COMPENSATED BAND 13 UPLINK FILTERS

	Standard SAW	LowDrift™ SAW	NoDrift™ SAW
Temperature Coefficient	-40 ppm/°C	-20 ppm/°C	-2.5 ppm/°C
Drift cold (25° to -20°C)	1.40 MHz	0.70 MHz	0.087 MHz
Drift hot (25° to +85°C)	-1.87 MHz	-0.93 MHz	-0.116 MHz

TABLE 3
DRIFT OF TEMPERATURE-COMPENSATED BAND 30 BAW FILTERS AT 2324 MHz

	Standard FBAR	LowDrift™ BAW	NoDrift™ BAW
Temperature Coefficient	-27 ppm/°C	-17 ppm/°C	-1 ppm/°C
Drift cold (25° to -20°C)	2.9 MHz	1.78 MHz	0.10 MHz
Drift hot (25° to +85°C)	-3.9 MHz	-2.37 MHz	-0.14 MHz

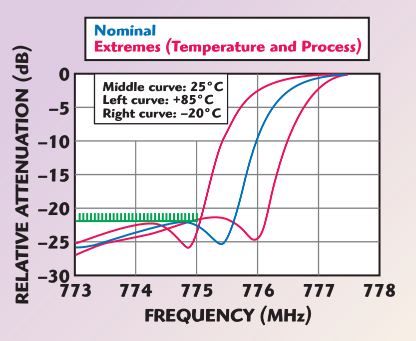

▲ *Fig. 2 Band 13 NoDrift™ filter performance.*

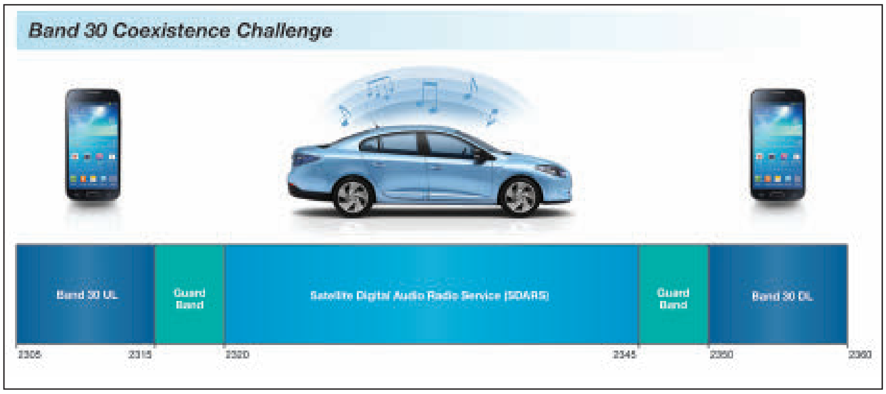

▲ *Fig. 3 Band 30 and satellite radio service coexistence challenge.*

shows the performance of the Band 13 NoDrift™ uplink filter in more detail.

BAND 30 AND SATELLITE RADIO

Another example of a situation requiring temperature-compensated filters is the challenge of Band 30 co-existence with satellite radio services, which are widely used to deliver in-car entertainment. The problem is shown in ***Figure 3*** where the satellite radio spectrum is sandwiched into the duplex gap between the Band 30 uplink and Band 30 downlink. The Band 30 spectral emission mask is tightly constrained to protect the satellite radio service as well as government bands below Band 30.

Mobile device makers and operators are very concerned about interference from satellite radio service signals (primarily the signals emanating from powerful terrestrial repeaters), and about meeting the specified emission mask. Similarly, satellite radio operators are concerned about interference due to Band 30 communications from mobile handsets or base stations.

Figure 4 shows the response required in a Band 30 uplink filter to achieve the spectral emission mask. The passband is 2305 to 2315 MHz, and the most difficult attenuation points are at 2296 and 2324 MHz. These are both 9 MHz away from the passband edge and require 11 dB of absolute attenuation.

As in the example of Band 13, the challenge is complicated by the need to meet the attenuation requirements over a wide temperature range. In the case of Band 30, a temperature-compensated BAW filter is needed. ***Table 3*** shows the response of new BAW filters at the critical 2324 MHz point. Only the NoDrift™ filter is capable of meeting requirements over the complete temperature range.

Filtering requirements for satellite radios are similarly challenging, requiring a temperature-stable filter that passes the satellite band but rejects adjacent Band 30 frequencies. This requirement is met by embedding a bandpass filter based on NoDrift™ BAW process into the car's antenna. ***Figure 5*** illustrates the response of this filter over a wide temperature range. As shown, the filter meets the requirements for low insertion loss across the entire passband, as well as the attenuation required to avoid interference with Band 30 uplink or downlink communications.

WI-FI COEXISTENCE IN CHINA

While the above two examples refer to filtering challenges in North America, similar challenging requirements

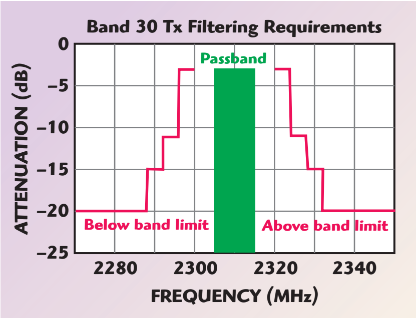

▲ *Fig. 4 Band 30 uplink filter requirements.*

exist in other regions. An example is LTE/Wi-Fi coexistence in China. The 2400 to 2482 MHz spectrum used by Wi-Fi lies between Bands 40 and 41, which are used to deliver TDD-LTE service in China. The upper edge of Band 40 (2400 MHz) directly abuts the Wi-Fi spectrum, with no transition band at all.

Solving this Wi-Fi coexistence challenge requires RF filters that are capable of rejecting closely adjacent frequencies. At the same time, the filters must minimize insertion loss in the WLAN transmission pathway, to help maintain the high signal-to-noise ratio and correspondingly low EVM required for 802.11n. BAW filters can achieve quality factors (Q values) that are superior to other traditional acoustic technologies. As a result of the high win SEMICONDUCTORS

Leading Global Communications

PD25-00 0.25μm E / D pHEMT

- 4th generation E/D PHEMT Technology
- High performance 0.25μm E-mode combined with latest generation 0.5μm D-mode switch
- E-mode device: Ultra low noise and high gain
- D-mode device: Compact layout and low Ron-Coff product

Fmin and Gain

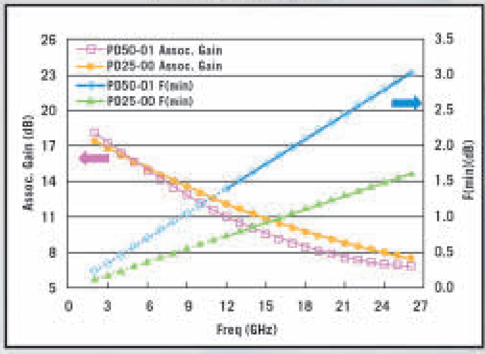

E-mode I-V Characteristics

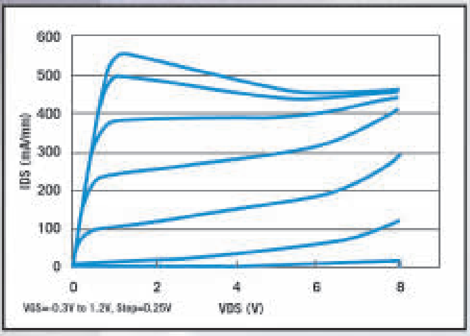

E-mode Transfer Curve

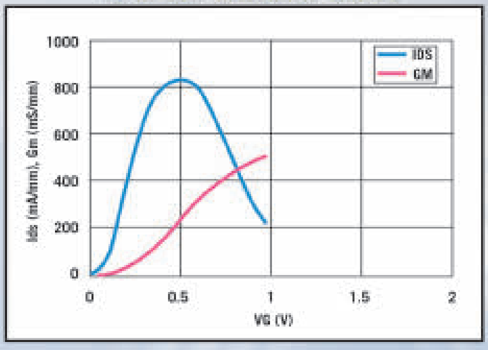

D-mode Switching Speed

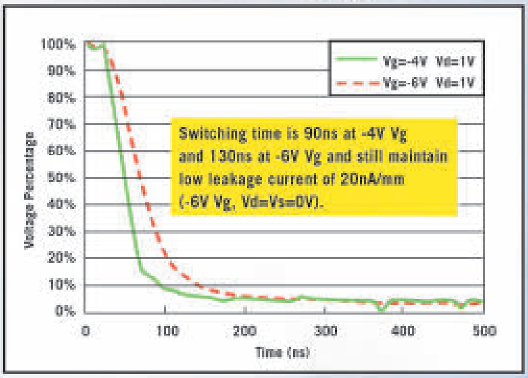

D-mode Device Performance

	PD50-01		PD25-00	
	Single	Triple	Single	Triple
Ron (ohm.mm)	1.9	3.7	1.3	2.2
Coff (fF/mm)	168	83	163	92
RonxCoff(ohm.fF)	316	310	209	198

DUT: NOF x UGW= 5 x 12μm

WIN SEMICONDUCTORS CORP.
Tel:+886-3-397-5999 Fax:+886-3-397-5069 http://www.winfoundry.com

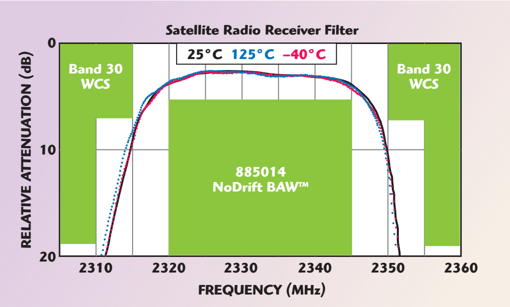

▲ *Fig. 5 Performance of NoDrift™ BAW satellite radio service filter over temperature range.*

Q values, the filter skirts will be very steep while insertion losses remain low even at the edges of the passband, minimizing the need to sacrifice LTE or Wi-Fi bandwidth.

SHRINKING FILTERS WITH NEW PACKAGING TECHNOLOGIES

Several factors are creating pressure to continuously reduce filter size. One is the trend for handsets to support an ever-growing number of frequency bands, requiring a corresponding increase in the number of filters. Another is the shift toward slimmer handset designs. Packaging technologies play important roles in reducing the size of filters and duplexers. Wafer-level packaging techniques that eliminate bulky ceramic packages mean filters occupy less PCB space. Flip-chip techniques, which replace wire bonds with more compact copper "bumps," also reduce horizontal space and height requirements. Together, these approaches can reduce space requirements by 50 percent and also reduce package height, facilitating slimmer designs. These can be particularly helpful for LTE RX diversity filters, in which small size is often an even more important concern than performance.

FUTURE FILTERING CHALLENGES

Demand for bandwidth is predicted to continue to skyrocket, largely due to growth in mobile video traffic. Globally, mobile data traffic is expected to increase 11-fold between 2013 and 2018 (Cisco Visual Networking Index, June 2014). Mobile video will grow at an even faster clip, increasing 14-fold over the same period and accounting for 69 percent of total mobile data traffic by 2018. Several developments are underway to help reduce – though not eliminate – the ever-growing pressure for more bandwidth. Each of these has implications for filtering requirements.

CARRIER AGGREGATION

One of these developments is Carrier Aggregation, a feature of LTE Advanced that helps operators create faster wireless data services. CA provides a method for overcoming the 20 MHz limitation on LTE component carrier bandwidth by enabling up to five fragments of spectrum to be combined into a single aggregate carrier that is up to 100 MHz wide. CA will be used to enable services faster than the 150 Mbps supported by a single component carrier (with LTE Category 4) today. Operators are rushing to put CA plans in place; by mid-2014, dozens of two-carrier and more than 50 three-carrier combinations had been proposed. CA will increase filtering challenges because each device will communicate simultaneously over multiple component carriers at different frequencies,

Introducing industry-leading GaN RF technology for military applications—new from Freescale, the global leader in RF power.

In the field, there's no time for second chances—or second best. As the largest, most deployed provider of RF power technology on Earth, Freescale now brings its industry-leading technology, design and manufacturing prowess to the defense electronics industry. Our new 125W GaN transistor provides breakthrough wideband and thermal performance, demonstrated in the available 200-2500 MHz reference design. Our RF power products are proven rugged and reliable in the harshest environments. US manufacturing and a 15-year product longevity warranty ensures long term security of supply. Freescale's dedicated support team of military systems and applications experts will back you up every step of the way. Out here, who will you count on? Talk to us.
Learn more freescale.com/RFmilitary

make it
freescale™

requiring stringent attenuation and isolation of each signal to eliminate potential interference between them.

NEW 3.5 AND 5 GHz LTE BANDS

New LTE bands will play a key role in operators' plans to support more users through network densification, while adding capacity for bandwidth-intensive applications such as video download. Network densification entails deploying a large number of small cells (compact network infrastructure devices with limited range) to increase the total number of users that can be supported in densely populated or crowded areas.

3.5 GHz BANDS

TDD-LTE Bands 42 (3.5 GHz band) and 43 (3.7 GHz band) are each 200 MHz wide, representing a significant addition to the available LTE bandwidth. Because of the propagation loss at the high frequencies used by these bands, their biggest value may be for relatively short-range applications, such as enabling speedy video downloads in dense urban areas.

Band 42 may see its first sizable deployment in Japan around 2016, as part of the program to support the 2020 Olympics. In a pilot test using Band 42, a Japanese carrier has already demonstrated very high throughput of 1 Gbps. BAW filters will be well suited to this band, providing better performance in a smaller package size than other technologies. Band 43 is likely to enter use later than Band 42; it presents similar benefits and challenges, and will likewise be best served by BAW filters.

Also on the horizon is LTE Unlicensed – the proposed use of LTE in unlicensed spectrum, notably the 5 GHz range. As with the 3.5 GHz bands, propagation characteristics in this band will likely mean LTE-U is used primarily for shorter-range communications. Some of the 5 GHz spectrum is already used for Wi-Fi. Transmitting data over LTE rather than Wi-Fi may offer advantages for video and other traffic types that can benefit from LTE's enhanced quality of service (QoS) and scheduling capabilities.

CONCLUSION

New spectrum bands and application requirements are creating increasingly difficult filtering challenges. The need to meet these requirements over a wide temperature range has driven the development of new, more temperature-compensated SAW and BAW filters. These filters enable system designers to solve coexistence problems in crowded RF spectrum which are as yet unaddressed by any other technology.

Temperature-compensated Low-Drift and NoDrift filters enable operators and manufacturers to achieve new levels of wireless spectral efficiency. Their extremely precise selectivity means operators and manufacturers can deliver higher speeds and greater bandwidth by utilizing spectrum that might be lost with older filtering technologies due to the need for additional design allowances.

As packaging technologies help to shrink filter size and enable handsets to support the growing number of bands, filter technologies are also evolving to meet future challenges such as new LTE bands that use higher-frequency regions of the spectrum. ■

HIGH POWER

100 MHz to 20 GHz

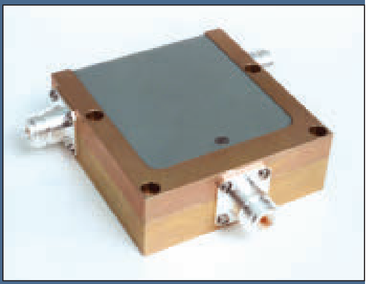

For Military/Radar Applications.

Isolators/Circulators

As one of the leading suppliers of ferrite components in the industry, UTE Microwave has pioneered innovative designs, quality craftsmanship and exceptionally high quality products. Custom designs, standards...many of them off-the-shelf, are the result of over 35 years of experience in the industry. UTE Microwave continues this tradition with new products for ever changing applications. Our broad line of HIGH POWER, low loss circulators and isolators spans the spectrum from below 100 MHz in coax/stripline units to waveguide devices at 18 GHz for both peak and average powers.

100 MHz HIGH POWER Circulator for Medical, Scientific and Industrial applications

A new HIGH POWER Circulator suitable for FM Broadcast, Scientific and Medical applications is now available. The unit provides 10 MHz bandwidth in the 85–110 MHz spectrum.

Specifications are 20 dB min. isolation, 0.3 dB max. loss and 1.25 max. VSWR. Operating power is 1 kW average and 25 kW peak. The 8-1/2" hex x 2" thick unit operates over a 15°–50° C temperature range. DIN 7/16 connectors are standard. Other units are available at higher frequencies.

HIGH POWER Drop-in Series

A broad line of low loss HIGH POWER Drop-in circulators are available from VHF to Ku band including Kilowatt average power levels at VHF thru S band. L and S band radar are a specialty. A few of these are shown here.

A) 2.7–3.1 GHZ 1 kW pk, 100 W av

B) 1.2–1.4 GHZ 3 kW pk, 300 W av

C) UHF TV Band 5 kW pk, 500 W av

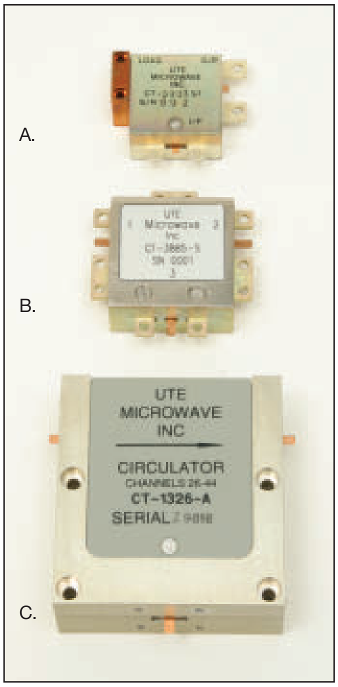

Our "POWER-LINE" serves the COMMUNICATIONS, TELECOM, MEDICAL, SCIENTIFIC, TV, PCS and INDUSTRIAL markets.

The following models are examples of our High Power units

Model No.	Power	Connectors	Freq. Range
CT-1542-D	10 Kw Pk 1 Kw Av	DIN 7/16	420–470 MHz
CT-2608-S	3 Kw Pk 300 W Av	"Drop-in"	1.2–1.4 GHz
CT-3877-S	2.5 Kw Pk 250 W Av	"Drop-in"	2.7–3.1 GHz
CT-3838-N	5 Kw Pk 500 W Av	N Conn.	2.7–3.1 GHz
CT-1645-N	250 W Satcom	N Conn.	240–320 MHz
CT-1739-D	20 Kw Pk 1 Kw Av	DIN 7/16	128 MHz Medical

Broadband Units • Common Band Devices • High Isolation Units • Multiport Devices • Drop-In Devices • Wireless/PCN Devices • High-Power Industrial/Medical Iso Adaptors Waveguide Junctions • High-Power TV Units • VHF and UHF Devices

sales@utemicrowave.com

FEATURES:

- Power levels to 5 KW CW, 75 KW Pk.
- Low Intermod Units
- Low Loss Options
- Extended Octave Bandwidths
- Power Monitors and DC Blocks
- Iso Filter-Monitor Assemblies

UTE MICROWAVE INC.

3500 Sunset Ave., Asbury Park, NJ 07712
Tel: 732-922-1009 Fax: 732-922-1848
E-mail: info@utemicrowave.com

Contact us for more information on our extensive product line and current catalog. We accept Visa, MC, Amex

Selecting Circuit Materials for Microwave Power Amps

John Coonrod
Rogers Corp.

Demand is growing for microwave power amplifiers (PA) due to an increasing number of applications, from commercial cellular systems to military radars that rely on amplified high-frequency signals. Solid-state microwave PAs depend on the characteristics of their active devices, but they also depend a great deal on the behavior and performance of their printed-circuit-board (PCB) materials for such functions as minimizing loss, maximizing gain and efficiently dissipating heat. Solid-state amplifier designers currently have a wide range of PCB materials to choose from. Sorting through these materials to make a suitable choice for a PA application can require careful comparison of some key PCB material properties, including the relative permittivity (or dielectric constant, ε_r) and the dissipation factor (tan δ). But many other PCB material parameters must be considered when choosing a substrate for a microwave PA, including thermal conductivity, temperature coefficient of dielectric constant (TCDk), copper surface roughness, tolerance of ε_r and even the tolerance of the PCB material's thickness. Understanding how these different PCB material properties relate to microwave PA performance can help in sorting through the many PCB material choices currently available and help enable the design of a microwave PA that not only meets its performance goals, but is dependable and reliable under a wide range of operating conditions.

Design and fabrication of a microwave PA requires control of a number of different parameters, with impedance control among the most important. Since a microwave PA may interact with or include many different types of components, such as impedance matching networks, quarter-wave transformers and 3 dB quadrature couplers as part of a larger circuit or system, the characteristic impedance of the amplifier circuitry, which is usually 50 Ω, should be tightly controlled. The circuit material ε_r tolerance is one key material parameter to consider when controlling impedance. Although designers may often assume that circuit material ε_r tolerance is the most critical material parameter for achieving good impedance control, this is typically not the case. In truth, when using a relatively well-controlled, high-frequency circuit laminate, the ε_r tolerance will generally be fairly tight and one of the lesser concerns in terms of impedance control. ***Table 1*** provides an example, assuming a 50 Ω microstrip transmission line on a high-frequency circuit laminate with nominal ε_r of 3.5 and ε_r tolerance of ±0.05.

TABLE 1

ILLUSTRATION OF TYPICAL VARIANCES IMPACTING THE CHARACTERISTIC IMPEDANCE OF A MICROSTRIP PCB

ε_r	Substrate Thickness (mils)	Copper Thickness (mils)	Conductor Width (mils)	Characteristic Impedance (ohms)	Difference of Impedance (ohms)	Comment
Microstrip transmission line circuit using 20 mil thick high frequency laminate						
3.5	20	2	43	50.07		Baseline for comparisons
3.5	18	2	43	46.86	3.21	Substrate is 10% thinner than baseline
3.45	20	2	43	50.39	0.32	ε_r lower by 1.4% from baseline
3.5	20	1	43	50.70	0.63	Copper thickness reduced by 1 mil from baseline
3.5	20	2	42	50.78	0.71	Conductor width reduced by 1 mil from baseline
Microstrip transmission line circuit using 10 mil thick high frequency laminate						
3.5	10	2	21	49.74		Baseline for comparisons
3.5	9	2	21	46.57	3.17	Substrate is 10% thinner than baseline
3.45	10	2	21	50.05	0.31	ε_r lower by 1.4% from baseline
3.5	10	1	21	50.78	1.04	Copper thickness reduced by 1 mil from baseline
3.5	10	2	20	51.16	1.42	Conductor width reduced by 1 mil from baseline

IMPEDANCE VARIABLES

Table 1 shows the impact of some common variables associated with PCB technology on the impedance of a PCB-based microstrip transmission-line circuit. It is divided into two groups of data, with the top section for a thicker circuit (20 mil thick substrate) and the lower section relating the same information for a thinner circuit (10 mil thick substrate). Comparing the two groups of data shows that thinner circuits are more sensitive to conductor effects, which means that variations in circuit conductor width and copper thickness will also impact the changes in impedance.

For example, a PCB with plated-through-hole (PTH) technology uses additional copper plated on top of the original laminate copper to achieve the PTH features. The amount of additional copper can vary from circuit-to-circuit and from batch-to-batch of fabricated circuits. Copper thickness plating tolerance of ±0.5 mils is common in the high-frequency industry although some circuit fabricators can achieve and maintain even tighter tolerances. Based on this tolerance value, a 1 mil range in different copper thicknesses for the same circuit design is not uncommon and, as noted earlier, the thinner the circuit material, the larger the impact in terms of impedance variations.

In addition to concerns of copper conductor thickness, the tolerance of the width of the conductor is also a concern in maintaining consistent impedance for a PCB-based PA. A tolerance of ±0.5 mils is again not uncommon in the high-frequency industry for the width of a copper conductor on a PCB, although many fabricators can achieve and maintain even tighter tolerances for the width of a copper conductor. For a tolerance of ±0.5 mils, the variation in copper conductor width is 1 mil, and thinner circuits will be more affected in terms of impedance by these conductor-width variations than thicker circuits.

One of the circuit material parameters shown in Table 1 with a significant impact on maintaining consistent impedance is the tolerance of the circuit substrate thickness. For the example in Table 1, the substrate thickness tolerance of ±10 percent has the greatest effect on the variations in circuit impedance. While this value of circuit material thickness tolerance is not uncommon, high-frequency laminates with better thickness tolerance values are available, which can maintain greater control of impedance for circuits such as microwave PAs.

The ε_r variation shown in Table 1 is one sided and only shows the negative portion of the tolerance. An ε_r tolerance of ±0.05 for a nominal circuit material ε_r of 3.5 represents a minus variation in ε_r of approximately 1.4 percent. But because it is a tolerance range with "plus" and "minus" limits, the actual deviations in ε_r can be a range that is twice that value, with changes of ε_r of 0.1 possible, or a percentage of 2.8 percent of the total circuit material ε_r value of 3.5. This parameter is not easy to portray in Table 1, but it should be noted that it will be the least-significant issue for the thinner (10 mil thick) circuit material and the next-to-least significant issue for the thicker (20 mil thick) circuit

Planar Monolithics Industries, Inc.

Offering State-Of-The-Art RF and Microwave Components & Integrated Assemblies From DC to 40GHz

PMI PUSHES THE LIMITS OF MIC & MMIC TECHNOLOGY & TECHNIQUES

- Amplifiers
- Attenuators - Variable
- DLVA & ERDLVA & SDLVA's
- DTO's & Frequency Synthesizers
- Filters
- Form, Fit & Function Products
- IFM's & Frequency Discriminators
- Integrated MIC/MMIC Modules
- I/Q Vector Modulators
- Limiters & Detectors
- Log Amplifiers
- Pulse & Bi-Phase Modulators
- Phase Shifters
- Rack & Chassis Mount Products
- Receiver Front Ends & Transceivers
- Single Sideband Modulators
- SMT & QFN Products
- Solid-State Switches
- Switch Matrices
- Switch Filter Banks
- Threshold Detectors
- USB Products

18.0 to 40.0GHz Millimeter Wave Quad Phase & Amplitude Matched, Diplexed & Selective Receiver Front End

PMI MODEL NO. DGM-18G40G-292FF-DS

- Frequency Range : 18.0 to 40.0GHz
- Gain : 3.0dB min, 7.0dB max
- Amplitude Ripple : ±1.0dB Over Every 500 MHz
- Phase Matching : 40° RMS, Channels 2,3,4 to Ref, Channel 1 Over Operating Temperature
- Diplexer K Band 1dB Passband : 18.0GHz min, 25.0GHz max
- Diplexer Ka Band 1dB Passband : 28.0GHz min, 40.0GHz max
- Crossover Band : 25.0GHz min, 28.0GHz max
- Crossover Excess Attenuation : 5dB
- Stopband Attenuation : 60dB
- Communication Interference Immunity : 53dBm Pulsed RF, 900MHz - 2.5GHz Without Limiter or Amplifier Saturation

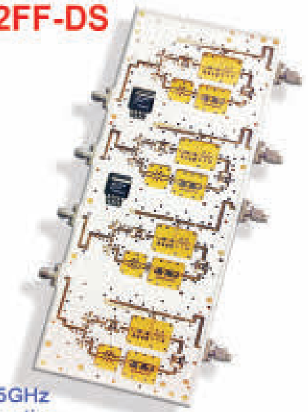

Functional Block Diagram

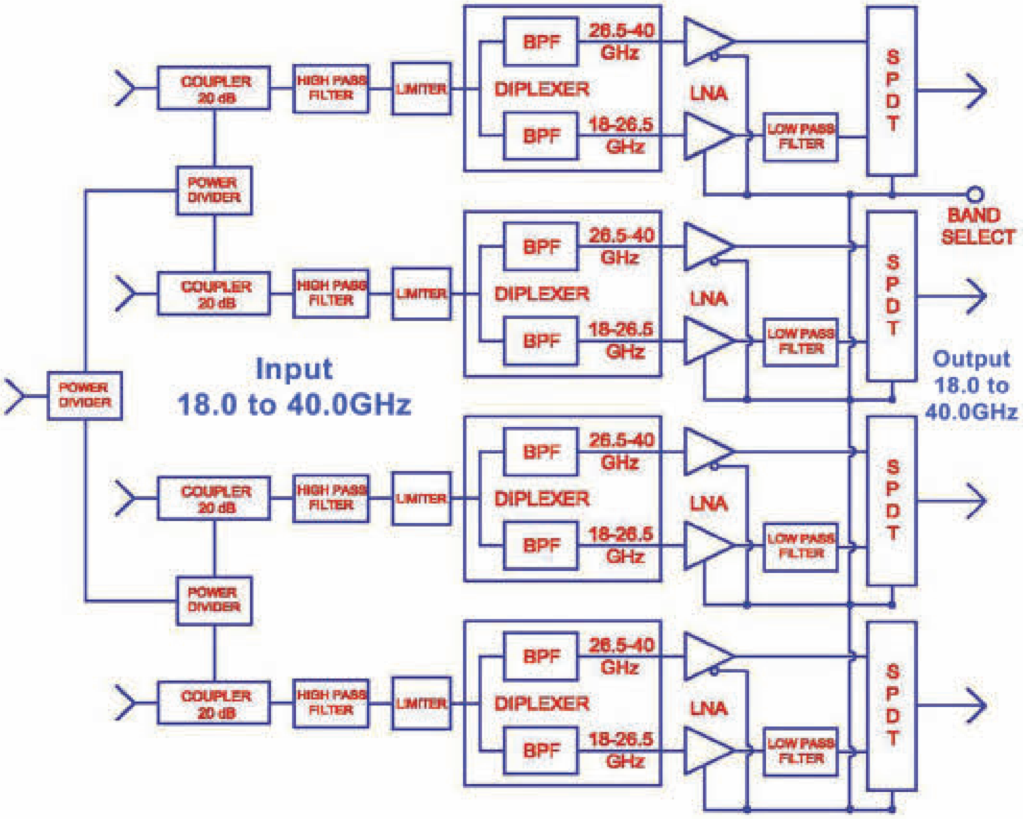

West Coast Operation:
4921 Robert J. Mathews Pkwy, Suite 1
El Dorado Hills, CA 95762 USA
Tel: 916-542-1401 Fax: 916-265-2597

East Coast Operation:
7311-F Grove Road
Frederick, MD 21704 USA
Tel: 301-662-5019 Fax: 301-662-1731

ISO9001:2008 REGISTERED
Email: sales@pmi-rf.com

ISO9001:2008 REGISTERED
Website: www.pmi-rf.com

Hermetic Sealing, High Reliability to Mil-Std-883, Small Quantity Requirements accepted & we offer Custom Designs too material. A circuit material with this nominal ε_r value and tolerance is considered quite good for many high-frequency circuit applications, although circuit materials are available with even tighter ε_r tolerance control.

INSERTION LOSS VARIATIONS

Circuit materials with low insertion loss play a major role in achieving maximum gain in a microwave PCB-based microwave PA. PCB insertion loss is made up of four components: conductor loss, dielectric loss, radiation loss and leakage loss. At lower microwave frequencies, dielectric and conductor losses account for most PCB insertion loss; which of the two parameters is dominant depends upon the thickness of the circuit substrate material. ***Figure 1*** shows three insertion loss charts for 50 Ω microstrip transmission-line circuits based on the same circuit material, although with different material thicknesses. The insertion loss models were generated with MWI-2014 circuit material analysis and modeling software from Rogers Corp. which uses closed-form equations from Hammerstad and Jensen[1] regarding microstrip impedance and loss predictions.

The three charts in Figure 1 compare measured and computer-modeled results. The measured insertion loss results were collected using a simple microstrip differential length method,[2] which minimized the contributions of insertion loss due to connectors and signal launches. The modeled insertion loss consisted of dielectric and conductor losses and, as can be seen from the plotted data, the modeled data for the total loss agreed fairly closely with the measured results. For simplicity, losses due to radiation and leakage were ignored in this comparison.

Figure 1 shows that insertion loss for a thin circuit (a) is dominated by conductor loss. For the thicker circuit (c), the dielectric and conductor loss contributions to circuit material insertion loss are about equal. If data for yet another, thicker (30 mil thick) circuit material had been added to Figure 1, it would have shown that dielectric loss would dominate the contribution to insertion loss. By knowing which loss components impact the insertion loss the most, a designer can select a material (and thickness) that will provide the optimum insertion loss performance for an application. In the 30 mil thick case not shown, changes in the dissipation factor had the greatest effect on the circuit material's insertion loss properties. For the thin circuit material in ***Figure 1a***, the inser-

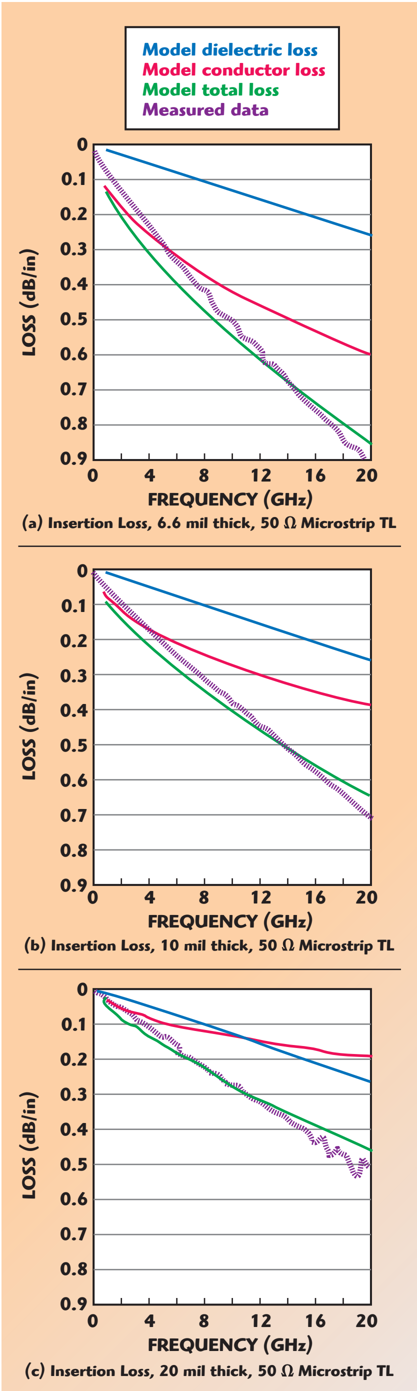

▲ *Fig. 1 Insertion loss showing the relationship of thickness to dielectric and conductor loss.*

tion loss was most affected by conductor loss, reiterating that changes to the circuit material's conductor properties will have the greatest impact on the circuit's insertion loss performance.

The copper surface roughness of a high-frequency circuit material can have an impact on the material's conductor loss.[3] A circuit material with a rough copper surface will have increased conductor loss compared to the same circuit material with a smooth copper surface. How much the circuit material's conductor loss will change with a change in copper surface roughness will depend on how much the conductor losses dominate the material's insertion loss. For the insertion loss of the thin circuit material shown in Figure 1a, a change in copper surface roughness will have a significant impact on the circuit material's insertion loss. For a thicker circuit material, the same change in copper surface roughness will not impact the material's insertion loss performance as much, and adjustments to the thicker material's dissipation factor would have more impact on the insertion loss of the thicker circuit material.

To better understand how the copper surface roughness of a circuit material can impact the insertion loss for different thicknesses of the same circuit substrate material, ***Figure 2*** shows microstrip transmission line circuits fabricated on the same substrate, but with different material thicknesses and copper surface roughness. The plots show circuit materials with a standard level of copper surface roughness at 2.8 µm RMS compared to LoPro™ laminate from Rogers Corp. with copper surface roughness of only 0.8 µm RMS. As shown, the benefits of a smoother copper surface for circuit insertion loss are much greater for the thinner circuits than the thicker circuits, with a difference in insertion loss of about 0.3 dB/in for the 7.3 mil thick circuit (when switching to the smoother copper surface) compared to a difference of about 0.1 dB/in for the 20 mil thick circuits.

Circuit material insertion loss is a concern for PA designers for a number of reasons, one of which is thermal management. A PA built on a PCB with higher insertion loss will generate more heat per applied amount of RF/microwave power than the same PA built on a PCB with lower insertion loss. This heat that is generated contributes to a PCB's maximum operating temperature (MOT) specification, and the PCB's MOT should not be exceeded for any prolonged period of time. PA designers typically try to minimize insertion loss with consideration of applied power and frequency to ensure that the MOT will not be exceeded. A thinner circuit can have more insertion loss than a thicker circuit; however, it can also enjoy the benefits of shorter heat flow paths to the ground plane and an attached heat sink to offset the heat generated by the higher insertion loss. Additional electrical-thermal interactions which impact thermal management were outlined in a recent article.[4]

A circuit material's TCDk is often overlooked by PA designers, and it is a parameter that greatly affects PA performance if not considered when selecting circuit materials. Quite simply, TCDk is the amount that the dielectric constant, ε_r, will change with a change in temperature. It is often apparent when a circuit has been operated in a controlled environment, in a laboratory, for example, which provides stable performance. When the PA is moved into the field, where

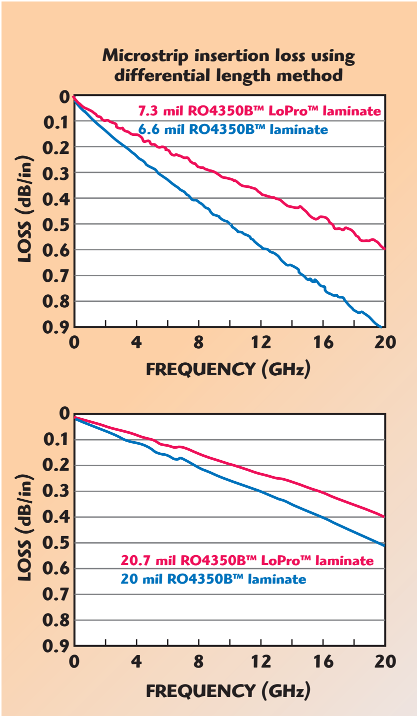

▲ *Fig. 2 Comparison of smooth and rough copper surface on the same substrate at different thicknesses.*

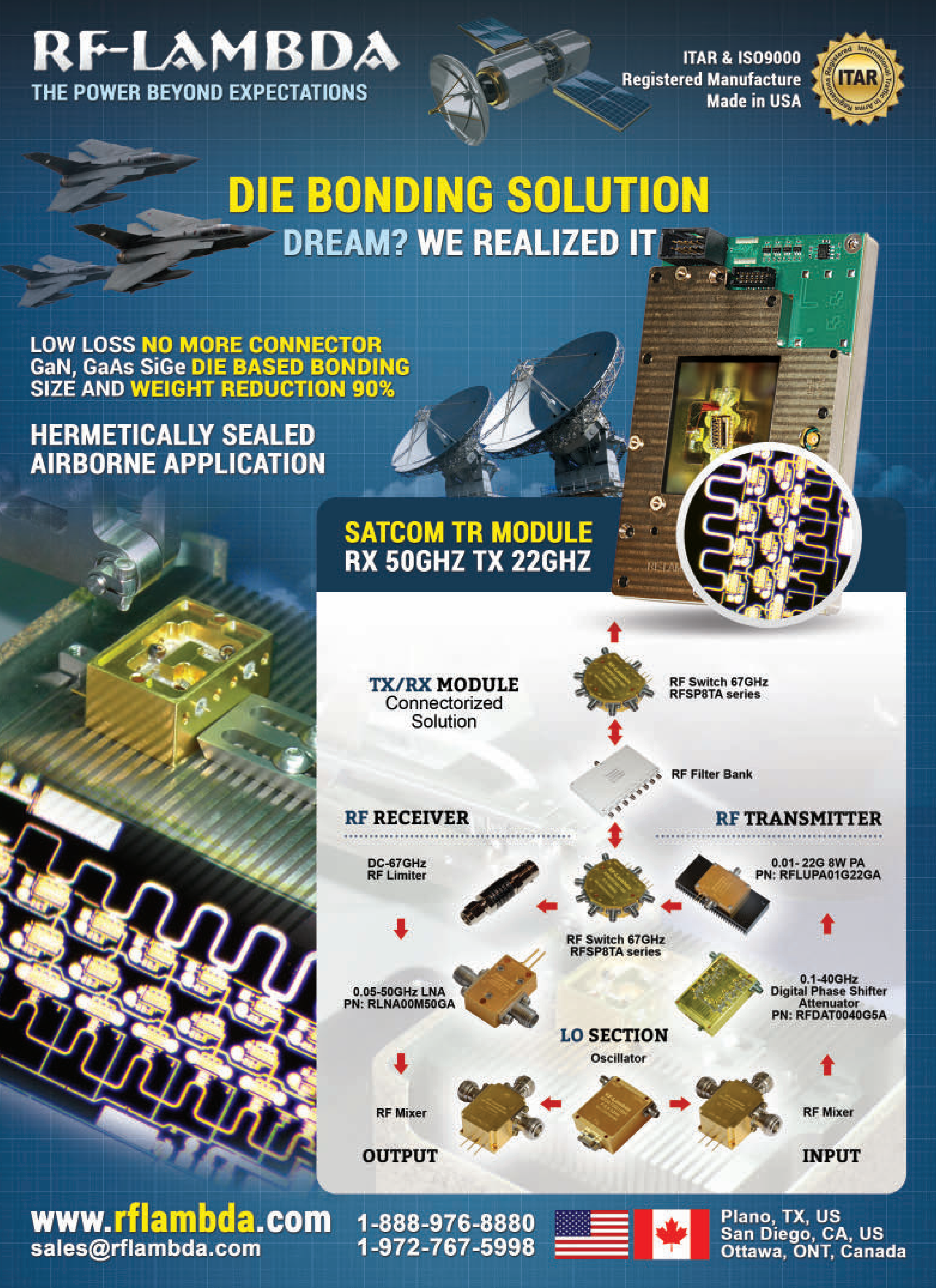
RF-LAMBDA
THE POWER BEYOND EXPECTATIONS
ITAR & ISO9000
Registered Manufacture
Made in USA
ITAR
DIE BONDING SOLUTION
DREAM? WE REALIZED IT
LOW LOSS NO MORE CONNECTOR
GaN, GaAs SiGe DIE BASED BONDING
SIZE AND WEIGHT REDUCTION 90%
HERMETICALLY SEALED
AIRBORNE APPLICATION
SATCOM TR MODULE
RX 50GHZ TX 22GHZ
TX/RX MODULE
Connectorized
Solution
RF Switch 67GHz
RFSP8TA series
RF Filter Bank
RF RECEIVER
RF TRANSMITTER
DC-67GHz
RF Limiter
0.01- 22G 8W PA
PN: RFLUPA01G22GA
RF Switch 67GHz
RFSP8TA series
0.05-50GHz LNA
PN: RLNA00M50GA
0.1-40GHz
Digital Phase Shifter
Attenuator
PN: RFDAT0040G5A
LO SECTION
Oscillator
RF Mixer
RF Mixer
OUTPUT
INPUT
www.rflambda.com
sales@rflambda.com
1-888-976-8880
1-972-767-5998
Plano, TX, US
San Diego, CA, US
Ottawa, ONT, Canada

TABLE 2
THERMAL PROPERTIES OF COMMON MATERIALS USED IN MICROWAVE PCB POWER AMPLIFIER APPLICATIONS

	TCDK (ppm/°C)	Thermal Conductivity (W/m/K)
Typical Woven Glass PTFE laminate	-150	0.25
Modified PPE laminate	70	0.35
Ceramic filled PTFE laminate	-30	0.50
RO4350B™ laminate	50	0.64
RT/duroid® 6035HTC laminate	-66	1.44

the temperature may be changing and spans a much wider range, the performance of the circuit changes with the change in temperature. The result is a change in ε_r which can cause impedance shifts and performance variations. The TCDk parameter provides a way to compare this behavior for different circuit materials. Many PCB-based PAs will generate heat during normal operation and can create their own temperature change in addition to temperature changes from environmental effects.

Some low-loss polytetrafluoroethylene (PTFE) laminates used for microwave applications exhibit relatively high TCDk values, which can be a concern for applications designed for a wide range of operating temperatures. Ceramic-filled PTFE circuit materials tend to provide better TCDk properties and are better suited for applications that must handle wide operating temperature ranges.

THERMAL CONDUCTIVITY

PCB thermal conductivity is an important circuit material parameter for PA designers. Because of the circuit trace heating exhibited by higher-power PAs, they are often mounted on heat sinks. For PAs with high levels of trace heating, the thermal path to the heat sink is often through the circuit substrate material, and the heat flow path will be through the substrate. In such a case, the PCB thermal conductivity will provide a measure of the circuit material's capability to transfer any heat generated in the circuit traces to the heat sink, with higher values of PCB thermal conductivity sought for PAs operating at higher power levels.

Table 2 shows typical values of circuit materials commonly used for PCB-based microwave PA applications. In general, TCDk numbers closer to zero in a mathematical absolute value sense are more ideal. In terms of thermal conductivity, higher values are better. As a rule of thumb, a good value of thermal conductivity for a PA circuit is 0.50 W/m/K or higher.

ATTACHING A HEAT SINK

Thermal management is a critical component for achieving high reliability in any microwave PA, and an important step in this process involves attaching the microwave PA PCB to a heat sink. Several options are available for attaching the PA PCB's ground plane to a heat sink, including mechanical screw-down fasteners, sweat soldering and applying thermally and electrically conductive adhesive (TECA). Each approach offers its own set of capabilities and limits. TECA can provide a very uniform and consistent bond without voiding or air gaps. In the past, some TECA materials have had issues with delamination through lead-free solder reflow, or they would suffer changes in electrical properties at elevated temperatures. But the latest generation of TECA materials solved these problems and provided consistent and reliable performance, even at elevated temperatures.

To better understand the use of TECA and its impact on PCB material insertion loss, a simple experiment was performed: a 10 mil thick microstrip transmission-line circuit, TECA and a thick copper heat sink was assembled in the configuration shown in ***Figure 3***. The transmission-line circuit was initially evaluated for insertion loss using the differential-length method, testing the circuit as a microstrip transmission line without the addition of the TECA or heat sink. The TECA and heat sink were then attached through a lamination process, and the insertion loss was tested with the TECA and heat sink as part of the ground return path, since end launch connectors were used and


You Have Our Undivided
ATTENTION
www.ewtfilters.com
We understand how critical your applications are. That's why you'll always have our *Undivided Attention*.
Offering more than 40 years of experience in custom design & manufacturing of RF and Microwave filters and filter based products to 50 GHz.
Military • Commercial
Wireless • Space
Eastern Wireless TeleComm, Inc.
Tel: 410.749.3800 Fax: 410.749.4852
sales@ewtfilters.com

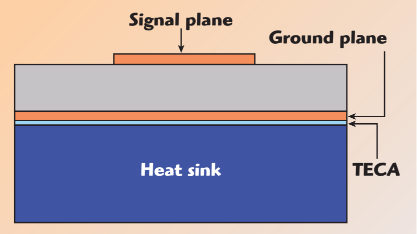

▲ *Fig. 3 Test vehicle configuration to evaluate the use of TECA and its influence on insertion loss.*

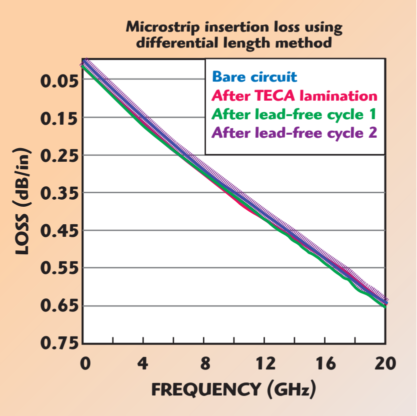

▲ *Fig. 4 Microstrip insertion loss testing of bare circuit, then following TECA attachment to heat sink and two lead-free solder reflow cycles.*

the ground was being picked up from the bottom of the circuit (the heat sink in this case). Following these measurements, the circuit assembly was subjected to a lead-free solder reflow cycle two times and the insertion loss was tested again. As ***Figure 4*** shows, there is no difference in insertion loss for the microstrip circuit with the addition of the TECA and heat sink, or with the completion of the lead-free solder reflow cycles. The TECA used in this study appears to perform after reflow cycles.

CONCLUSION

In general, some basic parameters can serve as guidelines when selecting circuit materials for microwave PA applications. A candidate PCB material for a microwave PA should have an ε_r tolerance that is ±1.5 percent or better, low dissipation factor, low insertion loss (possibly a PCB material with smooth copper), low TCDk and high thermal conductivity. In addition to these recommendations and the circuit fabrication guidelines of Table 1 for minimizing impedance variations, circuits with a conductor width tolerance of ±0.5 mil or better are recommended for microwave PA designs, as well as the same tolerance and value for copper plating thickness.

Selecting circuit materials for microwave PAs is never routine and it is always a good idea to have the circuit material supplier involved in the selection process, helping evaluate basic design and circuit fabrication considerations. A circuit material supplier's experience with many different high-frequency circuits can lend a great deal of valuable guidance to a specific microwave PA design. ■

References

1. E. Hammerstad and O. Jenson, "Accurate Models of Microstrip Computer Aided Design," *1980 MTT-S International Microwave Symposium Digest*, May 1980, pp. 407-409.
2. John Coonrod, "Methods for Characterizing the Dielectric Constant of Microwave PCB Laminates," *Microwave Journal*, May 2011.
3. J.W. Reynolds, P.A. LaFrance, J.C. Rautio and A.F. Horn III, "Effect of Conductor Profile on the Insertion Loss, Propagation Constant and Dispersion in Thin High Frequency Transmission Lines," *DesignCon 2010*.
4. John Coonrod, "The Impact of Electrical and Thermal Interactions on Microwave PCB Performance," *Microwave Journal*, February 2014.


THE FUTURE
IS CALLING...HOW WILL YOU
CONNECT TO IT?
4.1/9.5
Mini DIN
Delta's 4.1/9.5
Mini DIN series
of coaxial connectors were
developed to meet the growing
demands of today's high performance mobile communications systems.
The 4.1/9.5 Mini DIN has an operational frequency range of DC-14 GHz, offers excellent VSWR performance and Low Passive Intermodulation (Low PIM) >165 dBc, making it ideally suited for use in Base Stations, Distributed Antenna Systems (DAS) and Small Cell applications.
Features
• IEC standardization
• 30% smaller and lighter compared to 7/16
• Reduced center to center spacing
• Albaloy Plate
Benefits
• Global standard interface
• Increased package density
• LOW PIM: >165 dBc
Get your copy of our new 4.1/9.5 Mini Din catalog, contact Delta today!
DELTA
ELECTRONICS MFG. CORP.
Connect Here.
AS9100/ISO 9001:2008
CERTIFIED
ROHS
COMPLIANT
(978) 927-1060 • www.deltarf.com

MWJ REVIEW BOARD APPROVED

Second Harmonic Tuning for a Broadband High Efficiency GaN Power Amplifier

Qiao Ke, Tang Zongxi
University of Electronic Science and Technology of China, Chengdu, China

A new method for designing a harmonically tuned wideband power amplifier (PA) achieves high efficiency over a wide bandwidth. The operating bandwidth is divided into two bands in which the second harmonic output impedances of each are controlled for higher power added efficiency (PAE) and output power. To validate this approach, a broadband GaN power amplifier is designed to operate in the 2.1 to 2.7 GHz range. The frequency band is divided into two bands, 2.1 to 2.4 GHz and 2.4 to 2.7 GHz with their second harmonic output impedances each controlled to improve PAE and output power. The measured power output is greater than 40 dBm and the efficiency is better than 60 percent between 2.1 and 2.7 GHz. The power gain is better than 12 dB and the flatness is less than 1.5 dB in the design band.

In modern cellular base stations, output power, efficiency and linearity are the key requirements in the design of the PA. But with the growing number of wireless services, there is an increasing demand for wideband communication systems. The narrow frequency band power amplifier cannot meet future demands for massive data transmission; so bandwidth is another important design specification.

Although very high efficiencies have been recently reported for Class-F and Class-F^{-1} PAs,[1-3] the use of harmonic traps in the load network makes the bandwidth of these amplifiers rather narrow. Some wideband switched power amplifiers have been designed, including wideband Class E PAs,[4-6] but are limited by load conditions. Harmonic tuning is good for high efficiency,[7-10] but is not suitable for broadband operation. If the operating band is segmented, however, we show that harmonic tuning can provide broadband performance.

HARMONICALLY TUNED PA DESIGN

Generally, the second and the third harmonic output impedances are important for efficiency and output power. Impedances at higher harmonics have less effect on efficiency and increase the complexity of the circuit. Thus, in order to simplify the circuit and improve efficiency, only the second harmonically tuned GaN power amplifier is considered.

Figure 1a shows a typical second harmonically tuned circuit. The length of the TL2 transmission line is $\lambda/4$ at the fundamental center frequency (f_0), open for odd harmonics, but shorted for even harmonics. The optimal reflection coefficient for the second harmonic

(Γ_{2f0}) is obtained with the TL2 and TL1 transmission lines. Over a broad bandwidth, however, the λ/4 transmission line is not a perfect short at the second harmonic, and in turn, the reflection coefficients of second harmonic frequencies for wideband operation are not optimum. In order to optimize second harmonic output impedances for wideband performance, the operating band is divided into two frequency bands (low band and high band) and the harmonic impedances are separately controlled for each band.

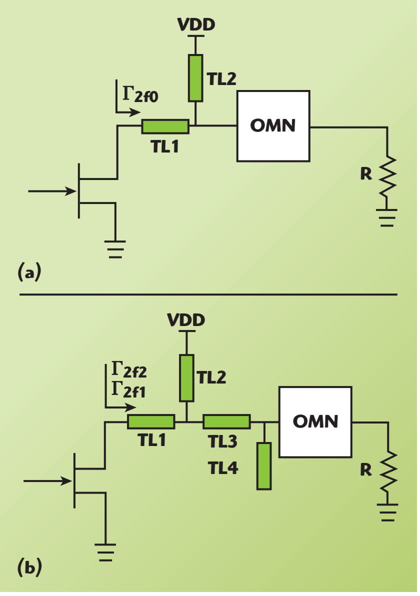

▲ *Fig. 1 Harmonically-tuned power amplifiers: traditional design (a) wideband design (b).*

In the new circuit, shown in ***Figure 1b***, the second harmonic reflection coefficients (Γ_{2f1}, Γ_{2f2}) are determined by TL1, TL2, TL3 and TL4. TL1 and TL2 are used to tune the low band, while TL1, TL3 and TL4 are used to tune the high band. The length of TL1 is λ/4 at the low band center frequency (f_1) and length of TL4 is λ/4 at the high band center frequency (f_2).

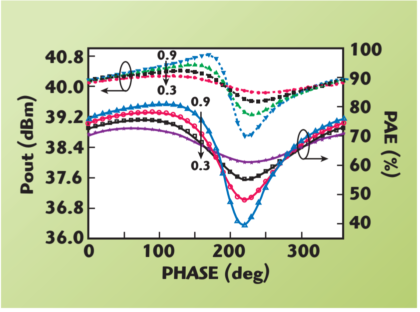

▲ *Fig. 2 Efficiency and output power versus second harmonic load reflection coefficient (f = 2.4 GHz, VDD = 28 V, VGS = –2.7 V).*

To determine the effect of the harmonic terminations at the output, the second harmonic reflection coefficients are swept during load-pull simulations while the fundamental source and load impedances are kept constant. ***Figure 2*** shows the efficiency and output power of the device versus phase variation of the second harmon-

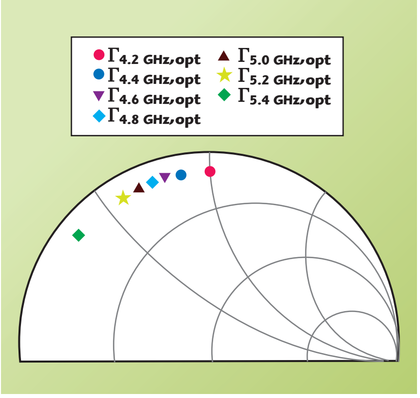

▲ *Fig. 3 Optimal second harmonic reflection coefficient.*

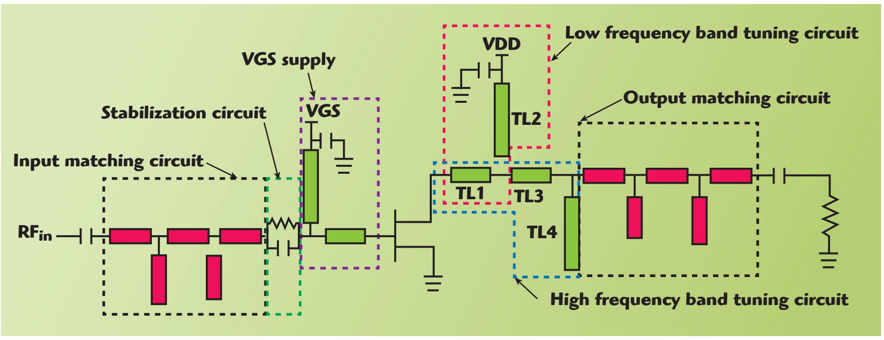

▲ *Fig. 4 Matching scheme of the harmonically-tuned power amplifier.*

ic reflection coefficient at different reflection coefficient magnitudes ranging from 0.3 to 0.9, with an interval of 0.2. The change of efficiency and output power with phase is apparent for a fixed magnitude of reflection coefficient. In particular, when the phase = 220°, PAE and Pout are significantly lower. In the process of designing the power amplifier, these phases should be avoided.

In general, the optimal second harmonic reflection coefficient is

$$\Gamma_{second,opt} = magnitude \cdot exp(j \cdot phase) \quad (1)$$

in which the magnitude is close to 1 on the edge of the Smith Chart (see ***Figure 3***). The second harmonic input reflection coefficient, which also has an impact on efficiency and output power can be adjusted with the input λ/4 line of the DC choke.

The design band is 2.1 to 2.7 GHz, which includes a number of communications standards like the W-CDMA downlink bands of 2.11 to 2.17 GHz, and 2.6 GHz as defined by TD-LTE. A 10 W GaN HEMT (CGH40010F) from Cree Inc., is selected as the PA device. Input and output fundamental impedances and output second harmonic impedances are obtained from load and source-pull measurements. Given that the length of TL2 is λ/4 at 2.2 GHz, TL1's electrical length is adjusted to provide suitable second harmonic output impedances over the operating band of 2.1 to 2.4 GHz. Given that the length of TL4 is λ/4 at 2.6 GHz, TL3's electrical length is adjusted to provide suitable second harmonic output impedances over the operating band of 2.4 to 2.7 GHz. Finally, input and output wideband matching is performed at the fundamental. The complete matching scheme is shown in ***Figure 4***.

Figure 5 shows the simulated drain voltage as a function of time for different frequencies. With optimized fundamental and harmonic impedances, the voltage waveform is similar to the ideal voltage waveform when the maximum PAE is achieved at an output power of 10 W. The bottom of the voltage waveform is flat and there is little overlap of current and voltage between 2.1 and 2.7 GHz, so the power dissipation is small.

EXPERIMENTAL CHARACTERIZATION

The broadband second harmonically tuned PA is fabricated on a dielectric substrate (RO4350, ε_r=3.66, h=0.508 mm) as shown in ***Figure 6***. With a continuous wave (CW) input signal and biased with VDD=28 V and VGS=-2.7 V, the PA has a small-signal

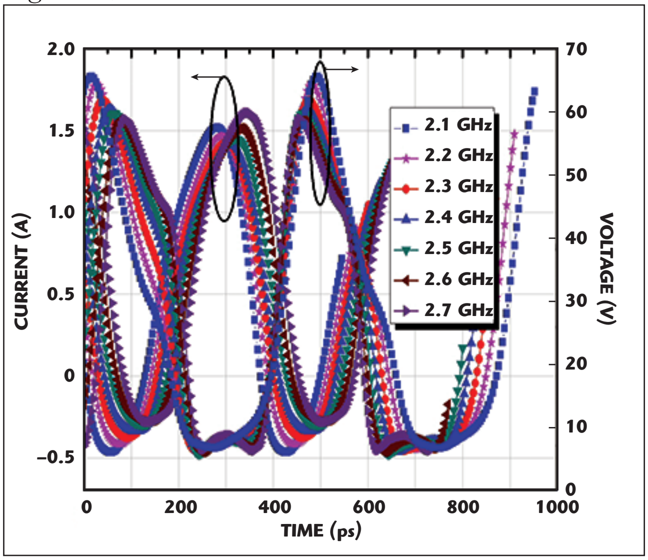

Fig. 5 Simulated drain voltage and current waveforms (VDD = 28 V).

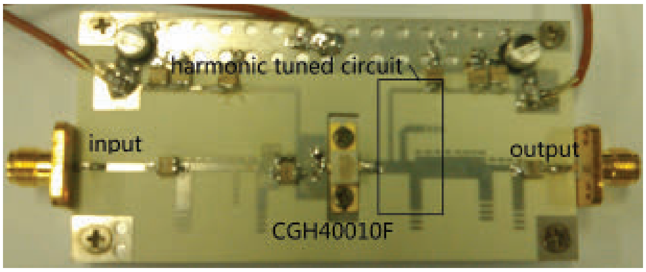

Fig. 6 Photograph of the assembled harmonically tuned power amplifier.

Control the comb.
Control the clarity.

COBHAM

The most important thing we build is trust

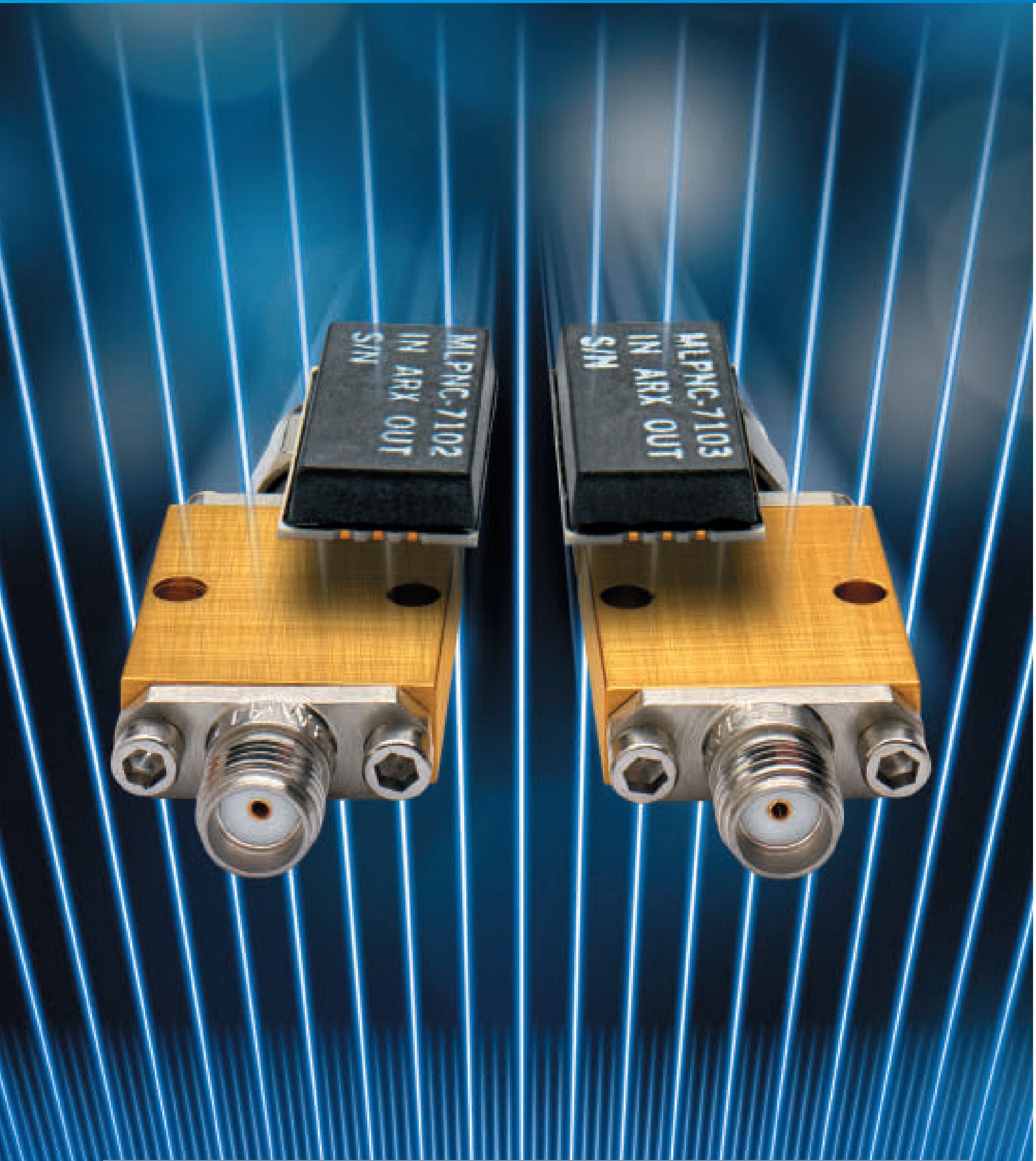

The sensitivity and the distance you've been striving for from your radar or surveillance receiver is now within reach. New GaAs comb generators from Aeroflex / Metelics are a best-in-class, nonlinear transmission line (NLTL) innovation that provides 10 to 18 dB lower phase noise for better sensitivity than Si step recovery diode (SRD) comb generators. Offering phase noise as low as -135 dBc/Hz at 100 Hz offset from the 12 GHz harmonic, the MLPNC series creates clean, low-conversion-loss harmonics to 30 GHz over variable input frequencies from 400 to 1300 MHz. Their variable input power from 21 to 23 dBm make them easy to drive and operate. They provide ultimate system design flexibility and the opportunity to simplify your system architecture.

Nonlinear Transmission Line GaAs Comb Generators

Part Number	Power (dBm)		Output Harmonics (dBm)*		
	Minimum	Maximum			
MLPNC-7100-SMA800	20 @ 100 MHz	24 @ 400 MHz	> -8 @ 4 GHz	> -18 @ 12 GHz	> -35 @ 20 GHz
MLPNC-7100-SMT680	20 @ 100 MHz	24 @ 400 MHz	> -8 @ 4 GHz	> -18 @ 12 GHz	> -35 @ 20 GHz
MLPNC-7102-SMA800	21 @ 400 MHz	23 @ 600 MHz	> -8 @ 4 GHz	> -16 @ 12 GHz	> -20 @ 20 GHz
MLPNC-7102-SMT680	21 @ 400 MHz	23 @ 600 MHz	> -8 @ 4 GHz	> -16 @ 12 GHz	> -20 @ 20 GHz
MLPNC-7103-SMA800	21 @ 800 MHz	23 @ 1.3 GHz	> -5 @ 6 GHz	> -15 @ 18 GHz	> -20 @ 30 GHz
MLPNC-7103-SMT680	21 @ 800 MHz	23 @ 1.3 GHz	> -5 @ 6 GHz	> -15 @ 18 GHz	> -20 @ 30 GHz

* Contact the factory for additional information or for products not covered in the table.

Aeroflex / Metelics is now a Cobham company

Aeroflex / Metelics

888-641-7364

www.aeroflex.com/metelics

TALENT • TECHNOLOGY • TRUST • 80 YEARS COBHAM 1934 - 2014 gain higher than 14 dB in the design frequency band, with a return loss better than 10 dB. ***Figure 7*** shows good agreement between simulation and measurements.

Measured output power, gain and PAE are shown in ***Figure 8***. An output power of at least 40 dBm and efficiency of greater than 60 percent are achieved across the operating band. The efficiency between 2.0 to 2.2 GHz and 2.55 to 2.7 GHz is better than at 2.4 GHz due to benefits of second harmonic tuning in the low and high bands. The gain is better than 12 dB in the 2.1 GHz and 2.7 GHz range, with the gain flatness less than 1.5 dB. Good agreement is achieved between the simulations and experimental results.

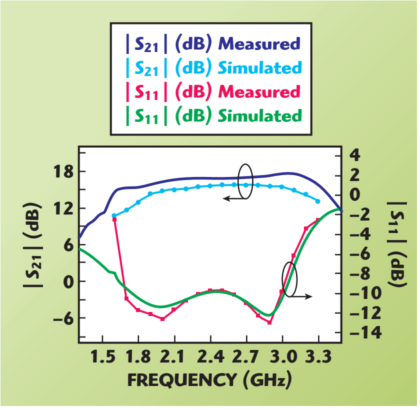

▲ *Fig. 7 Simulated and measured* $|S_{11}|$, $|S_{21}|$ *versus frequency.*

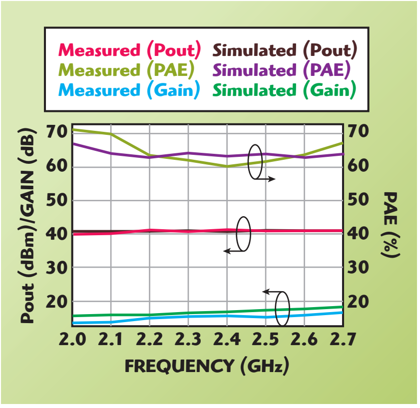

▲ *Fig. 8 Simulated and measured output power (Pout), PAE and gain versus frequency.*

CONCLUSION

A new method for the design of broadband harmonically tuned power amplifiers is described and demonstrated. The operating frequency band is divided into two for the control of second harmonic impedances to obtain high PAE and output power across the entire band. Performance of a wideband, high efficiency PA built using this design approach agrees closely with simulation. ■

References

1. J.Y. Hasani and M. Kamarei, "Analysis and Optimum Design of a Class E RF Power Amplifier," *IEEE Transactions on Circuits and Systems*, Vol. 55, No. 6, July 2008, pp. 1759-1768.
2. E. Cipriani, P. Colantonio, F. Giannini and R. Giofrè, "Theoretical and Experimental Comparison of Class F vs. Class F-1 PAs," *Proceedings of the 5th European Microwave Integrated Circuits Conference*, September 2010, pp. 428-431.
3. K. Chen and D. Peroulis, "Design of Broadband High-Efficiency Power Amplifier using in-Band Class-F&F-1 Mode-Transferring Technique," *IEEE MTT-S International Microwave Symposium Digest*, June 2012, pp.1-3.
4. Y.-S. Lee and Y.-H. Jeong, "A High-Efficiency Class-E GaN HEMT Power Amplifier for WCDMA Applications," *IEEE Microwave and Wireless Components Letters*, Vol. 17, No.. 8, August 2007, pp. 622-624.
5. K. Chen and D. Peroulis, "Design of Highly Efficient Broadband Class-E Power Amplifier Using Synthesized Low-Pass Matching Networks," *IEEE Transactions on Microwave Theory and Techniques*, Vol. 59, No. 12, December 2011, pp. 3162-3173.
6. N. Kumar, C. Prakash, A. Grebennikov and A. Mediano, "High-Efficiency Broadband Parallel-Circuit Class E RF Power Amplifier With Reactance-Compensation Technique," *IEEE Transactions on Microwave Theory and Techniques*, Vol. 56, No. 3, March 2008, pp. 604-612.
7. D. Gruner, K. Bathich, A. Al Tanany, and G. Boeck, "Harmonically Tuned GaN-HEMT Doherty Power Amplifier for 6 GHz Applications," *Microwave Integrated Circuits Conference (EuMIC)*, October 2011, pp. 112-115.
8. A. Al Tanany, D. Gruner, A. Sayed and G. Boeck , "Highly Efficient Harmonically Tuned Broadband GaN Power Amplifier," *Proceedings of the 5th European Microwave Integrated Circuits Conference*, September 2010, pp. 5-8.
9. R. Darraji and F.M. Ghannouchi, "High Efficiency Harmonically-Tuned GAN Power Amplifier for 4G Applications," *Canadian Conference on Electrical and Computer Engineering (CCECE)*, May 2011, pp. 1264-1267.
10. V. Carrubba, A. L. Clarke, M. Akmal, J. Lees, J. Benedikt, P. J. Tasker and S. C. Cripps, "On the Extension of the Continuous Class-F Mode Power Amplifier," *IEEE transactions on Microwave Theory and Techniques*, Vol. 59, No. 5, May 2011, pp. 1294-1302.

A Low Phase Noise Oscillator Based on an Active Substrate Integrated Waveguide Resonator

Chengjie Su, ZongXi Tang, Biao Zhang and YunQiu Wu
University of Electronic Science and Technology of China, Chengdu

An X-Band low phase noise oscillator based on an active substrate integrated waveguide (SIW) resonator uses series feedback to generate a negative resistance, compensating for the resonator's loss and improving its quality factor (Q). Performance of a negative-resistance oscillator designed using the active resonator is compared with that of a negative-resistance oscillator using a passive SIW resonator. The measured oscillation frequency of the active resonator oscillator is 10.19 GHz with an output power of 8.26 dBm. Its phase noise is -120.1 dBc/Hz at 1 MHz offset, which is about 8 dB lower than that of a similar oscillator with a passive resonator.

Microwave oscillators generally employ series and parallel feedback networks requiring frequency stabilization elements. There are several choices, such as dielectric resonators (DR),[1-3] elliptic filters,[4] ring resonators[5] and hairpin resonators.[6] The most important performance parameter is phase noise, since it determines a communication system's overall performance.[7] It is well known that low phase noise oscillators require high Q frequency stabilization elements. Although the DR has a high quality factor, it is not easily integrated with other circuit elements due to its bulky and non-planar profile; while microstrip resonators, though easily integrated, exhibit low Q values.

In recent years, substrate integrated waveguide structures have received much attention. SIW consists of two rows of metallic vias on a substrate and has similar propagation characteristics as that of rectangular waveguide; for example, an SIW cavity's resonant frequency is determined by its geometric dimensions. Moreover, SIW has several benefits, such as a potentially high-Q factor, low insertion loss and PCB compatibility.

Yet, the Q of an SIW resonator is still limited by dielectric, conductor and radiation losses, which compromise oscillator phase noise performance. This article discusses the use of an active SIW resonator for increased Q in an X-Band low phase noise oscillator.

HIGH-Q ACTIVE SIW RESONATOR DESIGN AND ANALYSIS

There are generally two alternatives for the design of an active resonator: coupling to a negative resistance to compensate for the loss of passive resonator, or equating an active feedback loop to a negative resistance.[8] For simplicity, the first one is chosen in this work.

Figure 1a is a top view of a passive SIW reflective resonator and its equivalent circuit (W=L=13.9 mm, R=0.3 mm, P=1 mm, Wp=0.1 mm, Lp1=2 mm, Wm=1.6 mm). The passive SIW resonator is modeled as a series RLC circuit. In this case, R_{loss} represents the combined dielectric, conductor and radiation losses, and L, C are determined by the SIW's physical dimensions to obtain the desired resonant frequency.

Because of its similarity with rectangular waveguide,[9] the propagation characteristics of the SIW's TE_{10} -like mode are very close to a rectangular waveguide's TE_{10} mode. Consequently, the resonant frequency of SIW resonator is determined from the following equation:

$$f_r\left(TE_{m0q}\right) = \frac{c_0}{2\sqrt{e_r}}\sqrt{\left(m/W\right)^2+\left(q/L\right)^2} \qquad (1)$$

where W and L are the length and width of the SIW resonator, and c_0 and ε_r are the speed of light in a vacuum and the relative dielectric constant of substrate, respectively. As shown in Figure 1a and the solid line of ***Figure 1d***, the simulated TE_{101} mode resonant frequency for the passive resonator is 10.09 GHz when W=L=13.9 mm, the unloaded Q is

$$Q_{passive} = \frac{wL}{R_{loss}} \qquad (2)$$

In order to increase the Q, the denominator R_{loss} must decrease. From Figure 1d and the method of Drozd and Joines,[10] the simulated loaded Q (Z_L=50 ohms) of a passive SIW resonator is about 500.

An active device operating in its unstable region can provide an equivalent negative resistance, and a transistor's unstable region can be enhanced by using series feedback. For a field effect transistor (FET), either a series-feedback inductor or a series-feedback capacitor of a few picofarads may be used.[11] In this article, the former is chosen and the series-feedback inductor is realized with two microstrip lines shorted to ground. ***Figure 1b*** is a top view of an active SIW reflective resonator and its equivalent circuit. Rneg (Rneg < 0) is the negative resistance. ***Figure 1c*** shows the simulated negative resistance Rneg. The equivalent resistance of the active SIW resonator is

$$R_a = R_{loss} + R_{neg} < R_{loss} \qquad (3)$$

Therefore, the unloaded quality factor is

$$Q_{Active} = \frac{wL}{R_a} \qquad (4)$$

It is apparent that $Q_{active} > Q_{passive}$ given the same dimensions and reso-

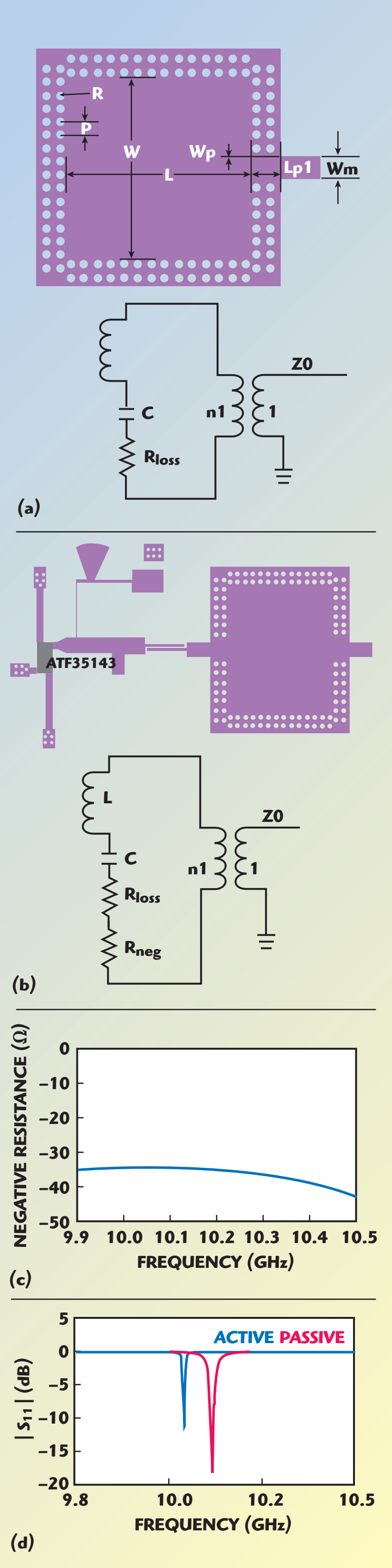

▲ *Fig. 1 Structure of the passive SIW resonator and its equivalent circuit (a) structure of the proposed active SIW resonator and its equivalent circuit (b) simulated negative resistance R_{neg} (c) and simulated S_{11} of active (blue) and passive (red) SIW resonator (d).*


RELEASE
THE POWER

nant frequency. As shown in Figure 1b and the dotted line of Figure 1d, the simulated TE_{101} mode resonant frequency for the active SIW resonator is 10.03 GHz , and the simulated loaded quality factor (Z_L=50 ohms) is about 2100. The resonant frequency of the active resonator is below that of the passive resonator due to the coupling capacitance, the parasitic capacitance and inductance of the active circuit.

OSCILLATOR DESIGN

In principle, a circuit will oscillate sustainably if the active device continuously supplies energy equal to the energy dissipated. In this case, an active SIW resonator is coupled to a microstrip line in series and then connected to the active device. If the lengths of microstrip line between the source electrode and ground, and the resonator and the active device, are properly chosen, the active device will provide sufficient negative resistance to sustain oscillation at the desired frequency.

The oscillator is designed based on large-signal measurement.[11] Let R_{IN} and X_{IN} represent the real part and imaginary parts of the active device impedance Z_{IN}, and let R_L and X_L be the real part and imaginary parts of the output matching network impedance Z_L. The necessary relation between R_{IN} and R_L to initiate oscillation is

$$R_{IN} - R_L < 0 \qquad (5)$$

In this case, the oscillation is unstable and its amplitude will grow. It will continue to build as long as equation 5 is satisfied; however, the absolute value of the negative resistance, R_{IN}, decreases due to the nonlinear performance of the active device until the oscillation reaches a steady state. When steady-state oscillation is reached, the relationships between R_{IN} and R_L, and X_{IN} and X_L are:

$$R_{IN} + R_L = 0 \qquad (6)$$

$$X_{IN} + X_L = 0 \qquad (7)$$

Oscillator design based on large-signal measurement can provide characteristics of oscillator performance such as power and harmonics. In this situation, the active device impedance Z_{IN} is a function of input power and frequency. According to equations 6 and 7, the output matching network impedance must satisfy the condition $Z_L = - Z_{IN}$.

The matching function requires that both the insertion loss and pass band attenuation ripple of the Chebyshev filter at the fundamental frequency be very small, while the harmonic suppression function requires that insertion loss of the Chebyshev filter at the harmonics be very large. To accomplish both functions, a six-order, short-step Chebyshev impedance transformer is selected.

A short-step Chebyshev impedance transformer[12] not only fulfills the output matching requirement at the fundamental, but also enhances harmonic suppression. Because the method and data of Matthaei[12] can match only two resistive terminations, however, complex impedance matching is performed using simulation tools per Chen and Peroulis.[13]

Figure 2 is a top view of the active resonator oscillator. It includes an active SIW resonator, a transistor with output matching network, and an output coupling capacitor to prevent DC current flowing into the measuring instrument.

MEASUREMENT

Figure 3a shows a negative resistance oscillator with an active SIW resonator fabricated on Rogers RT/Duroid 5880 with a relative dielectric constant ε_r = 2.2, loss tangent $\tan\delta$ = 0.0009 and thickness of 0.508 mm. For comparison, a negative resistance oscillator using a passive SIW resonator is also fabricated, as shown in ***Figure 3b***. The two resonators have the same physical dimension except that the active one has two terminations. The active SIW resonator uses Avago's ATF-35143 pseudomorphic high electron-mobility transistor (PHEMT). Its DC bias voltages are V_{gs} = 0 V, V_{ds} =2 V. Negative resistance for both the active and passive resonator oscillators is pro-

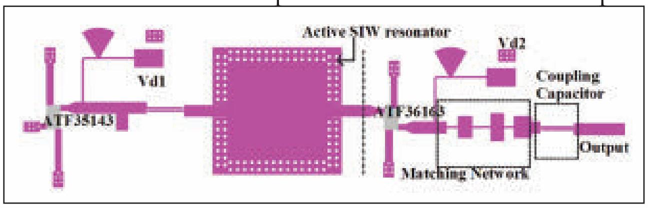

▲ *Fig. 2 Top view of the overall active resonator oscillator design.*

vided by Avago's ATF-36163 PHEMT. The two ATF-36163 PHEMT's gates are shorted because of the metallic via walls, and their V_{ds} =2 V.

The output spectrums of the two oscillators are measured with a Rohde & Schwarz FSP spectrum analyzer. ***Figures 4a*** and ***b*** show the phase noise and second harmonic suppression of the active resonator oscillator. Its oscillation frequency is 10.19 GHz with an output power of 8.26 dBm, and second harmonic suppression is greater than 30 dB. In addition, phase-noise for the active resonator oscillator is -120.1 dBc/Hz at 1 MHz offset, which is almost 8 dB lower than for the passive one. It is apparent from Figure 4a, however, that phase noise of the active resonator fails to decrease further beyond 1 MHz offset. There are two causes, one is noise floor deterioration due to the active device's noise figure, and the other is due to influences from external noise sources. The former may be alleviated through careful design of the active SIW resonator, and a metal shielded cavity will reduce the effects of the latter.

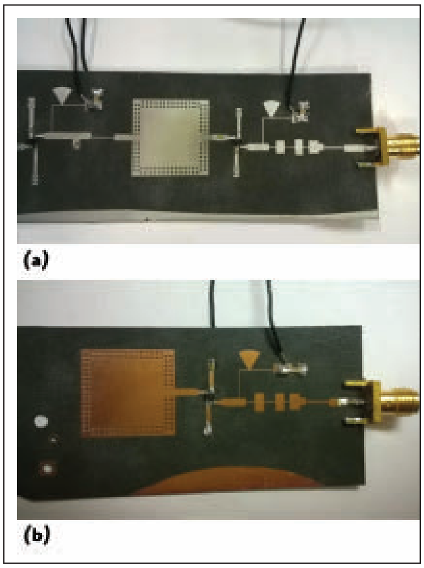

▲ *Fig. 3 Photograph of active resonator oscillator (a) and passive resonator oscillator (b).*

CONCLUSION

An active SIW resonator is designed to have a Q higher than that of a passive SIW resonator. The phase noise of an X-Band oscillator using the active resonator is -120.1 dBc/Hz at 1 MHz offset, which is about 8 dB lower than that of a similar oscillator with a passive resonator. The results indicate that the use of an active resonator is beneficial in reducing oscillator phase-noise. ■

ACKNOWLEDGMENT

This work is supported by National Natural Science Foundation of China (Grant No.61201004) and the Fundamental Research Funds for the Central Universities (ZYGX2011J011).

References

1. N.M. Mahyuddin, M.F. Ain, S.I.S. Hassan and M. Singh, "A 10 GHz PHEMT Dielectric Resonator Oscillator," *International RF and Microwave Conference Proceedings*, September 2006, pp. 26-30.
2. A.M. Pavio and M.A. Smith, "A 20-40 GHz Push-Push Dielectric Resonator Oscillator," *IEEE Transactions on Microwave Theory and Techniques*, Vol. 33, No. 12, December 1985, pp. 1346-1349.
3. B.I. Son, H.C. Jeong and K.W. Yeom, "Design of a Low Phase Noise Voltage Tuned DRO based on Improved Dielectric Resonator Coupling Structure," *Asia Pacific Microwave Conference Proceedings*, December 2012, pp. 1121-1123.
4. C.H. Tseng and C.L. Chang, "Design of Low Phase-Noise Microwave Oscillator and Wide Band VCO Based on Microstrip Combline Bandpass Filters," *IEEE Transactions on Microwave Theory and Techniques*, Vol. 60, No. 10, October 2012, pp. 3151-3160.
5. L.H. Hsieh and K. Chang, "Slow-Wave Bandpass Filters Using Ring or Stepped-Impedance Hairpin Resonators," *IEEE Transactions on Microwave Theory and Techniques*, Vol. 50, No. 7, July 2002, pp. 1795-1800.
6. L. Dussopt, D. Guillois and G.M. Rebeiz, "A Low Phase Noise Silicon 9 GHz VCO and an 18 GHz Push-Push Oscillator," *IEEE Microwave Theory and Techniques International Symposium Digest*, Vol. 2, June 2002, pp. 695-698.
7. Y.T. Lee, J. Lee and S. Nam, "New Planar High Q Active Resonator and Its Application to Low Phase Noise Oscillators," *IEEE Microwave Theory and Techniques International Symposium Digest*, Vol. 3, June 2004, pp. 2007-2010.
8. Z. Chen, W. Hong and J.X. Chen, "High-Q Planar Active Resonator Based on Substrate Integrated Waveguide Technique," *Electronics Letters*, Vol. 48, No. 10, May 2012, pp. 575-577.
9. F.F. He, K. Wu, W. Hong, L. Han and Xiaoping Chen, "A Low Phase-Noise VCO Using an Electronically Tunable Substrate Integrated Waveguide Resonator," *IEEE Transactions on Microwave Theory and Techniques*, Vol. 58, No. 12, December 2010, pp. 3452-3458.
10. J.M. Drozd and W.T. Joines, "Determining Q Using S Parameter Data," *IEEE Transactions on Microwave Theory and Tech-*

MIL-DTL-38999, Series 1 & 3 sealed cylindrical connectors

A full platform of environmental and hermetic class type connectors matching almost every environment in regards to number of ports, materials and plating, Availability: short deliveries.

Spectrum
Elektrotechnik GmbH

when Quality is needed

80905 Munich, Germany P.O. Box 450533

Telephone: +49-89-3548-040 Facsimile: +49-89-3548-0490

WWW.SPECTRUM-ET.COM Email: sales@spectrum-et.com

niques, Vol. 44, No. 11, November 1996, pp. 2123-2127.
11. Guillermo Gonzalez, *Foundations of Oscillator Circuit Design*, Artech House, 2007, pp. 251-343.
12. George L. Matthaei, "Short-Step Chebyshev Impedance Transformers," *IEEE Transactions on Microwave Theory and Techniques*, Vol. 14, No. 8, August, 1966, pp. 372-383.
13. K. Chen and D. Peroulis, "Design of Highly Efficient Broadband Class-E Power Amplifier Using Synthesized Low-Pass Matching Networks," *IEEE Transactions on Microwave Theory and Techniques*, Vol. 59, No. 12, December, 2011, pp. 3162-3173.

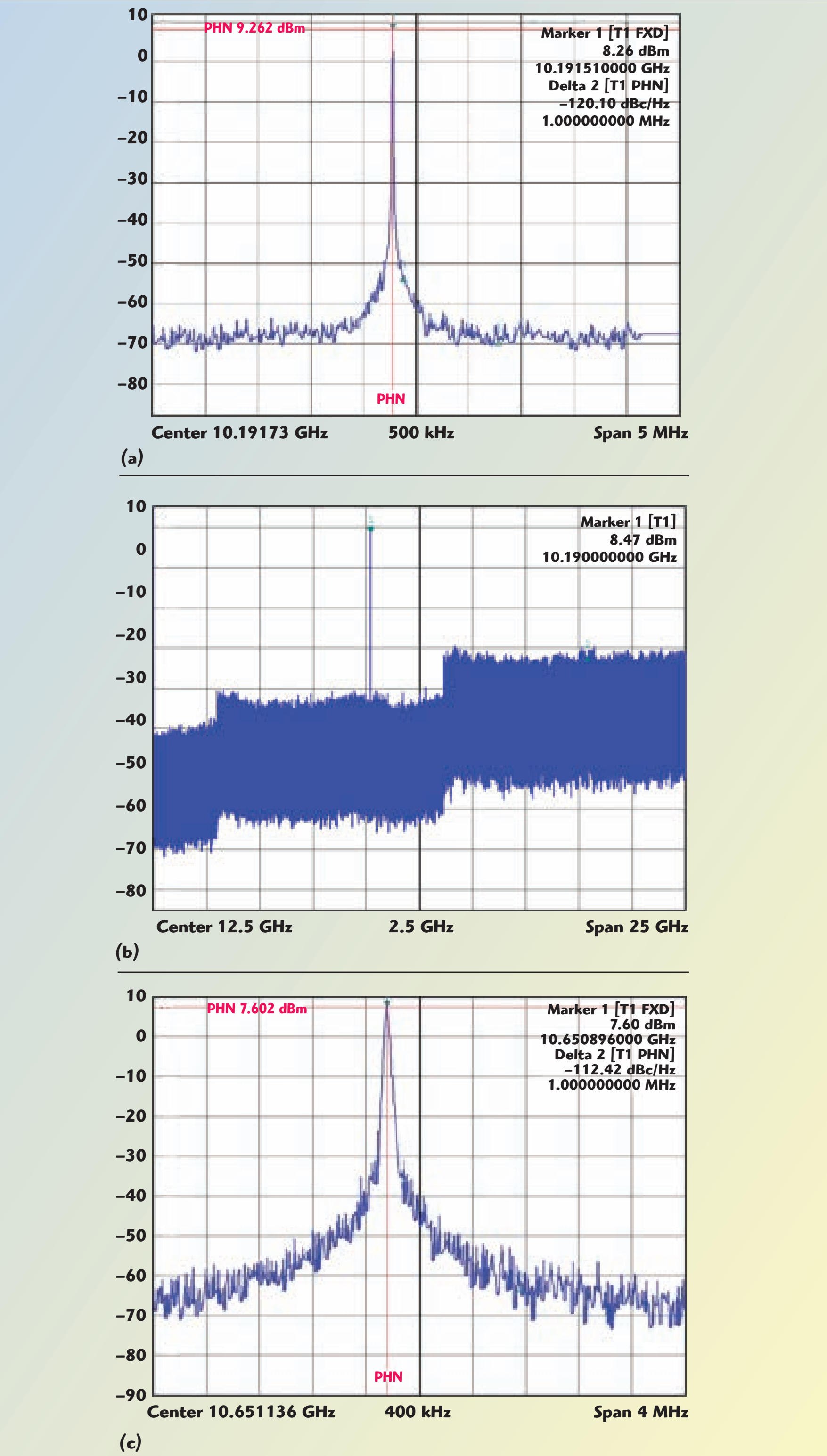

▲ *Fig. 4 Phase noise of the active resonator oscillator (a) second harmonic suppression of the active resonator oscillator (b) and phase noise of the passive resonator oscillator (c).*

HPXO series

High Performance Crystal Oscillators

Model	Frequency (MHz)	DC Bias VDC [Typ.]	Minimum Output Power (dBm)	Frequency Stability Over Temp. (ppm) [Typ.]	Phase Noise (dBc/Hz) [Typ.]			
					@ 100 Hz	@ 1 kHz	@ 10 kHz	@ 100 kHz
HPXO100	100	+12 @ 120 mA	+10	<+/-0.2	-140	-162	-174	-183
KHPXO100	100	+12 @ 120 mA	+10	<+/-0.2	-140	-162	-174	-183
HPXO125	125	+12 @ 120 mA	+10	<+/-0.2	-140	-162	-174	-183
HPXO128	128	+12 @ 120 mA	+10	<+/-0.2	-138	-160	-172	-180

RoHS

FEATURES:

- *Excellent Performance*
- *Oven / Voltage Controlled*
- *Ultra Low Phase Noise*
- *High Stability*
- *Standard Compact Package*
- *Low-G Sensitivity*

Talk To Us About Your Custom Requirements.

SYNERGY® MICROWAVE CORPORATION

Phone: (973) 881-8800 | Fax: (973) 881-8361
E-mail: sales@synergymwave.com
Web: WWW.SYNERGYMWAVE.COM
Mail: 201 McLean Boulevard, Paterson, NJ 07504

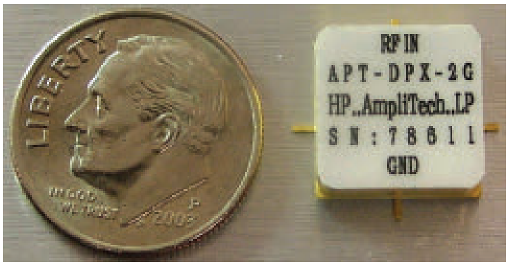

Surface Mount Diplexers with Variable Crossover Attenuation

Amplitech Inc.
Bohemia, N.Y.

A diplexer circuit, as shown in ***Figure 1***, is a very practical circuit for dividing the frequency spectrum into essentially two non-overlapping parts. Crossover attenuation (Ao) as a design parameter has been unavailable in the past, thus limiting the designer's options. This is no longer a constraint with Amplitech's new design. The designer now has the option to increase channel to channel isolation as required by using the variability of the crossover attenuation.

Complementary diplexers exhibit a near perfect input match across the entire band of coverage. The cost of this is an inherent restriction in the crossover attenuation to 3 dB (i.e., a half power split). For many applications, this level of crossover isolation is too small. Such design limitations can be circumvented only by giving up the match at the input and going to a non-complementary design.[1] This allows controlled interaction between the input impedances to each diplexer channel.

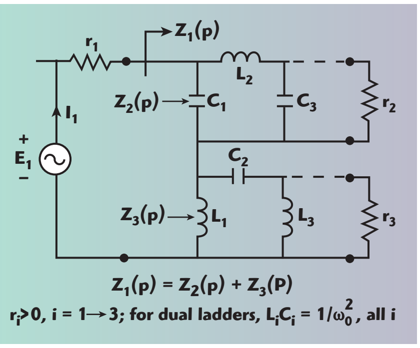

Fig. 1 Diplexer circuit.

A greater level of selectivity is also achieved for a given number of elements per ladder. This permits smaller size and lower loss for a given level of rejection.

For a given rate of cutoff in the complementary class, each channel with v elements per ladder, experiences a cutoff rate of "6v dB per octave," while in the non-complementary class described herein, each channel with v elements per ladder, experiences a cutoff rate of "2 × 6v dB per octave." This is due to the contributory influence of the neighboring channel resulting in designs which are able to fit in smaller volumes for the same selectivity, because fewer elements per channel are required when both channels contribute to the response. This provides more "bang for the real estate buck."

One may control the width of the transition region that exists between bands (i.e., where S_{11} is no longer to be matched) to any desired degree through the choice of ν with great effect.[1] Thus, the effect of the mismatch is limited to an inconsequential band of frequencies. Other approaches that attempt to increase selectivity in this region often include topologies which are more complicated, since they are

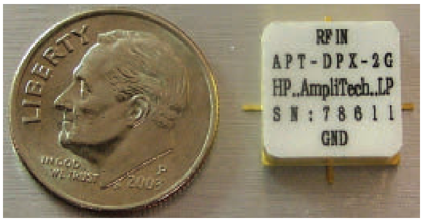

▲ *Fig. 2 Diplexer construction employing surface mount packaging.*

suboptimal and may involve the use of finite transmission zeros to improve selectivity where they might otherwise be avoided. Amplitech's topology avoids the use of finite transmission zeros altogether. Designs are built with a minimum of complications providing more "bang for the manufacturability buck."

CIRCUIT CONSTRUCTION AND DATA

The present goal for this design example was to complete the circuit construction while employing a surface mount (SMT) package and taking advantage of all of the benefits associated with such packaging. This includes size, ease of manufacturability and cost. The result of this effort is shown in ***Figure 2***.

The test data is shown in ***Figure 3***, where the attenuation for each channel is shown overlaid in the graph on the top and the SWR results are shown on the bottom of the figure for each of the three ports. The measured data was in good agreement with the initial design parameters. Good rejection was achieved with both good match and isolation.

A test fixture was developed as part of this effort. When the SMT package is loaded into this fixture, the assembly can be tested using a typical network analyzer test set-up employing

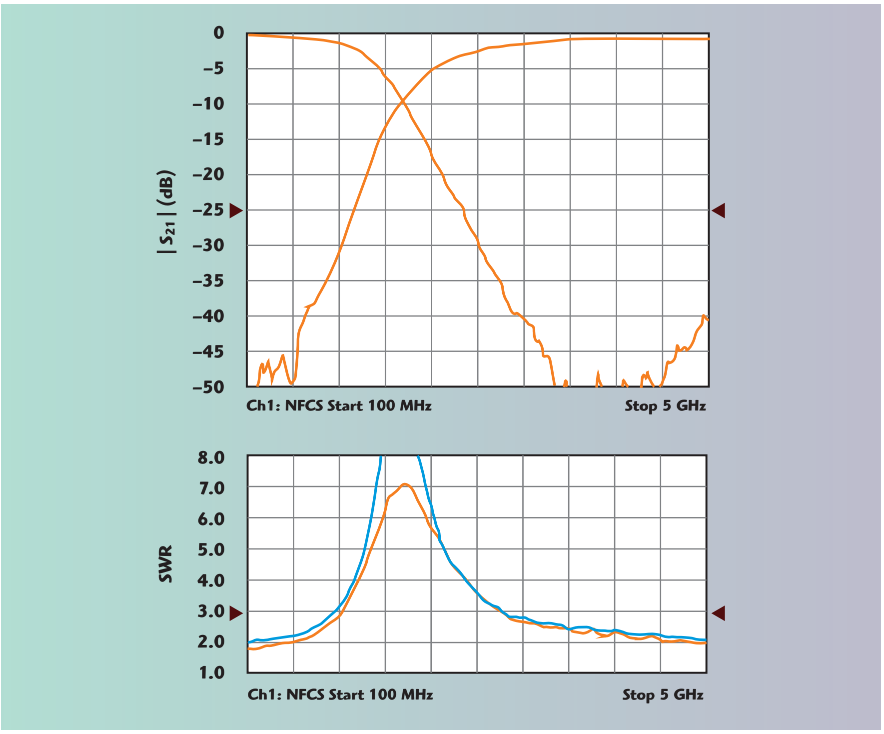

▲ *Fig. 3 Surface mount diplexer measured data.*

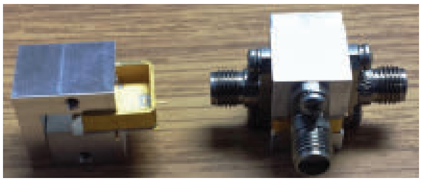

▲ *Fig. 4 New test fixture for the SMT diplexer.*

SMA (or other similar types) connections. Once tested, the SMT package may be removed from the test fixture. With connection tabs now exposed, the SMT diplexer may then be integrated into a higher level of assembly where it might be used in its intended application. The SMT diplexer may remain in the test fixture for continued use in system applications where the SMA connections are preferred to the tab connections. The fixture is shown in ***Figure 4***. A trade off comparison for each diplexer type is given in ***Table 1***.

TABLE 1

NON-COMPLEMENTARY DIPLEXER PERFORMANCE SUMMARY

Performance Parameter	Non-Complementary	Complementary
Crossover Attenuation	Variable	Fixed
Isolation	Higher than Complementary Case	Limited
Size	*Smaller*-Requires less elements for the same performance	*Larger*- Requires more elements for the same performance
Manufacturability	*Higher Yields*-Simpler Designs	*More Elements*-More Complexity
Input Match	*Unconstrained*-Under control of designer	Overconstrained

APPLICATIONS

The construction of Amplitech's new type of variable crossover, ladder realizable diplexer in an SMT package, has been practically demonstrated. The features of this design class are summarized in Table 1. The applications for this circuit include cell phone (separating GPS from other signals); mixer design enhancement; multi-channel communication systems; as well as SATCOM and EW systems. This circuit facilitates higher levels of system integration since passive circuits such as diplexers are often "tall poles" in the system size requirements. Future efforts will explore the use of even smaller packaging.

Reference

1. D.C. Youla, S.U. Pillai and F. Winter, "Theory and Design of Maximally Flat Low-Pass High-Pass Reactance Ladder Diplexers," *IEEE Transactions Circuits and Systems*, Vol. 39, No. 5, 1992, pp. 337-350.

Amplitech Inc.
Bohemia, N.Y.
(631) 521-7831
www.amplitechinc.com

Coaxial Attenuators, Terminations and Adapters

XMA Corp.
Manchester, N.H.

Technical advancements within the telecommunications industry as well as aerospace, defense and medical markets are driving manufacturers and carriers of wireless devices to push performance into the higher frequency bands. XMA Corp. has introduced a new 1.85 mm product family that includes coaxial attenuators, terminations and adapters, expanding its product offerings to meet the challenges of the 65 GHz millimeter wave market.

All three product types operate from DC to 65 GHz. They are Defense Federal Acquisition Regulation (DFAR) compliant and feature unique identification grooves located on the housing and coupling nut to visually differentiate them from similar looking lower frequency products. The materials and finishes used on all of XMA's 1.85 mm product lines are very durable and suitable for military/aerospace grade applications.

ATTENUATORS

XMA 1.85 mm, DC to 65 GHz, 1 W, 50 ohm attenuators are available in six different attenuation values: 3, 6, 10, 15, 20 and 30 dB and offer attenuation accuracy as low as ±0.75 dB from DC to 26.5 GHz. These models feature an air compensated, PTFE (Teflon®) dielectric support bead, passivated stainless steel housings and coupling nuts, and gold plated beryllium copper center conductors. ***Figure 1*** shows the typical S-parameter data for the 10 dB units.

TERMINATIONS

XMA 1.85 mm, DC to 65 GHz, 1 W, 50 ohm male terminations weigh 4.6 grams and operate from -55° to +100°C. VSWR performance is rated at 1.20:1 from DC to 18 GHz, 1.30:1 from 18 to 40 GHz and 1.35:1 from 40 to 65 GHz. These products feature a passivated stainless steel housing and coupling nut, a gold plated beryllium copper center conductor and a PTFE (Teflon®) dielectric. ***Figure 2*** shows the typical S-parameter data for these units.

ADAPTERS

XMA 1.85 mm, DC to 67 GHz, In-series adapters are offered in three standard configurations: female-to-female, male-to-male and male-to-female. They offer <1.35:1 VSWR from DC to 67 GHz, have an operational temperature range of -55° to +100°C and can handle a maximum average power of 20 W at 25°C. RF leakage is specified at > 90 dBc. A feature of the 1.85 mm adapter family is that they are all phased matched to within ±10° of each other. These models have gold plated stainless steel housings and coupling nuts, gold plated beryllium copper center conductors and PTFE (Teflon®) dielectrics.

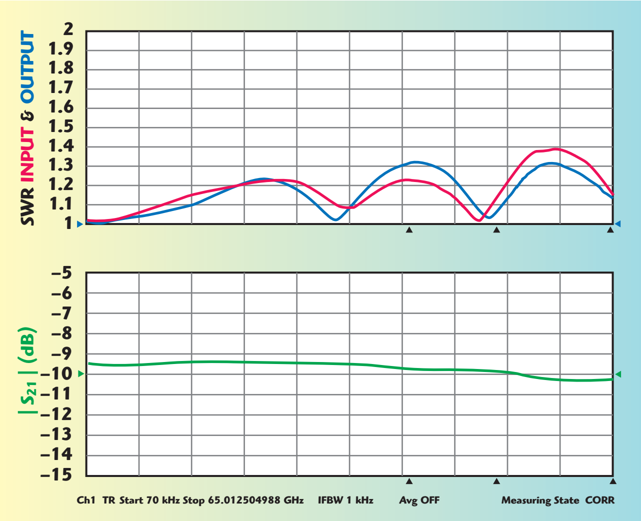

▲ *Fig. 1 Measured performance for 10 dB attenuators: Top shows SWR at input (red) and output (blue). Bottom shows* $|S_{21}|$.

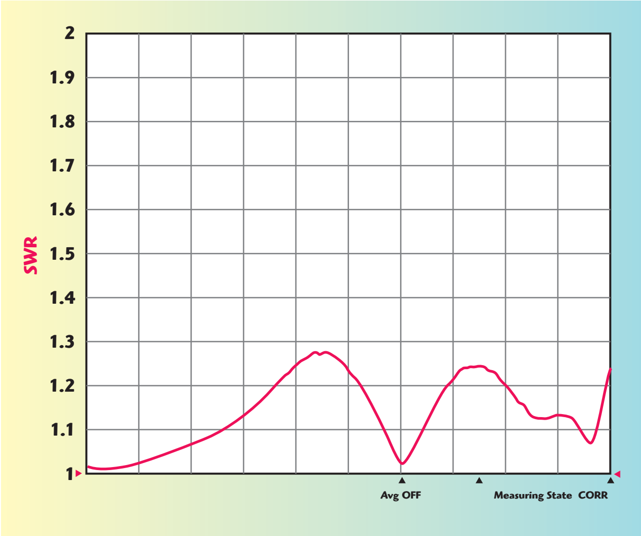

▲ *Fig. 2 Measured SWR for DC to 65 GHz terminations.*

XMA's line of rugged, high quality, 1.85 mm precision adapters, attenuators and terminations are designed to exceed the ever increasing demands of the 65 GHz market and provide "off-the-shelf" solutions for high frequency, millimeter wave applications.

XMA CORP.

XMA Corp. was established in 2003 through the acquisition of the Omni Spectra® product line from M/A-COM Inc. The 30 plus year legacy of Omni Spectra is well known in the RF and microwave industry and has been recognized as a "Gold Standard" when it comes to quality, performance and value.

XMA Corp.
Manchester, N.H.
www.xmacorp.com

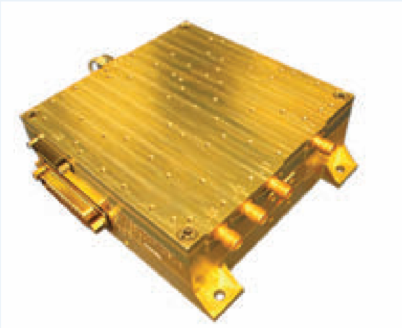

Block Upconverter with HPA for Ka-Band

Hittite Products from Analog Devices has introduced a new Ka-Band block upconverter with high power amplifier (HPA), designed for single carrier use in satellite communications. The HMC7056 upconverts an input signal between 1 and 2 GHz to an output between 29 and 31 GHz, which covers both the commercial (29 to 30) and military (30 to 31) satellite bands.

The upconverter has 65 dB of conversion gain and provides a linear output up to 37 dBm. The design employs dual upconversion with integrated local oscillators (LO) to ensure no phase inversion and maximum spurious rejection. The LOs require an external 100 MHz reference signal. Other features include digital gain control, thermal monitoring and gain compensation, HPA enable and an output isolator to ensure excellent output VSWR. The HPA output mates with WR28 waveguide.

The block upconverter operates over the -20° to +80°C temperature range and is designed to be used with conduction cooling. It meets military environment conditions. The unit weighs 2.11 lbs and measures 5.72" × 4.51" × 1.63".

The upconverter and HPA are also sold as separate products. The HMC7053 is a fully integrated Ka-Band upconverter, with SMA inputs and a 2.9 mm output connector. The HMC7054 HPA has a 2.9 mm input connector and WR28 waveguide output. The HPA, which utilizes GaAs MMIC technology, operates at 5 V and draws 14 amps.

Analog Devices Inc.
Norwood, Mass.
www.analog.com/hittitemw

5 MHz to 40 GHz Balun

The HL9404 broadband balun from HYPERLABS covers 5 MHz to 40 GHz and converts a single-ended input to differential outputs with tight amplitude and phase matching. Amplitude match is typically ±0.1 dB to 20 GHz and ±0.25 dB from 20 to 40 GHz. Phase match is specified at ±2 degrees at 10 GHz and ±4 degrees at 18 GHz.

A high-precision balun such as the HL9404 improves performance in high-speed ADCs, mixers, harmonic mixers, amplifiers, up/down converters and other systems. Exceptional amplitude and phase match ensure that second harmonic distortion is minimized at all frequencies.

The balun's insertion loss is approximately 6 dB and input power handling is greater than 30 dBm. The input and outputs are matched to 50 ohms, with K connectors used to interface with adjacent components. The size of the balun is 2.19" × 1.5" × 0.55" and it weighs 1.6 oz.

The HL9404 is priced lower than competitive solutions, according to HYPERLABS. It is available worldwide and lead times are usually less than a week.

The HL9404 is HYPERLABS' third balun. Its sister products, the HL9402 broadband balun and the HL9403 SMT broadband balun, are both specified to 20 GHz. Since their 2012 release, these components have been adopted by instrument manufacturers, IC designers and research labs around the world.

HYPERLABS products are designed and manufactured at the company's facility in Beaverton, Ore.

HYPERLABS
Beaverton, Ore.
www.hyperlabsinc.com

Software and Mobile Apps

Designer 15 for PCBs

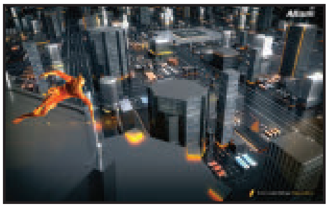

Altium Ltd., announced the upcoming release of its professional printed circuit board (PCB) and electronic system level design software, Altium Designer 15. It includes powerful new enhancements for designing the next generation of high-speed printed circuit boards and keeping up with industry trends, with support for new fabrication output standards as well as support for both IPC-2581 and Gerber X2. In addition, designers will no longer require external software or have to maintain complex lists of signals and nets, but instead will be able to plan and route groups of high speed nets with much greater efficiency and accuracy.

Altium Ltd.
www.altium.com

CST STUDIO SUITE 2015

VENDORVIEW

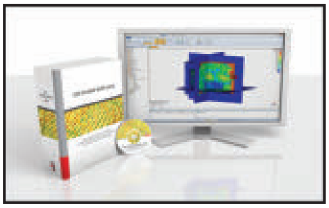

Computer Simulation Technology AG (CST) unveiled the upcoming version of its flagship electromagnetic simulation tool, CST STUDIO SUITE® 2015. The software is used by engineers and researchers working across the electromagnetic spectrum to model systems and optimize designs. Its tightly-integrated solvers cover a broad range of frequencies and geometrical scales and are complemented by more specialized technology for applications such as PCBs, cables, thermal analysis and charged particle devices. With CST STUDIO SUITE 2015, the links between the different simulation domains have been tightened and new tools have been added to allow users to go beyond what can be done with electromagnetic field simulation alone.

Computer Simulation Technology AG (CST)
www.cst.com

Impedance and Power-Handling Calculator

Isola's free impedance and power-handling calculator predicts the design attributes for microstrip and stripline based on the design's target impedance and dielectric properties of the company's RF, microwave and millimeter wave laminate materials. The software computes changes in the effective dielectric constant due to dispersion at higher frequencies. It then computes the total insertion loss, including the dielectric loss, conductor loss and the loss due to surface roughness. Visit isodesign.isola-group.com/phi-calculator to sign in and download.

Isola Group
www.isola-group.com

PXI Reference Solution

VENDORVIEW

Keysight Technologies announced a new PXI Reference Solution for RF power amplifier (PA) characterization and test. The Reference Solution, which performs S-parameter, harmonic distortion, power and demodulation measurements, enables rapid, full characterization of next-generation power amplifier modules, such as power amplifier-duplexers (PADs). The Reference Solution is optimized for high throughput and highly accurate measurement quality. It is the only small footprint, full characterization solution for design validation and product test of the RF power amplifier, as well as all of the passive devices surrounding the power amplifier, such as filters and duplexers.

Keysight Technologies Inc.
www.keysight.com

ChipScan-ESA 3.0

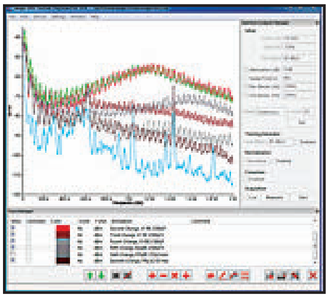

The ChipScan-ESA analysis software from Langer EMV-Technik GmbH has been designed for the clear and comparable recording of a spectrum analyzer's measurement curves. It allows users to visualize measuring curves quickly and interactively, perform complex analyses and export the curves easily. The software has been custom developed for measurements in the field of electromagnetic compatibility (EMC), specifically pre and post measurements during the EMC optimization of the device under test. The ChipScan-ESA software can also generate and export image data and measurement curves for documentation. (System requirements: Windows XP and later).

Langer EMV-Technik GmbH
www.langer-emv.com

Modelithics COMPLETE Library 11.3

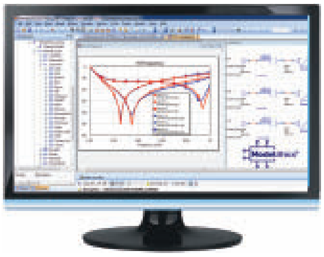

Modelithics announced this year's major release of the Modelithics COMPLETE Library, version 11.3 for NI AWR Design Environment/Microwave Office circuit design software. New simulation models have been added for passive capacitor, inductor, coupler and diplexer families, as well as active semiconductor devices from popular vendors, including AVX, Mini-Circuits, Coilcraft, MACOM, Passive Plus, Rohm and Murata. Other additions include over 60 new substrate- and part-value-scalable passive Global Models™, non-linear MACOM varactor diode models, Rohm and Toshiba non-linear transistor models, and over 15 coupler and diplexer models for AVX components.

Modelithics Inc.
www.modelithics.com

Software and Mobile Apps

RF Calculators and Conversion Tools

VENDORVIEW

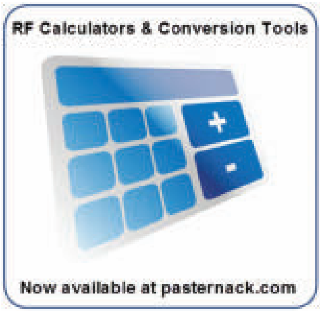

Pasternack has created and published a new set of RF calculators and conversion tools to assist engineers with answering complex RF-related product and design questions. The new RF calculators and converters include link budget, coax impedance, RF power conversion (such as dBm to W), attenuation, frequency, wavelength, VSWR/return loss, torque, noise, Free Space Path Loss (FSPL), unit conversion, microstrip and more. Each calculator page includes a diagram or illustrated depiction of what the calculator is used for as well as the mathematical formula for the chosen calculator. The calculator will also produce a "Find Related Products" button that directs users to Pasternack products that meet specific needs.

Pasternack Enterprises Inc.
www.pasternack.com

ROG Mobile

VENDORVIEW

Rogers Corp. launched ROG Mobile, a free mobile app for Apple and Android devices. The new app allows users to access Rogers' calculators, including the popular MWI (Microwave Impedance) simulation tool, literature, technical papers and to order samples, all while on the go with their smart phones and tablets. ROG Mobile includes tools and technical information to assist users with Rogers Corp.'s high performance printed circuit board materials. Users can also stay up to date by viewing articles and tech tips written by Rogers' experts.

Rogers Corp.
www.rogerscorp.com

New Vishay iPad App

Vishay Intertechnology announced the availability of a Vishay app for the Apple iPad® that makes it easy for users to access the company's Super 12 and Engineer's Toolbox collections of semiconductor and passive devices. Vishay's Super 12, a dozen key semiconductor and passive components, features new and improved technologies that can significantly improve the performance of end products and systems. Vishay's Engineer's Toolbox highlights innovative components that Vishay manufactures to help design engineers develop superior end products. The app provides key features, potential application ideas and links to datasheets and support materials for each product.

Vishay Intertechnology Inc.
www.vishay.com

New Products

FOR MORE NEW PRODUCTS, VISIT WWW.MWJOURNAL.COM/BUYERSGUIDE

FEATURING VENDORVIEW STOREFRONTS

Components

Wi-Fi Bandpass Filter

3H Communication Systems announced its low cost Wi-Fi bandpass filter. This is a 3 section cavity filter with a passband of 5725 to 5875 MHz and <0.25 dB insertion loss. The Wi-Fi filter provides >10 dB attenuation at 5570 and 6030 MHz and >70 dB @ DC to 2500 MHz and is capable of handling 50 W CW with a peak rating of 500 W. Size: 2.3" × 1.1" × 0.75" excluding sma connectors.

3H Communication Systems
www.3hcomm.com

SPDT Terminated Coaxial Switch

The D1 Series SPDT coaxial switch is a terminated switch with SMA connectors and operates at a frequency of DC to 22 GHz. Actuator options come in latching and failsafe modes, and units with TTL circuitry with integrated indicator circuits. Ducommun's design engineers can create custom versions for your specific applications.

Ducommun Inc.
www.ducommun.com

RF Adapters

Fairview Microwave Inc. introduced a comprehensive line of IP67 RF adapters commonly employed in the DAS, cellular, aviation and military industries due to their ingress protection from water and dust. Fairview Microwave's new RF adapters are IP67 rated, meaning they use advanced ingress protection to make them virtually impenetrable to contaminants like dust, sand and water. They are compatible with all like-series connectors, cables and passive and active components.

Fairview Microwave Inc.
www.fairviewmicrowave.com

Digitally Controlled PIN Diode Attenuator

Model A6P-69T-0BD is a digitally controlled PIN diode attenuator that operates from

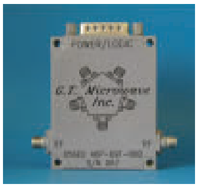

2 to 18 GHz. It is capable of 64 dB in monotonic 0.25 dB steps. The attenuation flatness is ± 5 dB with a 2.1:1 VSWR in 50 ohms and 4.5 dB insertion loss. This PIN diode attenuator is digitally controlled via 8 bits of TTL compatible binary logic with a switching speed less than 350 nsec. The operating temperature range extends from -45° to +85°C.

G.T. Microwave Inc.
www.gtmicrowave.com

DC to 3 GHz Voltage Limiter

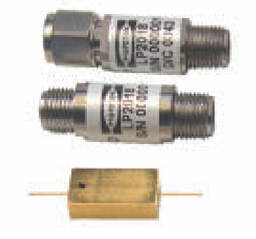

Herotek offers a DC to 3 GHz voltage limiter for DC, AC analog, digital, RF, impulse and microwave signals. LV3000A does not have a frequency break between DC and 3 GHz and no bias is required. The typical threshold level is ±0.7 VDC or 0 dBm microwave. LV3000A has low output leakage level (1.5 V typical @ ± 10 V input, +13 dBm typical @ +30 dBm input microwave). It has low harmonic generation (-20 dBc typical at rated input power).

Herotek, Inc.
www.herotek.com

Directional Coupler

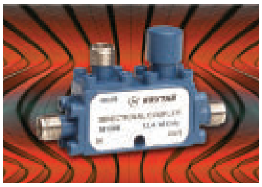

KRYTAR Inc. announced a new directional coupler covering 12.4 to 18 GHz with nominal coupling of 6 dB in an extremely compact package. It is uniquely designed for systems applications where external leveling, precise monitoring, signal mixing or swept transmission and reflection measurements are required. The coupler provides simple solutions for many applications including electronic warfare (EW), commercial wireless, SATCOM, radar, signal monitoring and measurement, antenna beam forming and EMC testing environments.

KRYTAR Inc.
www.krytar.com

Digital-to-Analog Converter

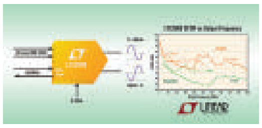

Linear Technology Corp. announced the LTC2000, a 16-bit 2.5 Gsps digital-to-analog converter (DAC) with exceptional spectral purity of 74 dBc SFDR at 200 MHz output, and better than 68 dBc SFDR for output frequencies from DC to 1 GHz, a 12 dB improvement over alternative 14-bit DACs. The LTC2000 features low phase noise and a wide 2.1 GHz, -3 dB output bandwidth, enabling broadband, or high frequency RF synthesis in applications such as instrumentation, broadband communications, test equipment, cable TV DOCSIS CMTS and radar.

Linear Technology Corp.
www.linear.com

Low PIM Adapters & Jumpers

MECA's Low PIM (-160 to -165 dBc typ) adapters and jumpers for DAS applications feature industry leading PIM performance of -155 dBc

min. Available in 7/16 DIN, Type N to SMA and 4.1/9.5 Mini-DIN connectors. Ideal for IDAS / ODAS, in-building, base station, wireless infrastructure, 4G and AWS applications. Made in U.S. and 36-month warranty.

MECA Electronics Inc.
www.e-meca.com.

DC Pass Matching Transformer

Z7550-NMNF+ is a DC passing matching transformer that allows impedance matching

between 50 and 75 ohms systems with minimum reflection into the circuit. This matching transformer will find its application in any system where 50 to 75 ohms matching is required.

Mini-Circuits
www.minicircuits.com

30 dB PIN Diode Attenuator

PMI Model DTA-26R5G40G-30-CD-1 is a 10-bit programmable 30 dB PIN diode attenuator with a step resolution of 0.03 dB over the frequency range of 26.5 to 40 GHz. This model

operates on a single +15 VDC supply and draws only 50 mA of current. Very high levels of attenuation accuracy of 0.03 dB are achieved. This attenuator provides ultra-fast switching speeds of 300 nsec and has an operating input power rating of +10 dBm. This model is supplied in a small, light weight housing measuring 2.0" × 1.8" × 0.5".

Planar Monolithics Industries Inc.
www.pmi-rf.com

Broadband Type N DC Block

Response Microwave Inc. announced the availability of its new broadband Type N DC block for use in automated test and production applications. The new RMDC.18000mf covers the 0.05 to 18 GHz band offering typical electrical performance of 0.6 dB insertion loss and 1.25:1 VSWR. Working voltage is 50 V and the unit is operational over the -55° to +85° C range. Mechanical package is 1.68" × 0.540" in diameter. Unit is made from SUS303F passivated stainless steel and connectors are precision N male to female.

Response Microwave Inc.
www.responsemicrowave.com

New**Products**

Capacitors

VENDORVIEW

Richardson RFPD Inc. announced the availability and full design support capabilities for two series of precision tolerance, NP0 RF microwave capacitors from American Technical Ceramics Corp. (ATC). The high-frequency, low-loss (Hi-Q) 400L Series and 400S Series capacitors feature a precision thin-film process that provides reliable and repeatable performance, industry-leading tolerances over a wide range of capacitance values, low ESR and high series resonant frequency.

Richardson RFPD/Arrow RF & Power
www.richardsonrfpd.com

2.9 In Series Adapter

United Microwave announced its new product the 370SF-40 which is available as a 2.9 mm male to 2.9 mm female right angle. The part meets or even exceeds all specifications per the MIL-C-39012 standard. The material for the body and coupling nut is stainless steel per QQ-S-764 Type 303. The contact material used is beryllium copper as per QQ-C-530, while the insulator material is teflon as per MIL-P-19468A. The mating dims are also in accordance with the MIL Standard-348.

United Microwave Products
www.unitedmicrowave.com

Octave-Band 180° Hybrid

Werbel Microwave is developing a standard line of wide and narrowband 180° hybrids. A signal applied to the sum port produces two outputs of equal amplitude and phase, while a signal applied to the delta port produces output signals of equal amplitude but opposite phase. Model 2JS600 covers the band of 4 to 8 GHz with 1.5:1 VSWR and ±10 degrees phase balance.

Werbel Microwave
www.werbelmicrowave.com

2-Way Combiner/Divider

Werlatone's breakthrough technology provides a new 2-way combining solution covering the full 3000 to 6000 MHz bandwidth. Model D9042 is rated for 250 W at the sum port, and operates with an insertion loss of only 0.35 dB max. This small package size measures just 2.03" × 2" × 0.87" and weighs only 5 ounces. Model D9042 offers excellent isolation of 15 dB min and is designed specifically for military and commercial applications.

Werlatone Inc.
www.werlatone.com

Amplifiers

Rack Mount RF Power Amplifier

The SSPA 0.960-1.215-2000-RM is a rack mounted, high power amplifier that offers high efficiency and high linearity. It is a microprocessor controlled unit and provides excellent performance across the 960 to 1215 MHz frequency band. This high power RF system contains a built-in, predistortion linearizer that allows for low level IMD's at high RF output power levels.

All controls are available on an LCD touch screen display that allows the operator to control all functions via this interface.

Aethercomm Inc.
www.aethercomm.com

Solid State Amplifier

VENDORVIEW

AR's 12500A225 RF solid state CW amplifier is the industry standard for radiated immunitytesting for entire automobiles, producing 12,500 W over the instantaneous 10 kHz to 225 MHz frequency band with harmonic distortion less than -20 dBc. Special features include gain control, internal automatic level control (ALC) and RF output level protection.

AR RF/Microwave Instrumentation
www.arworld.com

TWT Amplifier

dB Control introduces a Ka-Band traveling wave tube (TWT) amplifier for ground and mobile radar applications. Featuring an outdoor hub-mount configuration, the dB-3709i operates in the 34.5 to 35.5 GHz frequency range and provides 700 W minimum peak output power at a duty cycle of up to ten percent. The TWT amplifier is suitable for radar, test and measurement, antenna patterns and radar cross-section measurements. It is specifically designed for reliable performance in extremely harsh environments and for easy field maintenance.

dB Control
www.dbcontrol.com

High Gain Amplifier

The MMG20241H is a 1/4 W high gain amplifier designed as a driver or pre-driver for Doherty power amplifiers in wireless infrastructure equipment operating in the 450 to 3800 MHz frequency range. The device may also be used in a variety of general purpose amplifier applications including frequencies below 450 MHz and above 3800 MHz. At 2655 MHz, its P1dB is 24 dBm with a gain of 17.8 dB. The MMG20241H is biased with a single 5 V supply and draws 78 mA.

Freescale
www.freescale.com

Medium Power/Broadband Amplifier

Model AMFW-6F-18004000-29-8P is a recent addition to MITEQ's family of low noise, wideband and ultra-small waveguide LNAs in the 18 to 40 GHz band. The AMFW-6F-18004000-29-8P has a maximum noise figure of 2.9 dB in the full band, though the typical value is 2.6 dB. This LNA has over 35 dB of gain in a housing that is only 1.32" × 0.88" wide without the field-replaceable 2.93 mm connectors. Gain flatness is a maximum of ±3 dB.

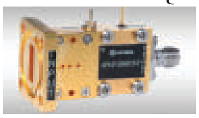

MITEQ Inc.
ww.miteq.com

Broadband Amplifiers

VENDORVIEW

Pasternack Enterprises Inc. announced the release of 10 new 1 and 2 W broadband amplifiers, which are ideal for defense, EW/ECM, radar, test instrumentation, telecom, satcom, microwave radio and industrial applications. These new medium power broadband amplifiers range in frequency from 2 to 18 GHz depending on the RF amplifier configuration.

Pasternack Enterprises Inc.
www.pasternack.com

W-Band Full Band Low Noise Amplifier

VENDORVIEW

Model SBL-7531142240-1010-S1 is a W-band low noise amplifier that covers the entire W-Band from 75 to 110 GHz. The amplifier exhibits more than 20 dB small signal gain with ± 1.5 dB gain flatness and about 4 dB noise figure. The output P1dB of the amplifier is 0 dBm typical and it draws 30 mA current from a single DC power supply in the range of +5 to +12 V. The low noise amplifier is equipped with WR-10 waveguide and UG387/U-M standard flange.

SAGE Millimeter Inc.
www.sagemillimeter.com

20 W GSM Frequency Power Amplifier

Model AHP0091-11-4243 is a GaAs based power amplifier offering 42 dB of linear gain and 43 dBm minimum output power at 1 dB gain compression over the frequency range from 860 to 960 MHz with excellent gain flatness and VSWR. The amplifier has built-in DC voltage regulator and requires a single +12 V DC power supply. The package size of the amplifier is 5.8" × 3.0" × 0.85".

Wenteq Microwave
www.wenteq.com

Networking

IF Transceiver

Innovative Integration announced the FMC-10GE which provides two 10 Gb Ethernet ports on a custom FMC module. Two standard RJ45 connectors support connection to CAT6e networks providing high speed connectivity to PCs, servers, embedded computers such as Innovative's ePC products or custom, intelligent IO. Aggregated burst rates of up to 20 Gbps are achievable. The two 10GE ports are fully independent on the module. Monitoring and control signals are mapped to the FMC interface for detection, loss-of-signal, rate and device control.

Innovative Integration
www.innovative-dsp.com

Sources

Ultra Low Noise Dielectric Resonator Oscillator

The EDRO-1035-10.00 is a 1 W, 10 GHz ultra low noise dielectric resonator oscillator (DRO), with TTL RF muting and variable attenuation feature. The unit draws only 360 mA with + 12 VDC and provides 19 dB of attenuation with -3 VDC. Small size and low cost make this unit attractive for sensor and beacon applications.

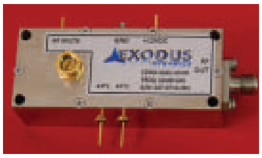

Exodus Dynamics
www.exodusdynamics.com

Greater than 2.5:1 BW VCO

DCMO80210-5 covers a 2.625:1 bandwidth in the frequency range of 800 to 2100 MHz, the full L-Band and more. Phase noise is -96 dBc/Hz at 10 kHz offset with an output power of +5 dBm minimum. The full bandwidth is achieved with a continuous tuning voltage of 0.5 to 24 V and DC bias power requirements of 5 V at 35 mA maximum current draw. The tuning sensitivity is less than 3:1 and the typical harmonic suppression is 10 dB.

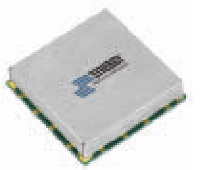

Synergy Microwave Corp.
www.synergymwave.com

Voltage Controlled Oscillator

Z-Communications Inc. announced a new RoHS compliant VCO model V844ME36-LF. The V844ME36-LF operates at 4100 to 4300 MHz with a tuning voltage range of 0.5 to 4.5 VDC and provides better than 1.1:1 tuning linearity. This high performance VCO features a spectrally clean signal of -110 dBc/Hz @ 100 kHz offset and a typical tuning sensitivity of 93 MHz/V. The V844ME36-LF is well suited for microwave radio links and satellite communication applications that require low phase noise performance.

Z-Communications Inc.
www.zcomm.com

Antennas

Dual-Channel Coaxial Rotary Joint

The AMCORJD-Ku dual-channel coaxial rotary joint has been specifically designed for use in the low-profile antennas that are a key element of Ku-Band satellite-on-the-move (SOTM) high-data-rate communication systems. The transmit channel has a frequency range of 13.75 to 14.5 GHz, with a power rating of 40 W CW, a maximum VSWR of 1.4:1 and a typical insertion loss

Statement of Ownership, Management, and Circulation (All Periodicals Publications Except Requester Publications)

1. Publication Title Microwave Journal	2. Publication Number 3 9 6 - 2 5 0	3. Filing Date September 30, 2014
4. Issue Frequency Monthly	5. Number of Issues Published Annually 12	6. Annual Subscription Price Domestic: $120.00 Foreign: $200.00
7. Complete Mailing Address of Known Office of Publication (Not printer) (Street, city, county, state, and ZIP+4®) HORIZON HOUSE PUBLICATIONS, INC. 685 Canton Street Norwood, MA 02062-2610		Contact Person Barbara Walsh Telephone 781-769-9750 x2025

8. Complete Mailing Address of Headquarters or General Business Office of Publisher (Not printer)
same as above

9. Full Names and Complete Mailing Addresses of Publisher, Editor, and Managing Editor (Do not leave blank)

Publisher (Name and complete mailing address)
Carl S. Sheffres, Horizon House Publications, Inc., 685 Canton Street, Norwood, MA 02062-2610

Editor (Name and complete mailing address)
Patrick Hindle, Horizon House Publications, Inc., 685 Canton Street, Norwood, MA 02062-2610

Managing Editor (Name and complete mailing address)
Jennifer DiMarco, Horizon House Publications, Inc., 685 Canton Street, Norwood, MA 02062-2610

10. Owner (Do not leave blank. If the publication is owned by a corporation, give the name and address of the corporation immediately followed by the names and addresses of all stockholders owning or holding 1 percent or more of the total amount of stock. If not owned by a corporation, give the names and addresses of the individual owners. If owned by a partnership or other unincorporated firm, give its name and address as well as those of each individual owner. If the publication is published by a nonprofit organization, give its name and address.)

Full Name	Complete Mailing Address
Horizon House Publications, Inc.	685 Canton Street, Norwood, MA 02062-2610
William M. Bazzy, CEO	" " " " " " "
Ivar A. Bazzy, President	" " " " " " "
Jared M. Bazzy, Vice President	" " " " " " "
Joan B. Egan, EVP	" " " " " " "

11. Known Bondholders, Mortgagees, and Other Security Holders Owning or Holding 1 Percent or More of Total Amount of Bonds, Mortgages, or Other Securities. If none, check box ✓ None

Full Name	Complete Mailing Address

12. Tax Status (For completion by nonprofit organizations authorized to mail at special rates) (Check one)
The purpose, function, and nonprofit status of this organization and the exempt status for federal income tax purposes:
☑ Has Not Changed During Preceding 12 Months
☐ Has Changed During Preceding 12 Months (Publisher must submit explanation of change with this statement)

13. Publication Title	14. Issue Date for Circulation Data Below	
Microwave Journal	YTD	September 30, 2014
15. Extent and Nature of Circulation 51,476	Average No. Copies Each Issue During Preceding 12 Months	No. Copies of Single Issue Published Nearest to Filing Date
a. Total Number of Copies (Net press run)	38,674	40,803
b. Paid Circulation (By Mail and Outside the Mail) (1) Mailed Outside-County Paid Subscriptions Stated on PS Form 3541. (Include paid distribution above nominal rate, advertiser's proof copies, and exchange copies)	30,285	29,797
(2) Mailed In-Country Paid Subscriptions Stated on PS Form 3541 (include paid distribution above nominal rate, advertiser's proof copies and exchange copies)	0	0
(3) Paid Distribution Outside the Mails Including Sales Through Dealers and Carriers, Street Vendors, Counter Sales, and Other Paid Distribution Outside USPS®	5,291	5,175
(4) Paid Distribution by Other Classes of Mail Through the USPS (e.g. First-Class Mail®)	0	0
c. Total Paid Distribution (Sum of 15b(1), (2), (3), and (4))	35,576	34,972
d. Free or Nominal Rate Distribution (By Mail and Outside the Mail) (1) Free or Nominal Rate Outside-Country Copies included on PS Form 3541	674	688
(2) Free or Nominal Rate In-Country Copies Included on PS Form 3541	0	0
(3) Paid Distribution Outside the Mails Including Sales Through Dealers and Carriers, Street Vendors, Counter Sales, and Other Paid Distribution Outside USPS®	0	0
(4) Free or Nominal Rate Distribution Outside the Mail (Carriers or other means)	2,301	5.035
e. Total Free or Nominal Rate Distribution (Sum of 15d (1), (2), (3) and (4))	2,975	5,723
f. Total Distribution (Sum of 15c and 15 e)	38,551	40,695
g. Copies not Distributed (See Instructions to Publishers #4 (page #3))	122	108
h. Total (Sum of 15f and g)	38,674	40,803
i. Percent Paid (15c divided by 15f times 100)	92.28%	85.94%

16. Publication of Statement of Ownership
✓ If the publication is a general publication, publication of this statement is required. Will be printed in the November, 2014 issue of this publication. ☐ Publication not required.

17. Signature and Title of Editor, Publisher, Business Manager, or Owner	Date
Carl S. Sheffres, Publisher	September 30, 2014

I certify that all information furnished on this form is true and complete. I understand that anyone who furnishes false or misleading information on this form or who omits material or information requested on the form may be subject to criminal sanctions (including fines and imprisonment) and/or civil sanctions (including civil penalties).

PS Form 3526, September 2007 (Page 2 of 3)

of 0.6 dB. The receive channel can handle DC to 2.15 GHz at a microwave power of up to 1 W CW.
Link Microtek Ltd.
www.linkmicrotek.com

Antenna Tuners

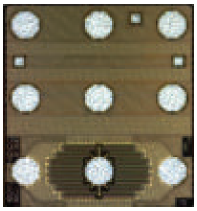

Cavendish's SmarTune antenna tuners are digitally variable capacitors used for LTE antenna tuning in smartphones and handheld devices. Cavendish's 32CK SmarTuners provide over 250 MHz tuning range in the LTE/3G spectrum bands between 700 to 960 MHz, and up to 1 GHz of tuning range between 1.7 and 2.7 GHz. The SmarTune performance gain exceeds 3 dB of added antenna efficiency. All 32CK devices come with a RFFEv1.1 MIPI standards compliant interface for easy integration into any LTE device.
Cavendish Kinetics
www.cavendish-kinetics.com

Test Equipment

Triggerable Impulse Generators

HYPERLABS has announced the release of two new high-speed triggerable impulse generators. The HL9201 (50 ps) and HL9101 (100 ps) generate fast pulses with a spectrum in the frequency domain that extends into the ultra wide band (UWB) communication range (2 to 5 GHz). These devices operate at a repetition rate between 10 Hz and 50 MHz. The products are available for direct purchase on the company's website, and generally ship within one week.
HYPERLABS INC.
www.hyperlabsinc.com

Signal Analyzer

VENDORVIEW

The new flagship of Keysight's X-Series, the N9040B UXA signal analyzer, delivers phase noise performance as well as 510 MHz analysis and real-time bandwidth. The UXA provides wider, deeper views of elusive wideband signals—known or unknown. In the development of mission-critical radar, electronic-warfare and communication systems, leading-edge signal analysis requires excellent phase noise performance. Keysight's proprietary local oscillator (LO) technology achieves phase noise of -136 dBc/Hz at 1 GHz, 10 kHz offset, and -132 dBc/Hz at 10 GHz, 100 kHz offset.
Keysight Technologies Inc.
www.keysight.com

Calibration Solutions

VENDORVIEW

SenarioTek offers calibration solutions for a wide variety of applications. Whether you need to perform automated inline calibration or do testing in a thermal vacuum chamber, the company's team will work with your engineers to create the best solution. By optimizing your calibration needs, SenarioTek will help you achieve the throughput and accuracy needed to get the most out of your equipment investment. Before you start making tradeoffs between speed and accuracy, contact SenarioTek and explore new ways to meet your calibration needs.
SenarioTek
www.senariotek.com

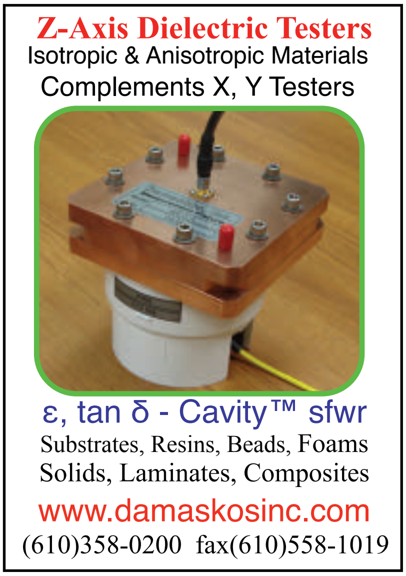
Z-Axis Dielectric Testers
Isotropic & Anisotropic Materials
Complements X, Y Testers
ε, tan δ - Cavity™ sfwr
Substrates, Resins, Beads, Foams
Solids, Laminates, Composites
www.damaskosinc.com
(610)358-0200 fax(610)558-1019


ES MICROWAVE LLC.
Since 1985 we have offered our custom design filters and sub-assemblies in combline, interdigital and suspended-substrate technologies.
Broadband
Suspended-Substrate
Filters, Diplexers, Triplexers, Quadruplexers, Quintuplexers, Sextuplexers...
DC-40 GHz Filters
Multiplexers &
Switch Filter Banks
ES Microwave, LLC
8031 Cessna Avenue, Gaithersburg, MD 20879
P: 301-519-9407 F: 301-519-9418
www.esmicrowave.com


KR Electronics
www.krfilters.com
ISO 9001:2008 Certified
Custom & Standard Filters
40+ Years of Military & Commercial Applications
Bandpass
Anti-Aliasing
Highpass
Video Filters
Diplexers
Delay Equalized
Surface Mount
Lowpass
Notch
Root Cosine
Equalizers
Linear Phase
Absorptive
Matched
KR Electronics, Inc.
Avenel, NJ
www.krfilters.com
sales@krfilters.com
Phone 732.636.1900
Fax 732.636.1982


LOGUS
Waveguide & Coaxial Switches
WR10 thru WR975
WR137
WR75
WR229
WRD580
VALUE · QUALITY · FAST DELIVERY
LOGUS.com
p: 561-842-3550
f: 561-842-2196


Frequency SYNTHESIZERS
• Applications up to 32 GHz such as SatCom
• Wide bandwidth single and multi-loop designs
• Low phase noise and low spurious
Phase-Locked OSCILLATORS
• Low phase noise and low spurious
• DROs to 32 GHz
• CROs to 5 GHz
• Crystal Osc. to 1.4 GHz
• Ref: 10 MHz / Internal
Low Cost Custom Designs are Our Specialty
Luff Research
Web: www.luffresearch.com
Tel: (516) 358-2880 Fax: (516) 358-2757
Email: sales@luffresearch.com

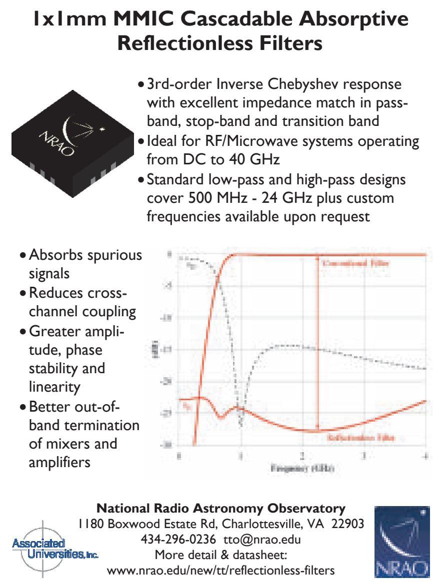
1x1mm MMIC Cascadable Absorptive Reflectionless Filters
• 3rd-order Inverse Chebyshev response with excellent impedance match in pass-band, stop-band and transition band
• Ideal for RF/Microwave systems operating from DC to 40 GHz
• Standard low-pass and high-pass designs cover 500 MHz - 24 GHz plus custom frequencies available upon request
• Absorbs spurious signals
• Reduces cross-channel coupling
• Greater amplitude, phase stability and linearity
• Better out-of-band termination of mixers and amplifiers
National Radio Astronomy Observatory
1180 Boxwood Estate Rd, Charlottesville, VA 22903
434-296-0236 tto@nrao.edu
More detail & datasheet:
www.nrao.edu/new/tt/reflectionless-filters
Associated Universities, Inc.
NRAO

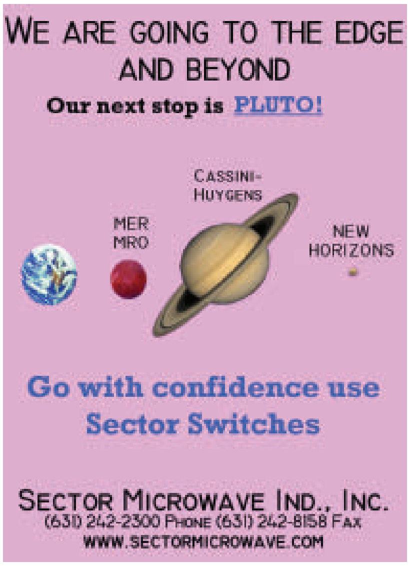
WE ARE GOING TO THE EDGE AND BEYOND
Our next stop is PLUTO!
CASSINI-HUYGENS
MER MRO
NEW HORIZONS
Go with confidence use Sector Switches
SECTOR MICROWAVE IND., INC.
(631) 242-2300 PHONE (631) 242-8158 FAX
WWW.SECTORMICROWAVE.COM


REVOLUTIONARY HERMETIC SMP CONNECTORS
These SMPs meet the requirements of MIL-STD-348, but utilize unique housing interface features, which significantly improves reliability and production assembly yields. Proprietary techniques are used to independently control plating thickness on pin and housing.
For use with Aluminum, Kovar and other package materials
SHP
SPECIAL HERMETIC PRODUCTS, INC.
PO BOX 269 – WILTON – NH – 03086
(603) 654-2002 – Fax (603) 654-2533
E-mail: sales@shp-seals.com
Web: www.shp-seals.com


Wright Technologies
Military Grade at Commercial Pricing
BATTLE TESTED
ASP26-3033
18-26.5 GHz
+33 dBm P-1dB
IN
OUT
S/N 0013 1814
Products that are made to Last!
• Amplifiers & Multipliers
• Subsystems & Converters
• Form, Fit & Function
• Operational Frequencies .1 to 96 GHz
+33 dBm P-1dB
(916) 773-4424 Ph (916) 760-2770 Fx
www.wrighttec.com
2015 CATALOG COMING SOON!

Millimeter Wave Wireless Communications

Theodore S. Rappaport, Robert W. Heath Jr., Robert C. Daniels and James N. Murdock

5G advanced communications systems are now in the research and development stages and millimeter wave wireless communications could be the next breakthrough for wireless networks in the mobile cellular industry, emerging wireless local area networks, personal area networks and vehicular communications. Completely new products, systems, theories and devices will be created to deliver mobile data rates of many Gigabits per second – thousands of times greater than today's cellular and Wi-Fi networks.

Millimeter Wave Wireless Communication Systems is one of the first comprehensive treatments of all technical elements of millimeter wave wireless communications systems that fuses key concepts from communications, circuits, antennas, propagation and emerging global standards into one complete, easy-to-read textbook. Written by four leading practitioners in the emerging field of millimeter wave wireless communications, this book allows engineers in both industry and academia to quickly become acquainted with the fundamentals needed to implement and explore the untapped potential of the higher spectrum that will provide unprecedented products and applications, never before imagined in the wireless industry.

Topics include:

- Digital communication: baseband signal/channel models, modulation, equalization, error control coding, multiple-input-multiple-output (MIMO) principles and hardware architectures
- Radio wave propagation characteristics: indoor and outdoor channel models and beam combining
- Antennas/antenna arrays: on-chip and in-package antennas, fabrication and packaging
- Analog circuit design: mmWave transistors, fabrication and transceiver design approaches
- Baseband circuit design: multi gigabit-per-second, high-fidelity DAC and ADC converters
- Physical layer: algorithmic choices, design considerations and impairment solutions; and how to overcome clipping, quantization and nonlinearity
- Higher-layer design: beam adaptation protocols, relaying, multimedia transmission and multiband considerations
- 60 GHz standardization: IEEE 802.15.3c for WPAN, Wireless HD, ECMA-387, IEEE 802.11ad, Wireless Gigabit Alliance (WiGig)

To order this book, contact:

Prentice Hall
230 Pearson Parkway
Lebanon, IN
www.mypearsonstore.com

680 pages, $125
ISBN: 978-0-13217-228-8

2015 Microwave Wireless Industry Exhibition in China (MWIE 2015)
2015 National Conference on Microwave and Millimeter Wave in China

MWIE 2015

Sponsor: Chinese Institute of Electronics (CIE)

Co-Sponsors: Microwave Society of Chinese Institute of Electronics
38th Research Institute of China Electronics Technology Group Corporation (CETC38)
University of Science and Technology of China
Hefei Normal University of China
Kingradio Technology [Shenzhen] Co., Ltd.
HT Microwave Co., Ltd.
Anhui University of China
Education Development Fund of Lin Weigan
Xi'an HengDa Microwave Technology Development Company

Collaborating Media: Journal of Microwaves(China), Radar Science and Technology(China), Microwave Journal (USA), Mwrfchina and Rfeda

2015 Microwave Wireless Industry Exhibition(MWIE2015) and 2015 National Conference on Microwave and Millimeter Wave in China (NCMMW2015) will be held in Anhui Kaiyuan Hotel, Hefei, China, in May 30 ~ June 2, 2015.
NCMMW2015 is China's largest conference on microwave and millimeter wave technologies. It is organized by Chinese Institute of Electronics (CIE) and held every two years (every odd year).
MWIE has already been held for over 20 years. It is one of most important events of the National Conference on Microwave and Millimeter Wave in China held every odd year, and the International Conference on Microwave and Millimeter Wave Technology held every even year.

MWIE2015 will be another grand exhibition after "MWIE2013" in Chongqing, "MWIE2012" in Shenzhen, "MWIE2011" in Qingdao, "MWIE2010" in Chengdu, "MWIE2009" in Xi'an, "MWIE2008" in Nanjing China!

Date: May 30~June 2, 2015 **Venue: Anhui Kaiyuan Hotel, Hefei, China**



"9th Committee Enlarged Conference of Microwave Society of Chinese Institute of Electronics" will be held during the period of MWIE2015. Nearly 80 Committee members from institutes, universities and companies of all parts of China will attend the conference and visit the exhibition. This is the best chance to let Chinese people know your company and products; exhibit in MWIE2015 is the best choice for your products to enter Chinese market.

Exhibitors to be attended:

Manufacturers / distributors for RF / microwave / millimeter wave devices / components: solid state device and circuits (including mmic): amplifiers, mixers, oscillators, etc. and passive components: filters, duplexers, couplers, attenuators, and antennas etc
Designer / distributor for RF / microwave / millimeter wave software
Manufacturers / distributors for RF / microwave / millimeter wave equipments
Manufacturers / distributors for RF / microwave PCB and connectors
Manufacturers / distributors for microwave absorber
Manufacturers / distributors for microwave / millimeter inductor, capacitor and high power resistor

Why you should attend?

MWIE2015 is the largest event of microwave, millimeter wave and RF field in China, which is sponsored by Microwave Society of Chinese Institute of Electronics
MWIE 2015 is where to provide a platform for enterprises engaged in microwave, millimeter wave and RF field to publicize your company/ products in China.
MWIE 2015 will provide a chromatic page of introduction for each exhibitor in List of Exhibitors, which is free.
MWIE 2015 is where to provide a nice opportunity for the scientists and engineers specialized in the field of microwave and millimeter wave to present your new ideas and learn from each other.

Contact: Mr. Wei Zilun, Gao Xin, Ms. Liu, Ms. Xu E-mail: mwrf@vip.163.com kingradio@188.com

AdvertisingIndex

Advertisers in blue are enabled with the layar app

Sales Representatives

Microwave Journal
Frequency Matters.

Eastern and Central Time Zones
Chuck Boyd
Northeast Reg. Sales Mgr.
(New England, New York, Eastern Canada)
685 Canton Street
Norwood, MA 02062
Tel: (781) 619-1942
FAX: (781) 769-5037
cboyd@mwjournal.com

Michael Hallman
Eastern Reg. Sales Mgr.
(Mid-Atlantic, Southeast, Midwest)
4 Valley View Court
Middletown, MD 21769
Tel: (301) 371-8830
FAX: (301) 371-8832
mhallman@mwjournal.com

Pacific and Mountain Time Zones
Brian Landy
Western Reg. Sales Mgr.
(CA, AZ, OR, WA, ID, NV, UT, NM, CO, WY, MT, ND, SD, NE & Western Canada)
144 Segre Place
Santa Cruz, CA 95060
Tel: (831) 426-4143
FAX: (831) 515-5444
blandy@mwjournal.com

International Sales
Richard Vaughan
International Sales Manager
16 Sussex Street
London SW1V 4RW, England
Tel: +44 207 596 8742
FAX: +44 207 596 8749
rvaughan@horizonhouse.co.uk

Germany, Austria, and Switzerland (German-speaking)
WMS.Werbe- und Media Service
Brigitte Beranek
Gerhart-Hauptmann-Street 33,
D-72574 Bad Urach
Germany
Tel: +49 7125 407 31 18
FAX: +49 7125 407 31 08
bberanek@horizonhouse.com

Israel
Liat Heiblum
Oreet International Media
15 Kineret Street
51201 Bene-Berak, Israel
Tel: +972 3 570 6527
FAX: +972 3 570 6526
liat@oreet-marcom.com

Korea
Young-Seoh Chinn
JES Media International
2nd Floor, ANA Bldg.
257-1, Myungil-Dong
Kangdong-Gu
Seoul, 134-070 Korea
Tel: +82 2 481-3411
FAX: +82 2 481-3414
yschinn@horizonhouse.com

Japan
Katsuhiro Ishii
Ace Media Service Inc.
12-6, 4-Chome,
Nishiiko, Adachi-Ku
Tokyo 121-0824, Japan
Tel: +81 3 5691 3335
FAX: +81 3 5691 3336
amskatsu@dream.com

China
Michael Tsui
ACT International
Tel: 86-755-25988571
Tel: 86-21-62511200
FAX: 86-10-58607751
michaelT@actintl.com.hk

Hong Kong
Mark Mak
ACT International
Tel: 852-28386298
markm@actintl.com.hk

Ed Kiessling
Traffic Manager/Inside Sales
685 Canton Street
Norwood, MA 02062
Tel: (781) 619-1963
FAX: (781) 769-6178
ekiessling@mwjournal.com

MicrowaveJournal's

STEM Works

Microwave Filter [mi-cro-wave fil-ter]

A circuit or structure that impedes the transmission of certain microwave frequencies, or frequency bands, while allowing the passage of others. Filters may be described as lowpass, bandpass, highpass or multiplexers, and may have functional characteristics such as Chebyshev, Butterworth or elliptic. Filters are essential components in radar and communications systems.

1897 Lord Rayleigh proposes the concept of waveguide for electromagnetic waves. He later develops wave theory to explain the Whispering Gallery waveguide mode of St. Paul's Cathedral that acts as a resonant cavity filter for acoustic waves.

1937 W.P. Mason and R.A. Sykes pioneer early analytical work in the field of microwave filters prior to WWII by deriving filter impedance and attenuation functions using ABCD parameters.

1948 "The MIT Radiation Laboratory Series," Vol. 9 (Chapters 9 & 10) by R.M. Fano and A.W. Lawson provides a classic introduction to the theory and design of microwave filters.

1957 S.B. Cohn provides the first comprehensive theory with practical application for designers.

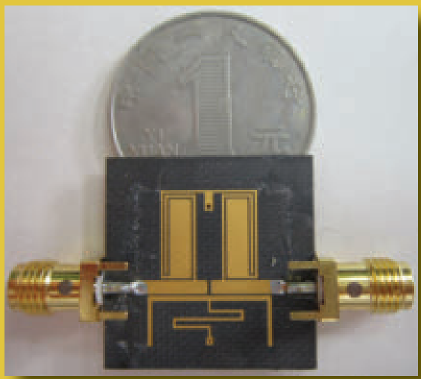

1964 G.L. Mathai, L. Young and E.M.T. Jones publish their well-known treatise on filters, impedance matching networks and coupling structures. This widely used reference is still in print.

1960s & 70s

Temperature stabilized dielectric resonator filters are introduced, providing high Q in a compact size.

1970s Linear phase filters are developed for low distortion in modern communications systems.

Subsequent Advances

The rapid synthesis of complex multimode/multiband structures in various media with improved in-band and out-of-band characteristics is enabled through the use of EM simulation and optimization algorithms.

Scan page using layar app

WERLATONE®

Truly Custom Designs

Couplers | Combiners/Dividers | Hybrids | Filters

Multi-Port Couplers
Model C7067

How Many Ports?

Custom Connectors !
Model C9219

What's your Interface?

Radial Combiners
Model D9706

How Many Inputs?

Big Stuff !
Model D8421

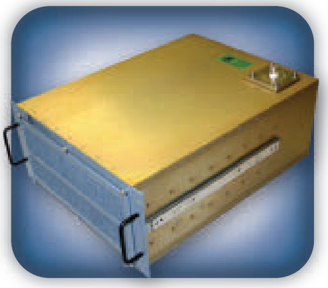

How Much Power?

Isolated N-Ways
Model D9714

Radial With Isolation?

Absorptive Filters
Model AF9350

Low Pass, High Pass?

Send Us Your Specs!!

Some of our Customer Driven Designs

Model	Type	Frequency (MHz)	Power (W CW)	Insertion Loss (dB)	VSWR
C7067	Directional Coupler, 4 Coupled Ports	123-133	2,250	0.15	1.20:1
C9219	Directional Coupler, Unflanged	640-660	3,500	0.1	1.15:1
D9706	16-Way Combiner / Divider	2,700-3,500	6,000	0.35	1.35:1
D8421	8-Way Combiner / Divider	1.5-30	12,000	0.3	1.30:1
D9714	5-Way Combiner / Divider	1,175-1,375	1,500	0.4	1.35:1
AF9350	Absorptive UHF Low Pass Filter	10-500	400	0.5	1.25:1

* Specifications are for reference only and subject to change without notice.

Werlatone, Inc. 17 Jon Barrett Road Patterson, NY 12563 (845) 278-2220 www.werlatone.com sales@werlatone.com

2014

Mobile Communications and Infrastructure

A Special Supplement to Microwave Journal

Contents

Cover Feature

Technical Features

Special Report

Product Features

Tech Briefs

Company Showcase

AUGMENTED REALITY: HOW IT WORKS

STEP 1
Download the free Layar app from the iTunes (iOS) or Google Play (Android) store.

STEP 2
Launch the app to view enhanced content on any page with the layar logo.

STEP 3
Frame the entire page in the screen and tap to experience enhancements (tap screen again for full screen view).

Refer to page 50 for this month's participants
AR pages may expire after 60 days

STAFF

Small Wavelengths – Big Potential: Millimeter Wave Propagation Measurements for 5G

Sijia Deng, Christopher J. Slezak, George R. MacCartney Jr. and Theodore S. Rappaport
NYU WIRELESS, NYU Polytechnic School of Engineering, Brooklyn, N.Y.

This article introduces wideband millimeter wave propagation measurements and the sliding correlator channel sounder system used to measure millimeter wave channels in New York City. The measurement system includes a 400 to 750 Megachips-per-second sliding correlator channel sounder that utilizes steerable directional horn antennas at both the transmitter and receiver. Several recent propagation measurement campaigns were conducted by the NYU WIRELESS research center in indoor and outdoor environments at the 28 and 73 GHz millimeter wave bands, resulting in directional and omnidirectional path loss models and multipath spread characteristics that are presented here. Measurement results for directional path loss, omnidirectional path loss and RMS delay spread are presented here. These results will help engineers design future millimeter wave wireless communications systems and will assist in the standardization of millimeter wave wireless networks.

As the wireless industry prepares for the impending fifth-generation (5G) wireless technology to meet the projected 1,000 × growth in user demand in the coming decade, there is a need for accurate and comprehensive channel models at millimeter wave frequencies.[1,2,4,5] Unlike previous generations of cellular technology, 5G will likely make use of the millimeter wave spectrum while also using existing UHF/microwave frequencies.

Millimeter wave frequencies (30 to 300 GHz) show great promise for the future of wireless communications because of the large raw available, unused bandwidth. In particular, over 14 GHz of available spectrum exists in the 28, 38/39, and 73 GHz bands, making these bands excellent candidates for new mobile spectrum that will increase capacity by several orders of magnitude over today's cellular and Wi-Fi allocations.[2,5] Recent advances in integrated circuit and antenna technology have made it possible to inexpensively and reliably manufacture wireless devices that operate at millimeter wave frequencies.[1,4,15,32]

Millimeter wave frequencies have not been widely used for personal communications to date because of a lack of available electronic components and a common belief that rain and atmospheric attenuation are too high for mobile access communications at these high frequencies. However, in reality the additional attenuation at millimeter wave frequencies will be negligible for coverage distances on the

order of several hundred meters.[5-7] Urban cellular deployments already use smaller cell sizes to meet growing capacity demands, thus millimeter wave cells will have similar density to deployments in use in today's urban areas.[6]

The uncharted millimeter wave spectrum requires carefully planned measurements in order to develop channel models to support equipment design and the standardization process of the air interface. Since 2012, the NYU WIRELESS research center has performed measurements at 28 and 73 GHz in New York City. These measurements have been used to develop channel models that are being used by researchers throughout industry and academia.[4-14,27,28] Earlier measurements in Austin, Texas during the summer of 2011 explored the 38 and 60 GHz bands, using a 400 and 750 Megachips-per-second (Mcps) spread spectrum binary phase shift keying (BPSK) channel sounder, very similar to the channel sounder used for the New York City measurements.[20,26,29,30,31]

MEASUREMENT APPROACH AND TEST SYSTEM

To conduct wideband millimeter wave channel measurements with angle of arrival and departure information, as well as high resolution multipath and received power, NYU WIRELESS makes use of a custom-built BPSK sliding correlator channel sounder. Unlike systems using vector network analyzers, there is no need for phasing cables between the transmitter (Tx) and receiver (Rx). Without the need for connecting the Tx and Rx, separation distances can be measured up to hundreds of meters in non-line-of-sight (NLOS) conditions. The system triggers from the strongest arriving multipath energy and is being upgraded with GPS-controlled cesium-standard clocks for absolute timing measurements.

The use of sliding correlation allows the channel sounder to measure over very large bandwidths.[3,25] Transmission begins with the generation of a baseband pseudorandom noise (PN) signal. The PN sequence is created by an 11-bit linear feedback shift register (LFSR), yielding a PN sequence with a length of 2^{11}-1 = 2047.

At the receiver, the signal is demodulated into its baseband in-phase (I) and quadrature (Q) components. These signals are then cross-correlated with a PN sequence identical to the Tx. The PN sequence at the Rx, however, is generated at a chip rate slightly offset from the Tx chip rate. For the outdoor New York City measurements, the Tx transmits at 400 Mcps and the Rx chip rate is 399.95 Mcps. The offset in chip rates gives rise to the slide factor, γ, which is calculated as:

$$\gamma = \frac{f_c}{f_c - f_c'}$$

where f_c and f_c' are the Tx and Rx chip rates, respectively.[3,16]

Due to the autocorrelation properties of PN sequences, the cross-correlation will be orders of magnitude larger when the two sequences are aligned than when not. These correlations can be performed separately but concurrently for the I and Q components, yielding two signals I(τ) and Q(τ).[17] The correlation peaks that occur when the sequences are aligned can be sampled and used to recover the channel's power delay profile (PDP) p(τ).

$$p(\tau) = I^2(\tau) + Q^2(\tau)$$

One of the most important features of the sliding correlator is the time dilation it provides. The sliding correlator has the effect of compressing the PDP's bandwidth drastically, equivalent to the original Tx chip rate divided by the slide factor.[3,18] For chip rates of 400 Mcps at the Tx and 399.95 Mcps at the Rx, the signals I(τ) and Q(τ) will each have a bandwidth of only 50 kHz.

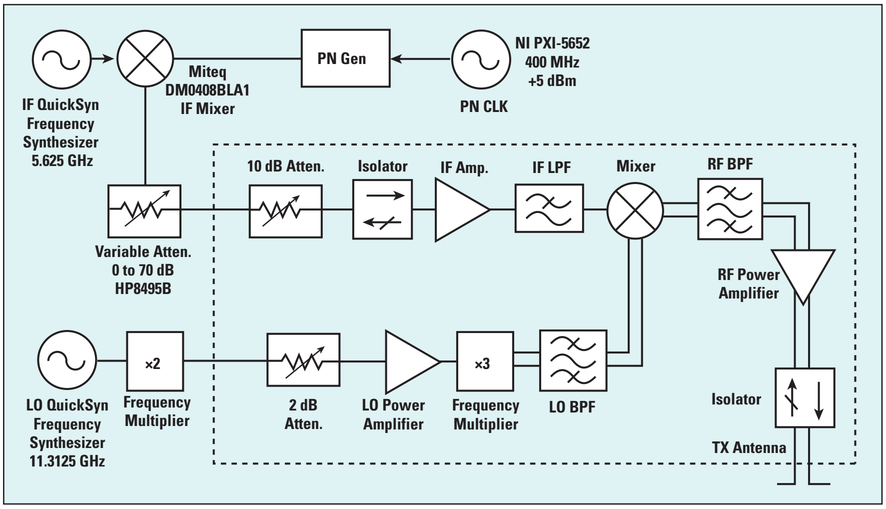

Fig. 1 Block diagram of the transmitter used to characterize the 73 GHz channel.

Although the sliding correlation process approximates the autocorrelation of a PN sequence, there is still improvement to be made after the time-dilated PDP has been recovered. The compression to a very narrow bandwidth offers the opportunity to lowpass filter the signal and reject a considerable amount of distortion that is present at higher frequencies.[16] Once this signal has been filtered, the true un-dilated PDP can be recovered.

There are several parameters that influence the performance of a sliding correlator, but the dynamic range in particular is often the greatest concern when considering channel sounder performance.[19] The theoretical dynamic range is determined from the length of the PN sequence, and is 66.2 dB for a sequence of length 2047.[19]

Figure 1 shows the block diagram of the transmitter system for the 73 GHz measurements. The channel sounding system uses QuickSyn signal generators provided by National Instruments (NI) for an intermediate frequency (IF) at 6.625 GHz. The 400 Mcps baseband PN sequence, produced by a PN sequence generator, is first mixed with the 5.625 GHz IF to obtain the second stage IF spread spectrum signal. The 22.625 GHz LO frequency is tripled by a frequency multiplier to 67.875 GHz, which drives the mixing operation with the spread spectrum IF signal. This generates a spread spectrum RF signal centered at 73.5 GHz with an 800 MHz first null-to-null RF bandwidth.[10]

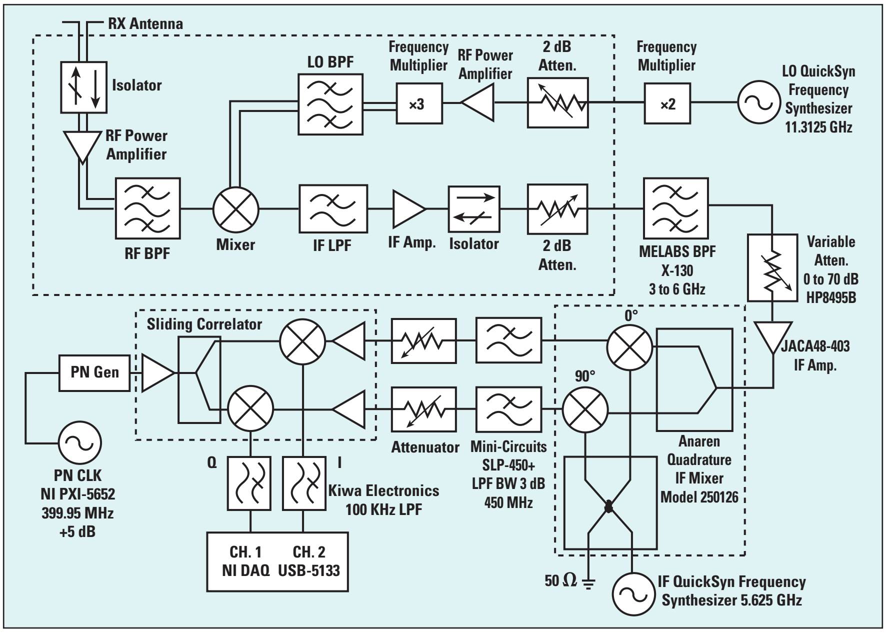

▲ *Fig. 2 Block diagram of the receiver used to characterize the 73 GHz channel.*

TABLE 1

SPECIFICATIONS FOR THE 28 AND 73 GHz CHANNEL SOUNDERS

Carrier Frequency	*28 GHz*	*73.5 GHz*
Chip Sequence Length	$2^{11} - 1 = 2047$	
Chip Sequence Clock Rate (Tx)	400 MHz	
Chip Sequence Clock Rate (Rx)	399.95 MHz	
First Null-to-Null RF Bandwidth	800 MHz	
Slide Factor	8000	
Tx Antenna Gain	24.5 dBi / 15 dBi	27 dBi / 20 dBi
Tx Antenna AZ HPBW	10.9°/30°	7°/ 15°
Tx Antenna EL HPBW	8.6°/30°	7°/ 15°
Rx Antenna Gain	24.5 dBi / 15 dBi	27 dBi / 20 dBi
Rx Antenna AZ HPBW	10.9°/ 30°	7°/15°
Rx Antenna EL HPBW	8.6°/ 30°	7°/15°
Antenna Polarization	VV	VV/VH
Maximum Tx Power	30 dBm	14.6 dBm
Maximum Measurable Path Loss	178 dB	181 dB

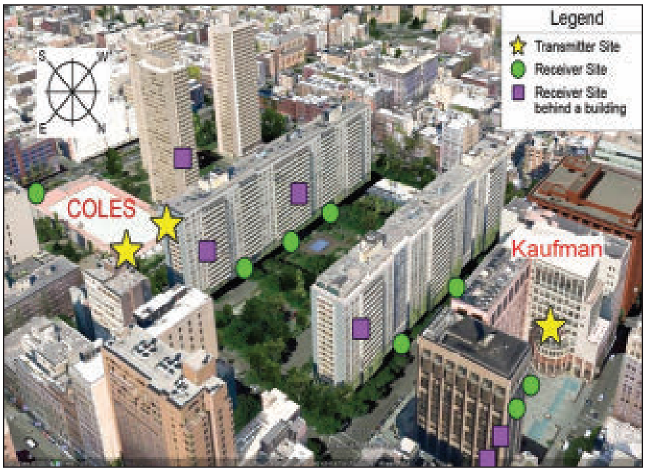

▲ *Fig. 3 28 GHz measurement sites near NYU's Manhattan campus.*

Figure 2 shows the block diagram of the receiver system for 73 GHz measurements. The received signal is down-converted from the 73.5 GHz RF to the 5.625 GHz IF. The LO frequency at 22.625 GHz is the same as on the Tx side. The sliding process correlates the 399.95 Mcps baseband signal generated by the Rx PN sequence generator and the baseband equivalent received I and Q signals from the downconverter, resulting in a time-dilated autocorrelation with a bandwidth of 50 kHz. The NI DAQ digitizer samples the time-dilated pulse on both the I and Q channels at 2 Megasamples-per-second (Msps). The Tx and Rx channel sounder block diagrams for 28 GHz are very similar to those shown for 73 GHz in Figures 1 and 2.

Directional horn antennas with various directive gains are used to provide spatial discrimination similar to what will be used in future millimeter wave systems.[1,15,32] By using directional antennas that can be rotated in the azimuth and elevation planes, angle of arrival (AOA) and angle of departure (AOD) information can be obtained by taking measurements across different AOA and AOD combinations.

Table 1 summarizes the specific parameters of the channel sounders used for each measurement campaign. AZ denotes azimuth, EL is elevation and HPBW is half-power beamwidth. VV indicates that the Tx and Rx horn antennas are both vertically polarized; VH denotes that the Tx antenna is vertically polarized and that the Rx antenna is horizontally polarized.

OUTDOOR MEASUREMENT CAMPAIGNS

The 28 GHz outdoor propagation measurements were conducted at three transmit locations and 25 receive locations in downtown Manhattan,[8] shown in ***Figure 3***. The three transmit locations are depicted with yellow stars, and the receive locations with green circles and purple squares. The green circles represent visible receive sites, and the purple squares depict receive locations blocked by obstructions in this view.

The 75 total Tx-Rx combinations comprised of Tx-Rx separation distances from 19 to 425 m. The channel sounder employed a 24.5 dBi gain antenna (10° HPBW) at the Tx, and either a 15 dBi (30° HPBW) or 24.5 dBi gain antenna (10° HPBW) at the Rx. The measurements were performed for a base station-to-mobile scenario, with Rx antennas at a mobile height of 1.5 m. Tx antennas were placed on relatively low rooftops, with two Tx locations 7 m above ground level (AGL) and one Tx location 17 m AGL. For each Tx-Rx location combination, 10 sets of measurements were conducted for various Tx and Rx azimuth and elevation angle configurations.

In addition to the Manhattan measurements, 28 GHz outdoor propagation measurements were also performed in downtown Brooklyn. These measurements were conducted for

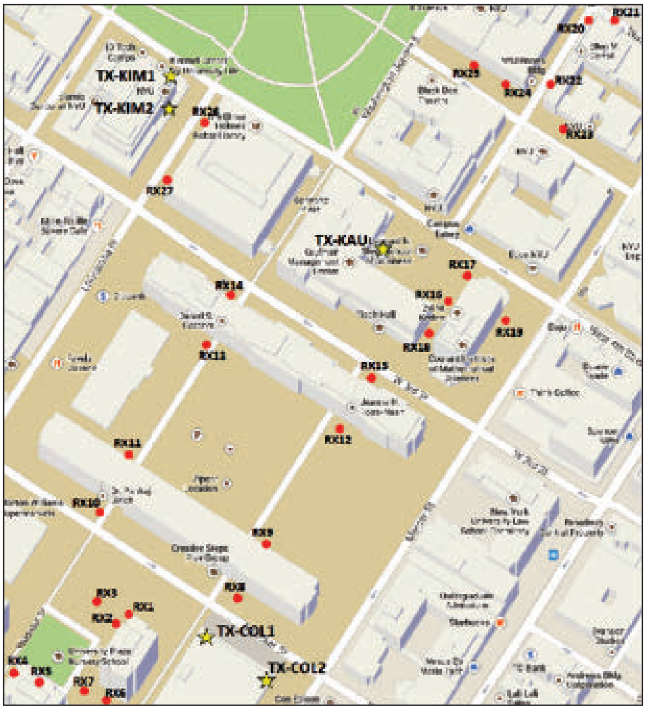

Fig. 4 73 GHz measurement sites around NYU's Manhattan campus.

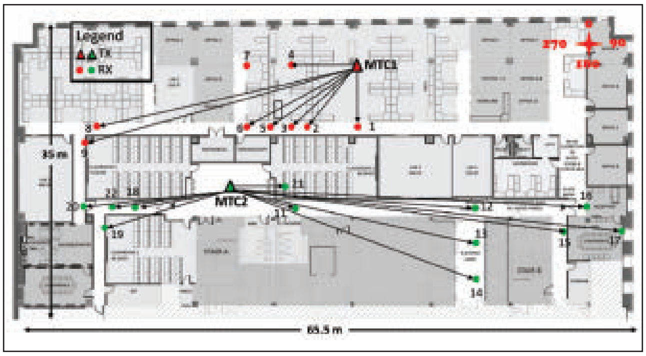

Fig. 5 Locations for the 73 GHz indoor measurements.[22]

one Tx and 11 Rx locations, with the Tx-Rx separation distance ranging from 75 to 125 m. At three locations, the Rx was moved in half-wavelength increments on an automated 10-wavelength long linear track. This configuration studied small-scale fading, which impacts MIMO performance.[23]

The 73 GHz outdoor propagation measurements were conducted in downtown Manhattan, at five transmit and 27 receive locations, as shown in ***Figure 4***. The five transmit locations are denoted by yellow stars. Two were on the two-story rooftop of the Coles Recreational Center (7 m high), two on the second floor balcony of the Kimmel Center (7 m high), and one on the fifth-story balcony of the Kaufman building of the Stern Business School (17 m high). Tx-Rx separation distances ranged from 30 to 216 m.

A total of 36 unique mobile access and 38 backhaul link combinations were measured. Rx antennas at heights of 2 and 4.06 m were used to emulate base station-to-mobile links and wireless backhaul links, respectively. For each Tx-Rx combination, up to 12 measurement sweeps were conducted to generate omnidirectional path loss models.[12]

INDOOR MEASUREMENT CAMPAIGN

An extensive indoor propagation measurement campaign at 73 GHz was conducted for different antenna polarizations to model a typical office environment. To measure the co- and cross-polarized channel characteristics, a pair of 20 dBi (15° HPBW) antennas was used. Two transmit and 21 receive locations, shown in ***Figure 5***, were chosen to investigate the complex indoor propagation channels.

The Tx-Rx separation distance ranged from 6 to 46 m. The Tx antenna was set at a height of 2.5 m near the ceiling to imitate current indoor wireless access points; the Rx was set at a height of 1.5 m (similar to the height of a mobile phone carried by a person). For each Tx and Rx location combination, eight measurements with various AOD and AOA and co- and cross-polarization combinations were measured.[21]

MEASUREMENT RESULTS

Measurement results from the 28 and 73 GHz outdoor and 73 GHz indoor campaigns include directional path loss models, omnidirectional path loss models and direction root mean square (RMS) delay spread characteristics.

Directional path loss values were obtained from individual unique pointing angles for all measurements. Directional path loss models are important, since 5G systems will use narrow beam directional antennas and will take advantage of beamforming and beam combining technologies.

Close-in free space reference distance path loss at a reference distance d_0 is expressed by the following equation:

$$PL(d)[dB] = PL(d_0) + 10\bar{n}\log_{10}\left(\frac{d}{d_0}\right) + X_\sigma \qquad (1)$$

where $\bar{n}$ is the best fit minimum mean square error (MMSE) path loss exponent (PLE), and X_σ is a zero mean Gaussian random variable with a standard deviation σ in dB, also known as the shadowing factor, caused by large-scale random variations in the channel.[3] The PLE is introduced to describe the propagation attenuation caused by the channel.

Figure 6 shows outdoor directional path loss models using a 1 m close-in free space reference distance for 28 and 73 GHz. Red crosses represent the NLOS path loss value measurements, blue triangles represent the best path loss values for a specific Tx-Rx location combination and green circles represent line-of-sight (LOS) path loss. Path loss models are simplified using a d_0 of 1 m, as it removes the denominator term seen in Equation 1.

For LOS scenarios, the PLE in outdoor and indoor environments for both 28 and 73 GHz is favorable, close to the theoretical free space path loss (FSPL) of n = 2.

The NLOS measurements also include measurements at LOS environment when the TX and RX antennas are not directly on boresight with each other. For NLOS scenarios, ***Figure 6a*** shows a PLE of 4.5 for all locations in 28 GHz outdoor measurements with 24.5 dBi narrow beam co-polarized antennas. ***Figure 6b*** shows a PLE of 4.7 for 73 GHz outdoor measurements, and ***Figure 6c*** shows a PLE of 5.1 for 73 GHz indoor measurements with co-polarized antennas.

NLOS-best denotes the lowest path loss observed at a unique point-

ing angle for the directional NLOS channel for each Tx-Rx location combination. Figure 6 shows that the NLOS-best PLE is 3.7 for 28 GHz outdoor and that the NLOS-best PLE is 3.6 and 3.3 for 73 GHz outdoor and indoor measurements, respectively. This improvement in PLE when considering the best NLOS angles is significant and shows the advantage of using beam searching and directional antennas at millimeter wave frequencies. The NLOS path loss experienced large attenuation per decade; however, the use of multiple antenna elements and beamforming and beam combining technologies can significantly decrease the path loss when considering the best possible paths.

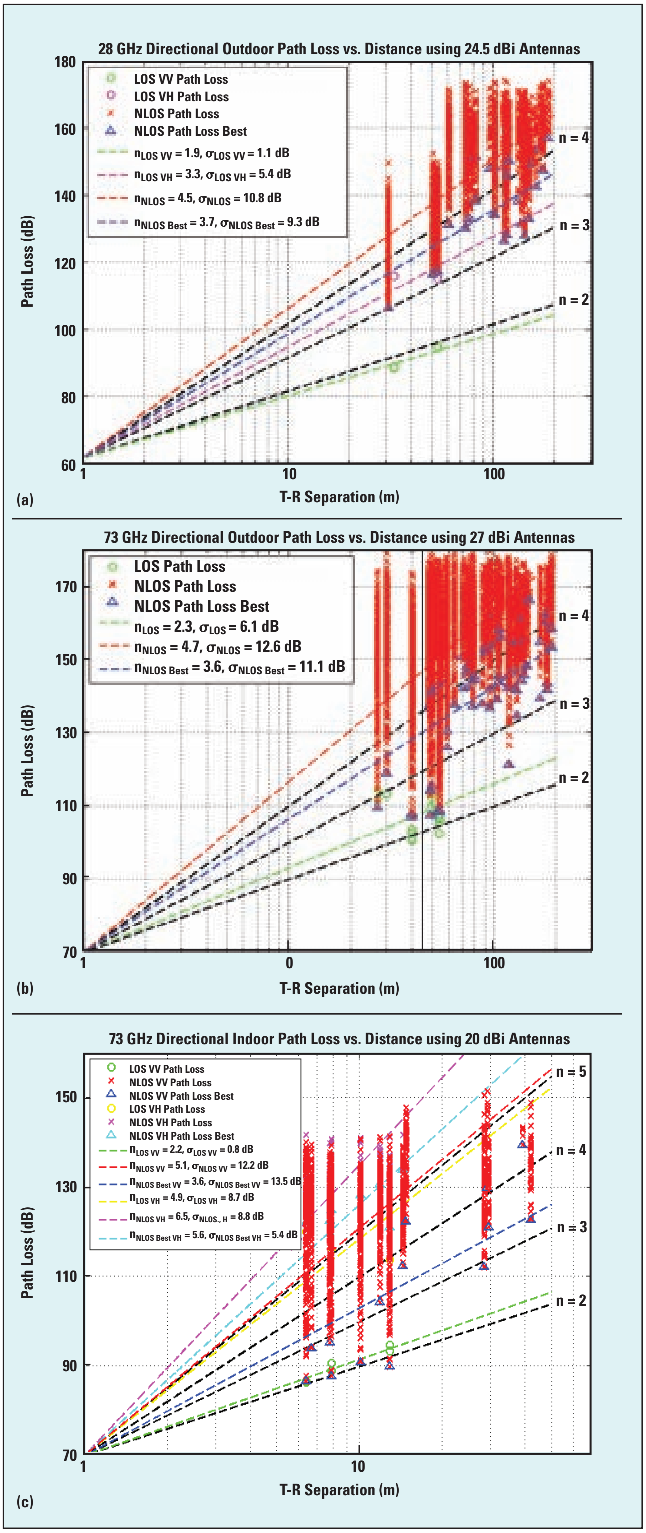

▲ *Fig. 6 28 GHz and 73 GHz close-in free space reference distance directional path loss in the outdoor urban environment of New York City, and indoor path loss models. 28 GHz outdoor directional path loss models (a). 73 GHz outdoor directional path loss models, considering access and backhaul Rx heights (b). 73 GHz indoor directional path loss models with VV and VH antenna polarization (c).*

The results show that beam combining can significantly reduce the propagation PLE[32]. PLE for certain Tx and Rx combinations reduces from 4.7 to 3.6 for 73 GHz outdoor scenarios using a 1 m free space reference distance. By coherently combining the four strongest signals from four distinct beams, compared to an arbitrarily pointed single beam, 28 dB of link improvement is achieved, and 10 dB of improvement when compared to a single optimum beam over a 100 m Tx-Rx separation at 73 GHz. For the 28 GHz outdoor measurements, the maximum possible improvement reaches 24 dB. The cross polarization measurements also show the potential for antenna polarization diversity systems in indoor millimeter wave communications systems.[21]

OMNIDIRECTIONAL PATH LOSS

Omnidirectional path loss models are important, since they allow an arbitrary antenna pattern to be used in simulation or analysis. The existing 3GPP WINNER II and other 3GPP-like models are omnidirectional for this reason. To create omnidirectional models for each Tx-Rx location combination, the received powers at every unique azimuth and elevation angle combination were summed after removing antenna gains. This yields an omnidirectional received power for each Tx-Rx location combination, used to compute an omnidirectional path loss model.[6,14,21]

Figure 7a shows the omnidirectional path loss models for 28 GHz outdoor LOS and NLOS measurements using a 1 m close-in reference distance. The LOS PLE of 2.3 is very close to the theoretical FSPL and has a small shadowing factor of 2.6 dB. The NLOS PLE is 3.4 with a standard deviation of 9.7 dB.[14] ***Figure 7b*** shows the omnidirectional path loss models for 73 GHz outdoor LOS and NLOS measurements, combining the access and backhaul scenarios. The LOS PLE and NLOS PLE are similar to the 28 GHz outdoor measurements. ***Figure 7c*** shows the omnidirectional path model for the 73 GHz indoor measurements. The LOS PLE for VV polarization is 1.5 with shadowing factor of 0.8 dB. The corresponding LOS PLE and shadowing factor for the cross-polarized antenna are 4.5 and 6.6 dB, respectively. The NLOS omnidirectional PLE and shadowing factor for co- and cross-polarized antenna are 3.1 and 8.9 dB; and 5.3 and 0.69 dB, respectively.

The indoor omnidirectional co-polarized path loss results are very promising for an indoor environment, as the LOS PLE is lower than true free space, due to ground bounces and constructive interference from reflections. The NLOS PLE of 3.1 is also reasonable for an indoor wireless network.[21]

RMS DELAY SPREAD

RMS delay spread is one of the most important characteristics of a radio propagation channel, as it describes

the multipath time dispersion of the channel used to estimate data rate and bandwidth limitations for multipath channels.[3,4] To build power-efficient millimeter wave mobile communication systems with simple equalization, the ideal situation is for particular beam pointing directions to offer both minimal path loss and minimal multipath delay spread. If the channel provides such paths, simplified receiver structures can be based solely on beamforming

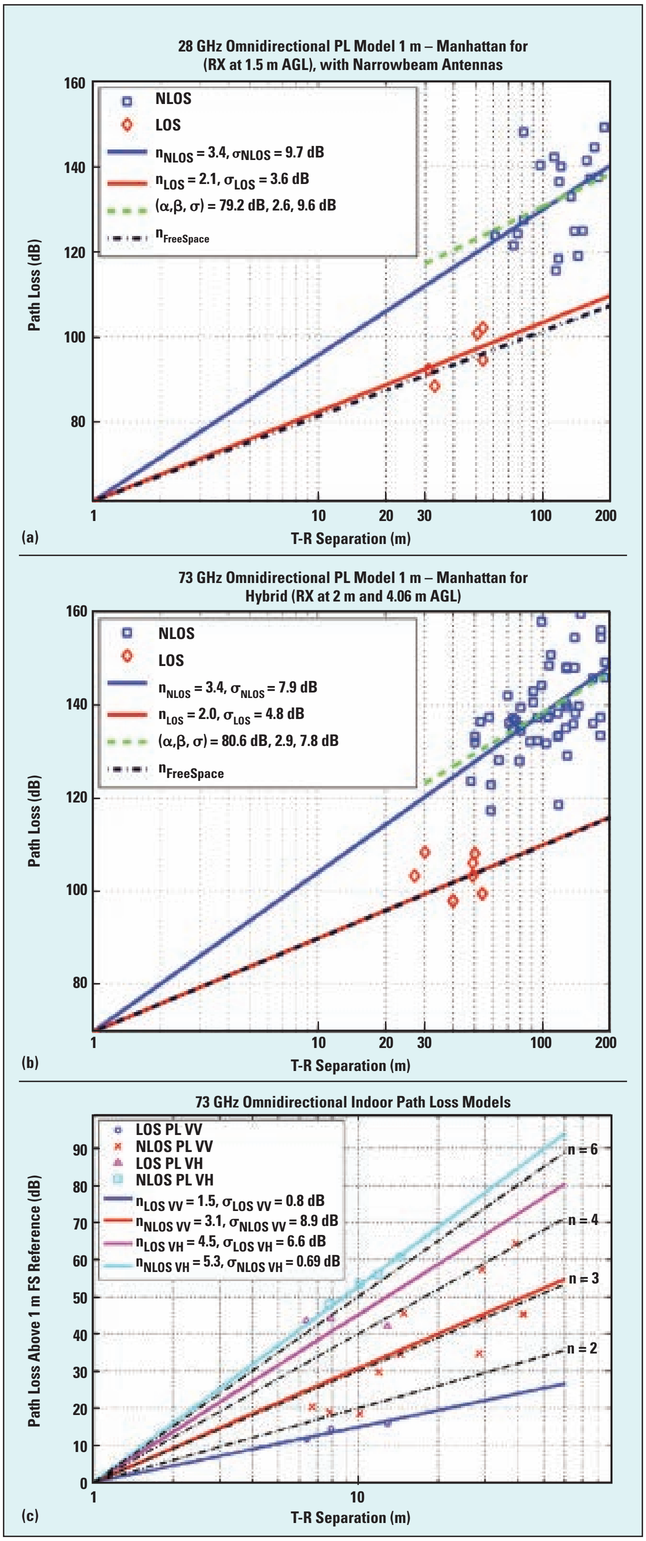

▲ *Fig. 7 28 GHz and 73 GHz close-in free space reference distance omnidirectional path loss in the outdoor urban environment of New York City, and indoor path loss models. 28 GHz outdoor omnidirectional path loss models (a). 73 GHz outdoor omnidirectional path loss models (b). 73 GHz indoor omnidirectional path loss models with VV and VH antenna polarization (c).*

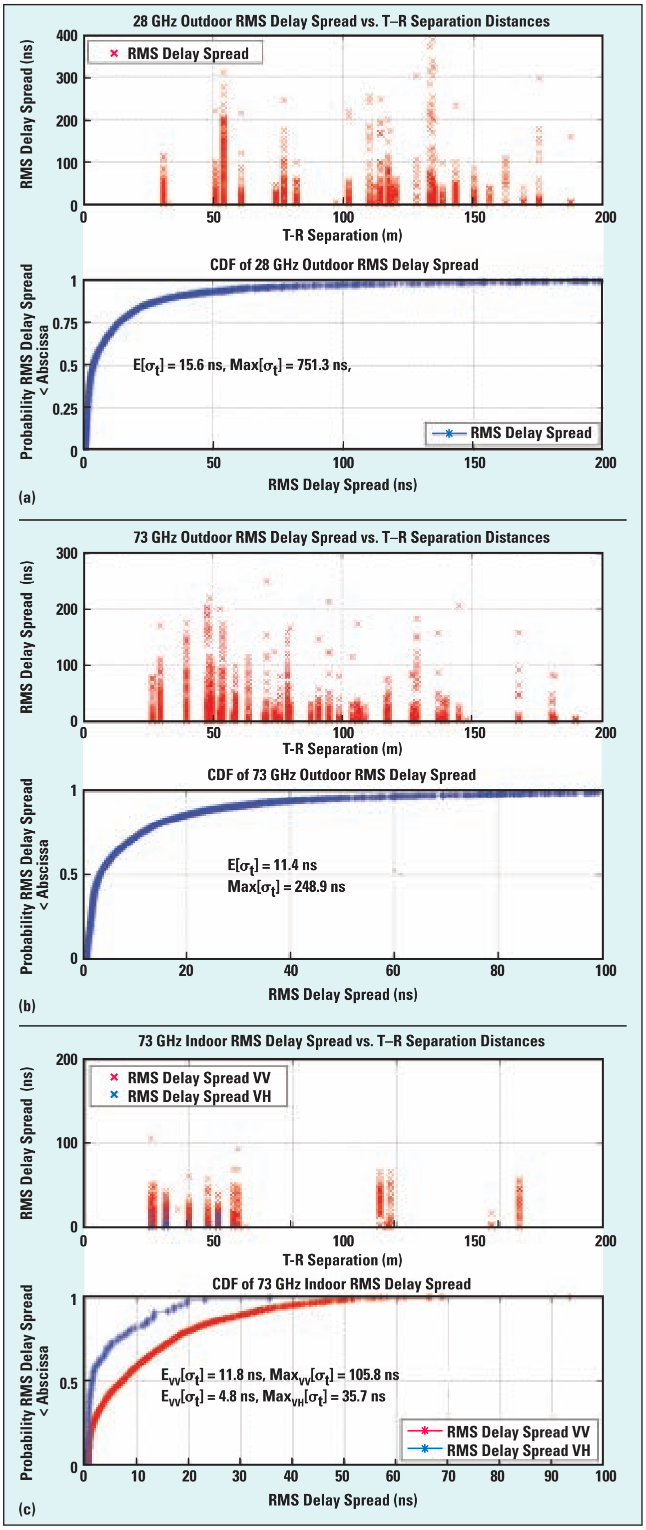

▲ *Fig. 8 28 and 73 GHz RMS delay spread CDFs and RMS delay spread as function of Tx-Rx separation distance. 28 GHz outdoor measurements (a). 73 GHz outdoor measurements (b). 73 GHz indoor measurements (c).*

TABLE 2

SUMMARY OF MINIMUM RMS DELAY SPREAD AND LOWEST PATH LOSS RESULTS FROM 28 GHz OUTDOOR AND 73 GHz OUTDOOR AND INDOOR MEASUREMENTS

Freq.	Scenario	Environment	Tx-Rx Separation Distance (m)	Path Loss (dB)	RMS Delay Spread (ns)	MED 10 dB (ns)	MED 20 dB (ns)
Multipath Delay Spreads for the Directional Beams with the Minimum RMS Delay Spread							
28 GHz	Outdoor	LOS	54	119.9	0.76	4.0	4.7
		NLOS	143	129.7	0.86	4.6	5.6
73 GHz	Outdoor	LOS	54	141.7	0.79	4.2	4.8
		NLOS	181	157.3	0.79	3.2	3.3
73 GHz	Indoor	LOS	6	141.5	0.54	2.1	2.1
		NLOS	29	86.3	0.56	1.9	1.9
Multipath Delay Spreads for the Directional Beams with the Lowest Path Loss							
28 GHz	Outdoor	LOS	33	88.4	0.84	4.5	5
		NLOS	114	126.2	165.10	7	1384.8
73 GHz	Outdoor	LOS	40	100.4	0.89	4.4	7.8
		NLOS	118	121.2	0.97	4.6	8
73 GHz	Indoor	LOS	6	86.3	0.85	4.6	5.3
		NLOS	10	90.7	0.80	4.4	5

and minimal equalization in the time domain, rather than using multi-tone, OFDM modulation and frequency domain equalization, as is done today.[4]

For this unique pointing angle scenario, ***Figure 8*** shows the RMS delay spread as a function of Tx-Rx separation and the associated cumulative distribution functions (CDFs) for 28 and 73 GHz outdoor and 73 GHz indoor measurements. The RMS delay spread in the 28 GHz outdoor measurements with 24.5 dBi gain narrow beam antennas shows that the majority of the multipath components arrive within about 50 ns. The RMS delay spread in the 73 GHz outdoor measurements with 27 dBi gain narrow beam antennas, combining backhaul and access scenarios, shows that a majority of the multipath components arrive within about 30 ns. For the 73 GHz indoor measurements, the majority of the multipath for co-polarized antennas arrives within about 35 ns, and for cross-polarized antennas within about 20 ns.

Generally, the RMS delay spread decreases as the Tx-Rx separation distance increases, since weaker components reaching the receiver at greater distances are not detectable above the receiver system's noise floor.[24]

Table 2 summarizes Tx-Rx separation distance, path loss, RMS delay spread, maximum 10 dB down excess delay[3] and maximum 20 dB down excess delay for specific antenna pointing angles. The characteristics are presented for two case-types in the table: values for one particular Tx-Rx angle pointing orientation that provides the minimum RMS Delay Spread for that case and values for one particular Tx-Rx angle pointing orientation that results in the minimum path loss, for the same Tx-Rx location combination. The values are determined from the entire measurement set that provided the smallest directional RMS delay spread and path loss.[21-23]

A simple algorithm to find the best beam directions will help simultaneously minimize both RMS delay spread and path loss (i.e., finding the best paths for both maximum SNR and very simple equalization).[23] By selecting a beam with both low RMS delay spread and path loss, relatively high power can be received using directional antennas without complicated equalization, meaning that low latency single carrier (wideband) modulations may be viable candidates for future millimeter wave wireless systems. The measured values presented here are useful to the research community for understanding values that may result when beamforming or beam searching algorithms are used to systemically search for the strongest Tx and Rx pointing angles, to achieve the lowest path loss or link attenuation.

CONCLUSION

This article describes the sliding correlator channel sounder system and presents the millimeter wave propagation measurements performed by NYU WIRELESS over the past two years. Results are shown for 28 GHz outdoor, 73 GHz outdoor base station-to-mobile (access), 73 GHz base station-to-base station (backhaul) and 73 GHz indoor scenarios. The measurement results include channel characteristics such as directional and omnidirectional path loss models relative to a 1 m free space reference distance, and directional delay spread.

The path loss model results obtained for unique pointing angles show that LOS free space propagation in outdoor ($n = 2.3$) and indoor environments ($n = 2.2$) for the 73 GHz band and outdoor environments ($n = 1.9$) for the 28 GHz band is favorable and close to the theoretical free space path loss ($n = 2$). The NLOS environment at 28 and 73 GHz experiences greater attenuation than the LOS environment yielding $n = 4.1$ for the 28 GHz outdoor directional measurements $n = 4.7$ for the 73 GHz outdoor scenario, and $n = 5.1$ for 73 GHz indoor measurements. However, with the use of multiple antenna elements, beamforming and beam combining technologies can significantly decrease the path loss when considering the best possible paths ($n = 3.7$ for 28 GHz outdoor, $n = 3.6$ for 73 GHz outdoor, and $n = 3.3$ for 73 GHz indoor co-polarization). The omnidirectional co-polarized path loss results are very promising for an indoor environment, as the LOS path loss exponent is smaller than for true free space, due to ground bounces and constructive interference from reflections.

RMS delay spread is generally inversely proportional to the Tx-Rx separation distance. Understanding RMS delay spread in the millimeter wave bands is important for wireless communications systems, especially where beam combining, beamforming and equalization are necessary to increase

the signal-to-noise ratio (SNR) and improve performance for a communication system.

The data described in this article will allow for the development of statistical channel models for millimeter wave small cell wireless communications systems in dense urban environments. Statistical models in the form of 3GPP standards have already been published based on the measurements described.[14,27,28] Given the large availability of spectrum at 28 and 73 GHz, millimeter wave bands will likely play a significant role in the next generation of cellular systems and these measurements and models will be an essential tool in their design. ■

References

1. T.S. Rappaport, J.N. Murdock and F. Gutierrez, "State of the Art in 60-GHz Integrated Circuits and Systems for Wireless Communications," *Proceedings of the IEEE*, August 2011, pp. 1390-1436.
2. A. Ghosh, T.A Thomas, M.C. Cudak, R. Ratasuk, P. Moorut, F.W. Vook, T.S. Rappaport, G.R. MacCartney, S. Sun and S. Nie "Millimeter-Wave Enhanced Local Area Systems: A High-Data-Rate Approach for Future Wireless Networks," *Selected Areas in Communications, IEEE Journal*, pp. 1152-1163, June 2014.
3. T.S. Rappaport, *Wireless Communications: Principles and Practice*, 2nd ed. Upper Saddle River, NJ: Prentice Hall, 2002.
4. T.S. Rappaport, R.W. Heath Jr., R.C. Daniels and J.N. Murdock, *Millimeter Wave Wireless Communications*, Pearson/Prentice Hall, c. 2015.
5. T.S. Rappaport, S. Sun, R. Mayzus, H. Zhao, Y. Azar, K. Wang, G.N. Wong, J.K. Schulz, M.K. Samimi and F. Gutierrez, "Millimeter Wave Mobile Communications for 5G Cellular: It Will Work!" *IEEE Access*, pp. 335-349, 2013.
6. S. Rangan, T.S. Rappaport and E. Erkip, "Millimeter-Wave Cellular Wireless Networks: Potentials and Challenges," *Proceedings of the IEEE*, pp. 366-385, March 2014.
7. G.R. MacCartney, Jr., J. Zhang, S. Nie and T.S. Rappaport, "Path Loss Models for 5G Millimeter Wave Propagation Channels in Urban Microcells," *2013 IEEE Global Communications Conference (GLOBECOM)*, December 2013, pp. 3948-3953.
8. Y. Azar, G.N. Wong, K. Wang, R. Mayzus, J.K. Schulz, H. Zhao, F. Gutierrez, Jr., D. Hwang and T.S. Rappaport, "28 GHz Propagation Measurements for Outdoor Cellular Communications Using Steerable Beam Antennas in New York City," *2013 IEEE International Conference on Communications (ICC)*, June 2013, pp. 5143-5147.
9. M.K. Samimi, K. Wang, Y. Azar, G.N. Wong, R. Mayzus, H. Zhao, J.K. Schulz, S. Sun, F. Gutierrez, Jr. and T.S. Rappaport, "28 GHz Angle of Arrival and Angle of Departure Analysis for Outdoor Cellular Communications Using Steerable Beam Antennas in New York City," *2013 IEEE 77th Vehicular Technology Conference (VTC Spring)*, June 2013, pp. 1-6.
10. S. Nie, G. R. MacCartney, S. Sun and T. S. Rappaport, "73 GHz Millimeter Wave Indoor Measurements for Wireless and Backhaul Communications," *2013 IEEE 24th International Symposium on Personal Indoor and Mobile Radio Communications (PIMRC)*, September 8-11, 2013, pp. 2429–2433.
11. S. Sun, G.R. MacCartney Jr., M.K. Samimi, S. Nie and T.S. Rappaport,"Millimeter Wave Multi-Beam Antenna Combining for 5G Cellular Link Improvement in New York City," *2014 IEEE International Conference on Communications (ICC)*, June 2014.
12. G.R. MacCartney Jr. and T.S. Rappaport,"73 GHz Millimeter Wave Propagation Measurements for Outdoor Urban Mobile and Backhaul Communications in New York City," *2014 IEEE International Conference on Communications (ICC), 2014 IEEE*, June 2014.
13. S. Nie, G.R. MacCartney, S. Sun and T.S. Rappaport, "28 GHz and 73 GHz Signal Outage Study for Millimeter Wave Cellular and Backhaul Communications," *2014 IEEE International Conference on Communications (ICC)*, June 2014.
14. G.R. MacCartney, M.K. Samimi and T.S. Rappaport, "Omnidirectional Path Loss Models in New York City at 28 GHz and 73 GHz," *IEEE 2014 Personal Indoor and Mobile Radio Communications (PIMRC)*, September 2014, Washington, DC.
15. F. Gutierrez, S. Agarwal, K. Parrish and T.S. Rappaport, On-Chip Integrated Antenna Structures in CMOS for 60 GHz WPAN Systems, *IEEE Journal on Selected Areas in Communications*, Vol. 27, Issue 8, October 2009, pp. 1367-1378.
16. R.J. Pirkl and G.D. Durgin, "Optimal Sliding Correlator Channel Sounder Design," *IEEE Transactions on Wireless Communications*, September 2008, pp. 3488-3497.
17. D.C. Cox. "910 MHz Urban Mobile Radio Propagation: Multipath Characteristics in New York City," *IEEE Transactions on Vehicular Technology*, November 1973, pp. 104-110.
18. R.J. Pirkl and G.D. Durgin, "How to Build an Optimal Broadband Channel Sounder," *2007 IEEE Antennas and Propagation Society International Symposium*, June 2007, pp. 601-604.
19. G. Martin. "Wideband Channel Sounding Dynamic Range using a Sliding Correlator," *IEEE 2000 Vehicular Technology Conference Proceedings*, 2000, pp. 2517-2521.
20. E. Ben-Dor, T.S. Rappaport, Y. Qiao and S.J. Lauffenburger, "Millimeter-Wave 60 GHz Outdoor and Vehicle AOA Propagation Measurements Using a Broadband Channel Sounder," *2011 IEEE Global Telecommunications Conference (GLOBECOM 2011)*, December 5-9, 2011, p. 1-6.
21. S. Nie, M. K. Samimi, T. Wu, S. Deng, and T. S. Rappaport, "73 GHz Millimeter-Wave Indoor and Foliage Propagation Channel Measurements and Results," NYU WIRELESS: Department of Electrical and Computer Engineering, NYU Polytechnic School of Engineering, Brooklyn, New York, Tech. Rep. 2014-003, July 2004.
22. T.S. Rappaport, G.R. MacCartney Jr., M.K. Samimi and S. Sun, "Wideband Millimeter-Wave Propagation Measurements and Channel Models for Future Wireless Communication System Design" invited, *IEEE Transactions on Communications*, to be published.
23. S. Sun, T.S. Rappaport, R.W. Heath, A. Nix and S. Rangan, "MIMO for Millimeter Wave Wireless Communications: Beamforming, Spatial Multiplexing, or Both?" *IEEE Communications Magazine*, Vol. 52, No. 12, December 2014.
24. T.S. Rappaport and D.A. Hawbaker, "Wideband Microwave Propagation Parameters using Circular and Linear Polarized Antennas for Indoor Wireless Channels," *IEEE Transactions on Communications*, February 1992, pp. 240-245.
25. W.G. Newhall, T.S. Rappaport and D.G. Sweeney, "A Spread Spectrum Sliding Correlator System for Propagation Measurements," *RF Design*, April 1996, pp. 40-54.
26. T.S. Rappaport, E. Ben-Dor, J.N. Murdock and Y. Qiao, "38 GHz and 60 GHz Angle-Dependent Propagation for Cellular and Peer-to-Peer Wireless Communications," *2012 IEEE International Conference on Communications (ICC)*, June 2012, pp. 4568-4573.
27. T.A. Thomas, H.C. Nguyen, G.R. MacCartney Jr. and T.S. Rappaport, "3D mmWave Channel Model Proposal," *2014 IEEE Vehicular Technology Conference (VTC Fall)*, 80th, September 14-17, 2014.
28. M.K. Samimi, T.S. Rappaport, "Ultra-Wideband Statistical Channel Model for Non Line of Sight Millimeter-Wave Urban Channels," *IEEE Global Communications Conference, Exhibitions & Industry Forum (GLOBECOM)*, December 8-12, 2014.
29. T.S. Rappaport, E. Ben-Dor, J.N. Murdock, Y. Qiao and J. Tamir, "Cellular and Peer-to-Peer Broadband Millimeter Wave Outdoor Propagation Measurements and Angle of Arrival Characteristics using Adaptive Beam Steering," *IEEE Radio and Wireless Symposium (RWS) 2012*, Santa Clara, CA, January 15, 2012.
30. J.N. Murdock, E. Ben-Dor, Y. Qiao, J.I. Tamir and T.S. Rappaport, "A 38 GHz Cellular Outage Study for an Urban Outdoor Campus Environment," *IEEE Wireless Communications and Networking Conference (WCNC)*, April 2012.
31. A.I. Sulyman, A.T. Nassar, M.K. Samimi, G.R. MacCartney Jr., T.S. Rappaport and A. Alsanie, "Radio Propagation Path Loss Models for 5G Cellular Networks in the 28 GHz and 38 GHz Millimeter-Wave Bands," *IEEE Communications Magazine*, September 2014, Vol. 52, No. 9, pp. 78-86.
32. W. Hong, K.H. Baek, Y. Lee and Y. Kim, "Study and Prototyping of Practically Large-Scale mmWave Antenna Systems for 5G Cellular Devices," *IEEE Communications Magazine*, Vol. 52, No. 9, September 2014.

50 MHz to 26.5 GHz

THREE AMPLIFIERS COVER IT ALL!

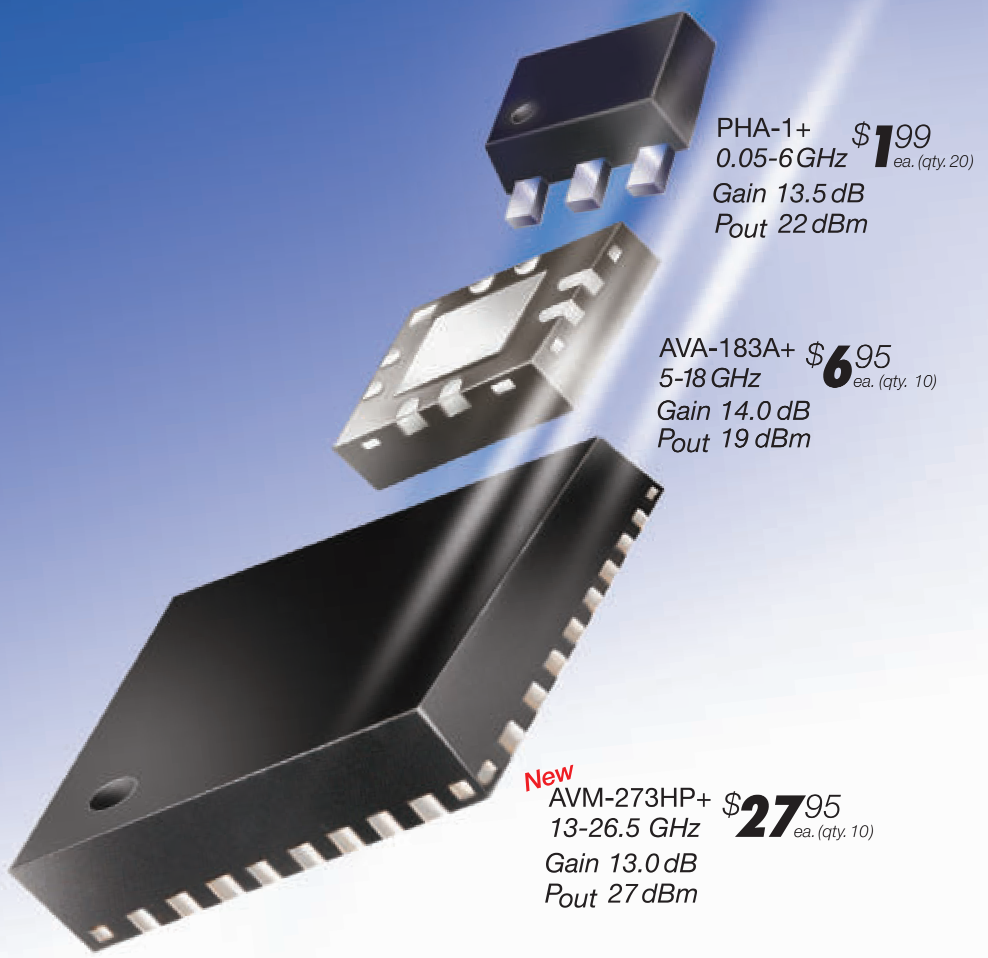

Mini-Circuits' New AVM-273HP+ wideband, 13 dB gain, unconditionally stable microwave amplifier supports applications from 13 to 26.5 GHz with 0.5W power handling! Gain flatness of ±1.0 dB and 58 dB isolation make this tiny unit an outstanding buffer amplifier in P2P radios, military EW and radar, DBS, VSAT, and more! Its integrated application circuit provides reverse voltage protection, voltage sequencing, and current stabilization, all in one tiny package!

The AVA-183A+ delivers excellent gain flatness (±1.0 dB) from 5 to 18 GHz with 38 dB isolation, and 19 dBm power handling. It is unconditionally stable and an ideal LO driver amplifier. Internal DC blocks, bias tee, and microwave coupling capacitor simplify external circuits, minimizing your design time.

The PHA-1+ + uses E-PHEMT technology to offer ultra-high dynamic range, low noise, and excellent IP3 performance, making it ideal for LTE and TD-SCDMA. Good input and output return loss across almost 7 octaves extend its use to CATV, wireless LANs, and base station infrastructure.

We've got you covered! Visit minicircuits.com for full specs, performance curves, and free data! These models are in stock and ready to ship today!

RoHS compliant

FREE X-Parameters-Based
Non-Linear Simulation Models for ADS

http://www.modelithics.com/mvp/Mini-Circuits.asp

Mini-Circuits®

www.minicircuits.com P.O. Box 350166, Brooklyn, NY 11235-0003 (718) 934-4500 sales@minicircuits.com

Understanding Envelope Tracking and Its Measurement Challenges

Yu Qian
Keysight Technologies Inc., formerly Agilent Technologies electronic measurement business
Santa Rosa, Calif.

Power amplifiers (PA) are a critical component in mobile communication devices like smartphones and tablets. To increase data rates, mobile devices are operating ever wider bandwidths with multiple-input multiple-output (MIMO) data streams and higher-order modulation, and orthogonal frequency division multiplexing (OFDM). This requires the PA to achieve both better linearity and efficiency to ensure long battery life. Unfortunately, this presents a bit of a problem for the PA, which is a power-hungry, nonlinear device. Fortunately, there is a technique that is helping overcome these issues: Envelope Tracking (ET). ET offers improved battery life and RF PA performance along with reduced heat dissipation. However, the technique is not without challenges. Let's take a closer look.

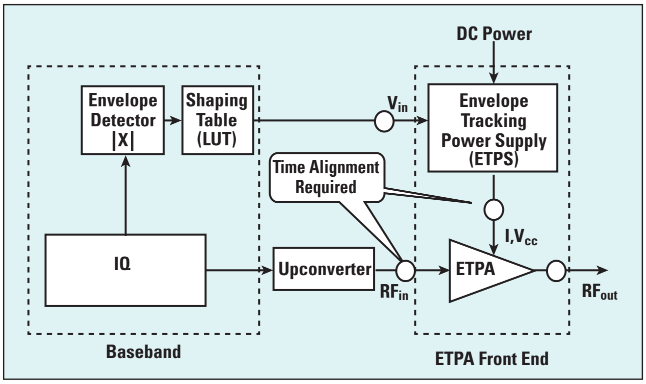

Fig. 1 Block diagram of a typical ET system.

ET: THE BASICS

ET improves the power amplifier's efficiency by tracking its bias voltage with the magnitude of the input signal envelope. ET dynamically adjusts the DC power supply voltage based on the envelope of the PA input signal, enabling the amplifier to be more linear, reach higher peak power, and achieve greater spectral and power-added-efficiency (PAE). It also reduces issues associated with distortion.

A block diagram of a typical ET system is shown in ***Figure 1***. Here, the envelope detector measures the magnitude of the IQ waveform, which is fed to a shaping table to determine the bias voltage supplied to the PA. The shaped envelope signal is supplied to the en-

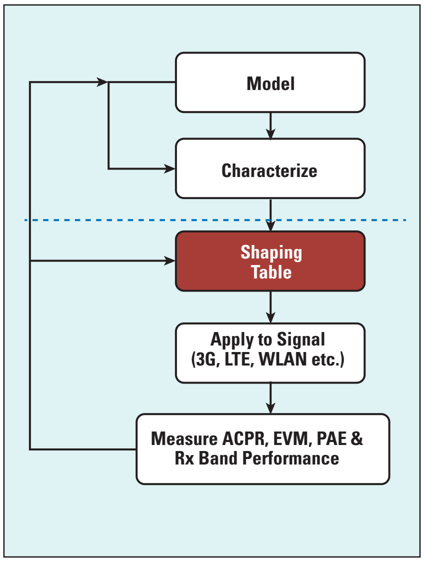

Fig. 2 Possible ET system design and test flow.

velope tracking power supply (ETPS), which modulates the bias voltage to track the RF input waveform. Finally, the PA amplifies the RF input signal.

ET does not apply a level limiter or operate with a fixed amplitude PA input signal, as is common with polar modulation. Instead, it may use a mixture of open and closed loop feedback, with delays introduced to the IQ or RF path to match those in the supply modulation path. In an open loop system, the shaping curve is applied to the envelope signal to match the supply voltage versus RF gain in the PA. Predistortion may also be used.

THE MEASUREMENT CHALLENGE

ET introduces an added complexity that makes configuring and testing an ET system especially challenging. Some of the specific challenges include:

PA Characterization for Simulation

ET requires additional testing, which drives up both test time and cost. A further complication, an ET PA must be treated as a 3-terminal active device. A low noise, high bandwidth power supply is also required, usually operating in a combination of switched and linear modes.

Shaping Table Design

The shaping curve or table determines the characteristics of the ET system. It must be properly designed and optimized to achieve the design goals, a process that is typically lengthy and difficult, often requiring many steps. Once designed, the shaping table and all the other components required to implement an ET system (i.e., ETPS, RF PA and radio design) must be tested or evaluated.

Antenna Tuning

While tuning the antenna is often performed by a specialist, the designer will likely need to check the operation of the ET system with antenna mismatch.

Time-Aligned Signal Generation

A timing misalignment of the envelope and RF signals of more than 1 ns will adversely impact the quality of the transmitted signal, affecting both adjacent channel power (ACP) and error vector magnitude (EVM). Timing misalignment results in an asymmetric adjacent channel leakage ratio (ACLR).

AM/AM and AM/PM Measurement

While an ACLR measurement will show a problem with the ET system, it won't provide much insight into its cause. Linearity measurements of AM/AM and AM/PM, on the other hand, are key metrics for assessing ET performance. To improve linearity, supply modulation may be used. It reduces the in-band and out-of-band intermodulation signals at higher powers.

Instantaneous PAE

Measuring the improvement in system performance is a big challenge when implementing an ET system. The performance of the RF PA can be measured by itself, but it is a very difficult undertaking requiring measurement of the current with sufficient bandwidth. The supply current, voltage and RF power measurements need to be accurately time aligned to provide an instantaneous PAE measurement. An alternate and considerably easier approach is to measure the performance improvement as a combination of the ETPS and the ET PA, using a bench supply to measure average current.

Group Delay Through the ETPS

The ETPS has a lowpass filter response, making ripples in group delay through it especially worrisome. These ripples can cause excess distortion in the RF PA output.

Receive Band Noise Floor

In an ET system, all but the RF carrier decoupling capacitors are removed. Any spurious signals and noise on the power supply line to the RF PA appear at the output. Of particular concern is any increase in the transmitter noise floor that appears at the receiver duplex frequency in a frequency division duplexing (FDD) radio. This noise is coupled through the antenna duplexer and reduces the receiver's sensitivity.

In addition to these technical challenges, engineers must deal with the logistical challenge of determining which parts of the ET system to test and how to perform all of the modeling and measurement.

CONFRONTING THE CHALLENGES

Dealing with the challenges to implement an ET system requires two essential components. The first is an ET design and test flow. One possible flow is illustrated in ***Figure 2***. It begins with modeling the PA's linear and nonlinear behavior and PA characterization. Next, the shaping table is designed. The envelope signal is then created, with the shaping table applied to the signal. Finally, the PA's PAE, ACLR and receive band performance are measured and analyzed.

The second element to evaluate ET components and ET-based radio designs is a highly flexible and accurate ET test system. Such a system should be comprised of a simulation environment, signal generator and analyzer with signal generation and analysis software, and an oscilloscope. For optimal flexibility, the system should support both LXI bench and PXI modular instruments and be based on common tools that enable effective teamwork, from R&D to design verification and into production.

A typical test system for the bench that can be used to perform the ET design and test flow is shown in ***Figure 3***. For system modeling and simulation, electronic system level (ESL) design software is used to trade off the ET system's baseband and RF performance. The software allows customized models to be developed and shared prior to simulation, so the performance and impact of different devices can be understood.

To generate both the RF and envelope signals required for evaluation and performance testing of the ET system, signal generation software with an ET option is employed. Once the envelope waveform is created, it is downloaded to a vector signal generator. An arbitrary waveform generator is used to generate the envelope waveform signal.

After downloading the waveforms, the timing of the RF and envelope signals is adjusted with the signal generation software. An oscilloscope measures the absolute time delay. The entire ET system performance (RF signal, envelope signal, ETPS and RF PA) is then evaluated using a signal analyzer and associated software.

Based upon the results, the PA can be adjusted to improve its output signal quality, using ET alone or with other PA technologies like crest factor reduction (CFR) and digital predistortion (DPD). A general-purpose signal generator, signal analyzer and arbitrary waveform generator can help optimize PA performance.

PA characterization, including swept frequency and pulse power measurements, is performed using a network analyzer and DC power analyzer with source measurement unit (SMU). If the DC power analyzer with SMU has a dynamic capability, pulsed PA performance may also be characterized. During PA testing, RF power modulation is measured using USB RF power sensors. A peak power analyzer and wideband sensor analyze the modulated power.

For production test, the following equipment is needed: waveform generation software, vector signal generator, arbitrary waveform generator, SMUs, digital inputs outputs (DIO) for device under test (DUT) control DC measurements, and a vector signal analyzer with appropriate measurement application software.

CONCLUSION

ET offers a number of performance advantages. However, to fully achieve these, designers must first understand and overcome the measurement challenges with configuring and testing an ET system. An accurate and flexible hardware/software test system specifically targeted at ET combined with an ET design and test flow offer designers an ideal way to mitigate challenges that may arise. ■

Yu Qian (Kevin) *is a wireless connectivity application expert and product marketing engineer with the Microwave Communications Division (MCD) at Keysight Technologies (formerly Agilent Technologies). Kevin has worked with Keysight for 13 years, with six years experience as an R&D software engineer and seven years experience as a marketing engineer and application expert. He is currently responsible for global wireless connectivity, new product introductions and business development. He also provides pre- and post-sale technical support and delivers training to internal field and application engineers and external customers. Kevin holds a master's degree in electrical engineering from Beijing University of Posts and Telecommunications (2001) and a bachelor's degree in electrical engineering from Shenyang Architecture University (1998).*

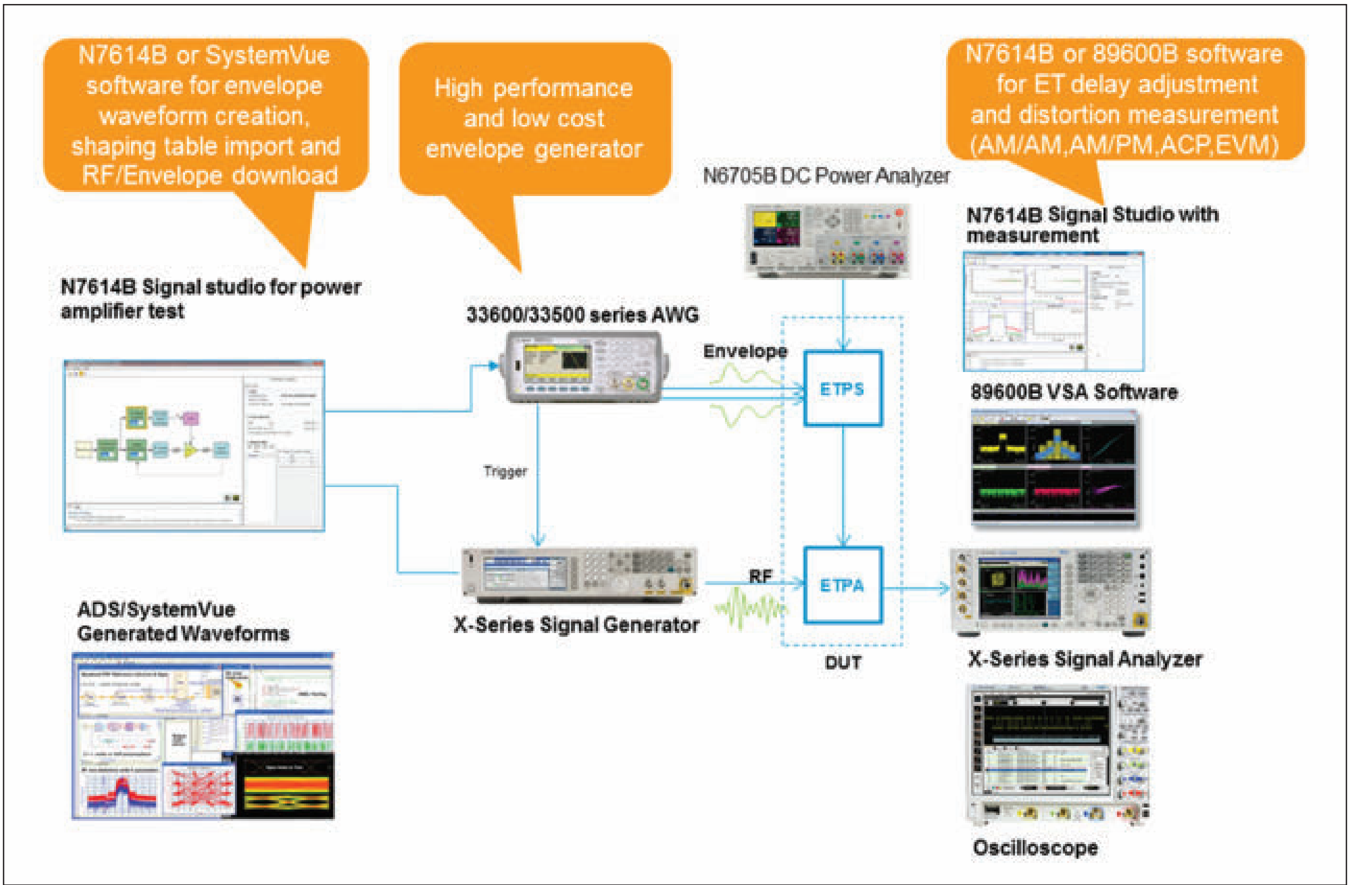

▲ *Fig. 3 A typical test solution for ET PAs.*

Six LTE Receiver Measurements Every Wireless Engineer Should Know

David A. Hall
National Instruments, Austin, Texas

From Wi-Fi devices to LTE handsets, today's wireless devices require several key measurements to characterize the ability of the receiver to demodulate an incoming signal from a base station or access point without distortion. Although many engineers are familiar with the notion of a sensitivity measurement (historically, the lowest signal level that can be received), this is just one of several measurements required to characterize receiver performance. There are actually six key measurements that engineers frequently use to evaluate receiver performance under a wide range of operating conditions.

Although this article describes these six receiver measurements in the context of an LTE receiver, the concepts apply to any wireless receiver. The 802.11 specifications are similar for wireless LAN radios.

LTE receiver metrics, shown in ***Table 1***, are defined in section 7 of the 3GPP TS 36.521 specifications. Although Table 1 actually lists seven measurements, spurious response is functionally similar to blocking characteristics, so they'll be combined in this article.

TABLE 1

LTE RECEIVER MEASUREMENTS

Measurement	3GPP TS 36.521 Section
Reference Sensitivity Level	Section 7.3
Maximum Input Level	Section 7.4
Adjacent Channel Selectivity	Section 7.5
Blocking Characteristics	Section 7.6
Spurious Response	Section 7.7
Intermodulation Characteristics	Section 7.8
Spurious Emissions	Section 7.9

When testing LTE receiver performance, the primary receiver figure of merit is receiver throughput. Each of the measurements listed in Table 1 defines conditions at which the device must meet minimum throughput requirements of 95 percent.

REFERENCE SENSITIVITY LEVEL

The reference sensitivity level describes the receiver's ability to operate within low signal power conditions. Unlike GSM and W-CDMA receivers that often use bit error rate (BER) to define the sensitivity requirements, LTE defines minimum performance in terms of throughput. Sensitivity is therefore defined as the lowest average power level at which the receiver can achieve 95 percent of the maximum throughput, when using QPSK modulation.

The hardware configuration for LTE reference sensitivity level requires a vector signal generator (VSG) directly connected to the receiver. It is common to use a fixed attenuator between the instrument and the device under test (DUT) or user equipment (UE) to improve the impedance match. As illustrated in ***Figure 1***, the VSG produces an LTE downlink signal and the receiver reports its throughput through a digital interface.

The power level at which an LTE receiver must meet the required throughput varies according to the E-UTRA frequency band and

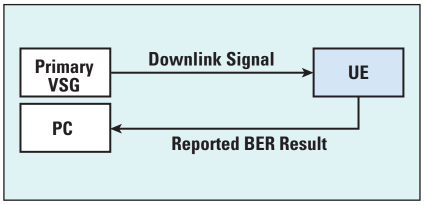

▲ *Fig. 1 Test setup for measuring LTE receiver sensitivity.*

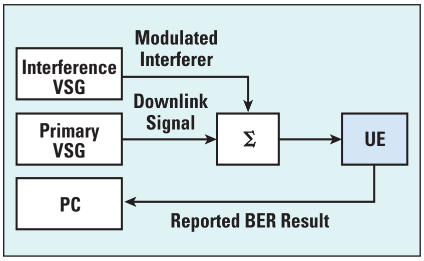

▲ *Fig. 2 Test setup for measuring adjacent channel selectivity.*

configured channel bandwidth. These conditions are defined in Table 7.3.3-1 of the 3GPP TS 36.521 specifications. The power levels range from -106.2 dBm for Bands 35 and 36 in a 1.4 MHz bandwidth to -90 dBm for Band 20 in a 20 MHz bandwidth.

MAXIMUM INPUT LEVEL

A second key metric of LTE receiver performance is maximum input level. Similar to the reference sensitivity level, the receiver's maximum input level characterizes its ability to achieve minimum requirements for throughput with large signal levels.

Receiver performance at relatively high power levels is primarily determined by the linearity of the front end, which is usually dominated by components such as the first LNA in the receive chain. The minimum conformance standards for maximum input level require that the receiver be able to achieve at least 95 percent of the maximum throughput in the presence of signal powers up to -25 dBm for all bands and in all channel bandwidths.

The test configuration for maximum input level is almost identical to reference sensitivity level. One minor difference is that it is not necessary to use substantial attenuation between the RF signal generator and the DUT when testing maximum input level. Instead, the signal generator is either connected directly to the DUT or through a small attenuator used for impedance matching.

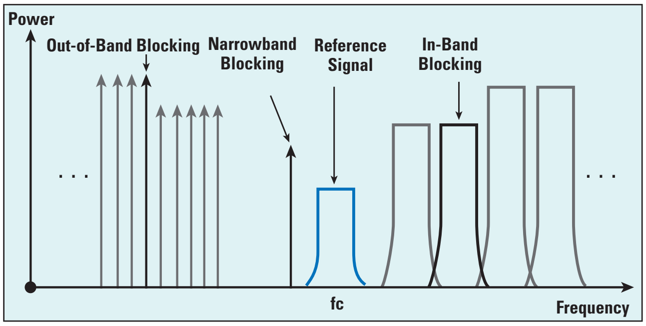

▲ *Fig. 3 Three types of interference signals are used to test the blocking characteristics of an LTE receiver.*

ADJACENT CHANNEL SELECTIVITY

Adjacent channel selectivity (ACS) is a third metric for LTE receiver performance. ACS measures a receiver's ability to achieve minimum throughput requirements in the presence of an adjacent channel signal, i.e., at a specific frequency offset from the given channel. This measurement is particularly useful in determining the receiver's performance at the band edge, when higher power out-of-band signals from other base stations are present. ACS can strictly be defined as the ratio (in dB) of the receiver filter's attenuation at the assigned channel frequency to the attenuation at the adjacent channel.

The test configuration for ACS requires two signal generators connected to a power combiner. One VSG produces the reference LTE signal, which is demodulated by the receiver. The other signal generator produces the interfering LTE signal at an offset frequency, illustrated in ***Figure 2***.

The outputs of both the primary downlink and interfering signal generators are combined to form a composite input to the UE. The specific requirements for LTE receiver ACS depend on the configured channel bandwidth and range from 33 dB in a 1.4 MHz channel to 27 dB in a 20 MHz channel.

Testing ACS generally involves two test configurations, one close to the sensitivity limit and one at the maximum input power to the receiver. When testing ACS at the lower end of the input power range, the primary RF signal generator generates a reference channel that is 14 dB above the receiver's sensitivity limits. The interfering RF signal generator produces an LTE signal at a higher output power, where the specific power level depends on the bandwidth of the transmission.

When testing ACS at the higher end of the receiver's input power range, the interfering RF signal generator produces an interferer at the maximum input level of -25 dBm. Then, the primary RF signal generator is configured to produce a reference channel that is substantially lower than the interfering signal. In this test, the absolute power level of the reference channel depends on the channel bandwidth.

BLOCKING CHARACTERISTICS

Blocking characteristics are a measure of the receiver's ability to accurately demodulate LTE signals in the presence of a wide range of interference. The specifications for LTE provide a more comprehensive range of interferers than the ACS measurement, including both continuous wave and modulated signals.

Figure 3 illustrates the range of blocking signals: continuous wave (CW) signals close to the band of interest (narrowband blocking), CW signals farther from the band of interest (out-of-band blocking) and modulated signals relatively close to the band of interest (in-band blocking).

A test configuration similar to that used for ACS is used to measure blocking characteristics, i.e., combining the outputs of two RF signal generators. If the signal generator producing the interfering signal cannot generate CW and modulated signals, a separate CW signal generator will be required.

Similar to sensitivity and ACS, the blocking characteristics measurements require the receiver to achieve a minimum throughput of 95 percent of its maximum throughput for each of the in-band, out-of-band and narrowband blocking measurements.

In-band blocking is a metric measure of the receiver's performance in the presence of an unwanted interfering signal in the UE receive band or in the first 15 MHz below or above the receive band. When performing this measurement, the primary VSG is configured to produce an LTE signal

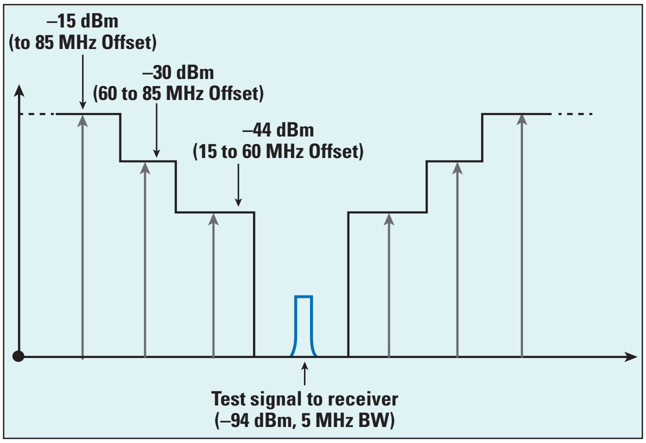

▲ *Fig. 4 Power levels and frequency offsets for out-of-band blocking characteristics.*

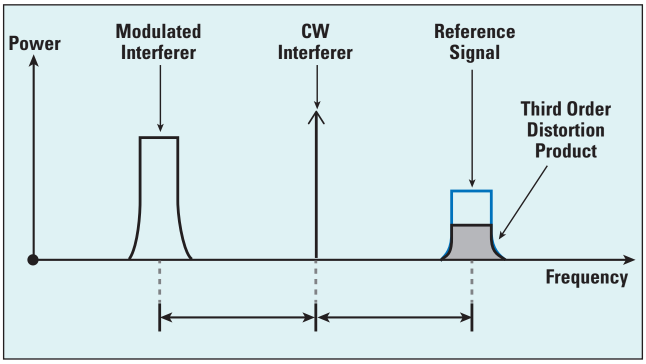

▲ *Fig. 5 Interfering signals are spaced so the third order distortion product interferes with the reference signal.*

6 to 9 dB above the reference sensitivity limit. The in-band interferer is a modulated LTE signal configured at either -56, -44 or -30 dBm, depending on frequency offset.

By comparison, out-of-band blocking characteristics evaluate the receiver's performance in the presence of higher power out-of-band signals. Unlike the in-band blocking characteristics that use a modulated signal, the out-of-band interfering signal is a CW signal at +6 dBm. When performing this measurement, the interference signal generator must be configured to generate a CW tone.

When testing out-of-band blocking, the reference LTE signal is generated at a power level that is 6 to 9 dB above the reference sensitivity level of the receiver, with the precise power level dependent on the bandwidth configuration. ***Figure 4*** shows that in the 5 MHz bandwidth configuration in E-UTRA Band 1, where the reference sensitivity requirement is -100 dBm, the test signal for out-of-band blocking is -94 dBm, which is 6 dB higher in power.

The final blocking measurement, narrowband blocking, is a measure of the LTE receiver's ability to achieve minimum throughput in the presence of an unwanted narrowband interferer, where the frequency offset is less than the channel spacing. Similar to the out-of-band blocking measurement, the narrowband blocking requires a test configuration that uses both LTE and CW signals.

Because the interferer for narrowband blocking is close in frequency to the band of interest, the power level of the interferer is much closer to the power level of the reference signal. Here, the reference LTE signal ranges from 16 to 22 dB above the sensitivity level of the receiver. Also, the interferer is generated at a power level of -55 dBm for all bandwidth configurations and is spaced at a frequency offset that is just over 200 kHz away from the band edge of the signal of interest.

INTERMODULATION CHARACTERISTICS

Receiver intermodulation characteristics mimic the effect of the intermodulation products that occur in a receiver experiencing multiple interferers simultaneously. To perform this measurement, two interference signals are simultaneously injected, creating third-order distortion products that directly interfere with the reference downlink signal.

As shown in ***Figure 5***, the frequency offset between the two interfering signals, both a CW interferer and a modulated interferer, is equivalent to the frequency spacing between the CW interferer and the reference signal to the receiver. Thus, the resulting third-order distortion product directly interferes with the reference signal.

The test setup for intermodulation characteristics requires three RF signal generators, two VSGs and one CW signal generator, and a three-way RF power combiner.

To pass the intermodulation characteristics measurement, a receiver must be able to achieve 95 percent throughput at power levels ranging from 6 to 12 dB above the sensitivity limit, depending on the channel bandwidth.

SPURIOUS EMISSIONS

The final critical LTE receiver measurement is spurious emissions. Unlike the other measurements, which define a receiver's ability to achieve a specified throughput under a range of signal conditions, the spurious emissions measurement characterizes the receive port's radiated emissions. It is the only receiver measurement that does not reference the throughput.

The hardware requirement for spurious emissions is straightforward and consists of connecting a spectrum analyzer to the receive port of the receiver. The spectrum analyzer measures emissions from 30 MHz to 12.75 GHz using a measurement bandwidth of either 100 kHz or 1 MHz (some exceptions apply to Bands 22, 42 and 43). The emissions requirement is -57 dBm in a 100 kHz bandwidth or -47 dBm in a 1 MHz bandwidth, with the measurement bandwidth dependent on frequency.

CONCLUSION

Although many engineers are most familiar with sensitivity as a metric for receiver performance, real-world environments require additional measurements. As the LTE receiver performance metrics indicate, receivers operate in the presence of a wide range of interfering signals that place requirements on both the noise floor and linearity performance. When testing an LTE radio for conformance with the 3GPP requirements, radio designers must consider a wide range of receiver performance metrics, from in-band emissions to intermodulation. ■

Note: This article is an abridged section from an application note entitled "Introduction to LTE Device Testing: From Theory to Transmitter and Receiver Measurements." For the full application note, visit: http://download.ni.com/evaluation/rf/Introduction_to_LTE_Device_Testing.pdf.

MMIC AMPLIFIERS

NOW! **DC to 26.5 GHz** from **73¢** qty.1000

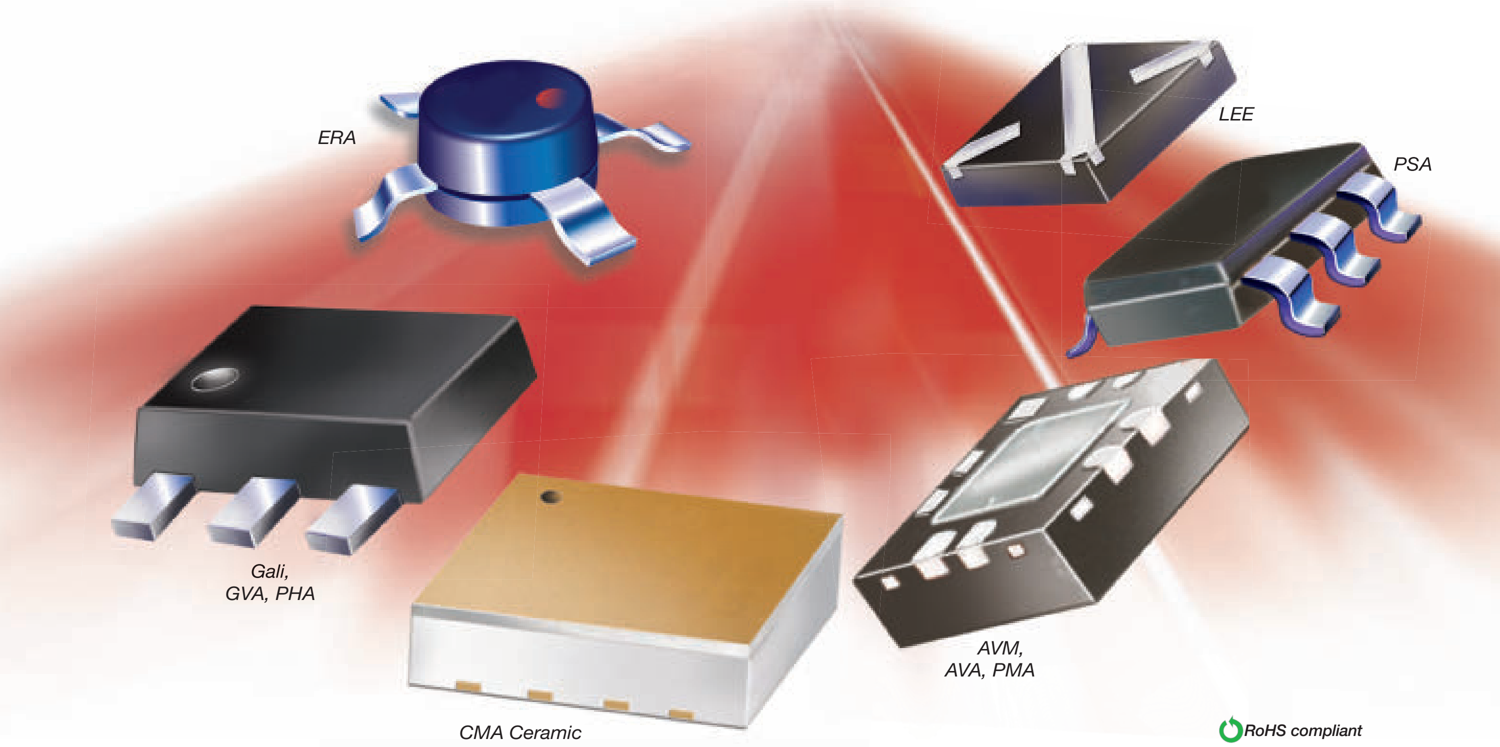

NF from 0.5 dB, IP3 to +48 dBm, Gain from 8 to 39 dB, Pout to +30 dBm

Now with over ~~145~~ 170 MMIC amplifier models covering frequencies from DC to 26.5 GHz*, chances are, Mini-Circuits has your application covered. Our ultra-broadband InGaP HBT and PHEMT amplifiers offer one of the industry's broadest selections of gain, output power, IP3, and noise figure to optimize your commercial, industrial, or military system performance. They can even meet your most critical size and power requirements with supply voltages as low as 2.8V, current consumption as low as 16mA, and packages as small as SOT-363 (1.35 x 2.25mm). Our tight process control guarantees consistent performance across multiple production runs, so you can have confidence in every unit.

Visit minicircuits.com and use our Yoni2™ search engine to search our entire model database by performance criteria for the model that meets your needs. You'll find pricing, full model specs, characterization data, S-parameters, and even free samples of select models! So why wait? Place your order today, and have units in your hands as soon as tomorrow!

*Low-end frequency cut-off determined by external coupling capacitors and external bias choke.

Yoni2™ Searching millions of actual data points to meet your specific requirements.

U.S. Patents 7739260
7761442

EZ To Get SAMPLES

FREE Samples On Demand!

www.minicircuits.com/products/ez_samples.shtml

Mini-Circuits®

www.minicircuits.com P.O. Box 350166, Brooklyn, NY 11235-0003 (718) 934-4500 sales@minicircuits.com

476 Rev K

Design of an 8×8 MIMO Broadband RF Subsystem for Future WLAN

Li Zhao, Jian-Yi Zhou, Wen-Wen Yang, Zhi-Qiang Yu and Li-Na Cao
Southeast University, Nanjing, China

This article describes a broadband 8×8 MIMO RF subsystem with large area coverage for next generation wireless local area networks (WLAN) in the 5 GHz band. Measurements demonstrate the capability to operate over a long range of 80 m at a high data rate of 1 Gbps, due to its 23 dBm transmitter, -70 dBm sensitivity, 50 dB dynamic range receiver and 8 dBi high gain antenna. The EVM of transmitter and receiver are 2.6 and 3.2 percent, respectively, for an 80 MHz 64 QAM signal. The 8×8 RF subsystem has been successfully integrated into an IEEE 802.11ac prototype system. Because broadband OFDM signals employed in 802.11ac WLAN standards are more sensitive to non-ideal RF system characteristics such as phase noise, I/Q imbalance and interference, their effects are analyzed and mitigations are incorporated. Design details, fabrication considerations and measurement results are presented.

Increasing demand on high data rate, long range wireless communication networks has driven the advancement of wireless local area network (WLAN) standards. In 1999, 802.11b dictated a maximum data rate of 11 Mbps at 2.4 GHz, increasing to 54 Mbps at 5 GHz with 802.11a and at 2.4 GHz with 802.11g in 2003.[1] In 2009, 600 Mbps was achieved in 802.11n by using additional multiple-input-multiple-output (MIMO) antennas. With the continuing development of laptops and smartphones, however, there is a need for even larger amounts of data sharing,[2] driving the creation of a new standard for higher data rate WLAN. The new 802.11ac standard, also known as very high throughput (VHT), is capable of a 500 Mbps data rate with one spatial stream in the 5 GHz band and greater than 1 Gbps with multiple spatial streams. It benefits from new features, such as wider channel bandwidth, a higher-order modulation scheme and more spatial streams.

There are three challenges in the design of an RF subsystem for future WLAN.[3] First is the transceiver's higher sensitivity to I/Q imbalance and channel gain flatness due to its wide channel bandwidth. Second is a higher sensitivity to carrier frequency offset and phase noise than single carrier systems.[4] Third is a higher peak-to-average ratio (PAR) caused by the complex modulation scheme, which requires more power back-off in the power amplifiers (PA).

Several methods are employed in this system to address these challenges and achieve excellent RF performance. Sufficient noise decoupling of the reference signal generation module and phase-locked loop (PLL) module improves the phase noise performance of the RF subsystem. The use of a broadband modu-

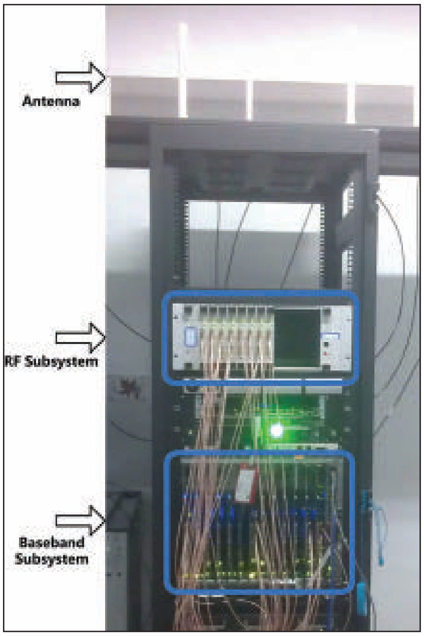

▲ *Fig. 1 Hardware platform.*

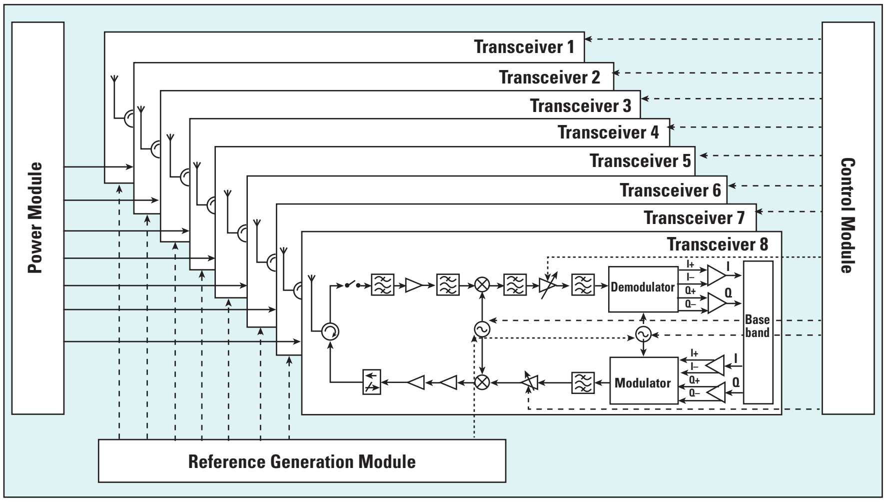

▲ *Fig. 2 RF subsystem block diagram.*

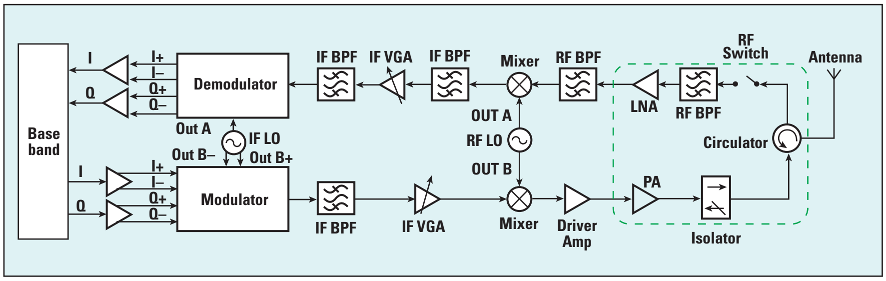

▲ *Fig. 3 5.8 GHz WLAN RF transceiver block diagram.*

lator and extra operational amplifiers ensures good I/Q balance within the 80 MHz bandwidth. Close attention to the printed circuit board (PCB) layout and metallic shields between modules reduces interference.

The measured communication range is as much as 80 m with a 1 Gbps data rate. Transmitter output power is as high as 23 dBm, which provides enough margin for the PA power back-off needed by the complex modulation scheme. The receiver operates over a large dynamic range of more than 50 dB. A parallel-fed twin-dipole array is used to form the 8 dBi high-gain antenna. The measured EVM of the transmitter and receiver using an 80 MHz 64 QAM signal is 2.6 and 3.2 percent, respectively.

SYSTEM OVERVIEW

The network is composed of one access point (AP) and user equipment (UE), which can be distributed throughout a building. The hardware platforms are the same at all the nodes (see ***Figure 1***). The RF subsystem block diagram is shown in ***Figure 2***. It has an operating frequency range of 5.76 to 5.84 GHz for an 80 MHz channel bandwidth and consists of one power module, one control module, one reference signal generation module and eight RF transceiver modules. The power module converts 48 to 6 VDC with a DC to DC converter. The control module guarantees communication between the baseband circuitry and RF transceivers. The reference signal generation module, which consists of a 10 MHz oven controlled crystal oscillator (OCXO) and a PLL, provides a 10 MHz reference signal to each of the eight transceivers.

It works in a time-division-duplex (TDD) mode. The transceiver has an RF port to the antenna and an I/Q interface to the baseband. The peak-to-peak voltage of I/Q signals between the RF subsystem and baseband circuitry is 500 mV. The transmitter and receiver share one antenna by using a circulator as shown in ***Figure 3***. Each transceiver has its own antenna, so there are eight antennas in total.

MITIGATION OF NON-IDEAL SYSTEM CHARACTERISTICS

Phase Noise

Improper setting of phase-locked loops (especially the loop filter bandwidth), a noisy power supply and reference frequency jitter are the main sources of phase noise. In the TDD mode, amplifiers on Tx and Rx paths are switched on and off with each communication burst in order to minimize power consumption. Power consumption changes dramatically between Rx mode and Tx mode, introducing noise. Unless the noise is thoroughly decoupled, it can affect the crystal oscillator and cause jitter in the reference. Phase noise is reduced by properly setting the crystal oscillator loop filter bandwidth, using an ultra-low noise, low dropout, linear regulator in the PLL power supply and employing tantalum capacitors for further decoupling.

It is also important that the 10 MHz reference be distributed to each RF transceiver without introducing jitter, especially when multiple RF boards are inserted in the RF subsystem. This is accomplished with an ultra-low jitter LVCMOS fan-out buffer to distribute the reference to the eight RF transceivers.

I/Q Imbalance

Theoretically, a phase imbalance (θ) and an amplitude imbalance (β) degrade SNR according to[5]

$$SNR' = \frac{P_S}{p_N + P_{N\theta} + P_{N\alpha}} = \frac{SNR}{1 + SNR\left[\tan^2(\theta/2) + \alpha^2\right]} \quad (1)$$

$$\text{where } \alpha = \left(10^{\beta/20} - 1\right) / \left(10^{\beta/20} + 1\right)$$

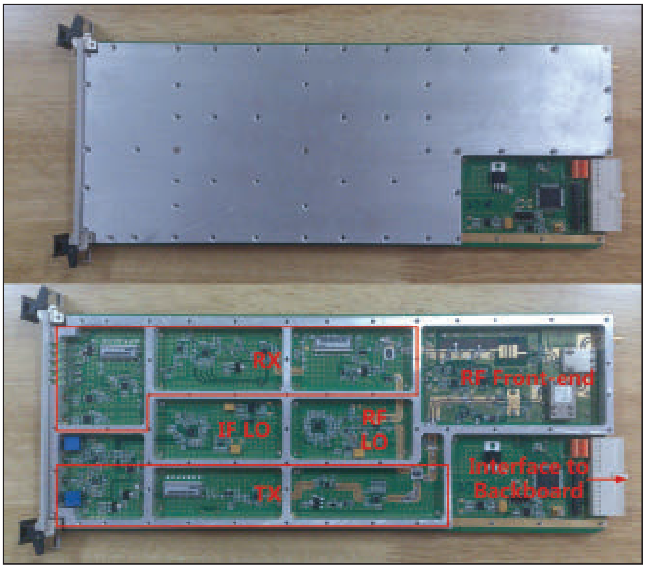

▲ *Fig. 4 5.8 GHz WLAN RF transceiver prototype.*

If SNR degradation of less than 2 dB is required to achieve an SNR = 21 dB, the phase imbalance should be less than 5 degrees and the amplitude imbalance should be less than 0.5 dB.[6] In practice, I/Q imbalance has a greater impact on wide bandwidth systems.

Asymmetry in the PCB layout and different trace lengths for the baseband I and Q signals contribute to I/Q imbalance. For a modulator or demodulator, impurities in the LO signal also contribute to I/Q imbalance. A bandpass filter placed between the PLL and the demodulator can help to filter out undesired harmonics, while amplitude imbalance is compensated by adjusting the feedback resistor of the operational amplifier and phase imbalance is compensated by placing shunt capacitors in I/Q signal paths.[7]

Interference

Shielding between different parts of the RF transceiver is critical, especially those parts with large power.[8] Different functional blocks are separated by a metal frame as shown in ***Figure 4***. The large LO signal and its harmonics can be coupled to the RF front end through the dielectric substrate or other paths. To address this, LC lumped filters in the output path of the LO signal filter out the relatively high LO harmonics. A high isolation mixer is also used to reduce LO leakage.

Carrier feedthrough is mainly caused by imbalances in the DC offset between I/Q signals at the input of the modulator. The operational amplifiers shown in Figure 3 act as buffers between the baseband signals and the modulator, and can also provide DC offset compensation for the I/Q signals. Tuning the DC offset of the I/Q paths can effectively suppress the carrier feedthrough to a level below -55 dBc.

RF TRANSCEIVER AND ANTENNA DESIGN

Structure

The transceiver is integrated on a 1.5 mm thick, four-layer PCB.[9] The first layer is on a Taconic TLX substrate, with ε_r =2.55, h=0.5 mm. The others are on FR-4. The RF front end, shown in the green dashed line box in Figure 3, uses a two-layer PCB (ε_r =2.55, h=0.5 mm) to provide

TABLE 1

TRANSCEIVER LINK BUDGET

Blocks	Specifications		
Transmitter			
Modulator	P1dB		+ 9 dBm
	Image Suppression		> 35 dB
IF Amplifier and Filter	Gain		10 dB
	P1dB		+ 18 dBm
Mixer	Conversion Loss		7 dB
	IP3		+ 23 dBm
Driver	Gain		10 dB
	P1dB		+ 15 dBm
Power Amplifier	Gain		25 dB
	P1dB		+ 34 dBm
Transmitter	Flatness		< 1 dB
Receiver			
2-stage Low Noise Amplifier	Noise Figure		2.3 dB
	Gain		30 dB
	P1dB		+ 15 dBm
Mixer	Conversion Loss		7 dB
	IP3		+ 23 dBm
IF Amplifier and Channel Select Filter	AGC=0	AGC=60	AGC=127
	Gain: 60 dB	Gain: 30 dB	Gain: 0 dB
	IP3		+ 18 dBm
Demodulator	P1dB		+ 13 dBm
	Image Suppression		> 30 dB
Receiver	Flatness		< 1.5 dB
Antenna			
	IRL and ORL*		< 15 dB
	Gain		> 8 dBi

* *IRL is the abbreviation of input return loss; ORL is the abbreviation of output return loss.*

a good ground connection and proper heat dissipation for the PA. The two PCBs are fixed on one metal base and interconnected with adjacent microstrip lines. The RF band is from 5.76 to 5.84 GHz, with a 4.2 GHz LO frequency and a 1.6 GHz IF.

Link Budget

IEEE 802.11ac stipulates operation over 5 to 6 GHz with a 293 Mbps data rate (80 MHz bandwidth, 1 spatial stream, and 64 QAM 5/6) and a sensitivity of -58 dBm. The sensitivity for an 80 MHz QPSK signal is -71 dBm. The relation between sensitivity (P_{sen}), thermal noise (P_{noise}), noise figure (NF) and signal to noise ratio (SNR) can be expressed as

$$P_{sen} = P_{noise} + NF + SNR \qquad (2)$$

A noise figure of 7 dB (P_{noise} = -95 dBm, SNR=17 dB for 80 MHz QPSK signal) is required to satisfy the -71 dBm condition. Gigabit-per-second data rates can be achieved by using multiple antennas and transceivers. The link budget

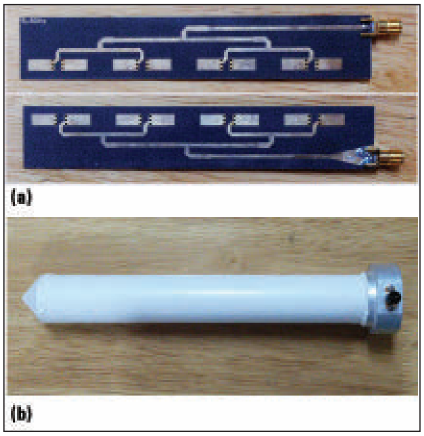

▲ *Fig. 5 Antenna prototype (a) and its package (b).*

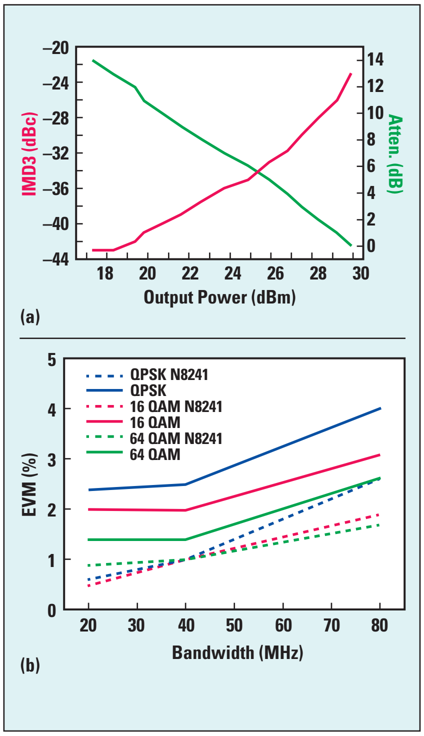

▲ *Fig. 6 Transmitter measured results; IMD3 (a) EVM at 23 dBm output power (b).*

TABLE 2

TRANSMITTER MEASUREMENTS

Parameters		Measurement Results
LO Phase Noise	4.2 GHz	-83 dBc @ 1 kHz, -91 dBc @ 10 KHz, -102 dBc @ 100 kHz, -127 dBc @ 1 MHz
	1.6 GHz	-93 dBc @ 1 kHz, -98 dBc @ 10 kHz, -110 dBc @ 100 kHz, -135 dBc @ 1 MHz
Tx Output IM3		-36 dBc @ P_{out} = + 23 dBm
Tx Gain Flatness		0.8 dB
Tx Carrier Suppression		> 55 dB
Tx Image Suppression		> 35 dB
Tx EVM (80 MHz QPSK)		4% @ P_{out} = + 23 dBm
Tx SNR (80 MHz QPSK)		28 dB @ P_{out} = + 23 dBm

of the transceiver is listed in ***Table 1***.

Antenna

The high gain parallel-fed twin-dipole array antenna consists of four identical printed twin-dipoles with half wavelength separation. The two arms of the twin dipole are printed on each side of the substrate and connected by metal vias. This structure can also effectively suppress cross polarization. The feed network acts as a two-stage power divider. It is realized by parallel strips of the same width on each side of the substrate. When the feed lines are connected to different arms, the two dipoles have a 180 degree difference in phase, which means the dipoles work in the even mode.[10] The antenna is fabricated on a 12.3 × 2.2 cm two-layer PCB, shown in ***Figure 5a***, and is packaged in a plastic cylinder with a 3.5 mm SMA connector to the cable, shown in ***Figure 5b***.

MEASUREMENT RESULTS

Performance is measured with a Keysight N8421A arbitrary waveform generator, R&S SMBV100A signal generator, Keysight N9020 spectrum analyzer and Keysight DSO91304A oscilloscope. Transmitter performance is summarized in ***Table 2***, including phase noise of the local oscillator. Transmitter IMD3 and EVM performance is shown in ***Figure 6***. Receiver performance is summarized in ***Table 3***. Receiver EVM performance becomes worse with increasing bandwidth as shown in ***Figure 7***. The receiver's maximum input power is -20 dBm, and its minimum input power (sensitivity) is -70 dBm, resulting in a 50 dB dynamic range.

The arbitrary waveform generator creates the baseband signal, which is upconverted to 5.8 GHz by the signal generator. The transceiver is tested using

TABLE 3

RECEIVER MEASUREMENTS

Parameters	Measurement Results
Rx Noise Figure	6 dB
Rx Gain Flatness	1.2 dB
Rx Dynamic Range	-20 to -70 dBm
Rx Image Suppression	> 35 dB
Rx EVM (80 MHz QPSK)	5% @ Pin = -40 dBm
Rx SNR (80 MHz QPSK)	26 dB @ Pin = -40 dBm

a 20 MHz LTE signal (which is also an OFDM signal) due to instrumentation bandwidth limitations. The measured transmitter and receiver EVM using the 20 MHz LTE signal is 2.1 and 2.2 percent, respectively (see ***Figure 8***). Because of the lack of calibration for I/Q skew, EVM performance of the N8241A is poor (3.5, 2.4, and 2 percent for 80 MHz QPSK, 16 QAM, 64 QAM signal, respectively); therefore,

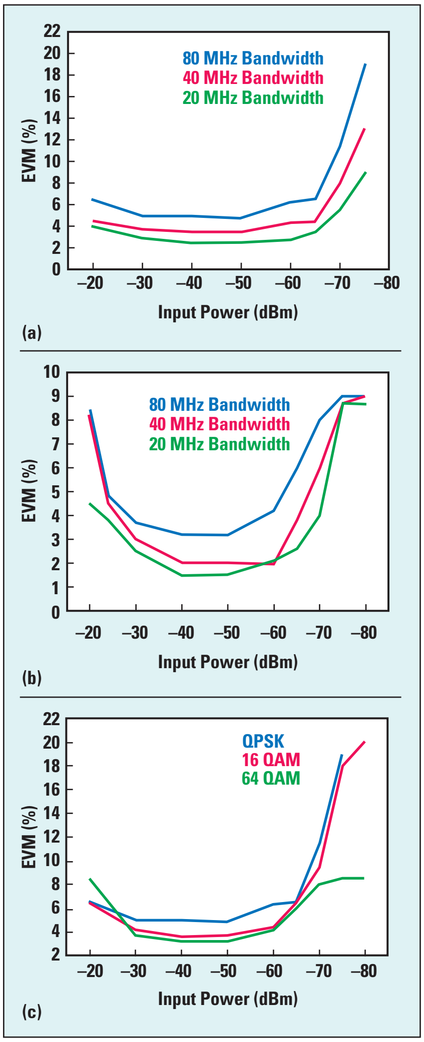

▲ *Fig. 7 EVM performance of the receiver for QPSK signal (a) 64 QAM signal (b) 80 MHz signal (c).*

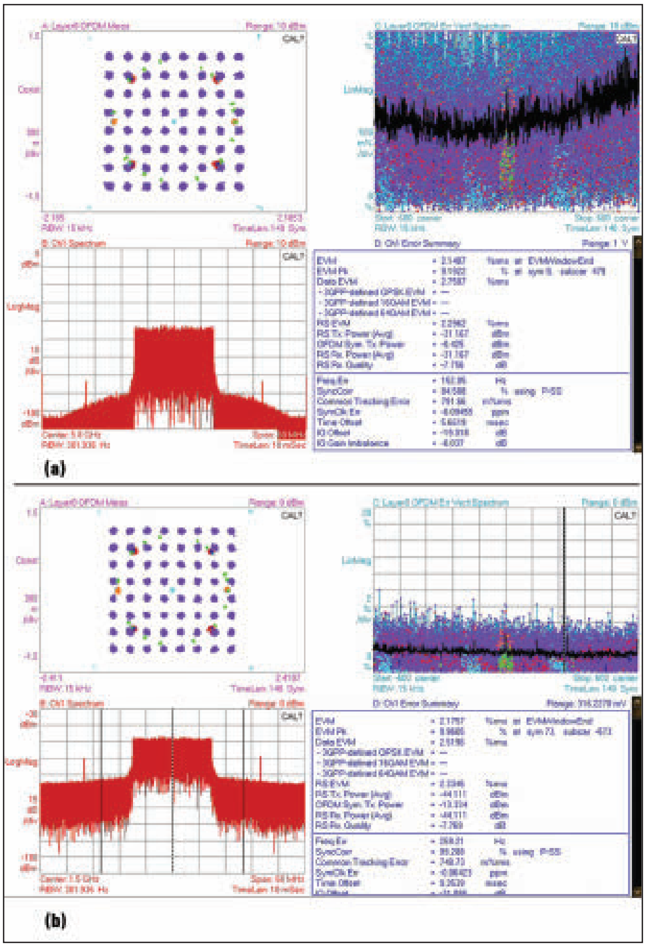

▲ *Fig. 8 EVM measurement of the transmitter at 23 dBm output power (a) and the receiver (b) for 20 MHz LTE signal with 100 resource block.*

the actual EVM might be better than the measured values. Measured versus simulated input return loss of the antenna and the radiation pattern at 5.8 GHz are shown in ***Figure 9***. The antenna has the gain of 8 dBi at 5.8 GHz and a wide impedance bandwidth from 4.8 to 6.5 GHz. ***Figure 10*** shows the operational system, where the cabinet on the left acts as a base station and the one on the right acts as the nearest mobile station. The data stream is transmitted and received through the antennas on the top of each cabinet.

CONCLUSION

An RF subsystem for future WLAN has been designed, fabricated and measured. The influences of phase noise, I/Q imbalance and interference are analyzed, and measures are taken to provide performance improvements. The RF receiver has low noise, wide dynamic range and high image rejection within the broad channel bandwidth. The RF transmitter has a high IMD3 and low EVM at 23 dBm output power. The antenna has 8 dBi gain at 5.8 GHz. The 8 × 8 RF subsystem has been used in an IEEE 802.11ac prototype system successfully with more than 1 Gbps throughput over an 80 m radius of coverage. ■

ACKNOWLEDGMENT

This work is supported in part by the National Natural Science Foundation of China under Grant 60702163, and in part by the National Science and Technology Major Project of China under Grant 2010ZX03007-002-01 and 2011ZX03004-003.

References

1. G. Hiertz, D. Denteneer, L. Stibor, Y. Zang, X.P. Costa and B. Walke, "The IEEE 802.11 Universe," *IEEE Communications Magazine*, Vol. 48, No. 1, January 2010, pp. 62-70.
2. Rolf de Vegt, "802.11ac Usage Models Document," IEEE, 802.11-09/0161r2, January 22, 2009.
3. Greg Jue, "Tackling MIMO Design and Test Challenges for 802.11ac WLAN," *Microwave Journal*, Vol. 55, No. 3, March 2012, pp. 88-96.
4. T. Pollet, M. van Bladel and M. Moeneclaey, "BER Sensitivity of OFDM Systems to Carrier Frequency Offset and Wiener Phase Noise," *IEEE Transactions on Communications*, Vol. 43, No. 234, February/March/April 1995, pp. 191-193.
5. C.L. Liu, "Impacts of I/Q Imbalance on QPSK–OFDM–QAM Detection," *IEEE Transactions on Consumer Electronics*, Vol. 44, No. 3, August 1998, pp. 984-989.
6. L.H. Li, F.L. Lin and H.R. Chuang, "Complete RF-System Analysis of Direct Conversion Receiver (DCR) for 802.11a WLAN OFDM System," *IEEE Transactions on Vehicular Technology*, Vol. 56, No. 4, July 2007.
7. Z.Q. Yu, J.Y. Zhou, J.N. Zhao, T. Zhao and W. Hong, "Design of a Broadband MIMO RF Transmitter for Next-Generation Wireless Communication Systems," *Microwave Journal*, Vol. 53, No. 11, November 2010, pp. 22-26.
8. Z. Chen, W. Hong, J.Y. Zhou, J.X. Chen and C. Yu, " Design of Miniature RF Transceivers for Broadband MIMO Systems in Ku-Band," *Microwave Journal*, Vol. 55, No. 11, November 2012, pp. 108-116.
9. J. Hendricks, "Printed Circuit Board Materials for Microwave Designs in Automotive Applications," *Microwave Journal*, Vol. 50, No. 12, December 2007, pp. 84-94.
10. W. Hong, Q. Jiang, Twin Dipole Wideband Printed Antenna, patent: ZL00 2 20230.1, 2001.2.24.

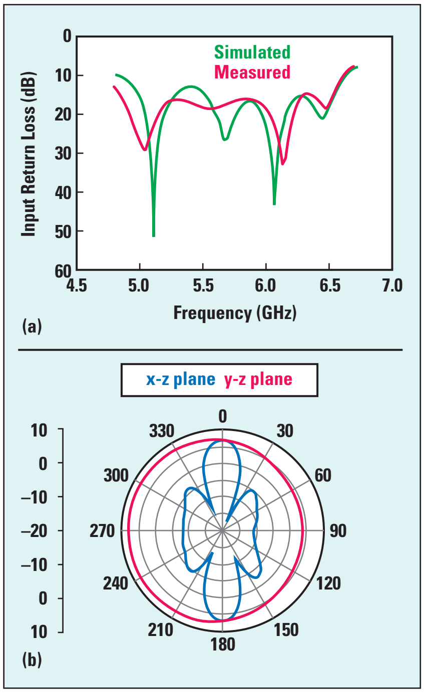

▲ *Fig. 9 Antenna input return loss (a) and radiation pattern at 5.8 GHz (b).*

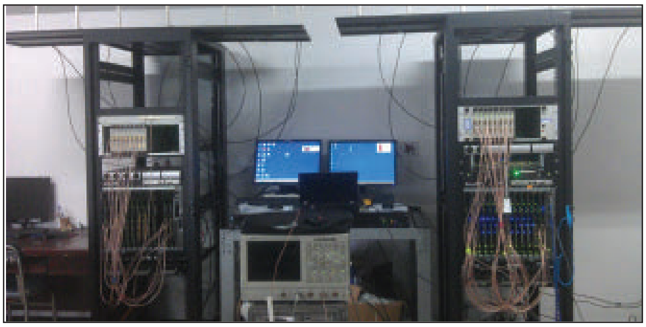

▲ *Fig. 10 WLAN system operation scenario.*


Reactel, Incorporated
Reacting First to All Your Filter Needs.
DCS
WLL
MMDS
VHF
UHF
REACTEL, INC
CDMA
REACTEL, INC.
Wireless
GSM
TX
Microcell
& Mobile
EGSM
AMPS
REACTEL, INC.
UMTS
RX
WLAN
REACTEL, INC.
Cellular
REACTEL, INC.
SMR
Crossband Coupler
WiFi
PCS
AWS
- Submitting a request for immediate attention will never be easier.
- Full featured App contains expanded RFQ capability, catalog, data sheets and more.
- Available for iPad, iPod and Android devices via the App Store and Google Play.
Available on the App Store
Google play
8031 Cessna Avenue • Gaithersburg, Maryland 20879 • Phone: (301) 519-3660
For general inquiries, please email reactel@reactel.com • http://twitter.com/reacteljim
Go online to www.reactel.com to download your Reactel catalog today.
3G
RoHS
@reacteljim

MWJ REVIEW BOARD APPROVED

Smart Antennas and Front End Modules in Q-Band for Backhaul Networks

R. Vilar, J. Marti
Universitat Politecnica de Valencia
R. Czarny
Thales Research and Technology
M. Sypek, M. Makowski
Orteh SP. Z O.O.
C. Martel, T. Crépin, F. Boust
Office National d'Etudes et de Recherches Aerospatiales
R. Joseph, K. Herbertz, T. Bertuch
Fraunhofer Institute for High Frequency Physics and Radar Techniques FHR
A. LeFevre
Thales Communications & Security SA
F. Magne
Bluwan Ltd.

As mobile operators face increasing base station density as well as growing bandwidth requirements, mobile backhaul has become the new challenge. This article defines the architecture for future mobile backhaul networks as proposed in the framework of the FP7 EU SARABAND project. The solution exploits a new and wider frequency band, Q-Band (40.5 to 43.5 GHz), to provide massive capacity. Since full deployment of Q-Band backhaul networks requires new technology development, an overview of disruptive antenna and front end technology developed within this project is also provided.

Demand for bandwidth is growing exponentially as consumers use their mobile devices in more bandwidth-intensive applications. The evolution to 3G and 4G/LTE mobile technologies provides a path to more efficient use of the radio spectrum and progressively higher uplink and downlink speeds to each user. Operators' forecasts show that additional steps are required to provide sufficient bandwidth.

As a result, operators have begun to introduce small cells into their networks, since this solution has recently emerged as a more cost-effective way for network mobile operators to improve the coverage and capacity of their mobile services. But there are some challenges to leveraging the benefits of small cells. One of the most significant is providing scalable, flexible mobile backhaul to connect small cells back into the network without breaking the small cell business case.

Operators typically use different backhaul

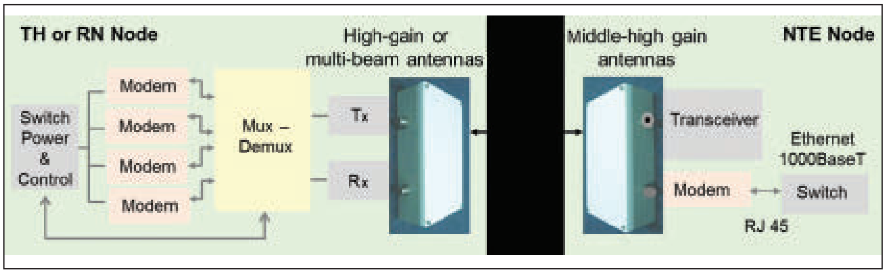

▲ *Fig. 1 Network node architecture.*

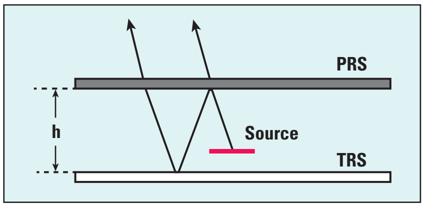

▲ *Fig. 2 Fabry-Perot cavity.*

technologies for their radio access networks. Nevertheless, existing alternatives such as fiber, digital subscriber line (DSL) and microwave backhaul do not provide the required CAPEX, OPEX and/or performance; therefore, an adequate backhaul upgrade in capacity and cost-efficiency is required. Millimeter wave technology, especially in Q-Band (40.5 to 43.5 GHz), offers a wide frequency spectrum, compactness and lightness of equipment and ease of implementing interference-free system configurations. This makes it very promising for high data rate backhaul applications.

The SARABAND project integrates Q-Band millimeter wave technology for point to multipoint (PMP) transmission to provide a cost-effective solution capable of supplying 150 to 200 Mbps per cell site.

WIRELESS BACKHAUL ARCHITECTURE

The wireless backhaul architecture proposed in SARABAND is a hierarchical, PMP Ethernet-based network composed of nodes linked by radio transmissions and remotely managed by a backhaul network management system (NMS). The solution is a distribution tree connecting a service provider's point of presence (PoP) to relay nodes ultimately reaching subscriber terminals, grouped terminals and mobile base stations. The main features are:

- A highly flexible PMP network topology that rapidly adapts to an operator's coverage and capacity requirements while simplifying radio deployment.
- The use of Q-Band, providing a large spectral bandwidth suitable for wide channels (40.5 to 43.5 GHz in 1 GHz sub-bands).
- A radio backhaul network composed of a multiplex of channels that aggregates several 100 Mbps half-duplex (TDD) channels to provide the required throughput (up to 2 Gbps half-duplex per 1 GHz radio transmission).
- Layer 1 and 2 of the network based on the 802.11n and then the 802.11ac standards and aggregation on 802.3ad.

The backhaul network architecture is composed of different types of nodes (see ***Figure 1***). The Transmission Hub (TH) carries traffic in the core network and connects several terminals or relay nodes (RN). Relay Nodes extend system range and avoid the limitations of line of sight. Network Terminal Equipment (NTE) delivers basic services to customers' points of presence.

To enable any configuration of hierarchical PMP links while meeting the required performance on each segment of the network, the SARABAND project is developing new Q-Band backhaul network technology to increase network node throughput, range and coverage, while reducing cost. Specific developments include:

- Q-Band low-profile, high-gain antennas that will enhance throughput between the TH and the remote sites. Two approaches have been analyzed: Fabry-Perot antennas and lens antennas for medium-gain (20 dBi) and high-gain (>30 dBi) applications, respectively.
- Q-Band programmable multi-beam antennas, which will enhance coverage, reduce interference and save energy. Circular Switched Parasitic Array (CSPA) antennas, for an agile antenna solution, have been analyzed.
- Q-Band miniaturized radio modules based on new substrate, packaging and interconnection processes with the objective of providing modules with low loss, high power and high reliability at a fraction of the price of any currently available radio.

TABLE 1

FP ANTENNA SPECIFICATIONS

Size	70 × 70 mm
Height	7 mm
Gain	16 to 25 dBi
Beamwidth -3 dB (E/H planes)	15° / 15°
Bandwidth at -10 dB	1 GHz
Side lobe levels vs main lobe	-13 dB

FABRY-PEROT ANTENNA

A Fabry-Perot (FP) antenna is a planar structure providing highly directive beams with properties such as a low profile, lightweight, simple feed mechanism and low cost. This makes it a good candidate to address Q-Band medium gain coverage requirements.

The FP antenna (see ***Figure 2***) is a type of leaky wave antenna, consisting of a partially reflective surface (PRS) at a proper distance from a totally reflective surface (TRS). The resulting cavity may be filled with air or a dielectric material and is excited by a source that is placed inside the cavity.[1] With an appropriate design, parallel plate modes are excited in the cavity by the source. The power carried by the modes leaks through the PRS, forming a broadside pencil beam in the far field. The distance between the two reflecting surfaces (h) of the cavity and the source position are important antenna parameters.

Considering that the source is positioned at the same level as the PRS, the power radiated in the boresight direction is at a maximum when the following condition is satisfied:

$$\phi_R + \psi_R - \frac{2\pi}{\lambda} \cdot 2h = 2n\pi \quad (1)$$

where ϕ_R is the reflection phase of the PRS, Ψ_R is the reflection phase of the TRS, h is the Fabry-Perot cavity height, and n = 0,1,2,3,...

For the SARABAND project, the FP antenna specifications are shown in ***Table 1***. It uses an air-filled FP cavity to reduce losses and provide the best compromise for maximum di-

TABLE 2 LENS ANTENNA SPECIFICATIONS		
Size	< 250 mm (f/D < 0.5)	< 150 mm (f/D < 0.5)
Gain	> 35 dBi	> 30 dBi
Beamwidth -3 dB	< 3° horizontal and vertical	< 5° horizontal and vertical
Bandwidth at -10 dB	3 GHz (or 1 GHz centered in each Q-Band)	
Diffused lobes	Mean value < 30 dB between 45° and 90°	

rectivity and pattern bandwidth. The PRS is made of periodic patches (2.88 × 2.88 mm with a 4.2 mm square periodicity) printed on a 0.51 mm thick dielectric substrate placed 2.79 mm above the TRS. A patch within the air-filled cavity is the source of excitation.

An FP antenna produces a highly directive beam with a single feed source, where

$$\text{directivity}(D) = \left(4\pi/\lambda^2\right)A \qquad (2)$$

for an aperture with an area A. While it is possible to reach up to 90 percent of the theoretical maximal directivity with a few lambda size aperture and a highly reflecting PRS, practical realizations achieve directivities around 50 percent of this limit.

FP antennas, however, are narrowband. Jackson et al.,[1] have shown that for a simplified configuration, the product of directivity and 3 dB bandwidth is a constant that can be estimated by the formula:

$$D \cdot BW \approx \frac{2.5}{n^2} \qquad (3)$$

with n being the cavity refraction index.

The high-gain antenna for the SARABAND project requires a 7.2 percent fractional bandwidth. Basic FP antennas have a fixed directivity-bandwidth product insufficient to meet this requirement; however, the gain can be increased through several complementary means. One is to extend the size of the radiating aperture making the surface through which the leaky wave radiates electrically large, achieving medium to high gain. Typically the PRS can be extended to a size of about 10 × 10 λ. A larger PRS size may not lead to a further gain increase since energy usually leaks from the cavity area being close to the source.

Antenna gain can be further increased by using multiple sources inside the cavity, making more efficient use of the large radiating surface. Furthermore, due to the presence of the PRS, the sources can be spaced 1.5 λ apart without generating grating lobes in the radiation pattern. This excitation mechanism requires a small feed network to distribute the energy between the multiple sources. ***Figure 3*** shows FP antennas with 1 and 16 sources, which have been designed to provide maximum gain. In both cases, the antenna size is 60 × 60 mm (~8.3 × 8.3 λ at 41.5 GHz). Maximum gain is achieved at 41.5 GHz with 1 source (19.2 dBi) and 41.75 GHz with 16 sources (23.3 dBi).

LENS ANTENNAS

In lens antennas, a quasi-point source (the feed) generates a spherical wave which is collected and collimated by a dielectric lens. This results in a plane wave at the antenna output that may provide diffraction-limited gain. Current lens antenna technology is either bulky (refractive design) or low-profile but less efficient (e.g., Fresnel lens).[2] To achieve a lower profile, yet efficient design, an innovative lens based on "quasi-optical" RF components is being investigated. It is the transposition of an optical approach, in terms of wavefront control and component design, to the RF domain. This enables the synthesis of an efficient, flat, high numerical aperture lens for controlling and reshaping the wavefront emitted by the Q-Band antenna feed.

Lens antenna operation is based on diffraction and constructive interference between zones composing the lens. The use of sub-wavelength structures and a hybrid lens design overcomes the usual Fresnel-lens limitations and does not suffer from loss of efficiency and bandwidth reduction when implemented in a low-profile configuration.

For the SARABAND project, this approach is applied to two different antennas of different sizes in order to cover both TH and NTE requirements. Specifications for the high-gain lens antennas are shown in ***Table 2***. The distance between feed and

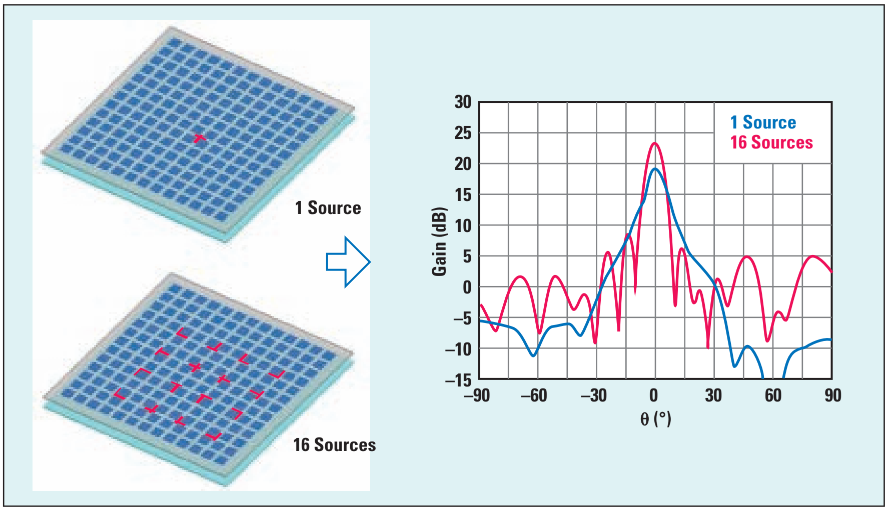

▲ *Fig. 3 FP antenna gain in the E-plane.*

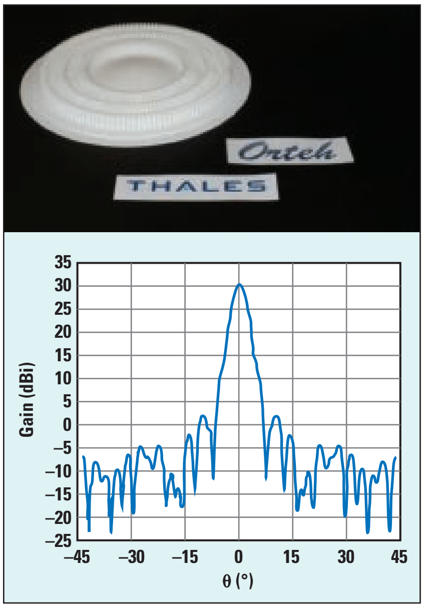

▲ *Fig. 4 Simulated gain of a low-profile high-gain lens in the H-plane at 42 GHz.*

lens must be optimized to take into account the feed radiation pattern, the lens size and the local sub-wavelength structure. For a given antenna volume, we can compute the configuration giving the highest antenna efficiency and therefore the highest gain. An example is shown in ***Figure 4***.

CSPA ANTENNA

An attractive concept for electronic beam steering is the circular switched parasitic array (CSPA) antenna, which is proposed for the agile Q-Band antenna with a large field of view to be used in the repeaters. The basis of this concept for electronic beam scanning is a well-known principle for the controlled forming of radiation patterns of an active antenna element using parasitically coupled passive antenna elements.[3] It allows for controlling the radiation pattern in the horizontal (azimuth) plane and steering the beam over a wide field of view. Simple electronic components such as PIN or varactor diodes may be used to tune the parasitic array elements and control beam shape and direction.

A CSPA antenna for a high-power data link application in C-Band (4.4 to 5 GHz) has been previously developed.[4] This design uses wire monopole antennas as active and parasitic radiators, sharing a common metallic ground plane of circular shape with the active element placed at its center. These monopoles must have a height of approximately λ/4 and spacing between the active element and the parasitic elements of approximately λ/4. ***Figure 5*** shows a 3D model of a C-Band CSPA antenna.

For the SARABAND project, the specifications of the Q-Band CSPA antenna are shown in ***Table 3***. At Q-Band the monopole-based CSPA is not feasible because of the height of the monopoles (only 1.8 mm) and the relative size of the additional circuitry (much larger than the antenna elements). Instead, printed microstrip technology is used, based on the CSPA concept.

A demonstrator fixed-beam antenna (without switching elements) is shown in ***Figure 6a***. In a forthcoming version, the beam will be steered by tuning/de-tuning the reflector elements through PIN diode biasing. Because the central active antenna element cannot achieve high gain by itself, the radiated signal is guided through a circular flared horn. At the center frequency of 42 GHz, a standard horn structure would have a length

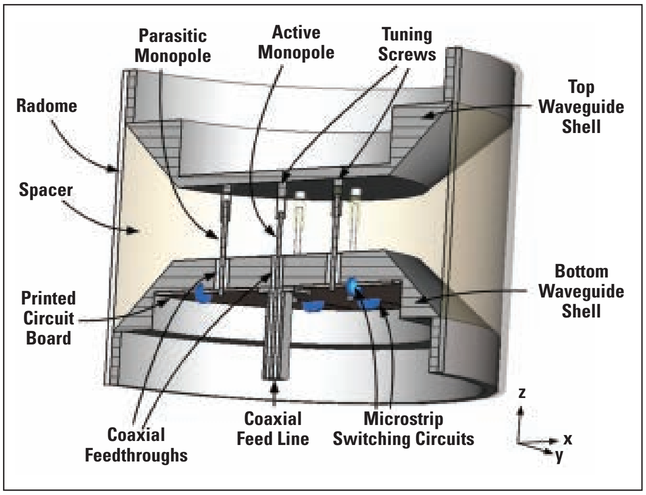

▲ *Fig. 5 C-Band CSPA antenna 3D model.*

TABLE 3

CSPA ANTENNA SPECIFICATIONS

Antenna Diameter	< 300 mm
Gain	16 dBi
Polarization	Vertical
Beamwidth (E/H plane)	6°/60°
Bandwidth at -10 dB	1 GHz (41.5 to 42.5 GHz)
Ideal coverage	270° in H plane (large field of view)

TABLE 4

TARGET PARAMETERS FOR THE TH-RN RADIO MODULES AND ANTENNAS

Radio Module TH-RN	Parameters	Values	Variances
Receiver			
	Noise Figure	4 dB	0.5 dB over temperature range
	Saturation P_{in}	-30 dBm	
	Gain	31 dB	Temperature: ± 1.5 dB Frequency: ± 1.5 dB
Transmitter			
	P_{sat}	29 dBm	Temperature: ± 1.5 dB Frequency: ± 1.5 dB
	P_1	26 dBm	Temperature: ± 1.5 dB Frequency: ± 1.5 dB
	Gain	26 dB	Temperature: ± 1.5 dB Frequency: ± 1.5 dB

TABLE 5

TARGET PARAMETERS FOR THE NTE RADIO MODULES AND ANTENNAS

Radio Module NTE	Parameters	Values	Variances
Receiver			
	Noise Figure	6 dB	0.5 dB over temperature range
	Saturation P_{in}	-30 dBm	
	Gain	30 dB	Temperature: ± 1.5 dB Frequency: ± 1.5 dB
Transmitter			
	P_{sat}	19 dBm	Temperature: ± 1.5 dB Frequency: ± 1.5 dB
	P_1	16 dBm	Temperature: ± 1.5 dB Frequency: ± 1.5 dB
	Gain	21 dB	Temperature: ± 1.5 dB Frequency: ± 1.5 dB

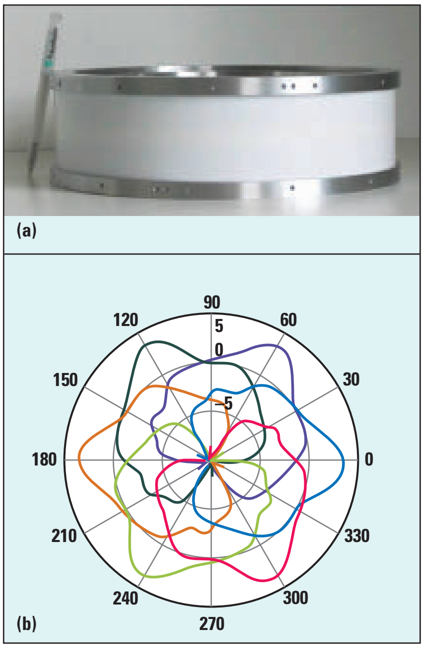

Fig. 6 *Photograph of the fabricated fixed-beam CSPA Q-Band antenna (a) simulated radiation patterns (b).*

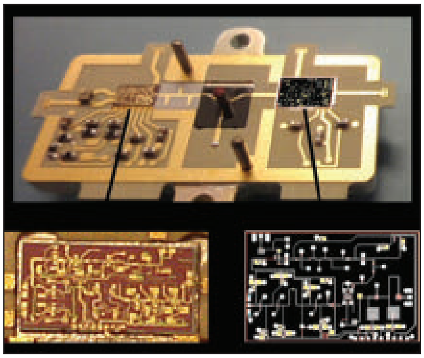

Fig. 7 *NTE transceiver.*

of approximately 300 mm. Due to external limitations the size of the horn must be reduced without reducing its gain; therefore, special measures are incorporated in the horn structure to reduce its size and increase the gain to achieve the desired characteristics. The antenna has an impedance bandwidth of 4.87 percent centered at 42 GHz. Simulated radiation patterns in the horizontal plane at 42 GHz are shown in ***Figure 6b*** for various scanning directions, corresponding to different configurations of tuned/detuned reflector elements.

RF MODULES

Front end radio modules use advanced GaAs-based monolithic microwave integrated circuit (MMIC) elements and benefit from system-in-a-package (SIP) technology integration to reduce the printed circuit board (PCB) footprint. Specific MMIC chip-sets for the up and downconverters have been developed by the project. These integrate several different functions and provide gain improvements, achieving the 18 dBm power target for the upconverter and 31/33 dB gain for the downconverter with 2.5 dB noise factor. These two chipsets, together with a power amplifier, are the core elements of the front end radio modules for the network nodes. ***Tables 4*** and ***5*** list target parameters for the NTE and TH-RN radio modules and antennas.

Specific SIPs using a supporting PCB etched on an organic substrate and including the MMIC chip-sets, filters, isolator/circulator and the antenna interconnection have been designed and manufactured for the SARABAND demonstrator. An example of a manufactured SIP design is the NTE transceiver shown in ***Figure 7***, which consists of a 42 × 25 mm rectangular module. It is composed of the upconverter and downconverter chip-sets soldered on a metallic plate, and a circulator which isolates the uplink from the downlink and allows alternative transmission and reception. A specific connector adapted for 40 to 45 GHz is used for the antenna interface. Signals coming from the local oscillator and the intermediate frequency amplifier and power are supplied through the PCB. Finally, a cover plate shields the module.

One of the biggest challenges has been to successfully miniaturize the front end radio modules. The use of SIP integration and GaAs-based MMIC modules has made this possible. In addition, miniaturization has reduced circuit losses, reduced cost (low site rental, easy installation) and enhanced acceptability. In the future, novel technologies such as SiGe-based devices and high frequency switch components could easily be incorporated to improve the performance of the chipsets and the SIP.

CONCLUSION

The Q-Band PMP backhaul architecture developed through the SARABAND project provides multi-gigabit capacity in a cost-effective manner by exploiting PMP transmissions and the Q-Band spectrum. In addition, the project has several on-going antenna and radio module developments. In particular, a 23 dBi gain Fabry-Perot antenna using multiple sources for medium-gain applications has been designed. Moreover, sub-wavelength structured lens antennas with gains higher than 30 dBi to cover both TH and NTE requirements have been manufactured. For electronic beam steering, a CSPA antenna has been proposed. The designed antenna has a relative impedance bandwidth of 4.87 percent, centered at 42 GHz, and a gain of 16 dBi with a beamwidth of 6°/60° (E/H plane) to cover a horizontal angular range of 270°. Finally, miniaturized front end modules with SIP integration have been designed and manufactured.

References

1. D. Jackson, P. Burghignoli, G. Lovat, F. Capolino, J. Chen, D. Wilton and A. Oliner, "The Fundamental Physics of Directive Beaming at Microwave and Optical Frequencies and the Role of Leaky Waves," *Proceedings of the IEEE*, Vol. 99, No. 10, October 2011, pp. 1780-1805.
2. A. Petosa, N. Gagnon and A. Ittipiboon, "Effects of Fresnel Lens Thickness on Aperture Efficiency," *Proceedings of the 10th International Symposium on Antenna Techniques and Applied Electromagnetics*, July 2004, pp.175-178.
3. R.F. Harrington, "Reactively Controlled Directive Arrays," *IEEE Transactions on Antennas and Propagation*, Vol. 26, No. 3, May 1978, pp. 390-395.
4. T. Bertuch, "A Circular Switched Parasitic Array Antenna for High Power Data Link Applications," *Proceedings of the 3rd European Conference on Antennas and Propagation (EuCAP)*, March 2009, pp. 2483-2487.

Ruth Vilar *received her M.Sc. and Ph.D. degrees in Telecommunications from the Universitat Politècnica de València, Valencia, Spain, in 2007 and 2010, respectively. She joined the Nanophotonics Technology Center as a researcher in 2004. Her research activities are focused on backhaul and access networks, advanced optical techniques for microwave signals and ultra-high speed data transmission. Other research interests include optical performance monitoring and packet-switched networks.*

Javier Martí *received his Ingeniero de Telecomunicación degree from the Universidad Politécnica de Catalunya, Spain in 1991, and his Ph.D. degree from the Universidad Politécnica de Valencia, Spain in 1994. In 1989 and 1990, he was an assistant lecturer at the Universidad Politécnica de Catalunya.*

From 1991 to 2000, he held the positions of lecturer and associate professor at the Telecommunication Engineering Faculty. Martí is currently the director of a national research centre for photonic technologies at the Valencia Nanophotonics Technology Centre (NTC), in Valencia, Spain. He has authored 7 patents and over 185 papers in refereed international technical journals in the fields of broadband hybrid fiber-radio systems and microwave/millimeter wave photonics, access networks, terabit/s OTDM/WDM optical networks, advanced optical processing techniques for microwave signals and ultra-high speed data transmission and silicon photonics.

Romain Czarny received his Engineering degree from ENST Paris (Ecole Nationale Supérieure des Telecommunications, now Télécom ParisTech) in 2002. He joined Thales Research & Technology (TRT) in 2006 where he received a Ph.D. in collaboration with IEMN working on optically driven sub-millimeters sources. After three years as project manager in a Thales subsidiary, Czarny joined the TRT LCDT Laboratory (Component, Technologies Integration & Demonstration Lab) with activities dedicated to optical concepts applied to RF technologies such as millimeter wave imaging and lens antenna technologies.

Maciej Sypek received his M.Sc., Ph.D. and habilitation degrees from the Warsaw University of Technology in 1987, 1992 and 2009, respectively. He is now the CEO of the Polish innovative company Orteh, active in the areas of information technologies and optics. He deals with optical design and numerical simulations of propagation electromagnetic radiation in demanding configurations from the extreme ultra-violet to the terahertz range. Sypek is an expert in the design and characterization of sub-wavelength elements. He is an author and co-author of more than 50 articles published in pre-reviewed scientific journals.

Michal Makowski received his M.Sc. and Ph.D. degrees from the Warsaw University of Technology in 2001 and 2007, respectively. His activities in Orteh are focused on the fabrication and characterization of sophisticated, optical, diffractive and holographic elements for the wide range of frequencies. Makowski is an author and co-author of more than 40 articles published in pre-reviewed scientific journals.

Cédric Martel joined the antenna department of ERA Technology (UK) in 1997. In 2002, he received his Ph.D. degree following a part-time research program in collaboration with ERA Technology and the University of Surrey. Since January 2006, he has been working as an antenna research engineer in the department of electromagnetism and radar (DEMR) of ONERA in France. Martel's research interests include leaky wave antennas, reconfigurable antennas, phased arrays, metamaterials and their antenna applications.

Thomas Crépin received his M.S. degree in physics from University of Lille, France, in 2002 and his Ph.D. degree from the University of Lille, France, in 2006. From 2002 to 2006, he was with Institut d'Electronique, de Microélectronique et de Nanotechnologie (IEMN), Lille, France, where he worked on terahertz technology and metamaterials. Crépin is currently working in the field of antenna and metamaterial design at ONERA, The French Aerospace Lab, in the Electromagnetism and Radar Department, Toulouse, France.

Fabrice Boust received the Agrégation of Physics in 1981 from the École Normale Supérieure de l'Enseignement Technique. He earned a Doctorate of Science in 1989 from the Paris Sud University. Boust is currently a senior expert in the Radar Department of ONERA (the French Aerospace Lab) and in SONDRA (a joint laboratory established between Supelec, ONERA, the National University of Singapore and DSO National Laboratories). His research interests are dynamics of magnetic particles, radar absorbing materials and metamaterials for antennas.

Ronald Joseph received his Ph.D. degree from Kumamoto University, Japan in 2011. He was a Lecturer in Electronics at Christ Junior College, Bangalore, India from 2002 to 2008. Joseph is currently working at the Fraunhofer Institute for High Frequency Physics and Radar Technique, FHR, Wachtberg, Germany. His research interests are antenna design and electromagnetic modeling.

Kai Herbertz received his Ph.D. in electrical and electronic engineering from Imperial College London, U.K., in 2010. Since 2011, Herbertz has been working as a researcher for the Fraunhofer Institute for High Frequency Physics and Radar Techniques (Fraunhofer FHR). His research interests include metamaterials and electromagnetic modeling.

Thomas Bertuch received his Ph.D. from RWTH Aachen University, Aachen, Germany, in 2003. His doctoral research was developed at the Research Institute for High Frequency Physics and Radar Techniques of the Research Establishment for Applied Natural Science e.V. (FGAN-FHR), Wachtberg, Germany. In 2004, he was a senior antenna scientist with the Defence, Security and Safety Institute of The Netherlands Organization for Applied Scientific Research (TNO), The Hague, The Netherlands. Since 2005, Bertuch has been with the FGAN-FHR which, since 2009, is the Fraunhofer Institute for High Frequency Physics and Radar Techniques (Fraunhofer FHR); where he is currently Team Leader of Antennas and Front End Technology. From 2000 to 2009, he was Lecturer of RF engineering at the Bonn-Rhine-Sieg University of Applied Sciences, Sankt Augustin, Germany. Since 2012 he has been Lecturer of Antennas and Wave Propagation at the Aachen University of Applied Sciences, Aachen, Germany. Bertuch's research activities include antenna and microwave circuit design, engineered electromagnetic materials (metamaterials), radar system design and electromagnetic modeling.

Alain LeFevre graduated from the Conservatoire des Arts et Métiers specializing in Macromolecule Polymers. He joined the Thales microwave department in 2000 to develop microwave component industrial activities and became involved in IFF (Identification Friend or Foe) microwave and X-Band activities. He has been in charge of studying a Q-Band Solid State Power Amplifier in the Thales microwave department.

François Magne is responsible for research and development at Bluwan. He began his career at the French DGA (French department of defence), creating missile guidance and directional radar systems. He later became director of industrial relations at French research think tank CNRS, and went on to lead advanced research at TRT-Philips and Thomson CSF. When the Thales Group acquired Thomson CSF, he became the chief scientist for the Thales CNI (communication, navigation and identification) division. Magne was a critical contributor in the development of advanced communications systems, as well as the development of satellite and high speed broadband technologies. In 2002, he became the vice president of technology in charge of innovation and industrialization at Thales, with whom he co-founded Bluwan in 2005.

Disruptive Factors in the Global Long Haul Market

Emmy Johnson
Sky Light Research, Scottsdale, Ariz.

Last summer, Sky Light Research (SLR) published a special report on the long haul market for North America. Due to LTE and its IP data centric requirements, long haul radios in North America were undergoing a transformation – becoming much more compact, flexible, powerful and fast. As of summer 2013, these slimmer, more agile radios were only available for the North American market, however, as SLR predicted, these radios are now available for the global market. Over the last year and a half, several vendors have added new or improved long haul product offerings to their portfolios.

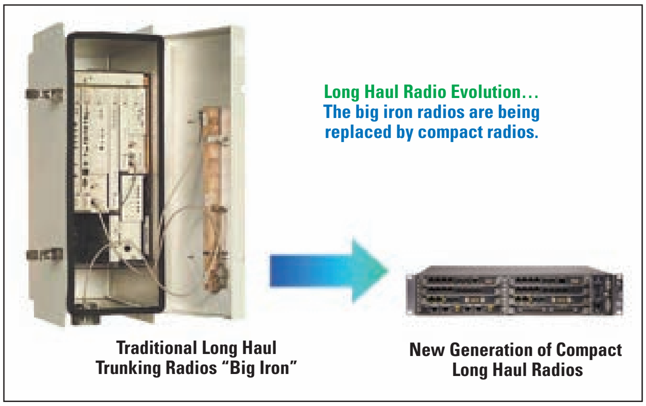

Fig. 1 Long haul radio evolution.

This new concept of IP based long haul radios has created two categories: (1) traditional big iron long haul radios, often referred to as trunk radios, and (2) new compact IP based long haul radios (see ***Figure 1***). Although the requirement for the traditional "big iron", high power trunking radios exists, Sky Light Research believes that growth in the long haul segment will be driven by the new IP based long haul radios.

CHANGING SPECIFICATIONS

The difference between the two types of long haul radios is illustrated in ***Table 1***. Often companies offer both types, with traditional radios appeasing legacy customers and projects, while compact IP based long haul radios attract customers modernizing their networks with IP. The changing specifications that are highlighted in Table 1 include:

Agile Architecture: Many vendors offering traditional trunking radios have updated their products to have a split mount version, since many operators cannot afford or do not want the expense associated with the shelters and required air conditioning needed to support a traditional microwave trunking solution. By placing part of the radio outside, it

TABLE I

CHANGING SPECIFICATIONS

	Traditional Trunking/ Long Haul Radios	New IP Based Long Haul Radios
Architecture	Full Indoor	Split-Mount/All Outdoor/ All Indoor
Capacity	4 to 6 Gbps per Antenna	up to 16 Gbps per Antenna
Carriers	8 to 12	10 to 20
Transmission Protocol	TDM Based	IP Based/Hybrid
System Gain	< 100 dB with waveguide	> 100 dB with waveguide
Transmission Power (dBm)	25 to 30	30 to 35
OAM	SDH based	Ethernet Service Capable (IEEE 1588v2, Ipv6)
Power Consumption	100+ W per channel	Under 100 W per channel

reduces the footprint and the expense required to keep the shelter and the equipment cool.

Traditional long haul or trunking radios are "big iron" radios that have large footprints. In some cases, especially in the non-mobile verticals, these radios are still preferred. However, mobile operators are driving the growth in the long haul segment, and they require a different type of architecture to resolve the quandary of limited real estate that is becoming increasingly expensive. This is one of the driving changes for long haul radios. Newer, compact IP-based long haul radios can now be used outdoors, indoors or in a split mount configuration.

All outdoor radios can be hung on poles, eliminating the footprint in the cabinet. This architectural change has expanded the use of long haul not only to the core, where a cabinet exists, but also to the cell's edge, due to its smaller form factor.

With its MPR9500 MPT-HL for the North American market, Alcatel Lucent was first-to-market with this concept. Until 12 to 18 months ago, Alcatel-Lucent owned the IP based compact long haul market in North America. Other vendors quickly realized the market potential and developed their own radios. Operators now have several options for compact IP based long haul solutions as LTE rolls out across the globe.

Capacity: It is well known that capacity requirements in the network are on an upward trajectory. Long haul radios approach capacity slightly differently than short haul radios. The unique characteristic of long haul radios is its branching mechanism. This allows the aggregation of several carriers on one antenna, which creates a very high capacity radio.

For example, Huawei's new long haul IP based radio is able to reach 16 Gbps – by aggregating 16 carriers of 1 Gbps each to one antenna, making it one of the highest capacity radios on the market.

Power: Like capacity, power also is increasing. The defining characteristic for long haul or trunking radios is high power, which makes them able to send the signal a longer distance (hence the name long haul). Today, long haul radios are pushing the power threshold, reaching 35 dBm, which emasculates the traditional 20 to 26 dBm of a few years ago. SIAE's radio can reach 35 dBm with 20 dB automatic transmit power control (ATPC).

Hybrid/IP based: Long haul radios with TDM are still required in many cases, due to TDM's ability to handle issues such as multi-path fading. However, future growth in long haul radios will be driven by Hybrid and/or IP based radios. This movement is making hybrid radios a more strategic choice over TDM radios for those customers who need a smooth transition from TDM to IP. Trunking/long haul radios are often used at aggregation points or in the backbone of the network where various types of media come together. Hybrid radios, by definition, can natively service the various traffic types, making them an important piece in the microwave tool kit. IP based long haul radios, however, are ideal for mobile data networks, like LTE and HSPA, where increased capacity is a must in order to support more IP packet-based services and applications.

Green/Energy Efficient: As with all networking infrastructure equip-

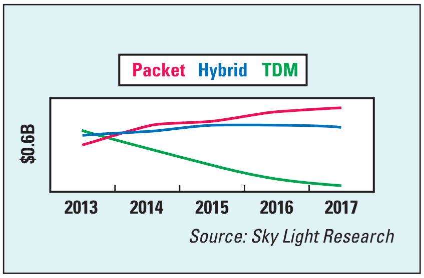

Fig. 2 Global long haul forecast.

ment, energy efficiency is important. Whether the trunk radio is being used in a fixed line provider's central office located in a remote region, or it's being hung on a pole in a mobile operator's network in a suburb, going green is important. Previously, radios were using over 100 W per channel; however, long haul radios today use less. Aviat's STR-600 long haul radio is one of the most efficient on the market, using less than 60 W per channel.

SLR expects 2014 to be the first year where we see IP based long haul radios out-ship TDM radios (see ***Figure 2***). This has already occurred in North America since the North American market is the region where long haul has the greatest demand. The shift in North America was driven by mobile operators rolling out LTE. Historically, mobile operators played a small part in long haul revenue generation due to their reliance on short haul radios. One of the central changes in the new long haul radios is its flexible architecture/compact footprint that is similar to short haul radios. Equipment vendors are taking full advantage of this feature, appealing to operators' desire to save real estate.

For example, both Ceragon's and Aviat's IP based long haul radios are available in split-mount. This architectural option has some resemblance to short haul radios that operators are used to deploying and building into their networks. Several vendors now selling compact IP based long haul radios will have a positive effect on growth for long haul radios through the forecast period.

Although compact IP based long haul revenue outside of North America is still in its infancy, SLR believes that this will change in the next 12 to 18 months, with strong growth occurring worldwide. There are just a handful of equipment manufacturers who offer compact IP based long haul radios for regions outside of North

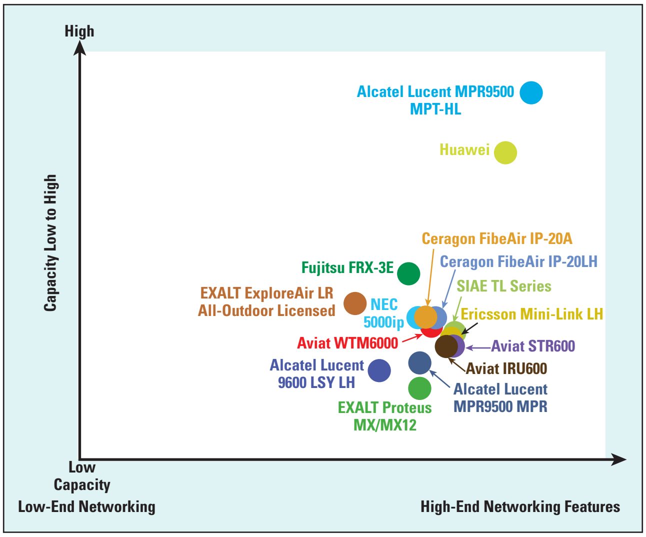

▲ *Fig. 3 Networking features – low end to high end.*

America, with Alcatel-Lucent and Huawei being among them. These two vendors represent a market bellwether of sorts because:

1) Alcatel-Lucent is the first to have compact IP based long haul radios, and they have had great success in the North American market. Even though most of the demand stemmed from just two customers, AT&T and Verizon, the company clearly sees the benefit that compact IP based long haul radios offers a mobile operator deploying advanced mobile broadband services.
2) Huawei is a leading microwave vendor and has never had a long haul offering. Since they are making their foray into the long haul market with an IP based compact long haul radio, they must have some very large customers asking for this solution. Huawei has been aggressive in winning 4G bids and SLR suspects that this latest radio is a product driven from customer requests.

THE LONG AND THE SHORT OF THE LONG HAUL MARKET

Historically, global long haul revenue has paled in comparison to short haul revenue. Despite this, long haul radios are a vital and steady market for the manufacturers that sell them worldwide. Although they are not used as much as short haul radios, their price points are much higher, with prices typically between $14,000 and $40,000 a link, depending on the application and load. The higher price points, combined with new applications for IP based compact long haul, will rejuvenate the market and drive up revenue.

Long haul radio applications run the gamut from backhaul to interconnecting buildings. Key verticals include utility companies, government agencies, enterprises, public service agencies, fixed line service providers and mobile operators. Private networks use long haul to connect remote locations to a headquarters for redundant links or for public safety, security and surveillance. Mobile operators use them nearer the central office to transport the traffic generated from cell sites on the edge back to the core. Public and private networks use long haul for connecting metro or building rings in the core of the network when fiber is not a practical solution. Because of their mission critical applications, long haul radios need to be highly reliable with high capacity data services. To achieve the multi gigabit capacity often required, most long haul radios support technologies like XPIC.

COMPETITIVE LANDSCAPE

The competitive landscape for long haul/trunk radios is dominated by less than a dozen equipment vendors. All of these, except Fujitsu, have a traditional short haul microwave radio offering as well. Some of these vendors are new to the long haul market, and are using their strong position in the short haul arena to leverage long haul sales.

Alcatel-Lucent: Alcatel-Lucent was the first to have a compact IP based long haul radio. Their innovative 9500 MPR platform has been tried and tested in real LTE deployments and thus, Alcatel-Lucent understands what mobile operators require for mobile broadband long haul deployments. The MPR 9500 long haul version offers 20 channels/antenna, up to 16 Gbps, and carrier class Ethernet services like redundancy, IEEE 1588 v2 and Synch E.

Aviat: Aviat has three long haul/trunking solutions – WTM6000, STR600 and IRU600, with the IRU600 only for North America. The WTM6000 is a traditional trunking radio, while the STR600 is split-mount. The trunking radio can support up to 16 channels, transport 4 Gbps of traffic and has a L2 carrier Ethernet switch. The STR600 does not require waveguides which makes the radio much more economical and provides better system performance than higher power all indoor trunking radios.

Ceragon: Ceragon's long-haul portfolio is built around the new, SDN-ready IP-20 platform and comes with a range of ANSI and ETSI configurations. Ceragon's fully protected longhaul solutions feature high density and high capacity and offer rich functionality. The IP-20 Platform simplifies the migration from Native TDM and Hybrid to all packet architectures. Because the new IDUs are completely backwards compatible with Ceragon's entire portfolio, including FibeAir and Evolution radio units, Ceragon customers require the replacement of only the IDU while keeping the radios, antennas, branching and waveguides/coax intact.

Ericsson: Ericsson has long been the leading microwave vendor and one of the leading vendors in the trunking/long haul radio market. They have recently made some changes to the Mini-Link LH radio, by offering a flexible, semi-compact or trunking version. The Mini-Link LH is part of its Mini-Link platform, offering interchangeable short haul and long haul radios for maximum flexibility and scaling.

Fujitsu: Fujitsu has one of the most OEM'd trunking/long haul radios around. Several microwave radio vendors private label their FRX-3E. Fujitsu prides itself on offering true hybrid quality. So instead of being solely focused on Ethernet services, and possibly sacrificing some traditional features, such as N+1 SDH, that can be critical for multi-path fading, Fujitsu is focused on helping customers facilitate a smooth migration from TDM to Ethernet.

Huawei: Huawei has been a leading vendor in the short haul market and has recently introduced a compact IP based radio for the long haul market. Their radio seems to have all the bells and whistles – compact, very high capacity (16 Gbps), up to 16 channels, up to 34 dBm transmit power and all the required Ethernet services.

NEC: NEC has two long haul radios – the 5000S (TDM) and the more recently introduced 5000IP (Hybrid/IP). Both radios are indoor, "big iron" radios. The 5000IP has ethernet OAM for fault management and performance monitoring as well as multiple clock sources such as synchronous Ethernet, IEEE 1588v2 and legacy TDM synchronization.

SIAE: SIAE's TL trunking radio is a hybrid radio that offers 16 channels per rack. It not only supports variable bandwidth options, but also supports Ethernet services such as Synch E and IEEE 1588 v2. Its very high power of 35 dBm is one of the highest available.

The features listed above are all important, but how do equipment vendors stack up on the key specifications? SLR surveyed radio vendors based on the metrics listed in Table 1 and then assigned a score to each. These were then tabulated for a networking score (see ***Figure 3***) – the higher the aggregated score, the further to the right of the chart the radio lies. The higher the capacity, the further to the top of the chart the radio lies.

Specifications were from vendors' data sheets and claims they made on surveys. Some of these claims were not able to be verified. If no information could be found, assumptions were made. ■

Emmy Johnson *is the founder and principal analyst of Sky Light Research, a third-party analyst firm specializing in wireless point-to-point mobile backhaul technologies such as microwave, sub 6 GHz and millimeter wave radios. The firm's popular services include quarterly market share reports and forecasts. Sky Light Research was founded in 2001 and is located in Scottsdale, Ariz. For more information, please email info@SkyLightResearch.com or call (480) 563-2251.*

Locating Sources of Interference

Cyril Noger, Anritsu S.A.
Villebon-sur-Yvette, France

The proliferation of RF devices has benefited the world in many ways, providing readier and more convenient access to communications, entertainment and information. But it has come with one unintended drawback: a huge increase in the frequency and severity of incidents of interference.

Cellular telephone networks have been hit particularly hard: the introduction of many new cellular technologies to an ever-growing number of subscribers has made it difficult for the network operators and spectrum regulation authorities to find clean spectrum unaffected by interference. Interference in cellular transmissions increases noise, with the effect of:

- reducing the effective size of a cell
- lowering data rates delivered to user equipment
- impairing the quality of voice and data communications

As a result, radio technicians spend much time travelling around the country, hunting the sources of interference. Only once a source is precisely located can action be taken to lower the power of its transmissions or to disable it entirely, if appropriate.

On occasion, filtering an unwanted in-band signal can solve the problem. Otherwise, the technician's job is to monitor the spectrum, uncover the nature of an interferer (permanent or intermittent) and track it to its source.

TYPES OF INTERFERENCE AFFECTING CELLULAR NETWORKS

The existence of interference affecting a cell is normally obvious to the operator, because it will have caused a drop in communications performance which will have been reported by the operator's networking monitoring systems. The first step in dealing with the problem is to observe what is happening in the affected frequency band. At this stage, the technician needs to know whether the interference is continuous or intermittent by measuring the amplitude and power of the interfering signal(s). This is best done by connecting an omnidirectional antenna to a spectrum analyzer, placing it in the cell in question and leaving it to log network activity for a period of time.

The analyzer may find one or more of a number of types of interference:

- In-band interference: an unwanted signal from a different transmitter type that falls inside the operating bandwidth of the desired signal. This corrupts the receiver as it is difficult to filter.
- Co-channel interference: similar to in-band interference, except that the unwanted signal originates from a transmitter in the same network, but located elsewhere.
- Out of band interference: in a wireless system designed to transmit in a different frequency band, part of a transmitted signal's energy can fall into the operating frequency band of the cell under test, impairing its performance.
- Adjacent channel interference: often seen in wideband transmission systems, when transmissions at the main operating frequency also generate lower-amplitude signals in directly neighboring channels (called the lower and upper channels or left and right channels).

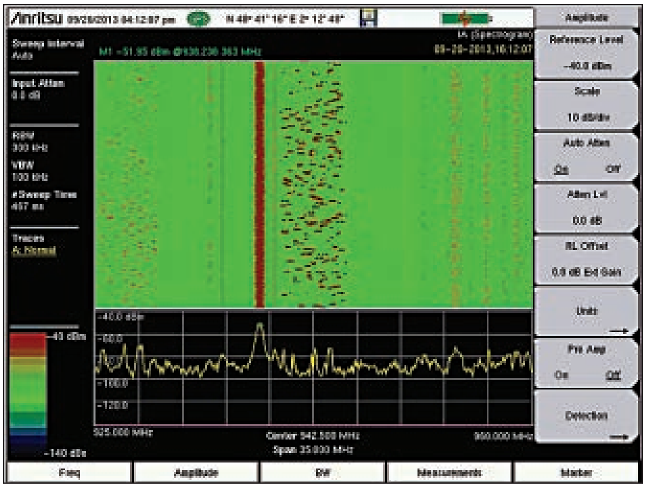

Fig. 1 *Spectrogram showing occurrences of signals in the GSM frequency band over a period of a few minutes.*

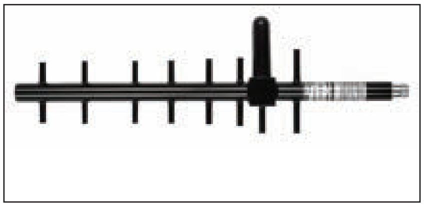

Fig. 2 *A Yagi antenna can isolate an interference source at a particular frequency.*

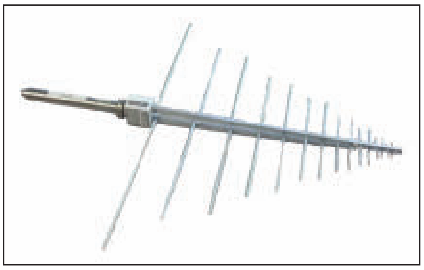

Fig. 3 *A Log Periodic antenna can capture a variety of interferers across a wide frequency spectrum.*

- Uplink and downlink interference: unwanted signals affecting the receiver (uplink) or the transmitter (downlink) of a base station when it communicates with a mobile terminal.
- Impulse noise: created whenever a flow of electricity is abruptly started or stopped, impulse noise can affect any transmitter's or receiver's characteristics, with the effect of scrambling communications.

Other types of interference may be found, but the most common types are those listed.

LOCATING THE SOURCE

In today's cellular telephone networks, the operator will be alerted to a problem by built-in alarms or dedicated sensors distributed through the network which can time-stamp instances of interference. Now, radio technicians have to identify the cause of the problem.

If the source of the problem is an RF emitter, one way to troubleshoot the system is to monitor the frequency band of the affected transmitter or receiver. A modern handheld spectrum analyzer connected to an omnidirectional antenna can accurately monitor a frequency band over a period of time (typically up to 72 hours) by continuously logging spectrum measurements.

Figure 1 shows the spectrogram display of continuous measurements. Its advantage is that the power (amplitude) of each detected frequency is color-coded, so when analyzing the measurements it is easy to see whether or not an unwanted signal appears in the frequency band under investigation. This first step will commonly identify the frequency and amplitude of the interfering signal, and the nature of its emissions (random, regular or continuous). Measurements taken from a single location are not sufficient to precisely locate the interferer.

The next step is to attempt to locate the source with the use of directional antennas (see ***Figures 2*** and ***3***). In the past, the preferred way to locate a source was to use an analog meter to measure the strength of a signal or carrier (see ***Figure 4***). These meters gave an audible beep which rose in frequency as the signal strength rose. This allowed technicians driving vehicles with roof-mounted antennas to gauge signal strength without taking their eyes off the road. While this was convenient, it was not an accurate means to locate interference, as the meter had no embedded mapping capability.

An improvement on this method is to perform a mapped drive test. Using the same omnidirectional antenna mounted on the roof of a car, the technician drives on a route through the affected area logging the power of signals at the suspected frequency. By

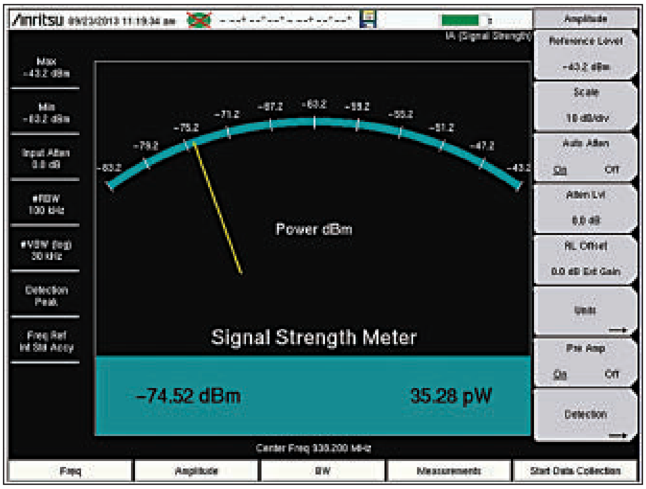

▲ *Fig. 4 A spectrum analyzer can emulate the display style of an analog meter to show signal strength.*

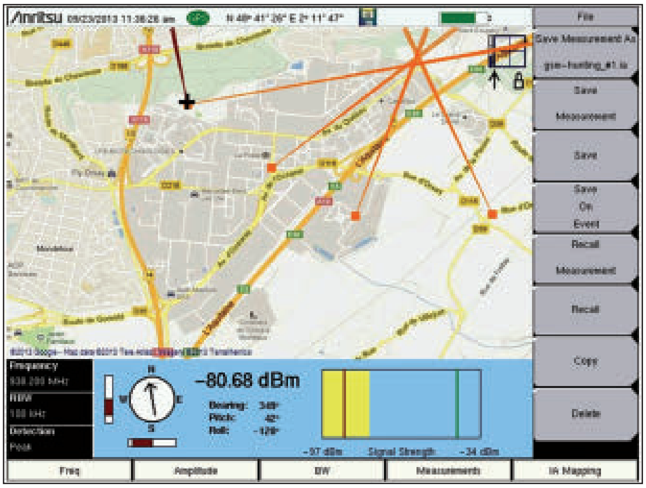

▲ *Fig. 7 Triangulation locates the source of interference on the instrument's map.*

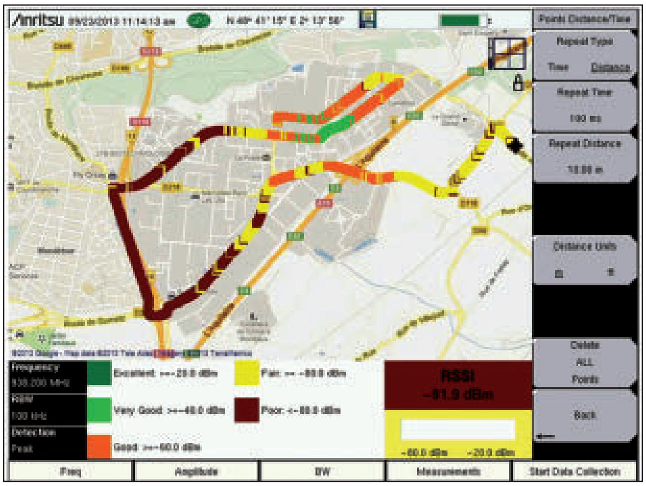

▲ *Fig. 5 A drive test records the signal strength at a chosen frequency over the course of a known route.*

▲ *Fig. 6 Direction finding in the field with a handheld spectrum analyzer and unidirectional antenna.*

pre-loading the route into a software application such as easyMap Tools, a map can be hosted on the spectrum analyzer and directly displayed while driving. As ***Figure 5*** shows, the analyzer can display the car's location in real-time (derived from a GPS signal) and the power of the received signal at the chosen frequency (known as Received Signal Strength Indicator, or RSSI).

The easyMap Tools software allows for the car's variable speed: the user can configure the spectrum analyzer to take a measurement at set distances, for example, every 10 m. Subsequent analysis of the drive test results might indicate the area in which the interfering signal is strongest.

To this point the interference-hunting process has narrowed the search down to a small area. But it has not precisely located the source: this means that the technician can still not identify it, so it cannot be attenuated, filtered or disabled. Finding the precise location of the interferer calls for the use of the same handheld spectrum analyzer, but now with a directional, narrowband antenna. The process of 'direction finding' in the suspected area is uncovered by the drive test.

Since this normally involves going out on foot in the area under investigation while holding a portable spectrum analyzer, it is helpful to have an accessory for holding the directional antenna. For example, Anritsu provides the MA2700A, an ergonomic handle that secures the antenna via a standard connector (see ***Figure 6***).

The MA2700A also includes a broadband pre-amplifier to boost the antenna's sensitivity and a built-in GPS receiver to enable the precise location at which measurements are taken to be logged in the spectrum analyzer. Finally, a built-in electronic compass (magnetometer) senses the exact direction in which the antenna is pointed. The user just has to pull a trigger and turn around 360° to find the direction of the strongest signal at the frequency in question. The location and direction are displayed on the instrument's screen.

By repeating this process from multiple locations, the user can perform triangulation (see ***Figure 7***); the various measurements should almost always point towards a single location on the map. This is the source of the interference.

This technique can be used by any network technician, since it uses familiar equipment and easy-to-operate software tools. Normally, this technique on its own is sufficient to enable the technician to find and fix the interference problem.

There are many kinds of interference sources that affect the performance of wireless transmission systems. The handheld spectrum analyzer, combined with omni- and unidirectional antennas, is the most convenient and effective instrument for identifying and locating the position of the interferer. In addition, by integrating GPS and mapping software in the spectrum analyzer, the time taken to troubleshoot interference problems is minimized.

VENDORVIEW

Anritsu S.A.
Villebon-sur-Yvette, France
www.anritsu.com

NATIONAL INSTRUMENTS

AWR | A National Instruments Company™

Try NI AWR Design Environment Today!

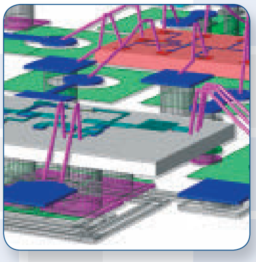
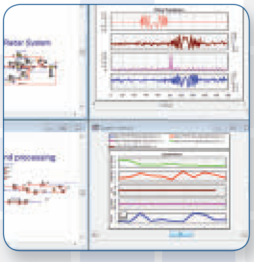
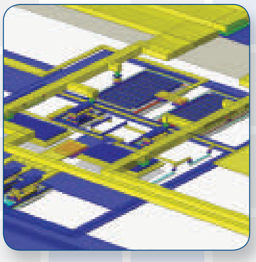
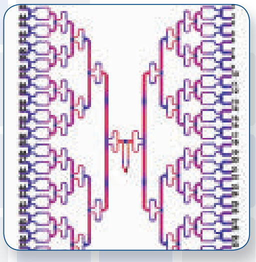
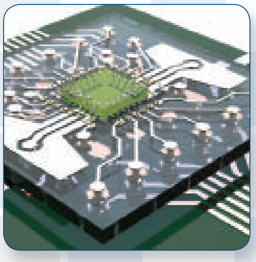

Microwave Office | Visual System Simulator | Analog Office | AXIEM | Analyst

Try NI AWR Design Environment

today and see for yourself how easy and effective it is to streamline your design process, improve end product performance, and accelerate time to market for MMICs, RFICs, RF PCBs, microwave modules, 3D/planar passive interconnects, antennas, communication systems, and more.

>> Learn more at ni.com/awr

NI AWR Design Environment consists of a comprehensive software product portfolio that offers a variety of high-frequency design tools that embrace system simulation, circuit simulation, and electromagnetic analysis.

- Microwave Office for MMIC, module, and RF PCB design
- Visual System Simulator for RF/comms. systems design
- Analog Office for analog and RFIC design
- AXIEM for 3D planar electromagnetic analysis
- Analyst for 3D FEM EM simulation and analysis

Visit **awrcorp.com/whatsnew** for a complete list of features found in the current version of NI AWR Design Environment.

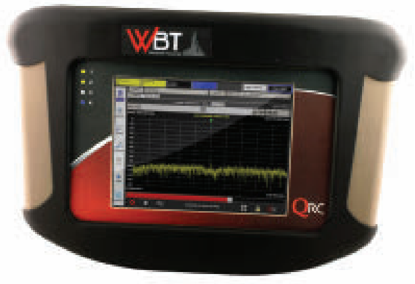

Transcorder Records 80 MHz Bandwidth Between 50 MHz and 6 GHz

QRC Technologies
Fredericksburg, Va.

The WBT-200 Wideband Transcorder® by QRC Technologies records and plays back 80 MHz of RF bandwidth, in two separately tunable 40 MHz sections, anywhere between 50 MHz and 6 GHz.

Contained in a single box and weighing less than 10 lbs, the WBT-200 is capable of playing back the recorded signals anywhere within the tuning range without the need for any additional equipment (see ***Figure 1***). It eliminates the need for a separate spectrum analyzer to digitize the signal, a signal generator to play back the RF and a PC to interface and control the unit. The WBT-200's simple user interface has a single button for RF record or playback.

Fig. 1 WBT-200 display showing RF playback.

Many other RF recording and playback systems require additional equipment with numerous interconnects, which increases the total cost of ownership and complicates the test setup and run procedures for the user. According to QRC Technologies, the WBT-200 has better performance and costs less than other similar products, most of which only collect data and can't reconstruct and play back the RF.

WBT APPLICATIONS

The WBT-200 can be used for the following applications:

Reference Signal Recording and Playback: A reference signal (e.g., test cases, standard compliance vectors) can be recorded, easily recalled and repeatedly played back. The WBT can replace expensive single-purpose communication test sets, which is especially advantageous in manufacturing operations that require numerous workstations to certify products.

Signal Analysis: Analysis can occur while the signal is being recorded, either by playing the recording back or directly analyzing the data.

Fig. 2 RF spectrogram obtained with the spectrum waterfall app.

Market Penetration: Utilization of licensed spectrum can be measured easily and quickly.

Competitive Analysis: A rough comparison of mobile operators can be obtained by measuring the amount of licensed spectrum each utilizes.

Interference Analysis: Looking directly at the spectrum can often determine the presence of an unlicensed signal. Playing back the recording can prove this to the interfering entity.

Training: The RF environment of interest can be recorded and played back to personnel being trained.

Receiver Test and Design: Particular signal configurations and tests can be recorded and played back for a deterministic design and test of RF receivers.

Security: The presence of unwanted transmissions can be detected anywhere in the frequency range.

Arbitrary Waveform Transmitter: Programmatically generated waveforms (e.g., in MATLAB) can be easily transmitted.

In the near future, the WBT-200 will also simultaneously record and retransmit 40 MHz of received spectrum in realtime at a different center frequency, enabling it to be used as a repeater or downconverter.

DATA STORAGE AND TRANSFER

The WBT platform records to and plays back from standard 2.5" commercial solid state drives (SSD) using the VITA 49 Radio Transport (VRT) industry standard open format. SSDs have the necessary read and write speeds and ensure a robust, portable product that will withstand shock and vibration.

The WBT-200 includes two drive bays. While data is recorded and played back using one SSD, the other SSD can easily be replaced without affecting the operation of the system. This unlimited disk swapping enables continuous recording and playback, limited only by the number of SSDs available.

Data on the drives can be visualized and analyzed using the WBT's Signal Analysis Toolkit or other analysis packages that utilize the QVRT file format.

If the signal has less than 80 MHz of instantaneous RF bandwidth, the recording bandwidth can be reduced to conserve disk space.

A gigabit Ethernet port is provided to transfer data from the SSDs over a network, remotely control a WBT and allow one WBT to control other WBTs. A future capability will allow data to be streamed directly to another device, at greatly reduced bandwidth. The interface supports both DHCP and static network configuration.

An eSATAp (powered eSATA) port enables additional high-speed disks to be directly connected to the WBT. In the future, data may be recorded directly onto the eSATA disks; however, maximum bandwidth may be reduced, depending on disk performance.

TIMING AND SYNCHRONIZATION

The WBT-200 contains an embedded GPS disciplined oscillator (GPSDO) that provides a precise internal 10 MHz timing reference, which is made available externally. The oscillator also generates a 1 pulse per second (PPS) signal with ±50 nanosecond accuracy, also available externally. These frequency and timing reference ports can be used to synchronize the WBT with other components, including additional WBTs for simultaneous recording and playback.

The 50-channel GPS receiver has an acquisition sensitivity of -144 dBm and tracking sensitivity of -160 dBm. The RF recordings are tagged with GPS geo-location.

WBT APPS

To expand the utility of the WBT-200, QRC has created a series of applications that supplement the role of many test systems. A patented, open architecture application programmer's interface (API) and VRT-based IQ file format (QVRT) make it possible. The WBT's core firmware provides the basic hardware level control of the system and application management. Everything else is available through the WBT API and open for anyone to use.

The following free apps will soon be available to download and install from the online WBT App Store:

Spectrum Waterfall: RF spectrogram (see ***Figure 2***).

AGC: Configurable automatic gain control of both WBT receivers.

SCPI Control: WBT control via Standard Commands for Programmable Instruments.

Timed Record/Playback: Record and/or playback files at specified times.

Tune and Dwell: Record specific sections of spectrum for a specific time and loop, if necessary.

Level Trigger: Record when power exceeds a threshold (peak or average), for a user-defined time, and stop recording when the signal falls back below a user-set power threshold.

RF DVR: In a temporary buffer, perpetually store the last received RF data for a user-defined duration. When a user-defined event has occurred, users can write the buffered RF information to the disk and continue to record the RF following the event.

Sweep To File: Sweep from a start to a stop frequency and save the spectrum results as a CSV file for analysis.

Users can also develop custom applications — even resell them through the WBT App Store — using common tools and languages such as C++, Python and familiar programming environments like Qt. QRC offers a full, prepackaged development environment and all necessary documentation.

QRC Technologies
Fredericksburg, Va.
(540) 446-2270
http://wbt.qrctech.com/

Field Analyzer with PIM Testing Capability

Anritsu Co. has introduced the MW82119B PIM Master™ that combines a 40 W, battery-operated PIM analyzer with a 2 MHz to 3 GHz cable and antenna analyzer, eliminating the need to carry multiple instruments to measure the RF performance of a cell site. The MW82119B provides tower and maintenance contractors, network installers and wireless service providers with the first handheld field passive intermodulation (PIM) analyzer with line sweep capability that fully certifies cell site cable and antenna systems.

The MW82119B PIM Master with Site Master™ option supports the full array of site tests. Field users can conduct PIM versus time, swept PIM, distance-to-PIM (DTP), return loss, VSWR, cable loss and distance-to-fault (DTF) measurements. In addition to eliminating the need to carry multiple instruments to the top of a tower, the integrated MW82119B PIM Master allows all site data to be stored in one location for fast retrieval.

The MW82119B PIM is MIL-STD-810G drop test rated and is designed to withstand transportation shock, vibration and harsh outdoor test conditions. The MW82119B PIM Master has also achieved an IP54 ingress protection rating, certifying its ability to operate without damage after exposure to blowing dust and water spray.

The MW82119B PIM Master has an outdoor viewable 8.4" display and intuitive user interface (UI) that is optimized for field conditions. New stainless steel lifting rings in the chassis and a padded soft case make the analyzer well suited for hoisting during tower-top testing. The analyzer's rugged design, lightweight and small size enable both PIM and line sweep testing at the top of the tower.

Covering various bands and featuring unprecedented measurement capability, the MW82119B PIM Master is well suited for a number of applications, including the deployment and maintenance of LTE remote radio heads (RRH), small cells and distributed antenna systems (DAS).

VENDORVIEW

Anritsu Co.
Morgan Hill, Calif.
www.anritsu.com

Low PIM, Plenum Rated Cable Assembly and mini-DIN Connector

The Times SPP-LLPL 50 ohm, low loss plenum rated/UL listed coaxial cable assembly family has been expanded to include SPP-375-LLPL 3/8" and SPP-500-LLPL 1/2" cables for even lower loss. With excellent electrical performance compared to many other copper cable assemblies, SPP-LLPL cables are well suited for in-building solutions for PIM-sensitive installations and system interconnects. Meeting the fire resistance requirements of UL 910 for plenum rated applications, the new larger sizes of SPP-LLPL cable assemblies are ideal for installations where lower loss is needed. High quality connectors assure excellent and reliable static and dynamic PIM performance: better than -155 dBc for applications up to 6 GHz. All Times plenum cables are UL listed and printed with the UL file number. SPP-LLPL cable assemblies are available in 1, 2 and 3 meter pre-assembled lengths with N, 716 DIN and SMA connector interfaces, and the new 4.1/9.5 mini DIN connectors.

The new 4.1/9.5 mini-DIN straight male connector, TC-SPP250-4195M-LP, is available for the SPP-250-LLPL (SuperFlexible Plenum PIM) 50 ohm low loss plenum rated coaxial cable assemblies for use in distributed antenna system (DAS) applications. SPP-250-LLPL is a ¼" super flexible type corrugated cable with low density PTFE dielectric and FEP jacket that meets the requirements of UL 910 for plenum applications. The cable assemblies are suitable for in-building jumpers and interconnects up to 6 GHz. The factory installable connectors attach via soldering of the center pin and induction soldering to the cable outer conductor, providing excellent VSWR performance and reliable PIM performance better: than -155 dBc.

Times Microwave Systems
Wallingford, Conn.
(203) 949-8400
www.timesmicrowave.com

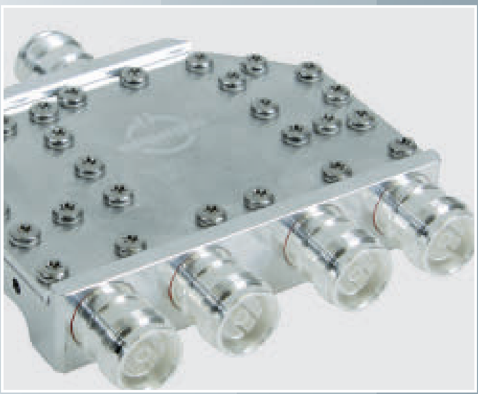

DC to 6 GHz SDR

Crimson is a flexible, wideband, high gain Software Defined Radio (SDR) platform that comes equipped with four independent receive and four independent transmit chains, each capable of up to 322 MHz of RF bandwidth to 6 GHz. At the core of the digital front, Crimson is powered by an Altera™ Arria V FPGA (5ASTMD3E3F31I3N) with an on-chip, dual-core ARM Cortex-A9 processor, and comes with a high stability internal reference clock.

Crimson has an RF tuning range of 100 kHz to 6 GHz with receive gain of 67 dB, SFDR of 55 dB at 200 MHz, SNR up to 73 dB and P1dB of -11 dBm. The transmit power is 10 dBm maximum at 6 GHz with P1dB of 14 dBm and SFDR of 61 dB from DC to 500 MHz.

Features

- Operating frequency from DC to 6 GHz (MF-HF-VHF-UF)
- Over 1200 MHz of RF bandwidth across four independent, controllable Rx channels, and over 1200 MHz across four independent, controllable Tx channels
- Low noise and high dynamic range
- High stability internal reference clock (± 5 ppb)
- On-board Altera ST FPGA with ARM processor
- Dual 10 Gigabit Ethernet backhaul

Applications

- Near real-time signals analysis
- Signal recording and spectrum monitoring
- Spectrum allocation analysis
- Multiple-input-multiple-output (MIMO) applications
- Mobile backhaul and base station
- Wideband communications

Per Vices
Toronto, Canada
solutions@pervices.com
www.pervices.com

COMPANY SHOWCASE

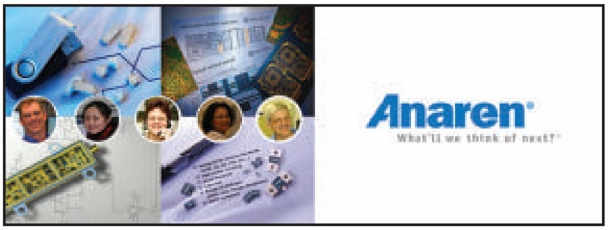

RF and Microwave Technology

VENDORVIEW

Anaren Inc. is a Syracuse-based, global leader in RF and microwave technology used in wireless infrastructure, satellite, defense and consumer-electronics applications. The company has approximately 1,000 employees and five state-of-the-art facilities worldwide. Product lines include: standard passive components (e.g., couplers, power dividers, baluns, resistors, attenuators, terminations), RF multichip modules, high-reliability softboard and ceramic PCBs, and complex assemblies (e.g., switching, beamformers, antenna feed networks, DRFMs, IMAs).

Anaren Inc.
www.anaren.com

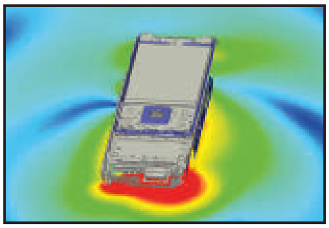

EM Simulation for Mobile Communications

VENDORVIEW

As mobile communication devices become thinner, smaller and more complex with every generation, designs need to meet new standards of performance. Using electromagnetic (EM) simulation, engineers can not only design and optimize the antenna of mobile devices, but also test its performance within the handset, for example, by evaluating coupling effects and the impact of dielectric materials, and investigating the influence of the human body on performance. Find out more about CST STUDIO SUITE®, an EM simulation tool, by visiting the company's website.

Computer Simulation Technology AG (CST)
www.cst.com

Flat Antennas SENCITY Matrix

As mobile data traffic levels continue to rise, small cells are increasingly being seen as a vital component of a modern heterogeneous network. The small size of HUBER+SUHNER SENCITY® Matrix antennas allows operators to access rooftop, wall and street level sites. HUBER+SUHNER offers a range of stand-alone antennas including radome, backplane and standard waveguide-interface that allows for quick adaption of this revolutionary technology. For entirely individual radio designs the antennas can also be purchased without housing. Visit www.hubersuhner.com for more information.

HUBER+SUHNER
www.hubersuhner.com

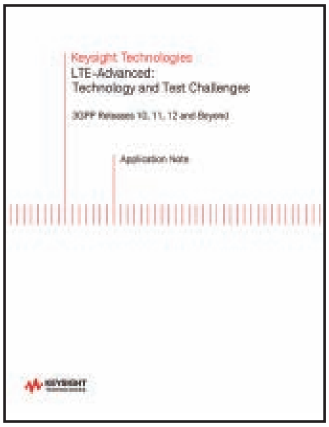

LTE-Advanced Application Note

VENDORVIEW

Keysight Technologies' LTE-Advanced: Technology and Test Challenges application note offers insights into 3GPP Releases 10, 11, 12 and beyond, with a focus on the LTE-Advanced air interface. It also covers 3GPP specifications for core network standards and services. Topics include LTE and LTE-Advanced, including summaries of LTE Release 8/9 features, ITU requirements for 4G, and 3GPP requirements for LTE evolution; Release 10 and LTE-Advanced; Release 11 LTE-Advanced enhancements; Release 12 radio evolution; Release 13 update; and LTE-Advanced product design and testing challenges.

Keysight Technologies Inc.
www.keysight.com

Equipment & Components Catalog

VENDORVIEW

Celebrating its 53rd anniversary, MECA (Microwave Equipment & Components of America) designs and manufactures an array of Low PIM DAS Equipment and RF/microwave components with industry leading performance. MECA is recognized worldwide as a primary source of supply for rugged and reliable components to commercial and military OEMs, service providers and installers by only providing products made in the U.S. Download the company's components catalog at www.e-meca.com/pdfs/MECA_catalogo-2014.pdf.

MECA Electronics Inc.
www.e-MECA.com

Custom Rack Mount Test Equipment Guide

VENDORVIEW

Mini-Circuits announced the publication of the 2014 Custom Rack Mount Test Equipment Guide, a 52-page, full color brochure showcasing a wide selection of custom test solutions ranging from DC to 18 GHz including amplifiers, signal generators, routing and distribution systems, and more. The brochure highlights Mini-Circuits' ability to deliver affordable, reliable custom test solutions with turnaround times as fast as two weeks and also introduces the company's user-friendly control software, programming support and test accessories. To request a copy, email sales@minicircuits.com.

Mini-Circuits
www.minicircuits.com

COMPANY SHOWCASE

Advancing the Wireless Revolution

VENDORVIEW

NI AWR software products accelerate the design and product development cycle of high-frequency ICs and systems found within the aerospace/defense, semiconductor, computer, consumer electronics and telecommunications markets by reducing the time it takes from concept through manufacturing. NI AWR Design Environment provides an intuitive use model that delivers an exceptional user experience and open design flow that supports third party tools, resulting in more compelling solutions. These unique aspects of NI AWR software maximizes user productivity by eliminating errors and design redundancies, quickening the pace to market.

National Instruments (formerly AWR Corp.)
www.ni.com/awr

Filters, Multiplexers and Multifunction Assemblies

VENDORVIEW

Reactel offers a variety of filters, multiplexers and multifunction assemblies for the mobile communication industry. Reactel's experienced engineers can come up with a creative solution for all of your Tx, Rx or cosite requirements. Reactel has designed a broad range of filters from high power units operating to 5 kW and beyond to extremely small ceramic units that are suitable for handheld or portable applications. The company's product line includes bandpass, lowpass, highpass and notch filters as well as multiplexers and multi-passband filters. Offering fast turnaround, competitive pricing and high quality, Reactel can satisfy most any requirement you may have.

Reactel Inc.
www.reactel.com

T&M Instruments That Meet Your Needs

VENDORVIEW

Whatever your job is, you do not always need the ultimate high-end T&M equipment. You do need precise, reliable, universal measuring instruments. That is what you get with Value Instruments from Rohde & Schwarz. They combine practical features with excellent measurement characteristics that are easy to use and easy on the budget. Find out more in the Value Instruments Catalog 2014 from Rohde & Schwarz. (Order number: PD 3606.6463.42).

Rohde & Schwarz GmbH & Co. KG
www.rohde-schwarz.com

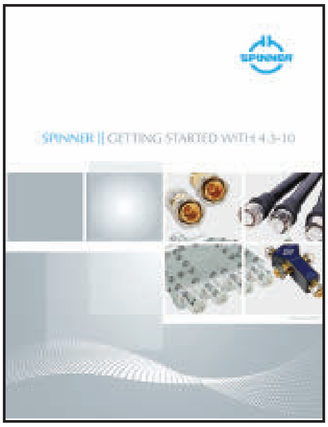

Getting Started With 4.3-10

SPINNER GmbH released their new 4.3-10 catalog. The catalog reflects the current 4.3-10 products showing connectors, jumpers, measurement and calibration, loads and attenuators, and couplers and splitters. The SPINNER Group has been setting standards with its RF technology products for more than 65 years. The company's high quality standards for design, material and manufacturing ensure the best possible connectivity, optimized installation and failure-free operation, even under the toughest environmental conditions. For more information visit the company's website at www.spinner-group.com.

Spinner GmbH
www.spinner-group.com

ADVERTISING INDEX & SALES REPRESENTATIVES

Ed Kiessling, Traffic Manager/Inside Sales
685 Canton Street Norwood, MA 02062
Tel: (781) 619-1963 FAX: (781) 769-6178
ekiessling@mwjournal.com

Eastern and Central Time Zones
Chuck Boyd
Northeast Reg. Sales Mgr.
(New England, New York, Eastern Canada)
685 Canton Street
Norwood, MA 02062
Tel: (781) 769-9750
FAX: (781) 769-5037
cboyd@mwjournal.com

Michael Hallman
Eastern Reg. Sales Mgr.
(Mid-Atlantic, Southeast, Midwest)
4 Valley View Court
Middletown, MD 21769
Tel: (301) 371-8830
FAX: (301) 371-8832
mhallman@mwjournal.com

Pacific and Mountain Time Zones
Brian Landy
Western Reg. Sales Mgr.
(CA, AZ, OR, WA, ID, NV, UT, NM, CO, WY, MT, ND, SD, NE & Western Canada)
144 Segre Place
Santa Cruz, CA 95060
Tel: (831) 426-4143
FAX: (831) 515-5444
blandy@mwjournal.com

International Sales
Richard Vaughan
International Sales Manager
16 Sussex Street
London SW1V 4RW, England
Tel: +44 207 596 8742
FAX: +44 207 596 8749
rvaughan@horizonhouse.co.uk

Germany, Austria, and Switzerland
(German-speaking)
WMS.Werbe- und Media Service
Brigitte Beranek
Gerhart-Hauptmann-Street 33,
D-72574 Bad Urach
Germany
Tel: +49 7125 407 31 18
FAX: +49 7125 407 31 08
bberanek@horizonhouse.com

Israel
Liat Heiblum
Oreet International Media
15 Kineret Street
51201 Bene-Berak, Israel
Tel: +972 3 570 6527
FAX: +972 3 570 6526
liat@oreet-marcom.com

Korea
Young-Seoh Chinn
JES Media International
2nd Floor, ANA Bldg.
257-1, Myungil-Dong
Kangdong-Gu
Seoul, 134-070 Korea
Tel: +82 2 481-3411
FAX: +82 2 481-3414
yschinn@horizonhouse.com

Japan
Katsuhiro Ishii
Ace Media Service Inc.
12-6, 4-Chome,
Nishiiko, Adachi-Ku
Tokyo 121-0824, Japan
Tel: +81 3 5691 3335
FAX: +81 3 5691 3336
amskatsu@dream.com

China
Michael Tsui
ACT International
Tel: 86-755-25988571
Tel: 86-21-62511200
FAX: 86-10-58607751
michaelT@actintl.com.hk

Hong Kong
Mark Mak
ACT International
Tel: 852-28386298
markm@actintl.com.hk